

WL-TR-97-4079

**PROCEEDINGS OF THE ANNUAL
MECHANICS OF COMPOSITES
REVIEW (17TH)**



Sponsored by:

**Air Force Wright Aeronautical Laboratories
Materials Laboratory**

APRIL 1997

FINAL REPORT FOR PERIOD 27-28 OCTOBER 1992

Approved for public release; distribution unlimited

**MATERIALS DIRECTORATE
WRIGHT LABORATORY
AIR FORCE MATERIEL COMMAND
WRIGHT-PATTERSON AFB OH 45433-7734**

DTIC QUALITY INSPECTED 3

19970711 019

REPORT DOCUMENTATION PAGE			Form Approved OMB No. 0704-0188	
Public reporting burden for this collection of information is estimated to average 1 hour per response, including the time for reviewing instructions, searching existing data sources, gathering and maintaining the data needed, and completing and reviewing the collection of information. Send comments regarding this burden estimate or any other aspect of this collection of information, including suggestions for reducing this burden, to Washington Headquarters Services, Directorate for Information Operations and Reports, 1215 Jefferson Davis Highway, Suite 1204, Arlington, VA 22202-4302, and to the Office of Management and Budget, Paperwork Reduction Project (0704-0188), Washington, DC 20503.				
1. AGENCY USE ONLY (Leave blank)		2. REPORT DATE April 1997		3. REPORT TYPE AND DATES COVERED Final Report 27-28 OCTOBER 1992
4. TITLE AND SUBTITLE PROCEEDINGS OF THE ANNUAL MECHANICS OF COMPOSITES REVIEW (17TH)			5. FUNDING NUMBERS	
6. AUTHOR(S)				
7. PERFORMING ORGANIZATION NAME(S) AND ADDRESS(ES) Air Force Materials Laboratory Nonmetallic Materials Division Wright-Patterson AFB OH 45433			8. PERFORMING ORGANIZATION REPORT NUMBER	
9. SPONSORING/MONITORING AGENCY NAME(S) AND ADDRESS(ES) Materials Directorate Wright Laboratory Air Force Materiel Command Wright-Patterson AFB Ohio 45433-7734 POC:Tammv Oaks, WL/MLBM, 937-255-3068			10. SPONSORING/MONITORING AGENCY REPORT NUMBER WL-TR-97-4079	
11. SUPPLEMENTARY NOTES				
12a. DISTRIBUTION AVAILABILITY STATEMENT APPROVED FOR PUBLIC RELEASE; DISTRIBUTION IS UNLIMITED			12b. DISTRIBUTION CODE	
13. ABSTRACT (Maximum 200 words) This report contains the basic unedited vu-graphs of the presentations at the "Mechanics" of Composites Review" sponsored jointly by the Non-metallic Materials Division of the Air Force Materials Laboratory, the Structures Division of the Air Force Flight Dynamics Laboratory and the Directorate of Aerospace Sciences of the Air Force Office of Scientific Research. The presentations cover current in-house and contract programs under the sponsorship of these three organizations.				
14. SUBJECT TERMS epoxy-matrix composites; composite materials; resin matrix composites; composite bonded joints; fatigue of graphite/epoxy composites; fracture and fatigue of bi-materials			15. NUMBER OF PAGES 302	
			16. PRICE CODE	
17. SECURITY CLASSIFICATION OF REPORT UNCLASSIFIED	18. SECURITY CLASSIFICATION OF THIS PAGE UNCLASSIFIED	19. SECURITY CLASSIFICATION OF ABSTRACT UNCLASSIFIED	20. LIMITATION OF ABSTRACT SAR	

AGENDA
MECHANICS OF COMPOSITES REVIEW
27-28 OCTOBER 1992

<u>TUESDAY, 27 OCTOBER 1992</u>	<u>PAGE</u>
0715 REGISTRATION	
0815 OPENING REMARKS	
0830 OBSERVATIONS AND MODELLING OF DEFORMATION AND FRACTURE IN NANO-STRUCTURAL MATERIALS - <u>E.C. Alfantis</u> , Michigan Technological University, Department of Mechanical Engineering & Engineering Mechanics, Houghton MI	1
0855 FAILURE MECHANISMS IN UNIDIRECTIONAL AND CROSSPLY CERAMIC-MATRIX COMPOSITES - <u>Issac Daniels</u> , Northwestern University, McCormick School of Engineering of Applied Science, Evanston IL	11
0920 MECHANISMS FOR THERMAL CYCLING DAMAGE IN METAL MATRIX COMPOSITES - <u>Minoru Taya</u> , William D. Armstrong and Martin L. Dunn, Department of Mechanical Engineering, University of Washington, Seattle WA	21
0945 SOME FRACTURE PROBLEMS IN UNIDIRECTIONAL BRITTLE MATRIX COMPOSITES (BMC) - <u>Nicholas J. Pagano</u> , Wright Laboratory, Materials Directorate, Wright-Patterson AFB OH	27
1010 BREAK	
1045 NAVY PERSPECTIVES ON COMPOSITES RESEARCH - <u>Yapa D. S. Rajapakse</u> , Office of Naval Research, Mechanics Division, Arlington VA	A-17
1110 LOCAL BUCKLING IN VISCOELASTIC COMPOSITES - <u>Richard A. Schapery</u> , University of Texas-Austin, Department of Aerospace Engineering and Engineering Mechanics, Austin TX	38
1135 COMPRESSIVE FAILURE MECHANISMS IN COMPOSITES - <u>N. A. Fleck</u> , W. S. Slaughter, Cambridge University, Engineering Department, Cambridge, UK; B. Budiansky, Harvard University, Div. Applied Sciences, Cambridge MS	48
1200 LUNCH	
1330 FIBER WRINKLING IN FILAMENT WINDING OF THICK CYLINDERS - <u>H. Thomas Hahn</u> , UCLA, Mechanical, Aerospace and Nuclear Engineering Department, Los Angeles CA	58
1355 BREAK	
1420 PRESSURE-INDUCED NONLINEAR BEHAVIOR OF FIBER-REINFORCED COMPOSITES - <u>George J. Weng</u> , Kook D. Pae, Rutgers University, Department of Mechanical and Aerospace Engineering, Piscataway NJ	68
1445 INTERACTIVE BUCKLING IN RING-STIFFENED COMPOSITE SHELLS - <u>Srinivasn Sridharan</u> , Akihito Kasagi, Washington University, Department of Mechanical Engineering, St. Louis MO	78
1510 BREAK	
1605 BEHAVIOR OF HYBRID GLASS/GRAPHITE REINFORCED THICK-SECTION COMPOSITE CYLINDERS UNDER HYDROSTATIC LOADING - <u>Himatlal J. Garala</u> , Naval Surface Warfare Center, Carderock Division, Bethesda MD	88
1630 ADJOURN	
1700 WORKING BUFFETT	

HIGH QUALITY REPRODUCED 3

WEDNESDAY, 28 OCTOBER 1992

- 0830 FAA PROGRAM OVERVIEW - D. W. Oplinger - FAA Technical, Atlantic City
Intn'l Airport, NJ A-31
- 0855 DAMAGE RESISTANCE AND TOLERANCE IN COMPOSITE STRUCTURES -
Paul R. Lagace, MIT, Cambridge MA NAAP*
- 0920 ANALYSIS OF COMPOSITE AIRCRAFT STRUCTURES CONTAINING ASSEMBLY
INDUCED DELAMINATIONS - Steven P. Wanthal, Carlos A. Fracchia, McDonnell
Aircraft Company, McDonnell Douglas Corporation, St. Louis MO 100
- 0945 DELAMINATION ANALYSIS - Han Pijn Kahn, Northrop Aircraft, Hawthorne CA NAAP*
- 1010 BREAK
- 1145 A SELF ALIGNED TEST FIXTURE FOR INTERLAMINAR TENSILE TESTING OF
TWO-DIMENSIONAL CARBON-CARBON - Ajit K. Roy, UDRI, Wright-Patterson AFB OH 108
- 1110 ANALYSIS OF AXISYMMETRIC MICROMECHANICAL CONCENTRIC CYLINDER
MODEL - H.W. Brown, III, Wright Laboratory, Materials Directorate,
Wright-Patterson AFB OH NAAP*
- 1135 MECHANICS OF PRESTRESSED COMPOSITES - Capt David H. Rose, Wright Laboratory,
Materials Directorate, Wright-Patterson AFB OH; J. M. Whitney, University of Dayton,
Dayton OH NAAP*
- 1200 LUNCH
- 1330 ANALYSIS OF THERMOMECHANICAL CYCLIC BEHAVIOR OF UNIDIRECTIONAL
METAL MATRIX COMPOSITES - Demirkan Coker, UDRI, Wright-Patterson AFB OH 118
- 1355 INFLUENCE OF PLY WAVINESS ON STIFFNESS AND STRENGTH REDUCTION IN
COMPOSITE LAMINATES - Travis A. Bogetti, U. S. Army Research Laboratory,
Aberdeen Proving Ground MD; John W. Gillespie, Jr., University of Delaware, Center
for Composite Materials and Associate Professor, Department of Mechanical
Engineering, Newark DE 128
- 1420 THREE-DIMENSIONAL EFFECTIVE PROPERTIES OF COMPOSITE MATERIAL FOR
FINITE ELEMENT APPLICATIONS - Jerome T. Tzeng, U.S. Army Research
Laboratory, Aberdeen Proving Ground MD; Amos Alexander, Custom Analytical
Engineering System, Inc., Flintstone MD 138
- 1445 BREAK
- 1510 A {1,2}-ORDER THEORY FOR THE ANALYSIS OF THICK COMPOSITE SHELLS -
T. Tsui, and E. Saether, U.S. Army Materials Technology Laboratory,
Mechanics and Structures Branch, Watertown MA 148
- 1540 DYNAMIC TESTING OF COMPOSITE CYLINDERS - Bob Neugebauer and
Aileen M. Voltmer, AAI Corporation, Hunt Valley MD 158
- 1605 CLOSING REMARKS AND ADJOURN

APPENDIX A: PROGRAM LISTINGS

A

*NOT AVAILABLE AT PRINTING


FOREWORD

This report contains the abstracts and viewgraphs of the presentations at the Seventeenth Annual Mechanics of Composites Review sponsored by the Materials Laboratory. Each was prepared by its presenter and is published here unedited. In addition, a listing of both the in-house and contractual activities of each participating organization is included.

The Mechanics of Composites Review is designed to present programs covering activities throughout the United States Air Force, Navy, NASA, Army and Federal Aviation Administration. Programs not covered in the present review are candidates for presentation at future Mechanics of Composites Reviews. The presentations cover both in-house and contractual programs under the sponsorship of the participating organizations.

Since this is a review of on-going programs, much of the information in this report has not been published as yet and is subject to change; but timely dissemination of the rapidly expanding technology of advanced composites is deemed highly desirable. Works in the area of mechanics of composites have long been typified by disciplined approaches. It is hoped that such a high standard of rigor is reflected in the majority, if not all, of the presentations in this report.

Feedback and open critique of the presentations and the review itself are most welcome as suggestions and recommendations from all participants will be considered in the planning of future reviews.



CHARLEEN VAUGHAN, Meeting Manager
Mechanics & Surface Interactions Branch
Nonmetallic Materials Division
Materials Directorate

ACKNOWLEDGEMENT

We wish to express our appreciation to the authors for their contributions; to the focal points within the organizations for their efforts in supplying the program listings; and to Barbara Hager for managing registration.

OBSERVATIONS AND MODELLING OF DEFORMATION AND FRACTURE IN NANOSTRUCTURAL MATERIALS

W.W. Milligan, S.A. Hackney and E.C. Aifantis
Center for Mechanics, Materials and Instabilities
Michigan Technological University, Houghton MI 49931

Abstract

A new technique and associated experimental observations are reported pertaining to the deformation and fracture of nano-grain gold and nano-scale gold/silicon composites. Based on these and related experimental results and speculations already advanced in the literature, an attempt is made to formulate a set of constitutive equations describing the evolution of strain and porosity at the nanoscopic level.

1. Introduction

Nanocrystalline materials and composites appear to be quite promising for structural applications, since they possess properties not found in conventionally-scaled materials. It has been reported, for example [1], that the mass density and elastic constants of nano-scale materials may be reduced with respect to their bulk counterparts by 25% and 20% respectively, while the thermal expansion coefficient, the fracture stress, and the activation energy for diffusion may be increased by 80%, 1000%, and 400% respectively.

The concept of improving material properties by using ultrafine microstructure has brought forth several intriguing questions. When the grain size of a ductile metal approaches the 30 nm range, application of the Hall-Petch equation or classical dislocation theory in general to describe the deformation and fracture initiation processes may be no longer valid. There has been some discussion of this point in the literature [2-4], and the usual amount of raw speculation as to the possible mechanisms of plastic deformation in nanocrystalline materials.

In particular, Gleiter and co-workers [2] found that the hardness of nanocrystalline Cu and Pd *decreased* with decreasing grain size below a certain threshold. They speculated that the decrease in strength, and an assumed increase in ductility, were due to a grain boundary sliding mechanism. On the other hand, Weertman and co-workers [3] found that the same metals followed a traditional Hall-Petch relationship, even in the nanocrystalline regime; *i.e.* the strength continued to increase with decreasing grain size. In these studies, mechanisms of deformation were not reported.

Nevertheless, questions pertaining to the existence or stability of intragranular dislocation structures in polycrystalline aggregates with grain sizes below 10 nm have already been raised in the literature. Moreover, the relevance of traditional dislocation-based plasticity mechanisms, such as the operation of Frank-Read sources and the formation of pile-ups or sub-grains has also been questioned for grain sizes at that level. In fact, interest in the plastic deformation of nanocrystalline materials has been piqued by observation of the "softening" of some materials as the grain size approaches 10 nm, as discussed above. Most of the speculation has centered around the increase in interfacial area and triple junction density leading to enhanced room temperature boundary sliding (or creep), and triple junction migration leading to deformation.

In addition to nanograin metals, nanostructural materials such as nanolayered metals, nanolayered metal/ceramic composites, and general nanocomposites are also of interest. The relevant question here is whether current theories of composite material behavior may be extrapolated to systems where the reinforcement size and spacing approach the range of 10 nm or less. A similar question may be asked for ductile/brittle layered materials, where the laminate spacing and laminate thickness approach the nanometer scale. It is not at all clear that continuum theories of plasticity and fracture will hold where the length scale is such that a dislocation

contained within a grain cannot be described using linear elasticity anywhere within the grain. This is easy to visualize, since the space available for a lattice dislocation is on the same order of magnitude as the size of the dislocation core in this grain size regime. A different situation may exist for grain boundary dislocations, whose motion and interactions with vacancies may be responsible for the uncommonly large rates of grain boundary sliding at room temperature when the grain size is reduced to the nanometer level.

A simple calculation shows that for an average grain size of 10 nm, approximately 25-30% of the atoms are located at grain boundaries. In view of this and the complex structure of the grain boundaries, one may argue that the deformation of nanograin materials takes place as a result of the combined local rearrangement and motion of both the "bulk" and "grain boundary" space in response to the external stress. In fact, the matter comprising the "grain boundary" space is at a different energetic (excited) state in comparison to the matter making up the interior of the grains, or "bulk space." Local exchange of mass and momentum occurs between the two spaces via vacancy or grain boundary dislocation mechanisms. Moreover, the development of nanoporosity is possible, especially at grain boundary triple junctions. It follows that nanopore nucleation, growth, and migration, which are realized by local vacancy diffusion, can contribute to the overall plastic deformation.

Based on the physical picture outlined above, as well as the experimental observations reported below, the following continuum model for the description of deformation at the nanoscale is advanced. A material point or elementary volume containing a sufficiently large number of grains is viewed as a superposition of "normal" (grain interior) and "excited" (grain boundary) states, with each one supporting its own density, stress and strain fields. These fields obey separate balance equations of mass and momentum which include, however, extra source terms to account for the exchange of mass and momentum that occurs between the two energetically distinct states. In fact, this proposal is an application of an earlier theory for continuously-distributed microstructures and dislocated states [5] to nanograin materials. Alternatively, one may envision the interior of the grain contributing to the overall rate of deformation by an elastic component and possibly a creep-like component due to lattice vacancy diffusion, while the grain boundary space contributes a creep-like component due to both grain boundary vacancy diffusion and grain boundary dislocation motion. Finally, nanopores contribute to deformation via cavity nucleation, growth and migration. In Section 2 we discuss experimental results pertaining to a class of nanocrystalline materials, and in Section 3 we outline some preliminary ideas and model equations for the description of deformation in these materials.

2. Experiments and Observations

Deformation behavior of nanocrystalline materials can be studied *in situ*, using a straining stage in the transmission electron microscope (TEM). Since the grain sizes are smaller than the film thicknesses, the behavior observed *in situ* should be fairly representative of bulk behavior. In this research, gold was sputter-deposited on electron-transparent aluminum films. The resulting specimen consists of a very ductile aluminum substrate and a relatively brittle nanocrystalline coating. *In situ* straining results in plane stress conditions in the coating. Typically, the coating will deform and fracture before the aluminum substrate, as shown schematically in Fig. 1. Large cracks initiate in the "hole" of the TEM foils and propagate into the thicker regions; deformation and fracture of the nanocrystalline gold may be studied in the regions ahead of the crack tip. Using a high resolution TEM along with a straining stage, deformation mechanisms can be observed and dynamically recorded. In these preliminary experiments, the composite specimens were deformed in bending and examined *post-mortem*. A similar procedure was used previously to study the behavior of thin film ductile-brittle laminates [7].

The sputtered gold films bonded well to the aluminum substrates. A small amount of internal porosity was observed in the vicinity of the gold grain boundaries, possibly at the Au/Al interface. The grain size of the gold was uniform, averaging about 8 nm in diameter. Work is in progress to determine the grain aspect ratios, *i.e.* the degree of columnar growth. Figure 2(a) is a brightfield micrograph taken in the wake of the crack tip. Figure 2(b) illustrates the portion of the

specimen in which Fig. 2(a) was taken and serves to explain some of the contrast observed in Fig. 2(a). The light areas are void space between the Al crack faces; the gray areas consist of Al which has necked prior to fracture, but no gold (See Fig. 1); and the dark areas consist of the gold film on top of the aluminum. The gray areas fully contained within the dark areas are secondary cracks in the gold, with aluminum underneath.

Several important observations may be elucidated from Fig. 2(a). First, *the nanocrystalline gold deformed in a very ductile manner*. This is clearly observable by examining the mating gold crack faces in the secondary cracking region; the material adjacent to the crack faces has deformed extensively, and the crack faces do not 'mesh' as they would in the case of brittle fracture. Additionally, one may observe ductile ligaments which are bridging the secondary cracks (indicated by "L's" in Fig. 2(a)). These ligaments are necking and deforming permanently as the crack tip opening displacement increases.

Figure 2(a) also shows evidence of crack growth by microvoid coalescence and link-up. These "nanopores" are indicated by arrows in Fig. 2(a), and appear to be growing along the grain boundaries. This leads to a grain boundary "grooving" effect which can be clearly observed in the nanopores in Figure 2(a). (For example, the pore above the uppermost "L" is not symmetric; it is semicircular on top, but a grain boundary groove has formed on the bottom.) It is difficult to imagine this type of void growth and grain boundary grooving occurring without the aid of extensive diffusion, even though the homologous temperature is very low.

The cracks observed in Figure 2(a) grew along the grain boundaries, apparently due to the growth and link-up of grain boundary voids. Another type of grain boundary cracking has been observed which does not appear to be related to nanopore coalescence. Figure 3 is a high resolution lattice image of a crack propagating through the nanocrystalline gold. It is clear from the lattice fringes that the crack is propagating in the grain boundaries. Grain boundary grooving was also observed in the wake of this crack, but the extent of plastic deformation was not as significant as that associated with the cracks shown in Fig. 2(a). The difference may be a film thickness effect; this is being studied presently.

Lattice imaging and atomic resolution imaging with an image intensifier revealed that the deformed gold grains were virtually dislocation-free. This was true even in the ductile ligaments which were extensively deformed. This lack of dislocations, in conjunction with the observation of rapid pore growth, suggests that a diffusive mechanism such as grain boundary sliding was responsible for the observed plasticity in the nanocrystalline gold with the 8 nm grain size. The dynamic *in situ* experiments which are currently under way should help confirm the mechanism of deformation.

Similar observations have been made on thin films of nanocrystalline gold (25 nm grain diameter) sputter-deposited on brittle carbon substrates. Fracture of these films in the transmission electron microscope allowed observation of the deformation and cracking patterns. Figure 4 shows brightfield micrographs printed such that the transmitted beam intensity was not altered during printing. The micrographs reveals a decrease in anomalous absorption near the edge of the crack, clearly indicating that the material was plastically deformed and thinned prior to fracture. A second observation, also seen in Fig. 2, is that the fracture surfaces do not match everywhere along the crack; this is further evidence supporting the existence of plastic deformation before and during fracture. In contrast to the 8 nm grain diameter gold, these 25 nm diameter grains showed some evidence of "bulk" deformation, and contained linear defects after deformation which may be dislocations or twins; further work is in progress to identify these structures. A final effect worth noting in Fig. 4(a) is the observation of some periodicity along the crack faces just before crack bifurcation occurs.

The aforementioned method of sputtering and then straining the films *in situ* is not limited to metals; unique composite structures can be synthesized as well. For example, we have co-sputtered gold and silica, as well as gold and silicon on aluminum (ductile) or carbon (brittle) substrates and then characterized the microstructures and deformation processes observed.

Figure 5 shows the evolution of the structure of such a nanocomposite material produced by the concurrent sputtering of Au and amorphous Si onto a 5 nm thick carbon film. The dark phase is crystalline gold and the light phase is amorphous silicon. There is very little solubility in this system, and no intermediate phases are formed. The Au and Si undergo phase separation during deposition, finally producing a bi-phase structure which is intricately interwoven on a very fine scale (90 sec). This structure is highly resistant to coarsening at temperatures which lead to rapid coarsening in pure gold.

The mechanical behavior of this composite is of interest. When pure Si is strained *in situ*, catastrophic failure by unstable crack propagation readily occurs. However, when 10 nm islands of Au were introduced into the brittle matrix, significant gains in toughness were obtained. This is observed during *in situ* straining experiments, in which stable crack growth and crack arrest are observed in the Au/Si composite laminates. Figure 6 shows, for the first time, a TEM image of a stable crack tip in a nanocomposite material. Figure 6 reveals the presence of microcracks ahead of the main crack in the brittle phase, and shows crack bridging and ligament formation in the wake of the crack tips (marked by "B" on the micrograph). This type of structure, which appears to be both tough and resistant to thermal coarsening, can be viewed as a possible foundation for a tough, high temperature composite material.

3. Modelling

To gain insight into the concept of superimposed bulk and grain boundary states, we assume an extreme case where both "phases" deform in a linear elastic fashion according to the one-dimensional rule

$$\sigma_i = E_i \epsilon_i \quad (\text{EQ 1})$$

where (σ_i, ϵ_i) denotes the local stress and strain carried by each of the two phases ($i = 1, 2$) and E_i corresponds to the Young's moduli. Each phase obeys a momentum balance equation which in one dimension takes the form

$$\frac{\partial \sigma_i}{\partial x} = f_i \quad (\text{EQ 2})$$

where f_i is an internal body force due to the mutual interaction of the two phases. In view of the assumption of small strains ϵ_i and small displacements u_i ($\epsilon_i = \partial u_i / \partial x_i$), the following constitutive assumption is adopted for f_i

$$f_1 = -f_2 = \alpha (u_1 - u_2) \quad (\text{EQ 3})$$

where α is an interaction "phenomenological" coefficient. Among other things, Eq. 3 implies that a total stress defined by $\sigma = \sigma_1 + \sigma_2$ will satisfy the usual equilibrium equation $\partial \sigma / \partial x = 0$ for the material considered as a whole. Upon combination of Eq. 1 - Eq. 3, the following uncoupled equation is obtained

$$E \frac{\partial^2 u}{\partial x^2} - c E \frac{\partial^4 u}{\partial x^4} = 0 \quad (\text{EQ 4})$$

where $u = u_1$ or u_2 and the new constants are given by the relations $E = E_1 + E_2$ and

$$c = \frac{E_1 E_2}{\alpha (E_1 + E_2)} \quad (\text{EQ 5})$$

If the surface tension-like coefficient $c \rightarrow 0$, then Eq. 4 becomes the usual equation of elasticity for the displacement in one dimension. The higher-order gradient equilibrium equation (Eq. 4)

could be arrived at by a different, perhaps less motivating but more direct argument. This is accomplished by considering the total stress σ , which is assumed to satisfy the usual local equilibrium equation

$$\frac{\partial \sigma}{\partial x} = 0 \quad (\text{EQ 6})$$

but a gradient-dependent constitutive equation of the form

$$\sigma = E \left(\epsilon - c \frac{\partial^2 \epsilon}{\partial x^2} \right) \quad (\text{EQ 7})$$

with the first term in the parenthesis designating homogeneous elastic response and the second term accounting for local heterogeneity. The three-dimensional counterparts of Eq. 6 and Eq. 7 have been utilized recently [8] to eliminate the strain singularity and obtain a "smooth-closure condition" for the crack opening displacement. It is argued that if elasticity can be useful at all in describing the deformation of nanoscale materials, in the small strain regime, then it should only be used in conjunction with the gradient term $c \partial^2 \epsilon / \partial x^2$, which accounts for the heterogeneous grain size distribution effects that become important at the nanoscale.

The situation becomes rather complex when one wishes to model plasticity effects at the nanoscale. Not only is the heterogeneity of plastic flow more difficult to treat, but also it is apparent from the discussion of the experimental observations that the homogeneous situation is not well understood. Nevertheless, a first modelling attempt is outlined below in analogy to various mechanisms of deformation assumed for superplastic deformation. Such an analogy with superplasticity may be argued on the basis of the very small grain sizes involved and the associated large volume fraction of grain boundary space. This large grain boundary space, along with the high observed grain boundary diffusivities, produce a situation resembling superplastic flow of traditional materials at high temperatures.

First, it is assumed that the contribution to the overall strain rate $\dot{\epsilon}$ is of the form

$$\dot{\epsilon} = \dot{\epsilon}_1 + \dot{\epsilon}_2 + \dot{\epsilon}_{12} \quad (\text{EQ 8})$$

where $\dot{\epsilon}_1$ is associated with diffusion, $\dot{\epsilon}_2$ is associated with dislocation climb and possibly glide in the grain boundaries, and $\dot{\epsilon}_{12}$ is associated with cavity nucleation, growth and migration. [It is evident from Fig. 2(a) that nanopores nucleate and grow during deformation, thus contributing to the overall strain rate.] Next, physically-based constitutive equations for the various strain rate components are adopted by involving arguments previously developed for related deformation mechanisms in superplasticity.

We confine attention to cases where elastic deformation is negligible, the local stress is adequately represented by the applied stress, and grain boundary sliding and rotation are accommodated by vacancy diffusion in both the bulk and grain boundary space, as well as by climb of grain boundary dislocations. Then, the following expressions can be written for $\dot{\epsilon}_1$ and $\dot{\epsilon}_2$ (see for example, reference [9] for a review)

$$\dot{\epsilon}_1 = K_1 \left(\frac{b}{d} \right)^2 D_{\text{eff}} \left(\frac{\sigma}{E} \right) \quad (\text{EQ 9})$$

$$\dot{\epsilon}_2 = K_2 \left(\frac{b}{d} \right)^2 D_B \left(\frac{\sigma}{E} \right)^2 \quad (\text{EQ 10})$$

where K_i are constants, b is the Burgers vector, d is the grain size, σ and E are the applied stress and Young's modulus, D_B is the grain boundary diffusivity, and the effective diffusivity, D_{eff} , is given by

$$D_{eff} = D_L \left(1 + \frac{3.3\delta}{d} \frac{D_B}{D_L} \right) \quad (\text{EQ 11})$$

where D_L denotes the lattice diffusivity, and δ is the grain boundary thickness.

Before we proceed with a corresponding expression for $\dot{\epsilon}_{12}$, it is noted that for constant strain rates, Eq. 10 and Eq. 11 predict a linear and quadratic flow stress vs. grain size dependence, respectively. This may serve as a basis for explaining the "softening" effect reported in [2], which is in contrast to the usual "strengthening" effect predicted by the Hall-Petch equation for traditional grain size metals.

It is not straightforward to write down an evolution equation for $\dot{\epsilon}_{12}$ by resorting to superplasticity arguments. One may do so, however, for the nanoporosity

$$\phi = \lambda n r^3 \quad (\text{EQ 12})$$

where λ is a numerical factor ($\lambda = 4\pi/3$ for spherical voids), n is the number of voids per unit volume, and r is the average pore radius. In cavitation damage theories, evolution equations for the nucleation rate \dot{n} and \dot{r} are provided. Then, the evolution of ϕ can be computed from the kinematic relation

$$\dot{\phi} = \phi \left(\frac{\dot{n}}{n} + 3 \frac{\dot{r}}{r} \right) \quad (\text{EQ 13})$$

along with appropriate equations for \dot{n} and \dot{r} . An equation for \dot{n} is given in [9] as follows

$$\dot{n} = \dot{n}_0 \exp \left(\frac{(\sigma - \sigma_a)}{\sigma_b} \right) \quad (\text{EQ 14})$$

where \dot{n}_0 , σ_a and σ_b are material constants. A relation for \dot{r} , for voids growing by diffusion processes and of a size comparable to the grain size, is given in [10]. It reads

$$\dot{r} = \frac{45\Omega\delta D_B}{kT} \left(\frac{\sigma}{d^2} \right) \quad (\text{EQ 15})$$

where Ω is the atomic volume, k is Boltzmann's constant, and T is the absolute temperature. Equations 13-15 can provide the desired equation for $\dot{\epsilon}_{12}$ by assuming that this is proportional to the nanoporosity, *i.e.*

$$\dot{\epsilon}_{12} = \Lambda \dot{\phi} \quad (\text{EQ 16})$$

This completes the set of equations which could be viewed as a basis for developing a three-dimensional flow theory for nanograin materials.

Acknowledgements

The support of the AFOSR, under grant number 91-0421, is gratefully acknowledged.

References

1. Report NMAB-454 of the National Materials Advisory Board, "Research Opportunities for Materials with Ultrafine Microstructures", National Academy Press, 1989.
2. A.H. Chokshi, A. Rosen, J. Karch and H. Gleiter: Scripta Met, **23**, 1989, p. 1679.
3. G.W. Nieman, J.R. Weertman and R.W. Siegel: J. Mater. Res., **6**, 1991, p. 1012.
4. T.G. Nieh and J. Wadsworth: Scripta Met, **25**, 1991, p. 955.
5. E.C. Aifantis: J. Eng. Mat. Tech., **106**, 1984, p. 326.
6. E.C. Aifantis: Int. J. Plast., **3**, 1987, p. 211.
7. S.A. Hackney and W.W. Milligan: Ultramicroscopy, **37**, 1991, p. 79.
8. B.S. Altan and E.C. Aifantis: Scripta Met., **26**, 1992, p. 319.
9. J.A. Colios and E.C. Aifantis: Res Mechanica, **5**, 1982, p. 67.
10. A.H. Chokshi and A.K. Mukherjee: in "Superplasticity in Aerospace", H.C. Heikkenen and T.R. McNelley, eds., 1988, p. 167.

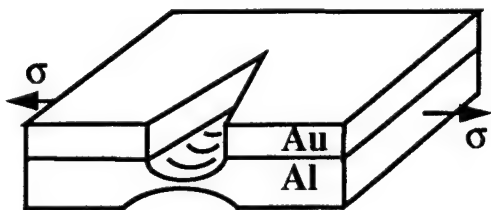
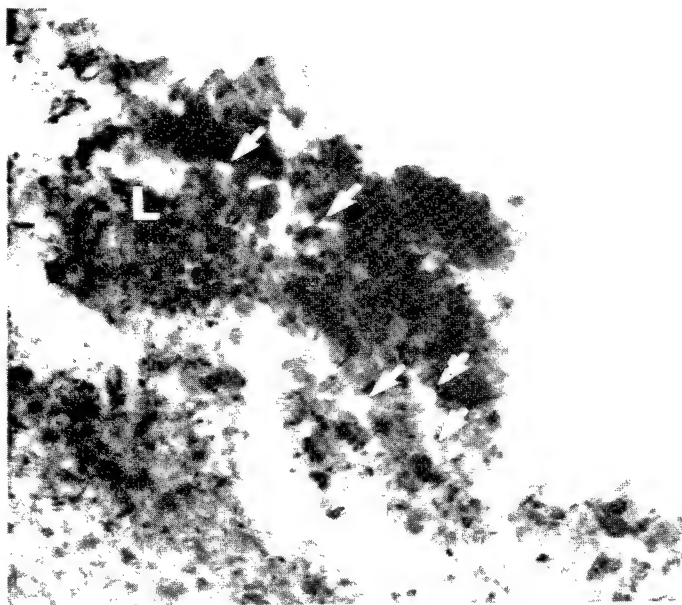
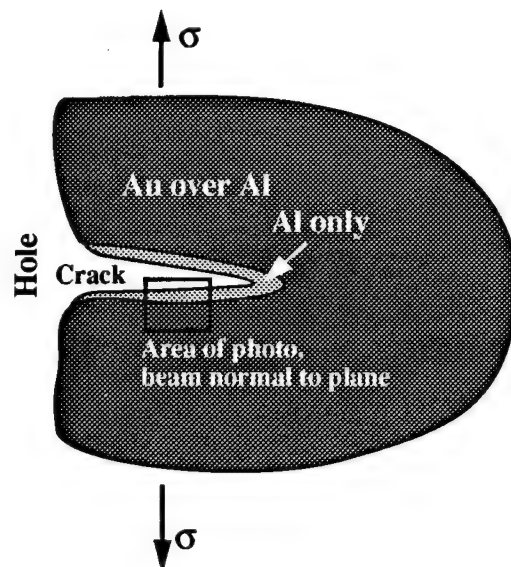


Fig. 1. Schematic diagram illustrating the geometry of the *in situ* deformation and fracture experiment.



(a) 100 nm



(b)

Fig. 2. (a) Brightfield TEM micrograph showing extensive plasticity, ligament formation, and crack growth by void coalescence and link-up in nanocrystalline gold. (b) Schematic diagram illustrating the area in which the photo was taken.



Fig. 3. High resolution TEM lattice image showing a crack propagating through a grain boundary in nanocrystalline gold, $d = 8$ nm.

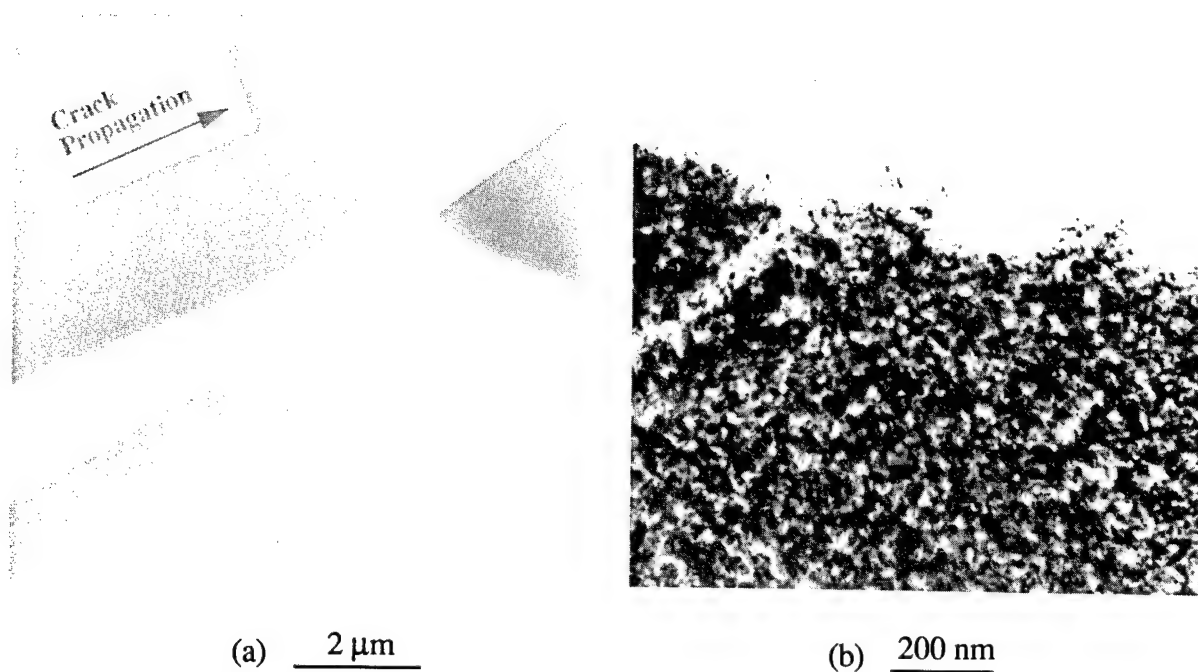
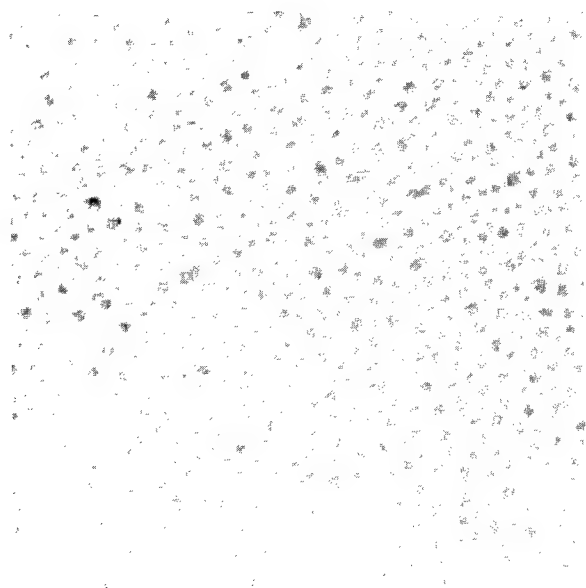
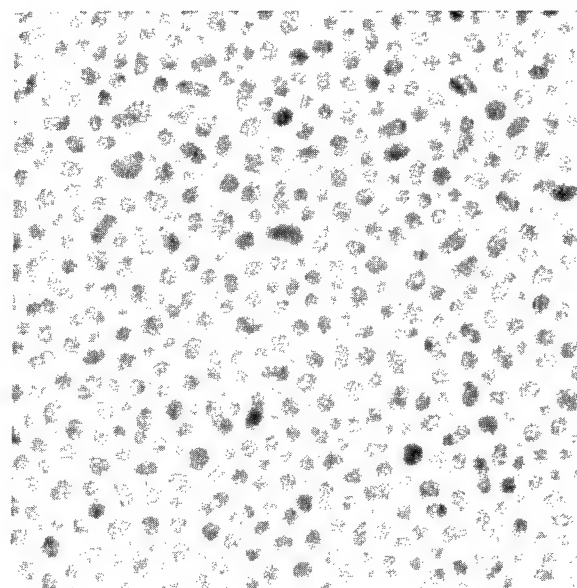


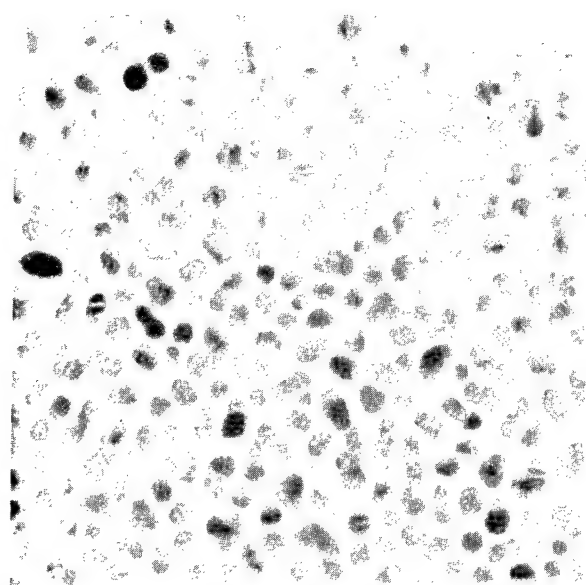
Fig. 4. Plastic deformation and fracture of 25 nm grain diameter gold on carbon. (a) Low magnification TEM micrograph showing periodicity before crack bifurcation. (b) High magnification TEM micrograph showing plastic thinning along crack face.



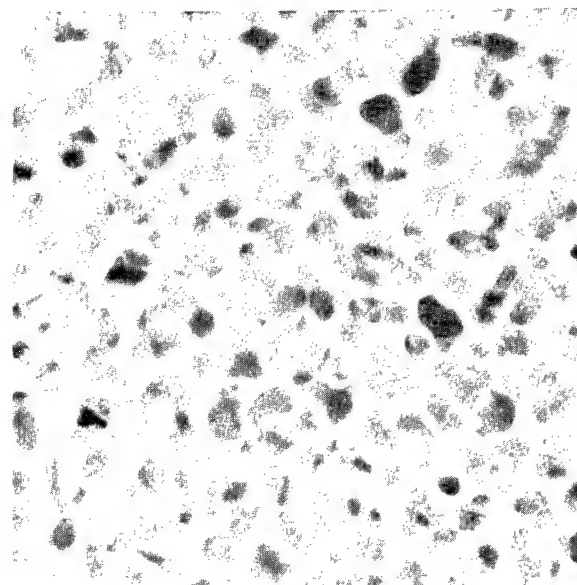
15 sec



30 sec



45 sec



90 sec

25 nm

Fig. 5. Evolution of structure in an Au/Si nanocomposite as a function of sputtering time, showing formation of interwoven bi-phase pattern.



50 nm

Fig. 6. Stable crack observed in bi-phase composite during *in situ* straining, showing microcracking ahead of major crack, ductile crack bridging (B's), formation of nanopores (arrows), and significant plasticity.

FAILURE MECHANISMS IN UNIDIRECTIONAL AND CROSSPLY CERAMIC-MATRIX COMPOSITES

I. M. Daniel
Northwestern University
Evanston, IL 60208

ABSTRACT

Failure mechanisms were studied by reflection light microscopy in unidirectional and crossply silicon carbide/glass-ceramic composite laminates under uniaxial tensile loading. A combined analytical/experimental investigation was conducted. A modified shear lag analysis was used to determine stress distributions, matrix cracking, fiber-matrix debonding and to correlate in-situ matrix tensile strength, residual stress and interface shear strength with measured experimental data.

The unidirectional material displays several characteristic features in the stress-strain behavior. Initially it behaves linearly elastically with no discernible damage. This is followed by a nonlinear region with decreasing stiffness, corresponding to transverse cracking in the matrix. Then, follows a region of stabilized stiffness reduction rate with matrix crack multiplication and fiber debonding. Then, there is a strain hardening region corresponding to more debonding and fiber failures ending with a quasi-linear region corresponding to nearly fully debonded and partially fractured fibers. Transverse matrix cracking starting at an applied stress of approximately 100 MPa (14.5 ksi) increased in density up to a saturation density of 8 cracks/mm or a minimum crack spacing of 120 μm (4.7×10^{-3} in.) at an applied stress of 269 MPa (39 ksi). There is evidence that some debonding starts before matrix crack saturation, but most of it occurs at crack saturation. Fiber breaks seem to follow debonding and always occur between matrix cracks. The macroscopic and microscopic information obtained from the tests was used to determine the interfacial shear strength. A value of 251 MPa (36.4 ksi) was obtained which is in good agreement with a published result for the same material based on a microindentation test.

In the crossply laminate failure initiation takes place in the 90° layer. It takes the form of radial cracks, followed by interfacial cracks, which in turn coalesce into transverse macrocracks. These transverse macrocracks in the 90° layer reach a characteristic saturation crack density with a minimum crack spacing of the order of the layer thickness. Subsequently, transverse matrix cracks are generated in the 0° layer increasing in density up to a minimum crack spacing of the order of five to eight fiber diameters. This stage of failure is accompanied by fiber-matrix debonding and some fiber-failures in the 0° layer. In the third stage of damage development, the macrocracks of the 90° layer branch off and connect with the 0° layer cracks in a characteristic "delta" pattern. This is finally followed by delamination and additional cracking in the 90° layer prior to ultimate failure. The various failure mechanisms and their interactions were discussed and compared with predictions of prior experimental and analytical studies of unidirectional composites.

OBJECTIVE

Conduct combined analytical/experimental study of failure mechanisms in unidirectional and crossply ceramic-matrix composite under uniaxial tension.

SCOPE

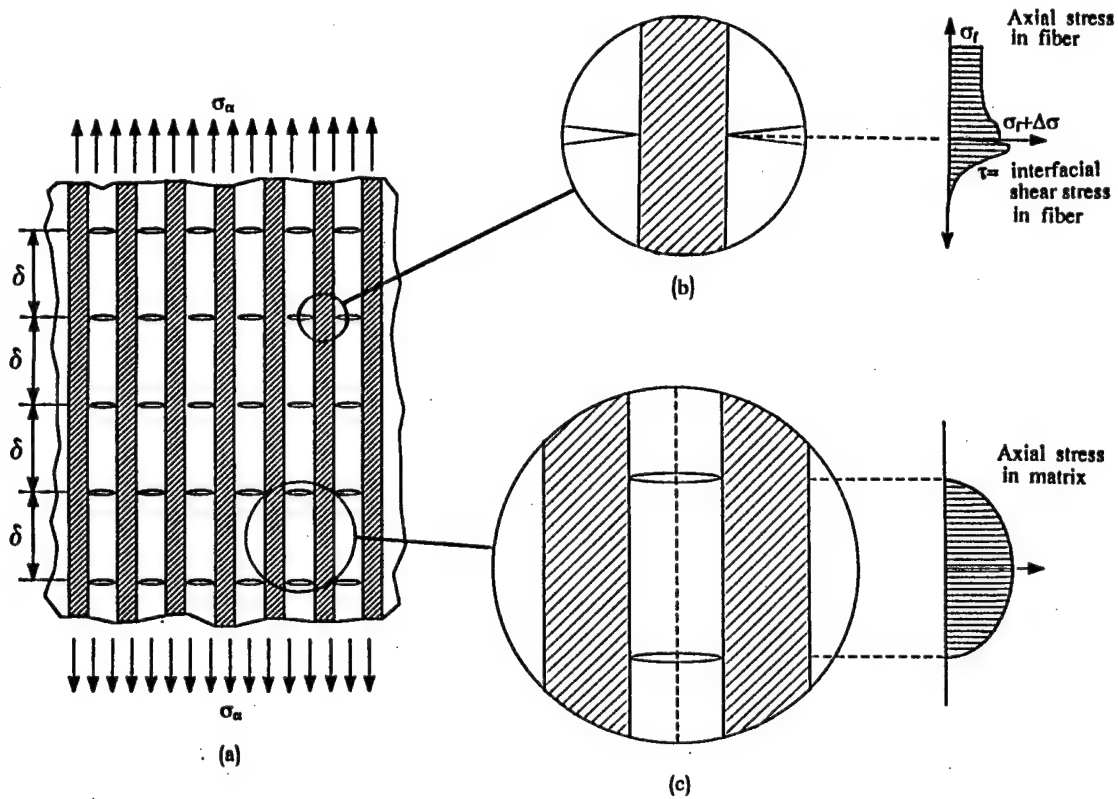
Material: Silicon Carbide Fiber in Calcium Aluminosilicate Matrix (SiC/CAS)
Layups: $0^\circ, 90^\circ, [0/90_2]_s$
Loading: Axial Tension

Table 1. Constituent Material properties

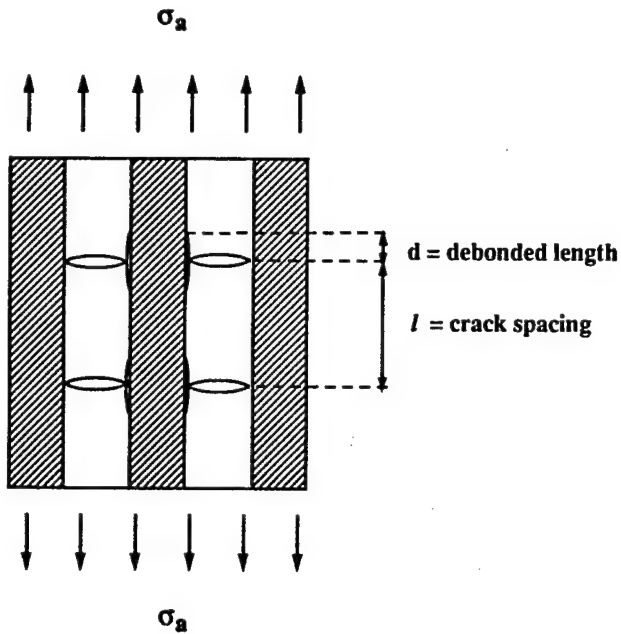
Property	CAS Matrix [19]	SiC Fiber [1,2]
Maximum Use Temperature, $^\circ\text{C}$ ($^\circ\text{F}$)	1350 (2460)	1300 (2370)
Fiber Diameter (μm)	-	15
Density (g/cm^3)	2.8	2.6
Coefficient of Thermal Expansion, $10^{-6}/^\circ\text{C}$ ($10^{-6}/^\circ\text{F}$)	5.0 (2.8)	3.2 (1.8)
Elastic Modulus, GPa (10^6 psi)	98 (14.2)	170 (25)
Tensile Strength, MPa (ksi)	124 (18) (flexural)	1930 (280)

Table 2. Measured Properties of SiC/CAS Unidirectional Composite

Property	Value
Fiber Volume Ratio, V_f	0.39
Ply Thickness, t , mm (in.)	0.38 (0.015)
Longitudinal Modulus, E_1 , GPa (Msi)	125 (18.1)
Transverse Modulus, E_2 , GPa (Msi)	112 (16.2)
In-plane Shear Modulus, G_{12} , GPa (Msi)	52 (7.5)
Major Poisson's Ratio, ν_{12}	0.18
Longitudinal Tensile Strength, F_{1t} , MPa (ksi)	393 (57)
Transverse Tensile Strength, F_{2t} , MPa (ksi)	55 (8)
Longitudinal Ultimate Tensile Strain, ϵ_{u1t}	0.0084
Transverse Ultimate Tensile Strain, ϵ_{u2t}	0.0005



Matrix Cracking and Local Stress Distributions in Longitudinally Loaded Specimen



CRACK INITIATION

$$\sigma_a = \frac{E_l}{E_m} (F_{mT} - \sigma_{rm})$$

where

σ_a = applied stress in composite

σ_{rm} = residual stress in matrix

F_{mT} = matrix tensile strength

E_m = matrix modulus

E_l = longitudinal modulus of composite

Composite Element with Matrix Cracking and Partial Debonding

STRESS DISTRIBUTIONS IN CRACKED SPECIMEN BEFORE DEBONDING

$$\sigma_m = \left(\frac{E_m \sigma_a + \sigma_{rm}}{E_1} \right) \left(1 - \frac{\cosh\left(\frac{\alpha l}{2} - \alpha x\right)}{\cosh\left(\frac{\alpha l}{2}\right)} \right)$$

$$\sigma_f = \frac{E_f}{E_1} \left(1 + \frac{E_m V_m}{E_f V_f} \frac{\cosh\left(\frac{\alpha l}{2} - \alpha x\right)}{\cosh\left(\frac{\alpha l}{2}\right)} \right) \sigma_a + \left(1 - \frac{\cosh\left(\frac{\alpha l}{2} - \alpha x\right)}{\cosh\left(\frac{\alpha l}{2}\right)} \right) \sigma_{rf}$$

$$\tau_i(x) = \frac{\alpha r_f V_m}{2 V_f} \left(\frac{E_m \sigma_a + \sigma_{rm}}{E_1} \right) \frac{\sinh\left(\frac{\alpha l}{2} - \alpha x\right)}{\cosh\left(\frac{\alpha l}{2}\right)}$$

where

σ_m = average axial stress in matrix

σ_f = average axial stress in fiber

τ_i = interfacial shear stress

σ_{rm} = axial residual stress in matrix

σ_{rf} = axial residual stress in fiber

E_f, E_m = fiber and matrix moduli, respectively

V_f, V_m = fiber and matrix volume ratios, respectively

x = axial coordinate measured from crack face

l = crack spacing

$$\alpha^2 = \frac{2}{A r_f} \cdot \frac{E_1}{E_f E_m V_m}$$

$$A = \frac{r_f}{4 G_f} + \frac{1}{G_m} \left[\frac{2}{3} \cdot \frac{V_f (r_f - r_m)}{(1 - V_f)^2} \left(4 + \frac{r_f}{r_m} + V_f \right) + \frac{r_f (1 + V_f)}{1 - V_f} \right]$$

G_f, G_m = fiber and matrix shear moduli, respectively

r_f, r_m = fiber and matrix radii in model, respectively

DEBONDING INITIATION

$$\tau_i(0) = \frac{\alpha r_f}{2} \frac{V_m}{V_f} \left(\frac{E_m \sigma_a + \sigma_{rm}}{E_1} \right) \tanh \frac{\alpha l}{2} = F_{is}$$

where

$\tau_i(0)$ = maximum interfacial shear stress (at $x = 0$)

F_{is} = interfacial shear strength

CRACK SPACING

(Prior to debonding)

$$l = \frac{2}{\alpha} \cosh^{-1} \frac{E_m \sigma_a + E_1 \sigma_{rm}}{E_m \sigma_a + E_1 (\sigma_{rm} - F_{mT})}$$

DEBONDED LENGTH

$$\tau_i(d) = F_{is} \quad (\text{at } x = d)$$

Neglecting friction

$$d = \frac{1}{2} \left[1 - \frac{1}{\alpha} \log \frac{1 + \xi}{1 - \xi} \right]$$

where

$$\xi = \frac{2 F_{is}}{\alpha r_f} \frac{V_f}{V_m} \frac{E_1}{E_m \sigma_a + E_1 \sigma_{rm}}$$

STRESS DISTRIBUTIONS IN CRACKED SPECIMEN AFTER DEBONDING

In debonded area ($0 \leq x < d$ and $l - d \leq x \leq l$)

$$\sigma_m = \frac{2V_f \tau_f x}{V_m r_f}$$

$$\sigma_f = \frac{\sigma_a}{V_f} - \frac{2\tau_f x}{r_f}$$

$$\tau_i = \tau_f$$

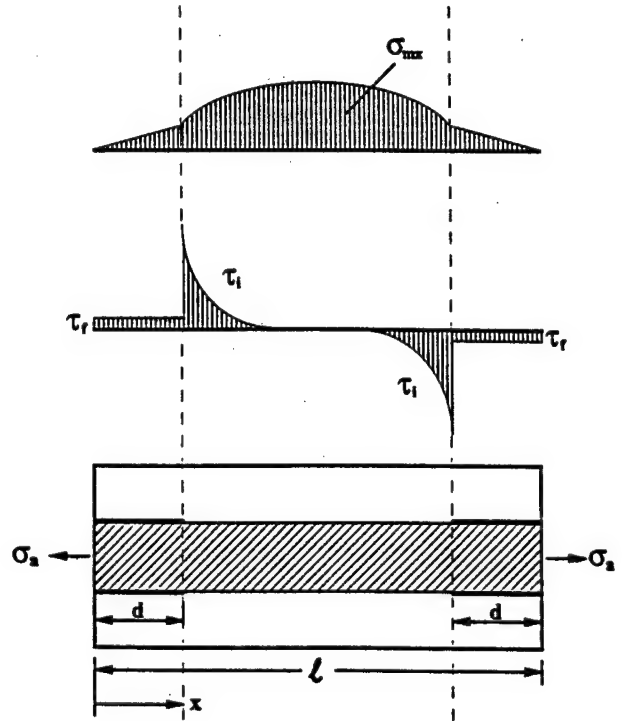
where τ_f = interfacial frictional stress

In the bonded area ($d \leq x \leq l - d$)

$$\sigma_m = \left(\frac{E_m}{E_1} \sigma_a + \sigma_{rm} \right) + \left(\frac{2V_f \tau_f d}{V_m r_f} - \frac{E_m}{E_1} \sigma_a - \sigma_{rm} \right) \frac{\cosh \alpha(l/2 - x)}{\cosh \alpha(l/2 - d)}$$

$$\sigma_f = \left(\frac{E_f}{E_1} \sigma_a + \sigma_{rf} \right) + \left(\frac{E_m V_m}{E_1 V_f} \sigma_a - \sigma_{rf} - \frac{2\tau_f d}{r_f} \right) \frac{\cosh \alpha(l/2 - x)}{\cosh \alpha(l/2 - d)}$$

$$\tau_i = \frac{\alpha r_f V_m}{2V_f} \left[\frac{E_m}{E_1} \sigma_a + \sigma_{rm} - \frac{2V_f \tau_f d}{V_m r_f} \right] \frac{\sinh \alpha(l/2 - x)}{\cosh \alpha(l/2 - d)}$$



Axial Matrix Stress and Interfacial Shear Stress Distributions in Cracked and Partially Debonded Composite Element

ESTIMATION OF INTERFACIAL SHEAR STRENGTH

$$\frac{F_{is}}{F_{mT}} = \frac{V_m}{V_f} \frac{\alpha r_f}{2} \coth \frac{\alpha l_{min}}{4}$$

where,

F_{is} = interfacial shear strength

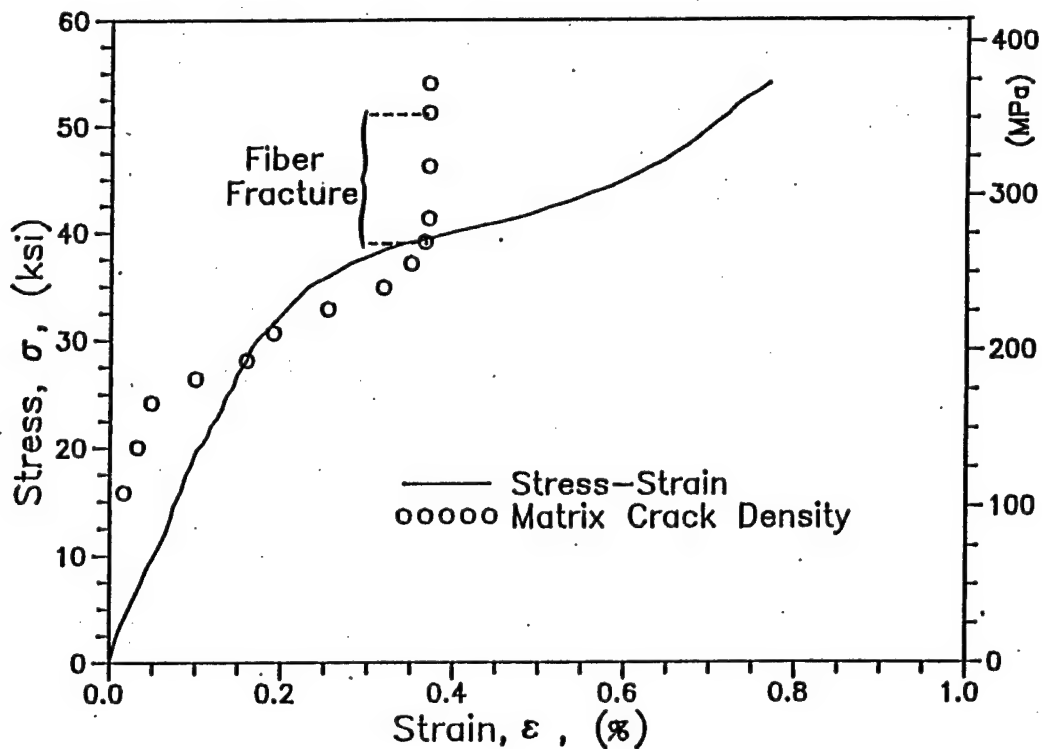
F_{mT} = matrix tensile strength

r_f = fiber diameter

l_{min} = minimum crack spacing

(prior to debond initiation)

α = function of geometric and constituent
material parameters

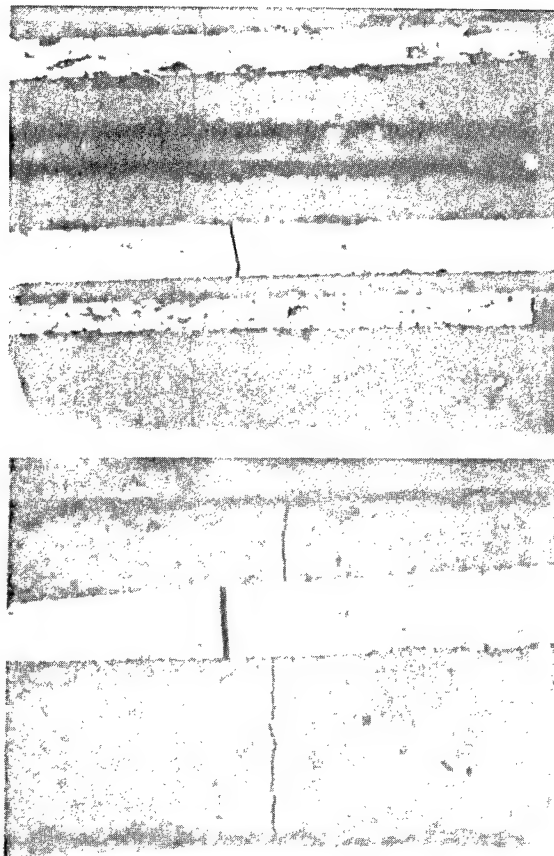


Normalized Crack Density, $6\lambda r_f$

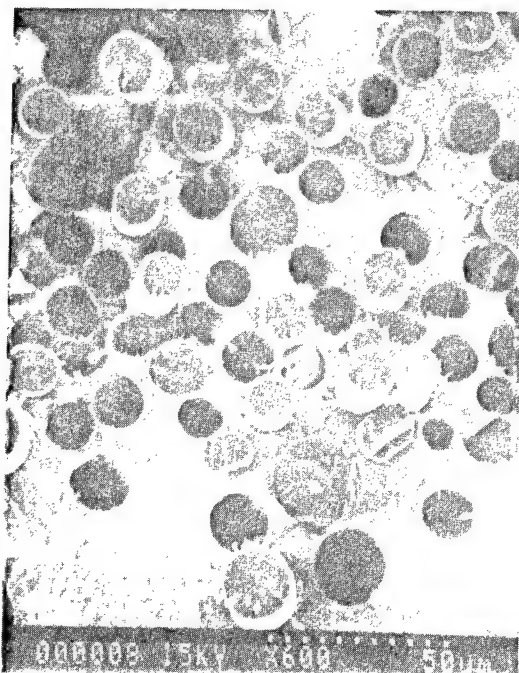
Stress-Strain and Stress Versus Matrix Crack Density for $[0_8]$ SiC/CAS Specimen Under Uniaxial Tensile Loading



Typical Photomicrographs Showing Initiation and Multiplication of Transverse Matrix Cracks under Longitudinal Tensile Loading

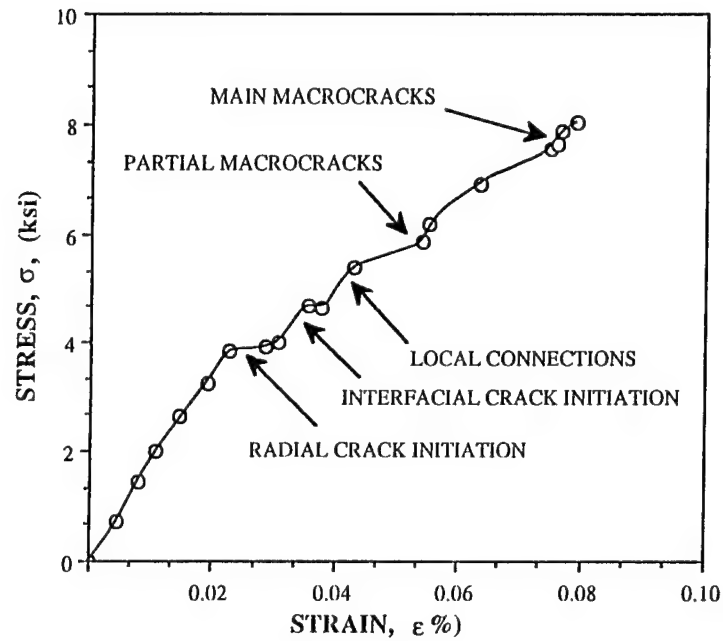


Typical Fiber Fractures Near Matrix Cracks with Fiber-Matrix Debonding

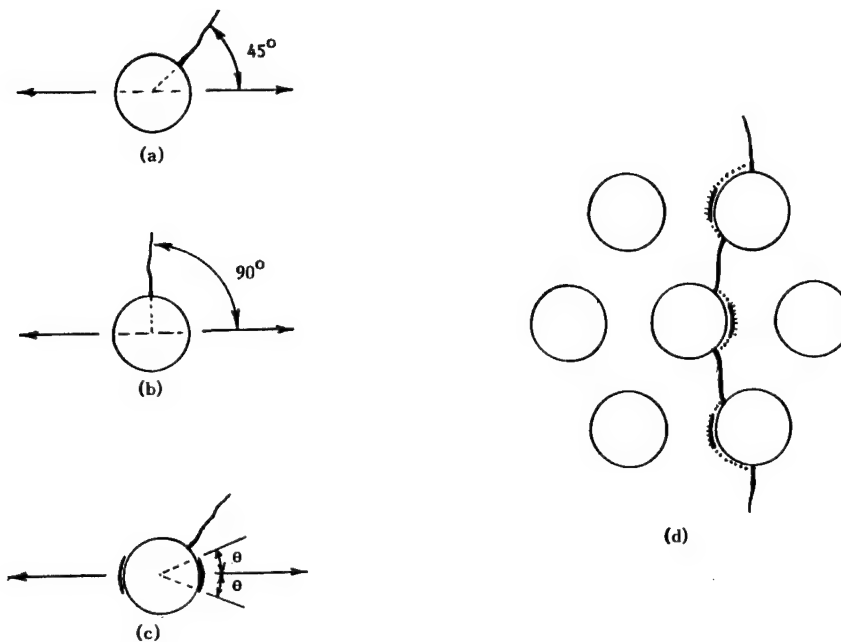


SEM Fractograph of Failure Surface under Longitudinal Tension
Illustrating Fiber Breaks and Pullout

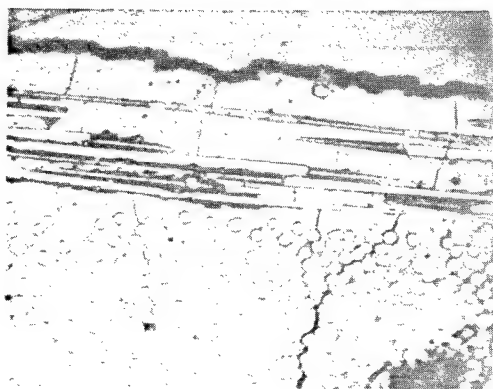
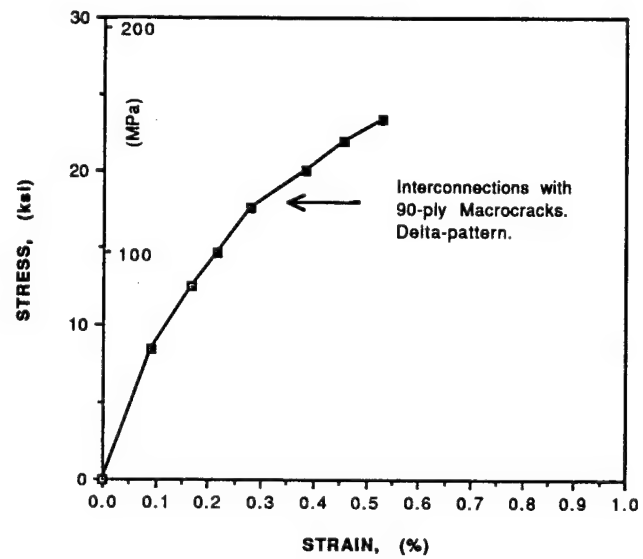
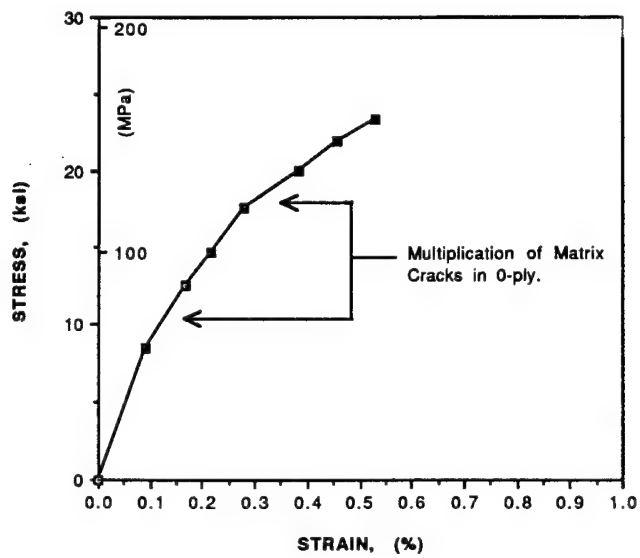
**Stress-Strain Curve for SiC/Cas
Cross-Ply Specimen**



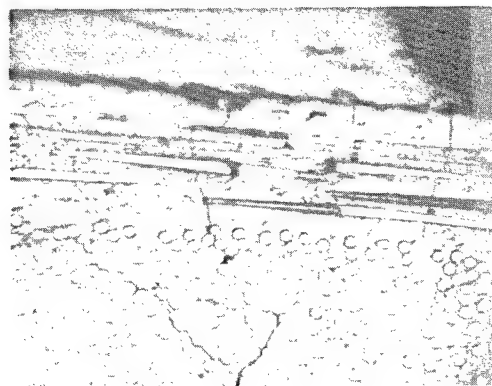
**Stress-Strain Behavior of Crossply Laminate with Corresponding Stages of
Damage Development in Transverse Layer**



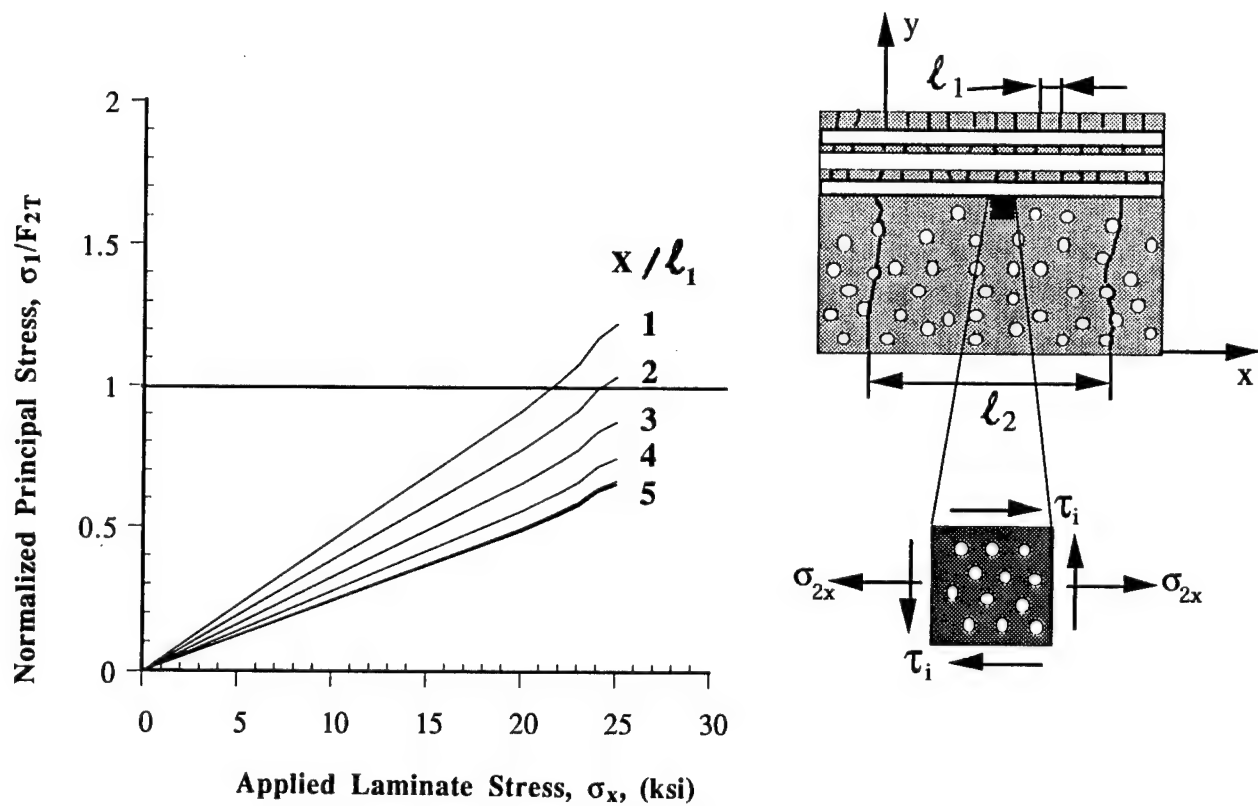
Development of Failure Mechanisms in Transversely Loaded Ceramic Matrix Composite (a) Initial Radial Cracks Around Closely Packed Fibers, (b) Initial Radial Cracks Around Isolated Fibers, (c) Interfacial Cracks, and (d) Interconnection of Radial and Interfacial Cracks



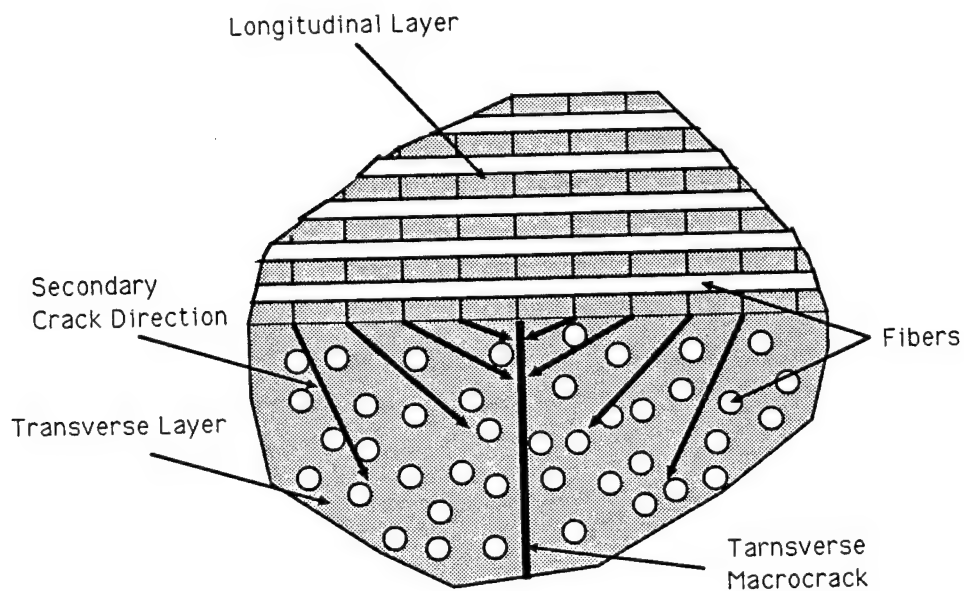
Matrix Cracking in 0° -Ply Following Saturation of Cracking in 90° -Ply



Interconnection of 0° -Ply and 90° -Ply Macrocracks (Formation of "Delta" Pattern)



Normalized Principal Tensile Stress in 90° Layer at Interface with 0° Layer After Crack Saturation in Both Layers as a Function of Applied Stress



Predicted Formation of "Delta" Pattern of Microcracks.

Mechanisms for Thermal Cycling Damage in Metal Matrix Composites

Minoru Taya, William D. Armstrong and Martin L. Dunn
Department of Mechanical Engineering
University of Washington
Seattle, WA 98195

Abstract

The major achievements of the AFOSR project (91-0234) during the past year can be categorized into analytical and experimental studies. The former includes construction of two models: one for dimensional change in a metal matrix composite (MMC) subjected to combined thermal cycling and creep loading [1] and the other for dislocation punching from a long fiber to relax the coefficient of thermal expansion (CTE) mismatch strain that would otherwise exist at the matrix metal-fiber interface [2]. The analytical model for the dimensional change of a MMC subjected to combined thermal cycling and creep loadings is an extension of our previous model for the dimensional change of a MMC subjected to thermal cycling only [3,4] and it can account for elastic-plastic-creep deformation of the matrix metal and temperature dependency of matrix yield stress. The temperature-time relation of thermal cycling used in the model is shown in Fig. 1 where the solid and dashed lines are the assumed and actual shapes, respectively. Figure 2 shows the analytical results of the axial strain (dimensional change) of a MMC subjected to thermal cycling and constant stress σ_0 where A_i , B_i , C_i and D_i (i is the number of thermal cycle) are defined in Fig. 1. Figure 2 clearly illustrates the strong applied stress (σ_0) dependency of the strain accumulation during thermal cycling. The present model (dashed line) is then compared with the experiment (open circles) [5], Fig. 3 where the analytical results based on elastic-plastic deformation of the matrix metal (solid line) are also shown. The present model appears to be able to predict the slope of the experimental data, i.e. the strain per cycle is linear with applied stress σ_0 .

Another analytical study is to construct a model for dislocation punching from a long fiber in a long fiber MMC as a result of relaxation of CTE mismatch strain at the matrix-fiber interface [2]. The analytical model for dislocation punching in a long fiber MMC is an extension of our previous models for a short fiber MMC [6] and a particle MMC [7], and it is shown in Fig. 4 where (a), (b) and (c) show the cross section view of a long fiber with unrelaxed CTE mismatch strain in terms of surface dislocations at the interface (before punching), the fiber with punched-out dislocations, and the glide mode of edge dislocations, respectively. The punching distance R (see Fig. 4) is obtained in a closed form [2]:

$$R = a \left\{ \frac{(1+2\nu)\mu}{2(1-\nu)k} \right\}^{1/2} \quad (1)$$

where a is the radius of the fiber, ν , μ and k are Poisson's ratio, shear modulus and friction (yield) stress of the matrix respectively.

The average dislocation density in the matrix, $\bar{\rho}$ is increased due to the dislocations so punched, resulting in the increase in the in-situ yield stress ($\Delta\sigma_{ym}$) of the matrix metal in a MMC over that of the unreinforced metal, and $\Delta\sigma_{ym}$ is estimated as

$$\Delta\sigma_{ym} = \gamma\mu b \sqrt{\rho} \quad (2)$$

where γ is a material constant of order 1, b is the Burgers vector, and μ is the shear modulus. The increase in the matrix in-situ yield stress is known to enhance thermal cycling resistance [3]. Motivated by the above, we have designed a hybrid MMC, Fig. 5 where chopped fibers embedded in the matrix are the sources of dislocation punching by the above mechanism, thus enhancing the matrix in-situ yield stress [8]. We will design another microstructure similar to the hybrid MMC, hybrid-gradient MMC, Fig. 6, whose mechanical properties are expected to be further enhanced, since the CTE mismatch at the matrix - fiber interface can be diffused into multiple interfaces, resulting in reduction in the stress concentration at the interface.

The progress in the experimental study is mainly in two areas: processing of W-ThO₂ fiber / FeCrAlY matrix composite and modification of creep thermal cyclers. The residue of binder in the as-processed MMC has been an inevitable problem, for it would degrade the mechanical properties. To minimize the residue, an attempt has been made to include the sintering process, Fig. 7 which provides less porous preform and ensures more complete degassing.

When a MMC is subjected to combined thermal cycling and creep loadings, its dimensional change is expected to be larger than that of thermal cycled MMC, see Fig. 2. The data of such a large strain should be evaluated under a constant stress rather than constant load. The current thermal cycler [9] was designed for a constant load. Thus, the modification of the present creep thermal cycler was made such that a constant stress be realized during combined thermal cycling and creep loadings, Fig. 8.

References:

1. M.L. Dunn and M. Taya, submitted to *Scripta Metall. Mater.*
2. S. Shibata, T. Mori and M. Taya, (1992) *Scripta Metall. Mater.*, **26**, 363.
3. M. Taya, W.D. Armstrong and M.L. Dunn, (1991) *Mater. Sci. Eng.* **A143**, 143.
4. W.D. Armstrong, M. Taya and M.L. Dunn, (1991) "Damage and Oxidation in the High Temperature Composites," ASME Bound Vol. AD 25-2, eds. G.K. Haritos and O.O. Choa, 51.
5. H. Zhang, G.S. Daehn, and R.H. Wagnor, (1991) *Scripta Metall. Mater.*, **25**, 2285.
6. M. Taya and T. Mori, (1987) *Acta. Metall.*, **35**, 155.
7. M. Taya, K.E. Lulay and D.L. Lloyd, (1991) *Acta. Metall.*, **39**, 73.
8. J. Echigoya, M. Taya, and W.D. Armstrong, (1991) *Mater. Sci. Eng.*, **A141**, 63.
9. W. D. Armstrong and M. Taya, (July/August, 1991), *Experimental Techniques*, 33.

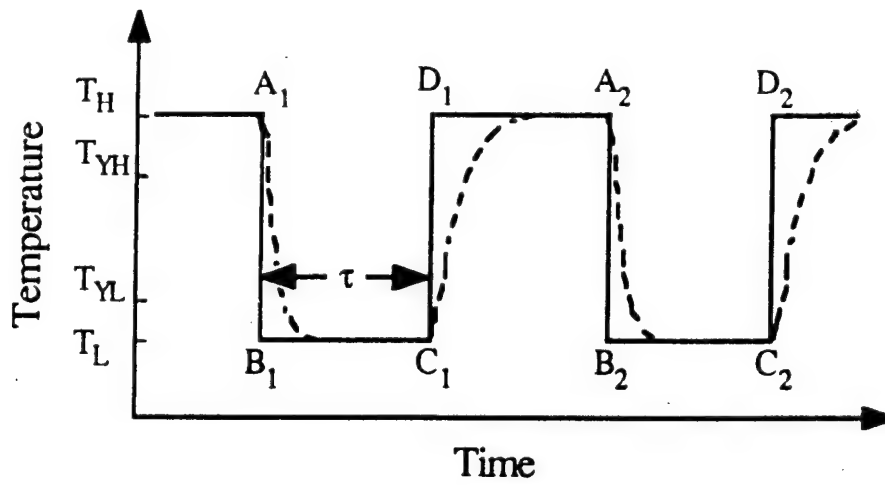


Figure 1. Temperature-time relation of thermal cycling: solid line (idealized), dashed line (actual)

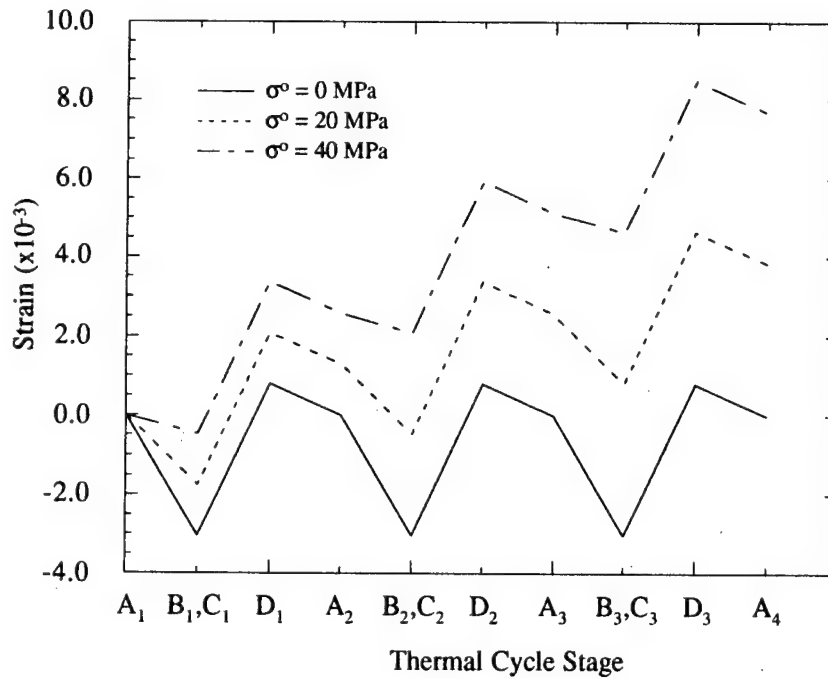


Figure 2. Strain (dimensional change) in a MMC subjected to thermal cycling with constant applied stress σ_0 .

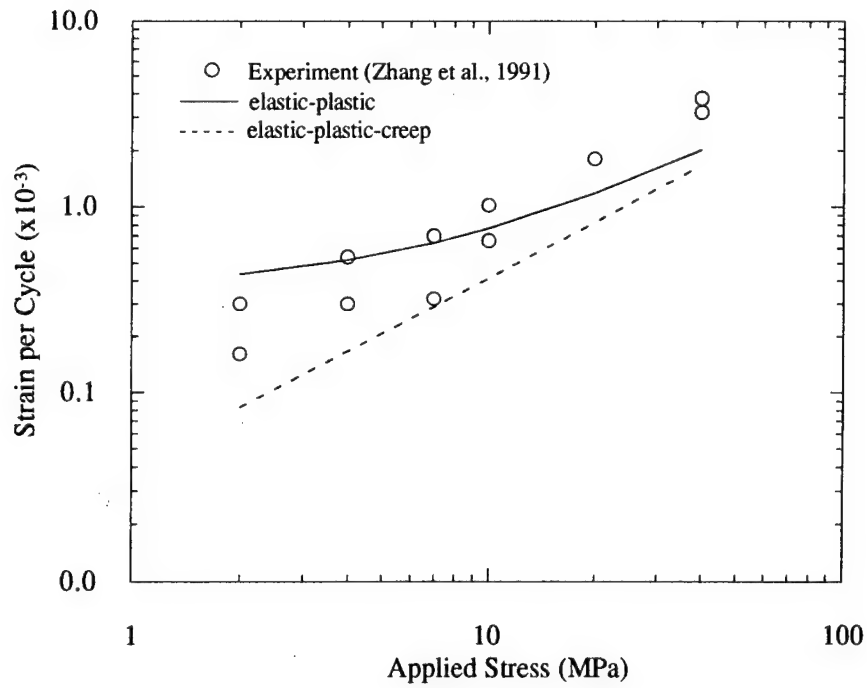


Figure 3. Strain (dimensional change) per cycle vs. applied stress for short fiber SiC/Al MMC subject to combined thermal cycling and creep loadings.

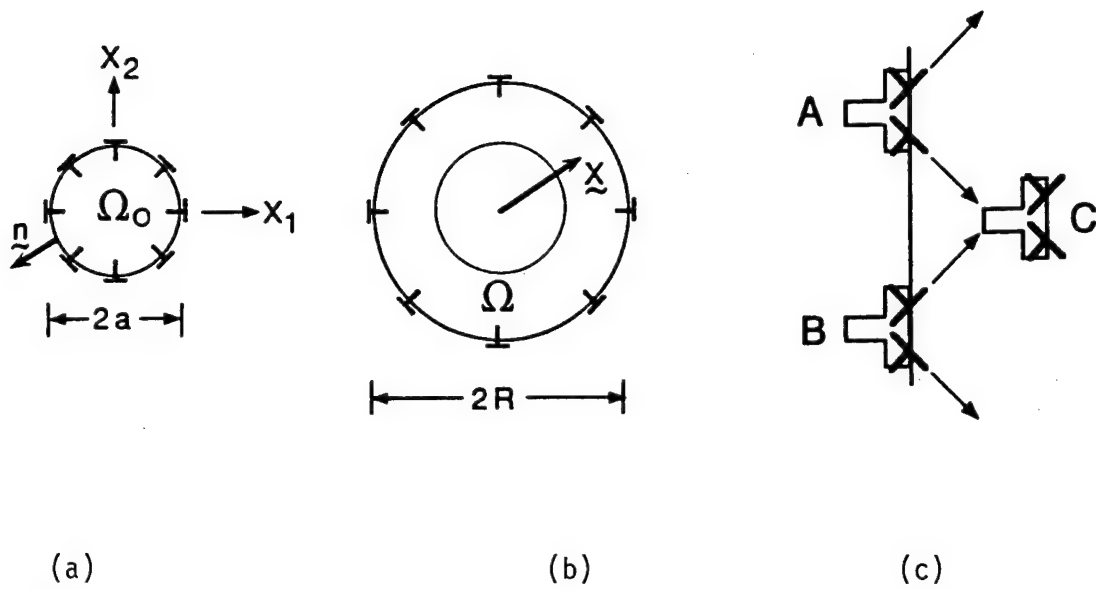


Figure 4. Dislocation punching model for a long fiber MMC (a) before, (b) after punching, (c) actual punching mode (glide motion of edge dislocations).

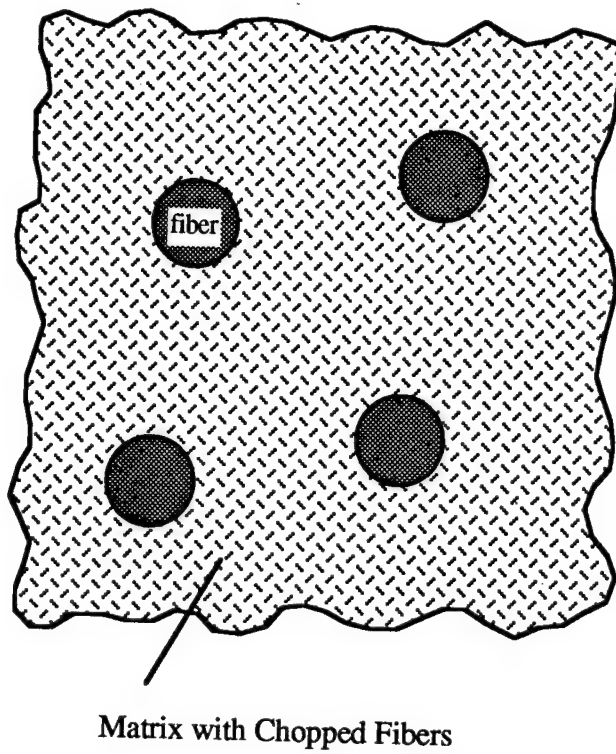


Figure 5. A schematic of hybrid MMC where chopped fibers are uniformly dispersed in the matrix, providing for the source of dislocation punching.

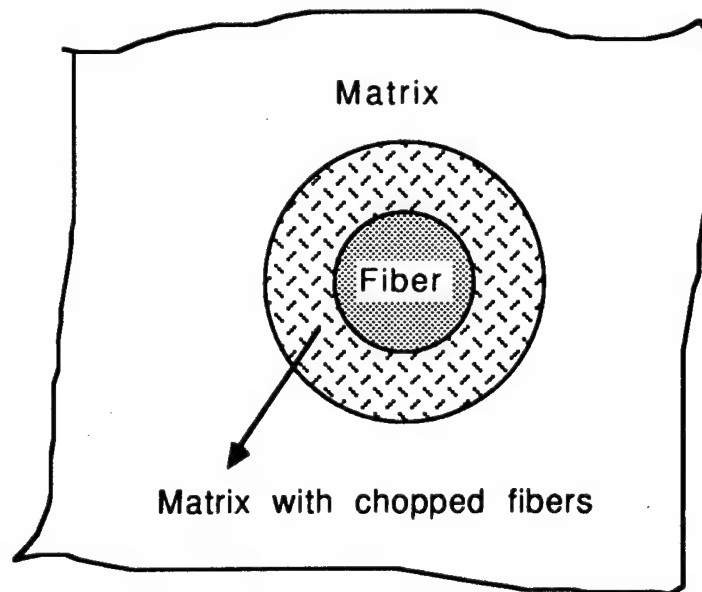


Figure 6. A schematic of hybrid-gradient MMC where chopped fibers are dispersed only in the doughnut area.

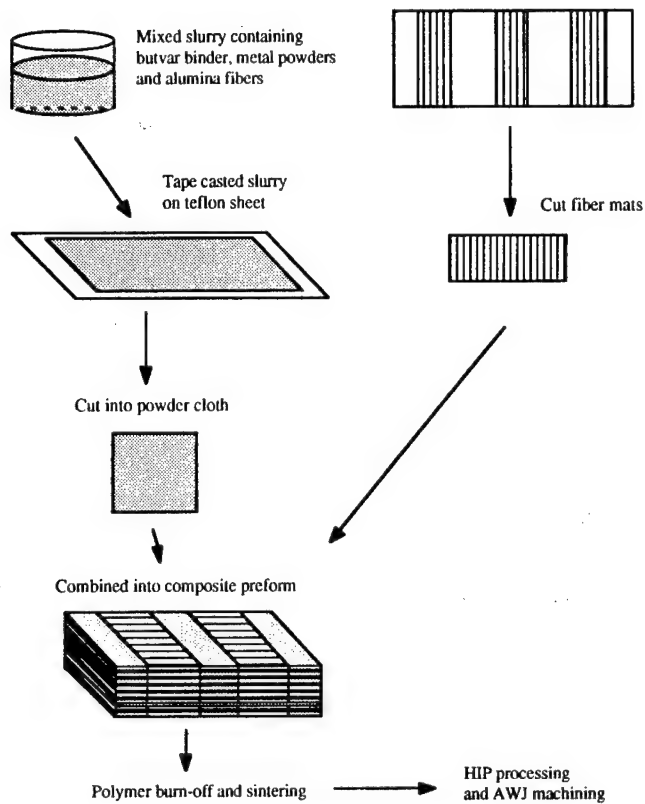


Figure 7. Processing route of MMC.

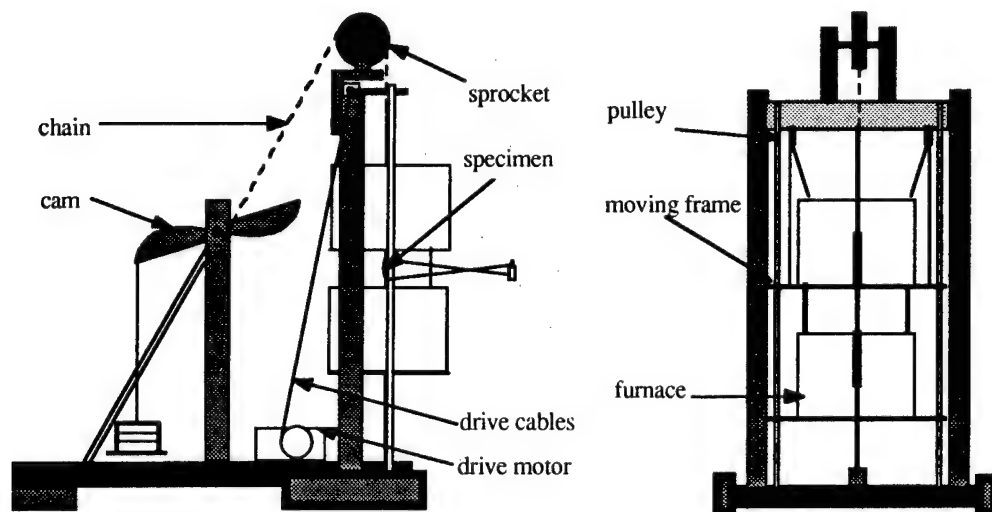


Figure 8. The creep thermal cycler modified for a constant stress.

SOME FRACTURE PROBLEMS IN UNIDIRECTIONAL BRITTLE MATRIX COMPOSITES (BMC)

Nicholas J. Pagano

WL/MLBM
Wright-Patterson AFB OH

Ceramic-and glass ceramic matrix composites are being touted for application in high-temperature structural components. Before their potential can be realized, however, understanding of the significance of the fracture modes that occur at very low stress levels will be essential. Unfortunately, at this point in the technology development, the precise definition of these mechanisms, i.e., the geography of the fracture plane(s), has been described rather incompletely in experimental research. In most cases, the experimental observations only provide views of these cracks at their intersection with a surface of the composite. Thus, in this presentation, we will provide some predictions of failure scenarios (what-if studies) based upon a hypothetical idealized initial flaw in the matrix-an annular crack in a plane normal to the fibers of an unidirectional composite. Although many of the properties needed for the modeling study have not been realistically determined, especially the in-situ strength/fracture properties, it is hoped that the modeling can serve to determine the nature of the parameters that require measurement and to help establish the sensitivity of the response to these parameters, as well as to guide experimental efforts to attempt validation of the failure processes hypothesized. The complexity of these processes seems to demand an iterative approach between the analyst and experimentalist.

We will make predictions employing a recently developed variational model¹ of an axisymmetric concentric cylinder which may contain damaged regions in the form of annular or penny-shaped cracks in the constituents and/or debonds between them. The work attempts to examine in closer detail than analyses currently available^{2,3} the mechanics of failure in BMC once a flaw has been formed within the matrix. It should be noted that we start with the viewpoint discussed by Kim and Pagano⁴ that initial failure in BMC occurs within a single cell or at random in various cells and is assumed to be a planar transverse matrix crack which is stopped (or deflected) as soon as it encounters the nearest fiber-matrix interfaces and does not extend any further. This is in contrast to the global steady state cracking mode in which a single matrix crack traverses and bridges all the fibers as studied in the famous ACK model⁵ and refined by Budiansky, Hutchinson, and Evans⁶. In this regard, it represents the cylindrical geometry counterpart to the model of Wang et al³ and the micromechanical version of the models that examine short cracks in homogeneous, orthotropic media, such as those by Marshall, Cox, and Evans⁷ and McCartney⁸. Unfortunately, such models that represent the fibers and matrix as "layers" provide inaccurate geometric details as, for example, the ratio of fiber spacing to fiber diameter is very much higher than that in a composite having the same volume fraction of fibers arranged in a hexagonal pattern. There is substantially less distortion of these details in the concentric cylinder model utilized in the present work. We have called this failure mechanism the *full-cell cracking mode*, which may or may not include interfacial debonding.

An important feature of this work lies in the fact that very large (non-singular) stresses can be developed on the fiber-matrix interface in or near its intersection with the plane of an annular matrix crack⁹ and that these stresses may cause damage in the matrix (possibly the fiber as well) at the interface prior to propagation of the annular crack. Various failure scenarios may then develop depending on the magnitude and mix of the interlaminar stresses, the matrix energy release rate, and the respective ultimate properties of the interface and constituents. One of these scenarios which will be further explored examines the possibility of crack deflection at the interface, which of course represents a key controlling feature of a useful BMC. Included in this work is the presentation of a model which approximates the response in a region where the volume fraction

differs from the average value. The behavior under consideration here is governed by numerous factors such as the thermoelastic and strength/fracture properties of the constituents, geometric details such as fiber diameter, spacing and volume fraction, initial annular crack dimensions and location, interface characteristics (which may not all be identified at this time), loading parameters, residual processing stress state, and, perhaps, interphase properties. Because of the multitude of parameters, we shall perform this investigation in the mode of a case study rather than attempting a systematic study of all the parameters and focus on bulk material properties typical of present composite systems under study in which the fibers are Nicalon and the matrix a glass-ceramic. Furthermore, we shall take advantage of the relative technical simplicity of a composite having a radial compressive stress at the fiber-matrix interface after processing. (The full-cell cracking mode may be generated by flaws other than the annular one assumed here, however, it seems quite reasonable to assume that such a flaw approximates one which must develop sometime prior to the formation of a full-cell transverse crack).

According to the new model, interface damage in the form of matrix cracking and/or debonding may be developed as a function of the stress concentration produced by the annular crack. This secondary damage may then set up a synergistic increase in the applied energy release rate. For the cases considered here, this enhanced energy release rate entered the population of matrix \mathcal{G}_c only for the non-uniform situation, where locally increased fiber spacing is encountered. Of course, this is partially due to the larger potential cracking area in the matrix. On the other hand, the small annular cracks permitted in the model in regions of large fiber volume fraction, were shown to be almost universally immobile. This suggests that uniform, high fiber volume fraction materials will be endowed with crack growth resistance. The fact that much higher values of \mathcal{G} are available in matrix-rich regions may be responsible for the observation³ that matrix cracking occurs in such regions, however, the small size and detection difficulty of potential matrix cracks in fiber-dense regions must also be considered.

The present model includes in its scope the perennial problem of the competition between the respective stresses causing crack deflection and fiber penetration at the fiber-matrix interface. The conclusion on this issue is that, for the composite class considered here, and ignoring dynamic and statistical effects, the state of stress on the interface at the point of maximum stress is such that matrix damage (due to σ_z^m) or debonding (due to σ_r) would precede fiber failure, even for the highest interface strengths that one can expect in these materials. Even when the annular crack impinges on the interface itself, the ratio σ_r/σ_z^f is so large that debonding would be expected. Therefore, practical efforts to degrade interfacial strength for the purpose of promoting crack deflection may be fruitless or even negative in many cases.

Somewhat representative (isotropic) values of elastic properties for the constituent materials will be assumed. The thermoelastic moduli and geometry are taken as

$$\begin{aligned} E_f &= 200 \text{ GPa} & E_m &= 100 \text{ GPa} \\ V_f &= 0.2 & V_m &= 0.4 \\ \alpha_f &= 2.7 \times 10^{-6}/^\circ\text{C} & \alpha_m &= 3.2 \times 10^{-6}/^\circ\text{C} \\ \Delta T &= -1000^\circ\text{C}, \frac{d^2}{a^2} = \frac{5}{3}, \frac{d}{a} = 20 \end{aligned}$$

The given ratio of d/a corresponds to a fiber volume fraction of 60% in the concentric cylinder. These dimensions will be subsequently modified by applying a factor of 8×10^{-6} , a realistic value of fiber radius (in m).

REFERENCES

1. Pagano, N.J., "Axisymmetric Micromechanical Stress Fields in Composites". Proceedings of 1991 IUTAM Symposium on Local Mechanics Concepts for Composite Materials Systems, Virginia Polytechnic Institute and State University, Blacksburg, VA, Oct. 29, 1991.
2. He, H. and Hutchinson, J.W., "Crack Deflection at an Interface Between Dissimilar Elastic Materials", Int. J. Solids Structures, **25**, 9 (1989), pp. 1053-1067.
3. Barsoum M., Kangukar, P., and Wang, A.S.D., "Matrix Crack Initiation in Ceramic Matrix Composites Part I: Experiment and Test Results"; Wang, A.S.D., Huang, X.G., and Barsoum, M., "Matrix Crack Initiation in Ceramic Matrix Composites Part II: Models and Simulation Results", Comp. Sci and Technology, **43**, 3 (1992), pp. 257-282.
4. Kim, R.Y. and Pagano, N.J., "Crack Initiation in Unidirectional Brittle Matrix Composites", J. Am. Ceram. Soc., **74**, 5 (1991), pp. 1082-1090.
5. Aveston, J., Cooper, G., and Kelly, A., "Single and Multiple Fracture", in The Properties of Fiber Composites, Conference Proceedings, National Physical Laboratory, Guildford, UK. IPC Science and Technology Press, Ltd. (1971), pp. 15-26.
6. Budiansky, B., Hutchinson, J.W., and Evans, A.G., "Matrix Fracture in Fiber-Reinforced Ceramics", J. Mech. Phys. Solids, **34** (1986), pp. 167-189.
7. Marshall, D.B., Cox, B.N., and Evans, A.G., "The Mechanics of Matrix Cracking in Brittle-Matrix Fiber Composites", Acta Metall., **33** (1985), pp. 2013-2021.
8. McCartney, L.N., "Mechanics of Matrix Cracking in Brittle-Matrix Fiber-Reinforced Composites", Proc. Roy. Soc. London, **A-409** (1987), pp. 329-350.
9. Kaw, A.K., and Pagano, N.J., "Axisymmetric Thermoelastic Response of a Composite Cylinder Containing an Annular Matrix Crack", to be published.

TABLE 1

 $\epsilon_o = 0$ $\epsilon_o = .001$

b/a	σ_z^f	σ_θ^f	σ_z^m	σ_θ^m	σ_r	τ_{rz}	\mathcal{G}	σ_z^f	σ_θ^f	σ_z^m	σ_θ^m	σ_r	τ_{rz}	\mathcal{G}
1.05	25.84	7.46	109.34	106.57	30.96	14.20	.146	344.95	48.06	323.42	211.34	117.57	42.01	1.280
1.10	-5.72	-4.36	79.69	81.88	5.87	7.78	.124	251.58	13.09	235.70	138.32	43.34	22.98	1.081
1.14	-18.76	-8.86	67.74	73.43	-2.60	4.56	.101	213.01	-0.20	200.38	113.32	18.29	13.48	.882
1.20	-29.93	-12.65	59.00	66.30	-10.75	1.86	.064	179.99	-11.43	174.52	92.23	-5.80	5.50	.557
1.291*	-35.96	-15.66	53.94	62.60	-15.66	-0-	-0-	162.14	-20.33	159.55	81.27	-20.33	-0-	-0-

*Uncracked

Energy Release Rates (N/m) and Maximum Interface Stresses (MPa) for imposed ϵ_o plus $\Delta T = -1000^\circ\text{C}$, $V_f = 0.60$

TABLE 2

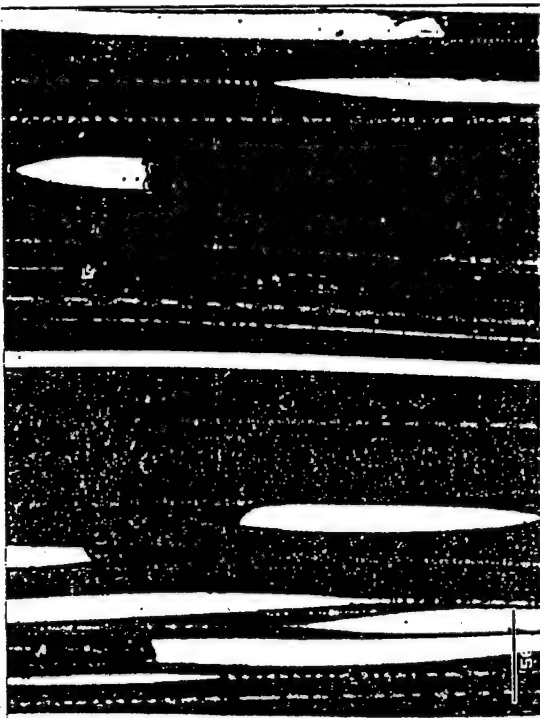
$\epsilon_0 = 0$ $\epsilon_0 = .001$

b/a	σ_z^f	σ_θ^f	σ_z^m	σ_θ^m	σ_r	τ_{rz}	\mathcal{G}	σ_z^f	σ_θ^f	σ_z^m	σ_θ^m	σ_r	τ_{rz}	\mathcal{G}
1.08	255.4	131.6	326.1	290.2	224.3	52.8	2.02	911.1	339.8	848.5	648.0	581.0	137.2	13.7
1.12	193.3	105.1	262.3	239.1	168.4	41.4	1.93	749.7	270.6	682.3	515.2	435.5	107.8	13.0
1.48	120.3	58.3	96.4	70.5	72.0	18.7	1.06	313.0	151.6	250.8	183.5	187.3	48.6	7.14
2.236*	-29.7	0.1	67.1	79.9	0.1	-0-	-0-	169.3	-2.3	174.6	101.0	-2.3	-0-	-0-

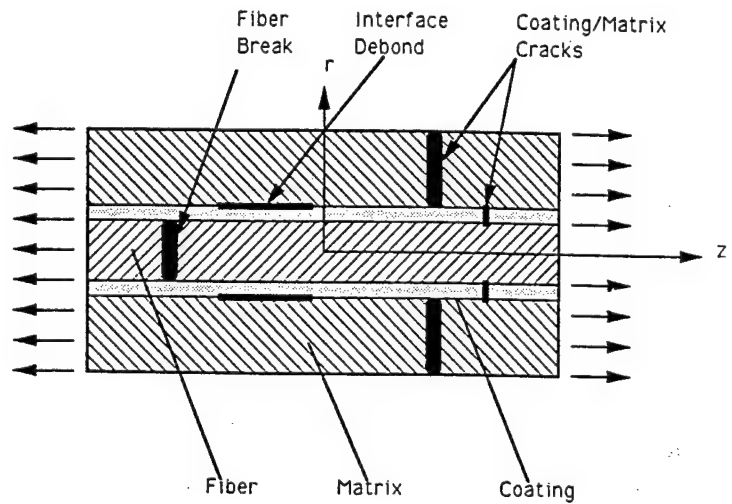
*Uncracked

Energy Release Rates (N/m) and Maximum Interface Stresses (MPa) for imposed ϵ_0 plus $\Delta T = -1000^\circ\text{C}$ in Non-uniform Composite

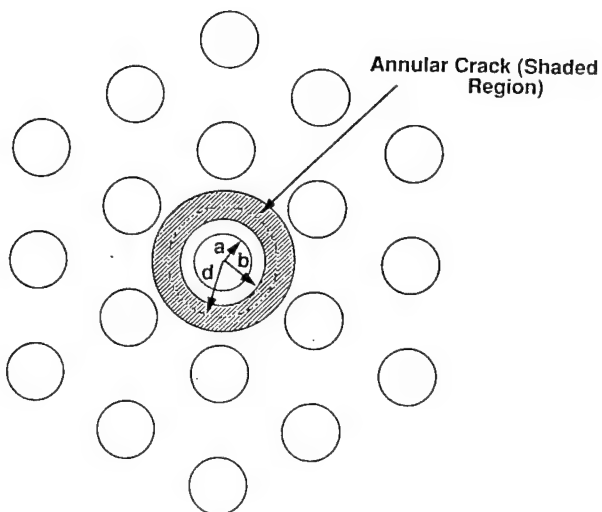
SiC/CAS [0]
70 MPa



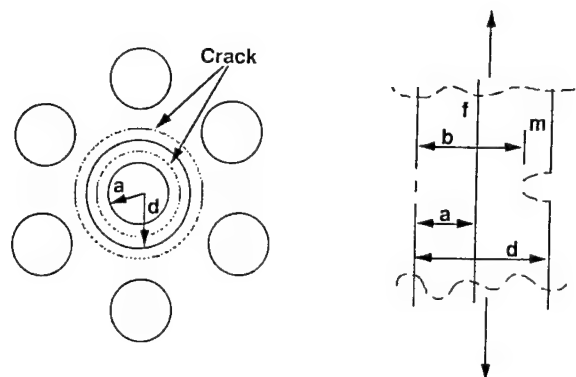
Observed Matrix Cracking in Nicalon-CAS Composite (dimension shown is 50 μm)



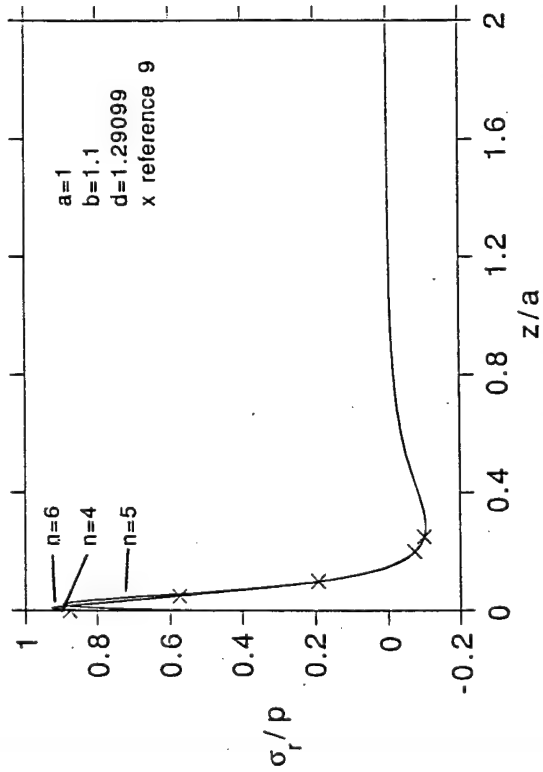
Damage Modes in Brittle Matrix Composites



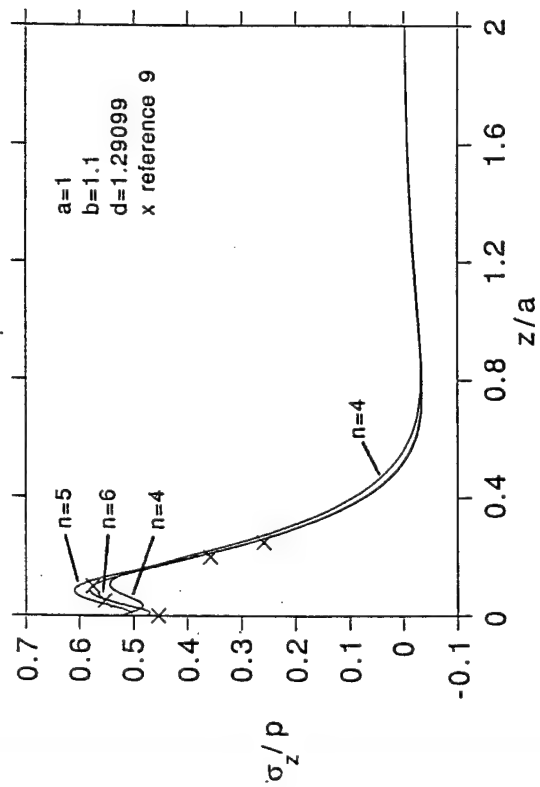
Postulated Annular Crack in a Hexagonal Array



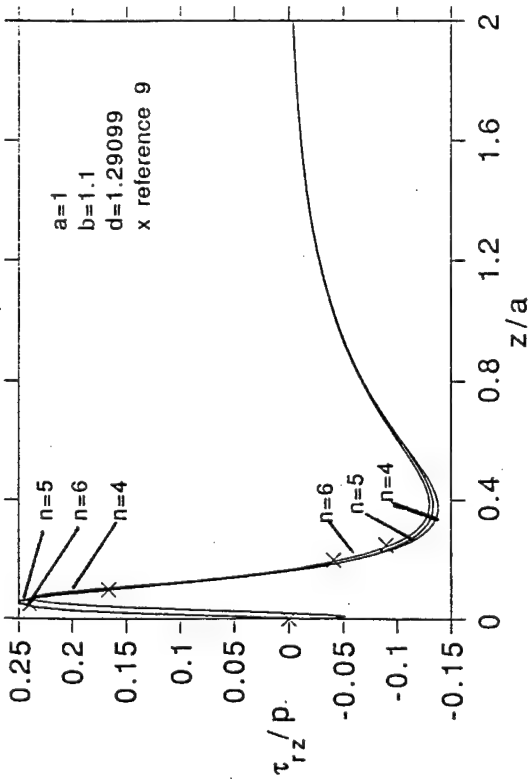
Geometry of Annular Crack in a Composite Cylinder



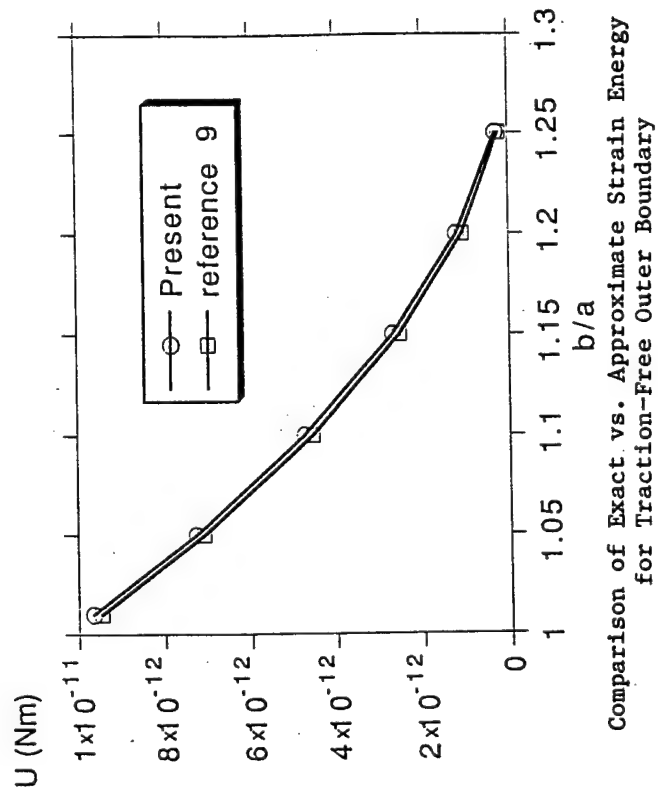
Radial Stress Distribution Along the Interface for Traction-Free Outer Boundary



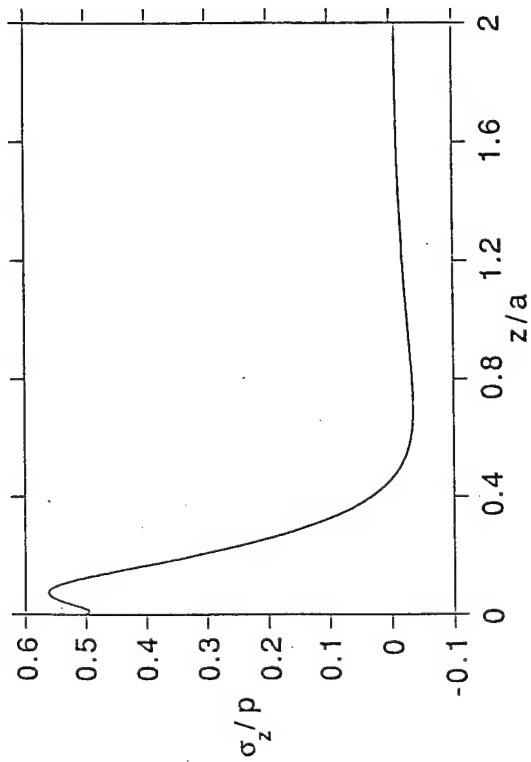
Axial Fiber Stress Distribution Along the Interface for Traction-Free Outer Boundary



Shear Stress Distribution Along the Interface for Traction-Free Outer Boundary

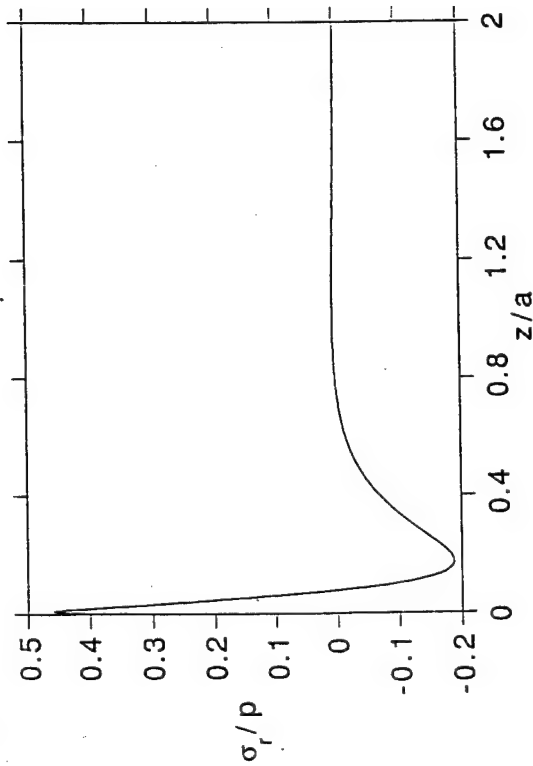


Comparison of Exact vs. Approximate Strain Energy for Traction-Free Outer Boundary

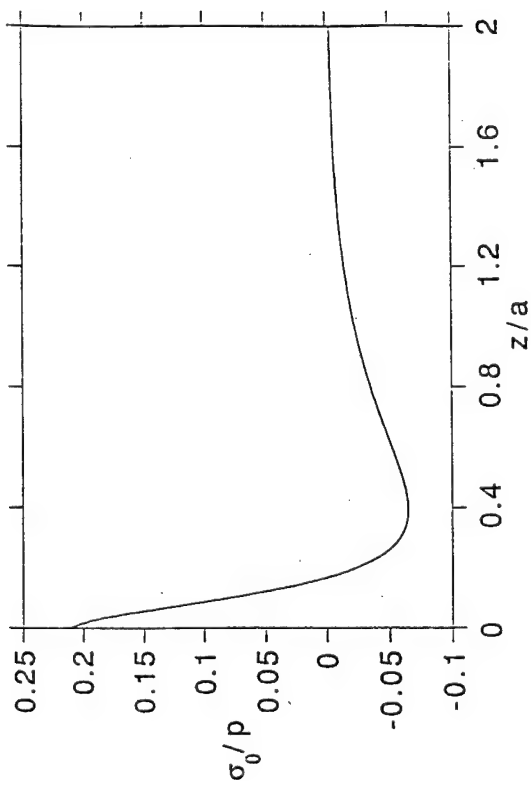


Fiber Axial Stress at Interface,
Constrained Boundary

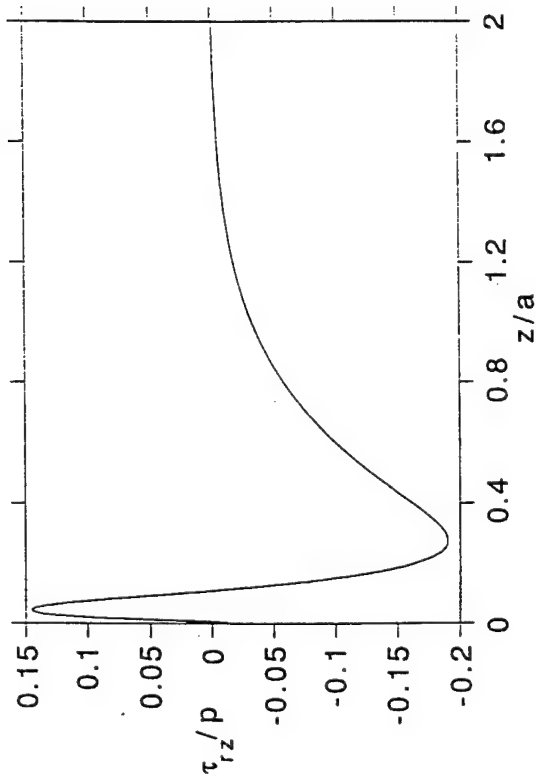
34



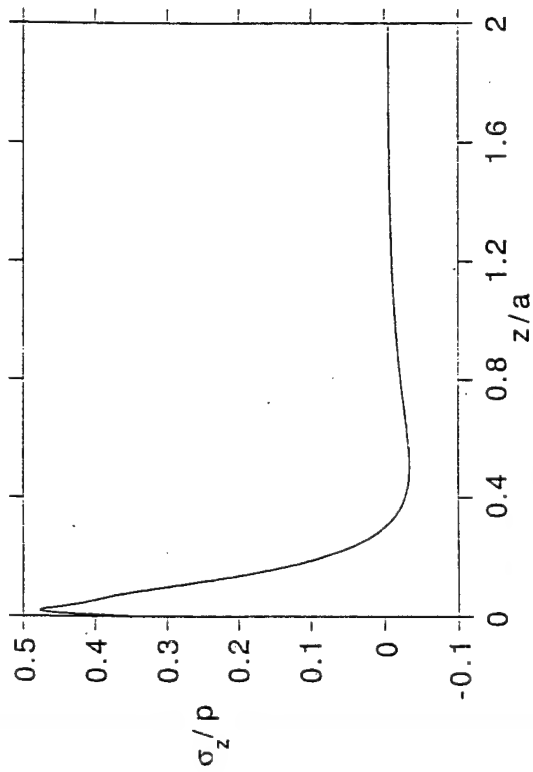
Radial Stress at Interface,
Constrained Boundary



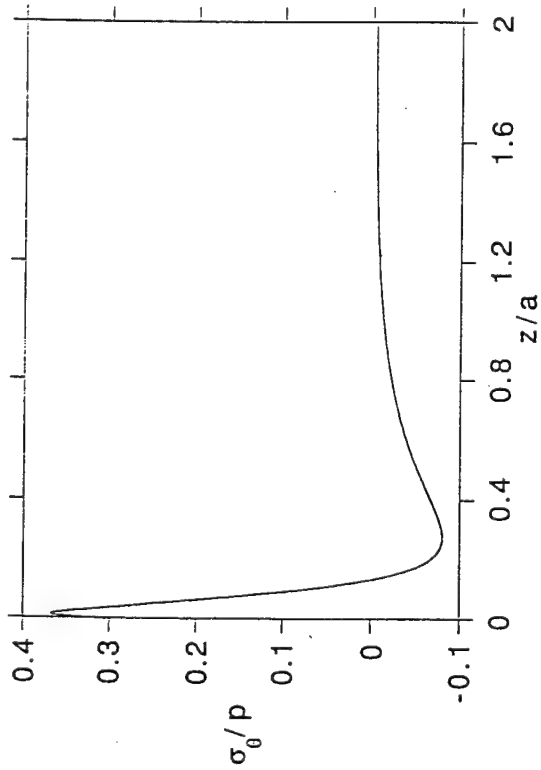
Fiber Hoop Axial Stress at Interface,
Constrained Boundary



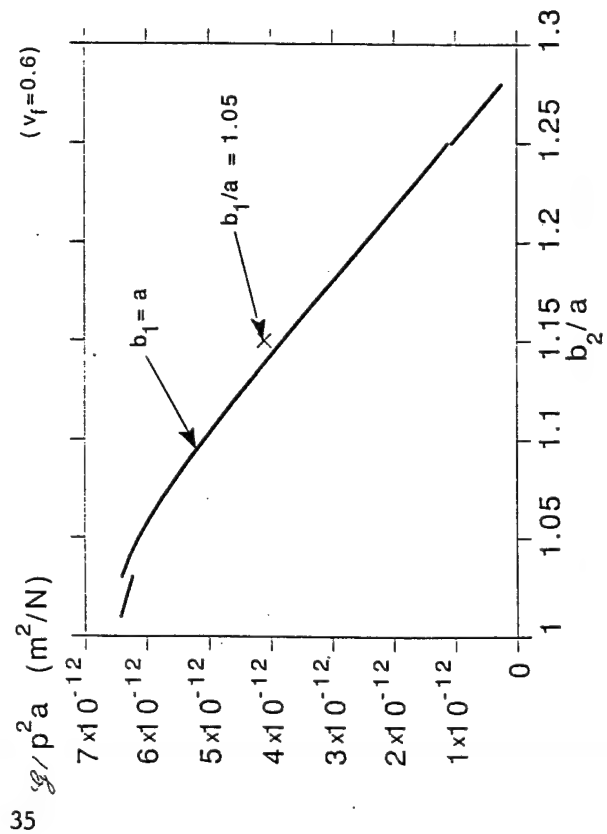
Shear Stress at Interface,
Constrained Boundary



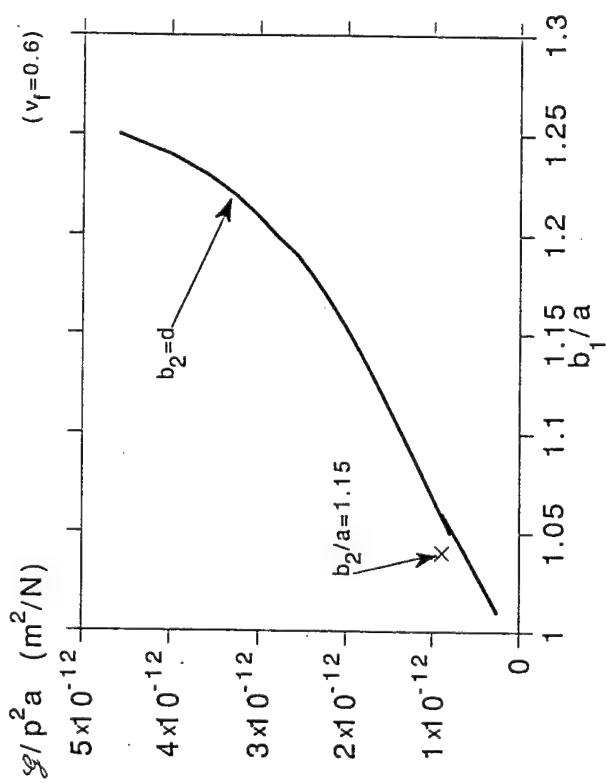
Matrix Axial Stress at Interface,
Constrained Boundary



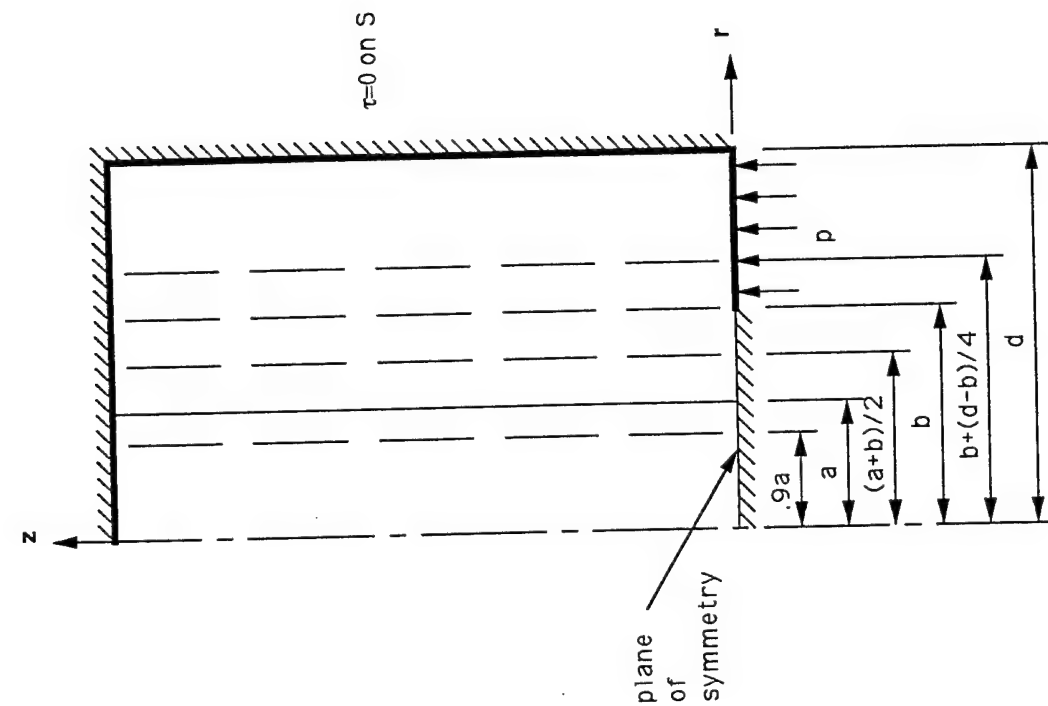
Matrix Hoop Stress at Interface,
Constrained Boundary



Energy Release Rate for Outer Crack

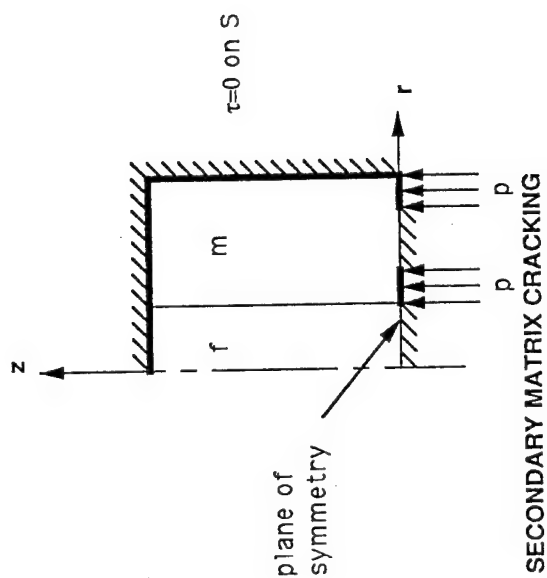


Energy Release Rate for Inner Crack

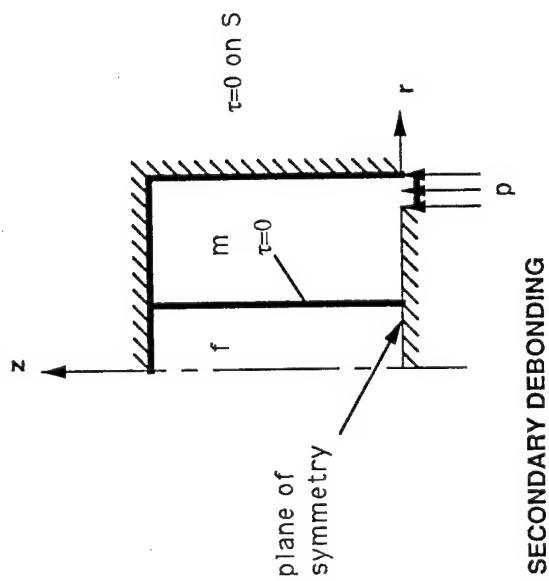


PRESSURIZED CRACK MODEL

Subregions Employed for the
Pressurized Crack Problem

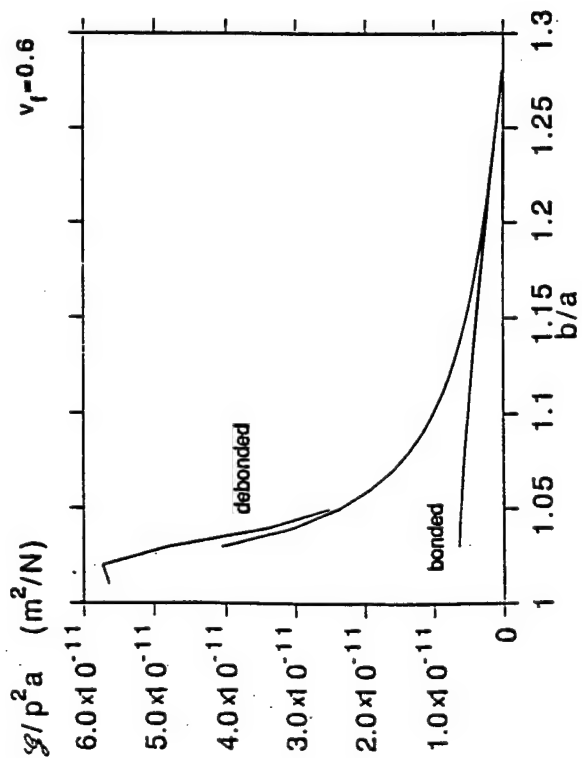


SECONDARY MATRIX CRACKING

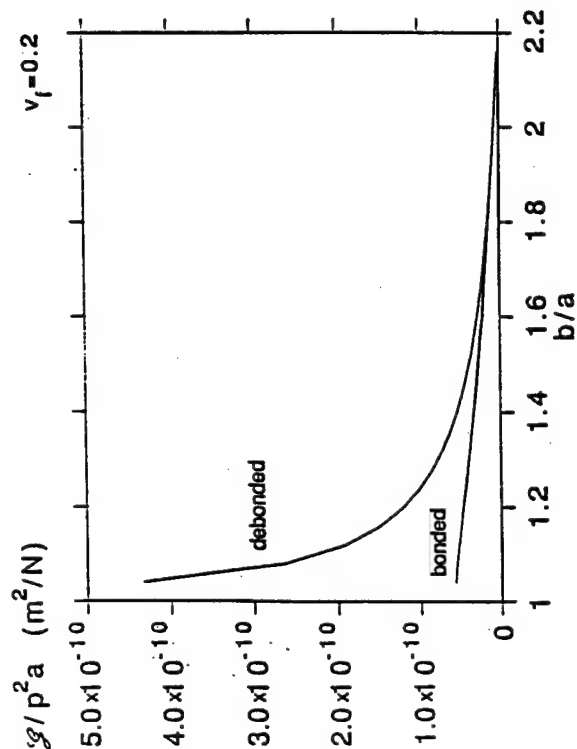


SECONDARY DEBONDING

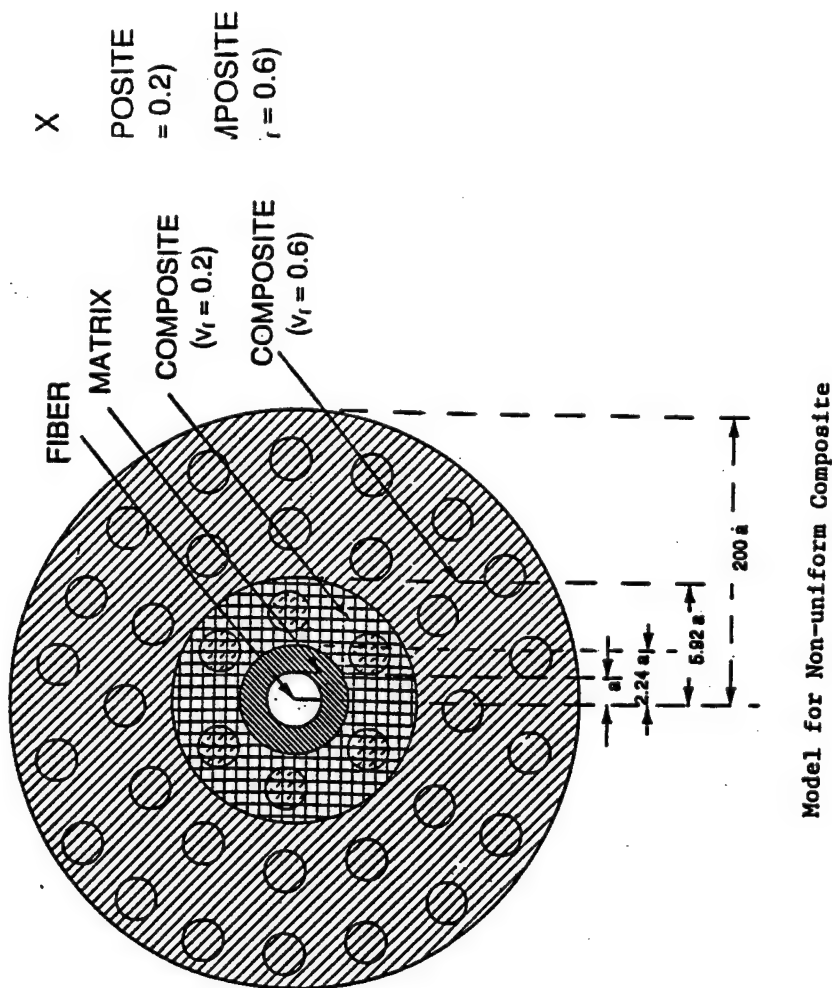
Transverse Annular Crack and Transverse
or Debond Crack at the Interface



Energy Release Rates for Bonded and Debonded Interface, $v_f=0.6$



Energy Release Rates for Bonded and Debonded Interface in Non-uniform Composite



Model for Non-uniform Composite

LOCAL BUCKLING IN VISCOELASTIC COMPOSITES

R. A. Schapery

Department of Aerospace Engineering and Engineering Mechanics
The University of Texas at Austin
Austin, Texas 78712, U.S.A.

ABSTRACT

Microbuckling appears to be the primary compressive strength-limiting mechanism in modern, highly anisotropic composites, such as unidirectional, carbon fiber-reinforced plastic. Over the past three decades, investigators have used linear theory of varying degrees of complexity in studies of failure by fiber buckling. For the commonly used levels of fiber volume fraction, the critical deformation mode is one in which the wave length is long compared to the fiber diameter and is characterized locally by simple shearing deformation. These linear analyses predict a strength which is approximately equal to the principal shear modulus G_{12} . Measured strengths are commonly one-third to one-fifth of this modulus. Kink bands are observed in compression failed specimens and, as a result, elastic and plastic buckling analyses of kink bands have been made in an effort to resolve this discrepancy. Alternatively, assuming a state of local, uniform, simple shear deformation, the combined effects of shear nonlinearity and realistic amounts of initial fiber misalignment are sufficient to reduce the compressive strength from the linear theory value of G_{12} to observed levels. One may interpret the simple shear analysis as applying to a kink band which is normal to the fibers. However, shear buckling may simply represent the local failure initiation event, which is followed by a kink band propagating from the site of the initial event.

In this paper the effects of linear and nonlinear viscoelasticity on local buckling and compressive strength in axially loaded, unidirectional composites are described. In order to not obscure the basic effects of viscoelastic behavior with geometric complexities, we consider here only the uniform, shear mode of deformation. It is believed the primary factors which influence compressive strength are contained in this simple model as it predicts realistic values of strength.

First, the simple shear mode of buckling is reviewed and the governing equation for the growth of an imperfection (fiber misalignment angle) is given. This equation is then solved for a linear viscoelastic composite under constant and cyclic axial loading.

An approximate analytical solution for the growing fiber misalignment angle is developed and compared with a direct numerical solution. Unstable (exponential) growth in time occurs in certain cases. It is therefore of engineering interest to know when the growth is stable (i.e. the fiber angle is bounded for all time) or, at least, the angle does not exceed a specified value over a specified time period. The analytical solution enables one to readily estimate the time-dependent fiber angle.

Next, nonlinear effects are described. In the nonlinear case the fiber misalignment angle is predicted to grow without bound as a finite (failure) time is approached (in contrast to the exponential growth for the linear material). The compressive strength is predicted for specified failure times, which is illustrated using material property data for a carbon/rubber-toughened epoxy composite. The effect of initial fiber misalignment angle on the strength is also shown. (This initial angle could be taken as the residual fiber angle following a period of cyclic loading in the linear viscoelastic range of behavior.) Finally, the effect of constant axial stress on failure time is illustrated for the same material.

Related Publications

R. A. Schapery, "Analysis of Local Buckling in Viscoelastic Composites," August 1991, Proc. IUTAM Symp. on Local Mechanics Concepts for Composite Material Systems, VPI&SU, October 1991.

R. A. Schapery, "Compressive Strength Based on Local Buckling in Viscoelastic Composites," April 1992. To be published in Proc. 3rd Pan American Cong. of Appl. Mech., São Paulo, Brazil, Jan. 1993.

R. A. Schapery, "On Nonlinear Viscoelastic Constitutive Equations for Composite Materials," April 1992. Proc. VII Int. Cong. on Exp. Mech., Las Vegas, June 8-11, 1992.

Acknowledgment

Sponsorship of this research by the Office of Naval Research Solid Mechanics Program, under Grant No. N00014-91-J-4091, is gratefully acknowledged.

OVERALL OBJECTIVE OF THE PROJECT

INVESTIGATE, THEORETICALLY AND EXPERIMENTALLY, THE EFFECT OF NONLINEAR AND VISCOELASTIC BEHAVIOR OF THE RESIN IN THICK-SECTION, CONTINUOUS FIBER COMPOSITES. EMPHASIZE DEVELOPMENT OF DEFORMATION AND FAILURE MODELS WHICH ACCOUNT FOR THE GROWTH OF INITIAL FIBER/PLY WAVINESS UNDER COMPRESSIVE STATIC AND FATIGUE LOADING.

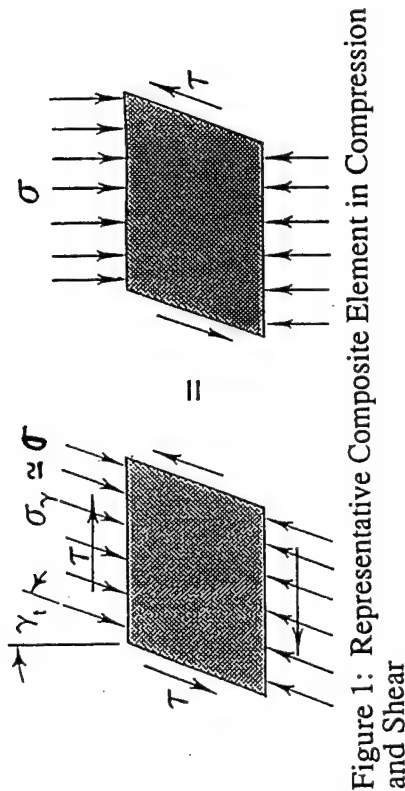


Figure 1: Representative Composite Element in Compression and Shear

FOR VERTICAL LOAD ONLY ON THE CROSS-SECTION

(1) $\tau = \sigma \gamma_t$ where $|\gamma_t| < 1$

SHEAR STRESS-STRAIN EQN:

(2) $\tau = \tau[\gamma]$ where $\gamma = \gamma_t - \gamma_0$

and γ_0 = INITIAL FIBER ANGLE

(1) & (2) YIELD

FOR LINEAR VISCOELASTICITY:

(3) $\tau[\gamma] - \sigma\gamma = \sigma\gamma_0$
OR
 $\sigma = \frac{\tau[\gamma]}{\gamma + \gamma_0}$

$\tau[\gamma] = \int_0^t G(t-t') \dot{\gamma} dt'$

WHERE $G(t)$ IS THE PRINC. SHEAR RELAX. MODULUS

ANALYTICAL SOLUTION FOR $\sigma = \text{CONSTANT}$
 $= \sigma_c$

USE THE LAPLACE/CARSON TRANSFORM:

$$\bar{\gamma}_c = \frac{\gamma_0 \sigma_c}{\bar{G} - \sigma_c}$$

where

$$\bar{f} \equiv \bar{P}f = P \int_0^\infty e^{-Pt} f(t) dt \quad (\text{CARSON TRANSFORM OF } f)$$

APPROXIMATE TRANSFORM INVERSION:

$$f(t) \approx \bar{f}(\alpha/t) \quad \text{if} \quad \left| \frac{d^2 \log f}{(d \log t)^2} \right| \ll 1$$

where

$$\alpha = [\Gamma(1 + \beta)]^{1/\beta} \quad \text{If } -0.1 \leq \beta \leq 0.1 \text{ then } \alpha \approx 0.56$$

and

$$\beta = - \frac{d \log \bar{f}}{d \log P}$$

- BEHAVIOR OF $\tilde{G}(P)$:

$$G(\infty) \leq \tilde{G} \leq G(0^+) \quad \text{and} \quad \frac{d\tilde{G}}{dP} > 0$$

- IF

$$G(\infty) < \sigma_c < G(0^+)$$

THEN A SIMPLE POLE EXISTS ON REAL (P) > 0 AT P_c , WHERE

$$\tilde{G}(P_c) = \sigma_c$$

- RECALL THAT

$$\tilde{\gamma}_c = \frac{\gamma_0 \sigma_c}{\tilde{G} - \sigma_c}$$

- TO INVERT, WRITE $\tilde{\gamma}_c = \Delta \tilde{\gamma}_c + \frac{\gamma_0 \sigma_c}{\tilde{G}_c (P - P_c)}$

$$\text{where} \quad \tilde{G}_c \equiv \frac{d\tilde{G}}{dP} \text{ at } P = P_c$$

THEN

$$(5) \quad \gamma_c \equiv \Delta \tilde{\gamma}_c \left(\frac{\alpha}{t} \right) + \frac{\gamma_0 \sigma_c}{P_c \tilde{G}_c} (e^{P_c t} - 1)$$

ANALYTICAL SOLUTION FOR CYCLIC LOADING

- WRITE σ & γ AS:

$$\sigma = \sigma_c + \Delta \sigma, \quad \gamma = \gamma_c + \Delta \gamma$$

WHERE σ_c IS SELECTED SO THAT

$$\int_t^{t+T} \Delta \gamma dt = 0 \quad (T = \text{period})$$

- THEN, USING EQN. (3), γ_c AND $\Delta \gamma$ SATISFY:

$$(6) \quad \{Gd\gamma_c\} - \sigma_c \gamma_c = \gamma_0 \sigma_c \Rightarrow \gamma_c = \gamma_c(t)$$

$$(7) \quad \{Gd\Delta\gamma\} - \sigma \Delta\gamma = (\gamma_0 + \gamma_c) \Delta \sigma$$

- TO ESTIMATE $\Delta \gamma$ ANALYTICALLY, SUPPOSE $\sigma(t)$ IS SUCH THAT $\Delta \gamma = \gamma_a \sin \omega t$ WHERE $\omega = \frac{2\pi}{T}$.
IF $t \gg 0$, THEN $\{Gd\Delta\gamma\} = \gamma_a |G^*| \sin(\omega t + \Phi)$

$$\text{WHERE } \{Gd\Delta\gamma\} \equiv \int_0^t G(t-t') \Delta \dot{\gamma} dt'$$

- FOR ARBITRARY CYCLIC $\sigma(t)$:

IF $\Phi \equiv 0$ AND $|G^*| \equiv |G^*| \left| \frac{2\pi}{T} \right|$

FOR ALL SIGNIFICANT FOURIER COMPONENTS, THEN

$$\{Gd\Delta\gamma\} \equiv |G^*| \Delta\gamma$$

AND THE SOLUTION TO

$$\{Gd\Delta\gamma\} - \sigma\Delta\gamma = (\gamma_0 + \gamma_c) \Delta\sigma$$

(8) IS
$$\Delta\gamma \equiv \frac{(\gamma_0 + \gamma_c) \Delta\sigma}{|G^*| - \sigma}$$

- THEN σ_c IS FOUND FROM
$$\int_t^{t+T} \Delta\gamma dt = 0,$$

(9) GIVING
$$\int_t^{t+T} \frac{\sigma - \sigma_c}{|G^*| - \sigma} dt = 0$$

- THE CONDITION FOR STABLE RESPONSE IS

$$\sigma_c < G(\infty)$$

- EXAMPLES

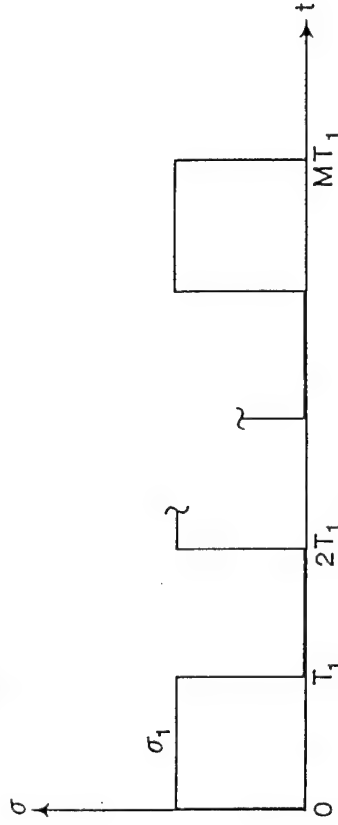


Figure 2: Cyclic Axial Stress History Used in the Examples

FROM (9):
$$\sigma_c = \frac{\sigma_1}{2 - (\sigma_1 / |G^*|)}$$

- FOR STABILITY ($\sigma_c < G(\infty)$):

$$\sigma_1 < \frac{2G(\infty)}{1 + (G(\infty) / |G^*|)}$$

- USE FOR THE RELAXATION MODULUS

$$G(t) = \left(\frac{t}{t_s} \right)^{-m} G_s + G_e$$

WHERE, TYPICALLY,

$$0 \leq m \leq 0.5$$

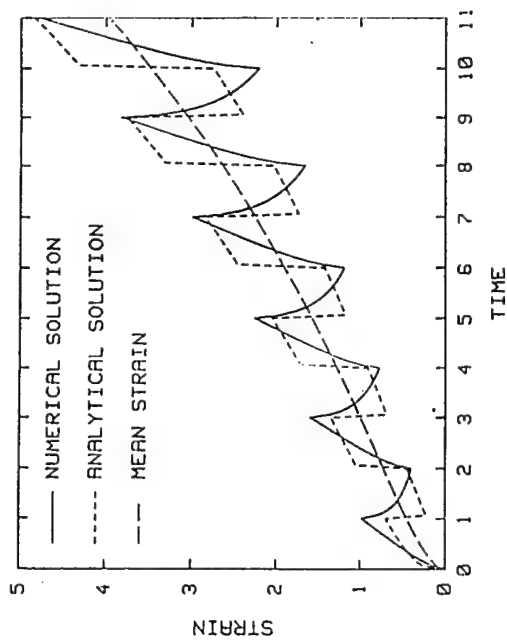


Figure 3: Strain Ratio γ/γ_0 vs. Dimensionless Time t/T_1 for $m = 0.5$, $\hat{G}_e = 0$, $\hat{i}_e = 11$

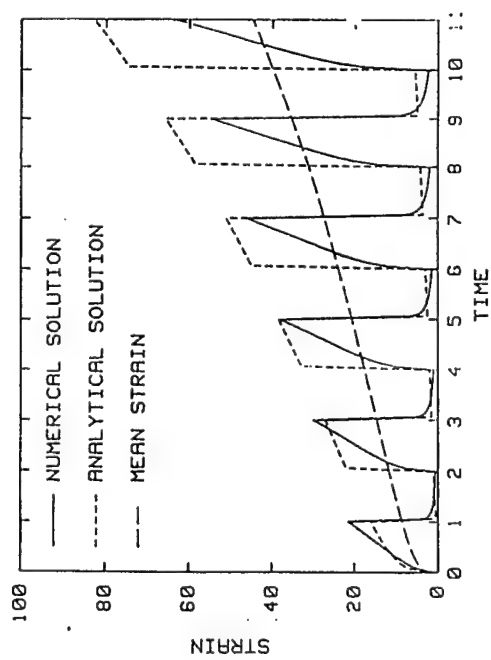


Figure 4: Strain Ratio γ/γ_0 vs. Dimensionless Time t/T_1 for $m = 0.05$, $\hat{G}_e = 0$, $\hat{i}_e = 11$

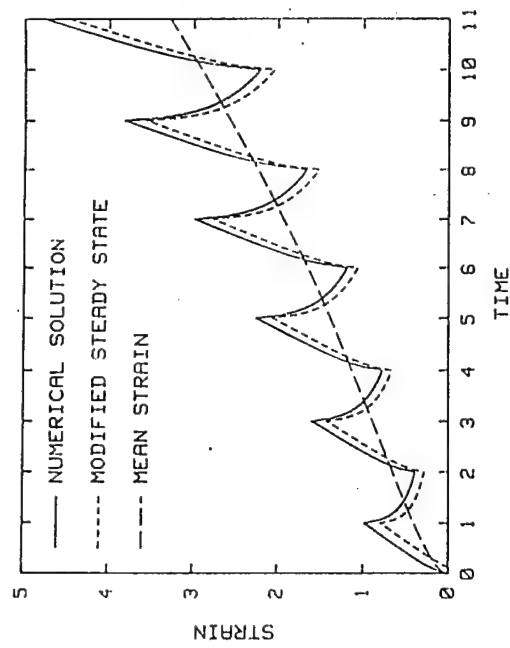


Figure 5: Strain Ratio γ/γ_0 vs. Dimensionless Time t/T_1 for $m = 0.5$, $\hat{G}_e = 0$, $\hat{i}_e = 11$

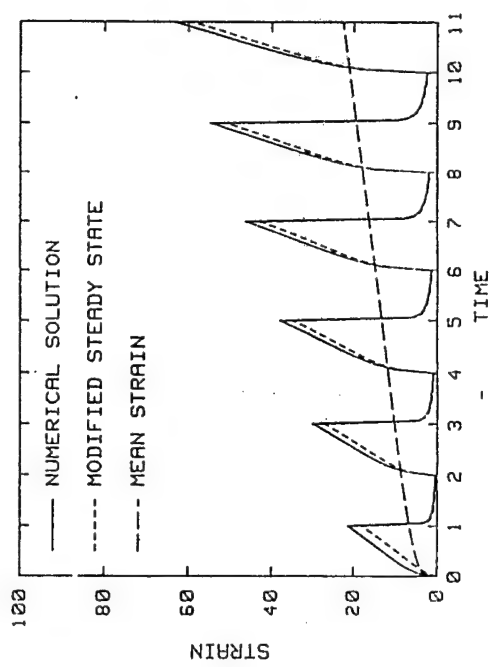


Figure 6: Strain Ratio γ/γ_0 vs. Dimensionless Time t/T_1 for $m = 0.05$, $\hat{G}_e = 0$, $\hat{i}_e = 11$

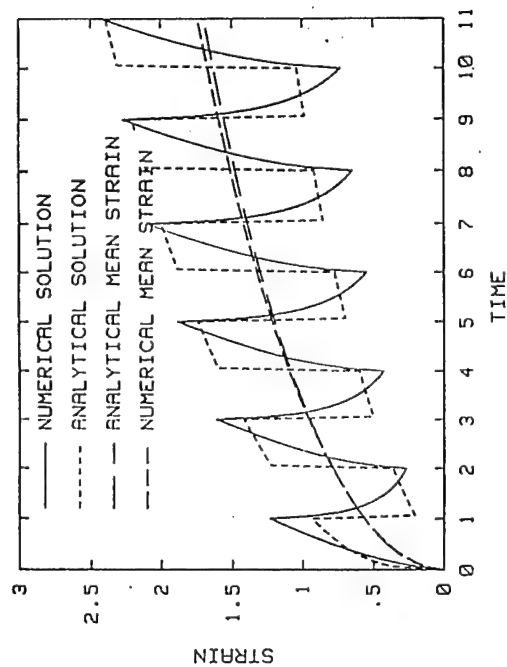


Figure 7: Strain Ratio γ/γ_0 vs. Dimensionless Time t/T_1 for $m = 0.5$, $\hat{G}_e = 1$, $\hat{\sigma}_1 = 1.5$

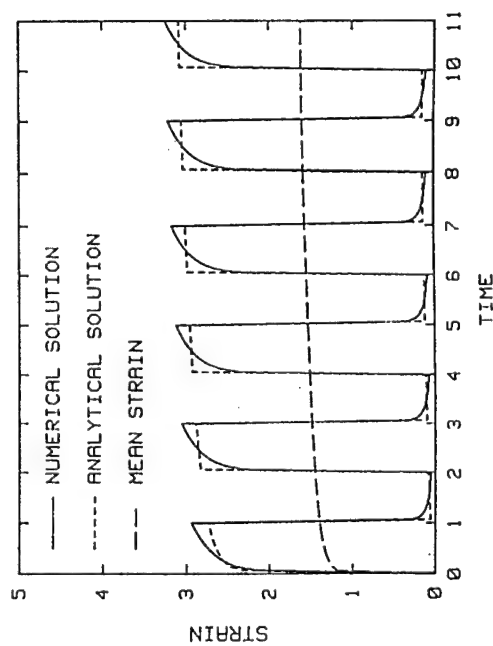


Figure 8: Strain Ratio γ/γ_0 vs. Dimensionless Time t/T_1 for $m = 0.05$, $\hat{G}_e = 1$, $\hat{\sigma}_1 = 1.5$

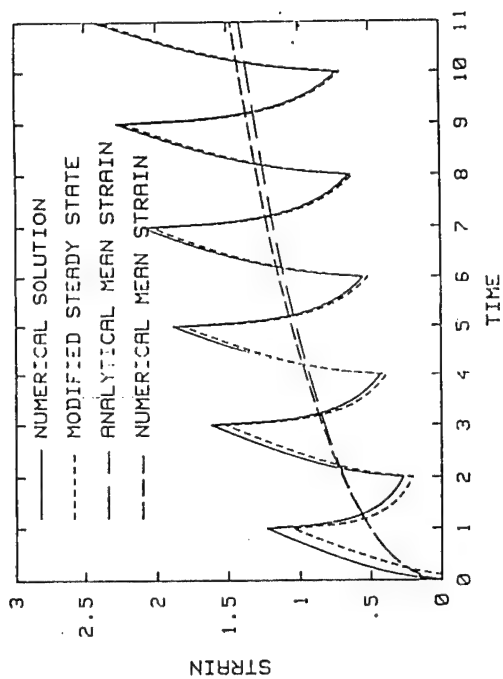


Figure 9: Strain Ratio γ/γ_0 vs. Dimensionless Time t/T_1 for $m = 0.5$, $\hat{G}_e = 1$, $\hat{\sigma}_1 = 1.5$

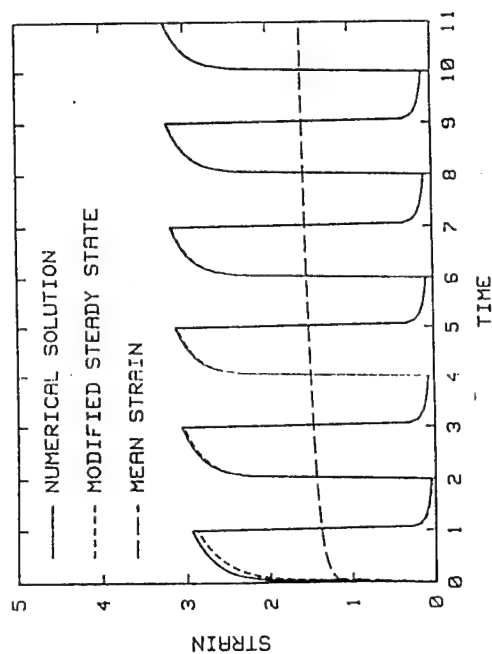


Figure 10: Strain Ratio γ/γ_0 vs. Dimensionless Time t/T_1 for $m = 0.05$, $\hat{G}_e = 1$, $\hat{\sigma}_1 = 1.5$

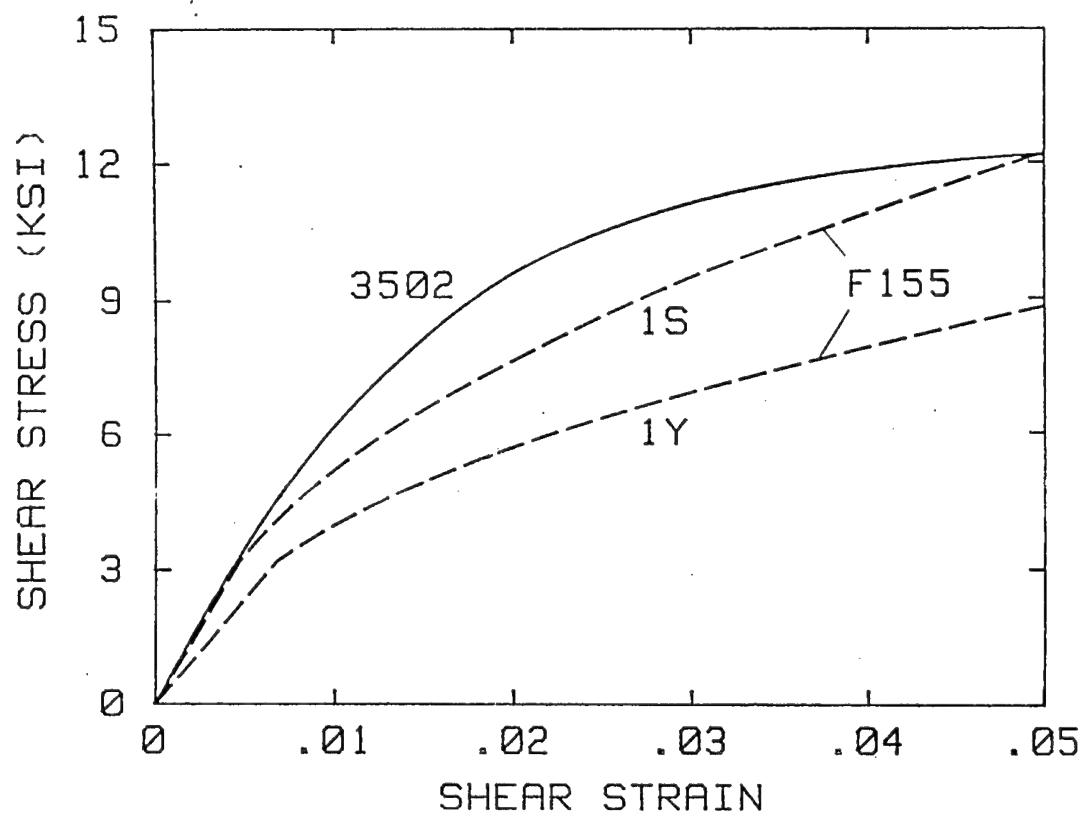


Figure 11. Stress vs. Strain for Two Composites.

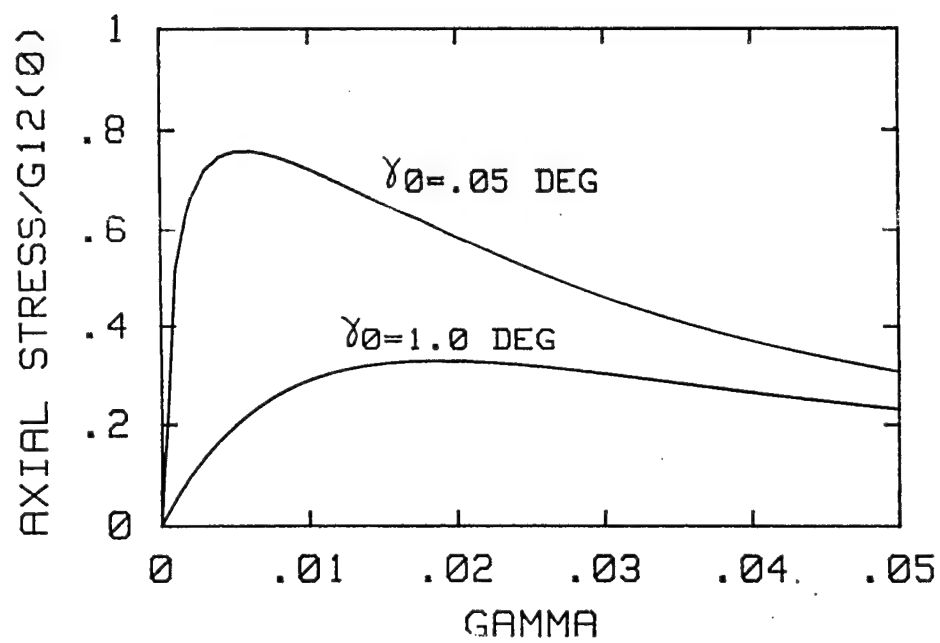


Figure 12. Effect of Initial Angle γ_0 for the AS4/3502 Composite.

CREEP BUCKLING FOR A NONLINEAR
VISCOELASTIC MATERIAL (CARBON/RUBBER-
TOUGHENED EPOXY)

(10) EQUILIBRIUM EQN: $\tau - \sigma\gamma = \sigma\gamma_0$

(11) CONSTITUTIVE EQN:

$$\gamma = J_0\tau + J_1 \int_0^t (t-t')^m \frac{d\tau^q}{dt'} dt' \quad \text{FOR } t \geq 0$$

• QUASI-ELASTIC APPROX TO (11):

$$\gamma = J_0\tau + J_1 t^m \tau^q$$

• MAXWELL MODEL: USE $m = 1$ IN EQN. (11).
EQNS. (10) AND (11) GIVE

(12)
$$S_r - k \int_0^{t_r} (t_r - t')^m \frac{dS_r^q}{dt'} dt' = 1$$

where

$$S_r \equiv \frac{\tau}{\tau_0}, \quad t_r \equiv \frac{t}{t_q}, \quad k \equiv \frac{1}{q} \left(\frac{q-1}{q} \right)^{q-1}$$

t_q = quasi-elastic failure time

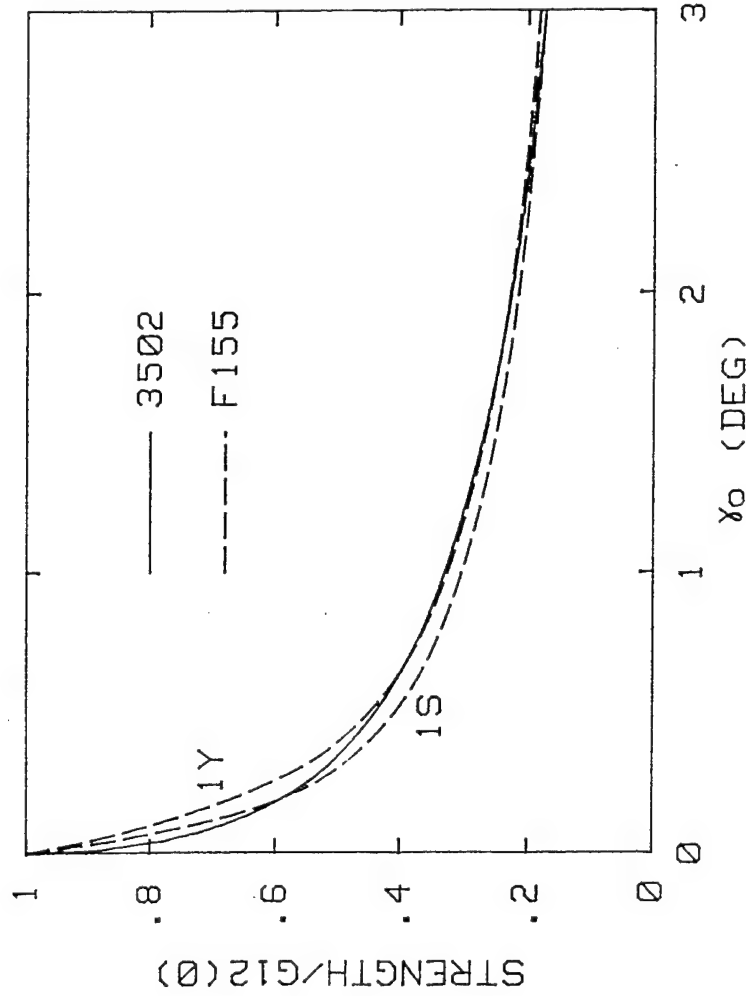


Figure 13. Effect of Initial Fiber Angle γ_0 on Strength.

CONCLUDING REMARKS

• USING LINEAR THEORY:

TIME-DEPENDENT BUCKLING WAS PREDICTED FOR THE SHEAR MODE OF LOCAL DEFORMATION.

AN ACCURATE, APPROXIMATE ANALYTICAL METHOD WAS DEVELOPED FOR CONSTANT LOAD.

FOR CYCLIC LOADING, TIME-DEPENDENT BUCKLING WAS ACCURATELY PREDICTED BY COMBINING STEADY-STATE, CYCLIC DEFORMATION WITH THAT DUE TO CONSTANT LOAD.

THE METHODS HAVE BEEN USED FOR SOME COMPLEX MODES OF DEFORMATION WHICH INCLUDE BENDING.

SHEAR NONLINEARITY AND A MEASURE OF THE PRE-EXISTING (ZERO-LOAD) FIBER ANGLE ARE NEEDED FOR REALISTIC PREDICTIONS OF COMPRESSIVE STRENGTH OR FAILURE TIME.

THE PRE-EXISTING FIBER ANGLE IN THE NONLINEAR ANALYSIS CAN BE THAT WHICH EXISTS AFTER CYCLIC LOADING IN THE LINEAR RANGE.

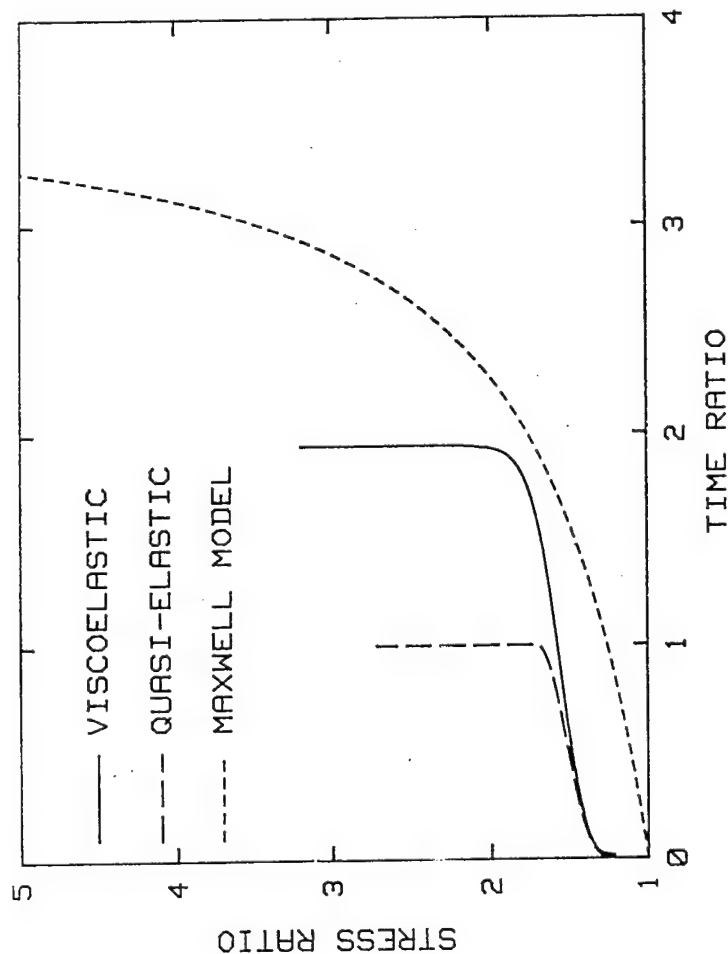


Figure 14. Stress Ratio τ/τ_0 vs. Time Ratio t/t_0 .

COMPRESSIVE FAILURE MECHANISMS IN COMPOSITES

N.A. Fleck^{*}, B. Budiansky[#] and W.S. Slaughter^{*}

^{*}Cambridge University Engineering Department
Trumpington St., Cambridge CB2 1PZ
England

[#]Div. Applied Sciences, Harvard University,
Oxford St., Cambridge, Mass., 02138, USA

Modern engineering fibre composites are used increasingly in primary load bearing structures because of their high specific tensile strengths and elastic moduli. The most widely used of these are polymer matrix composites. Other examples include ceramic matrix and metal matrix composites, both of which remain largely in the developmental stage. Wood, in many circumstances, also behaves as an aligned fibre composite. One problem impeding widespread use of fibre composites is their low compressive strength. Typically, the uniaxial compressive strength can be less than 60% of the tensile strength.

Microbuckling has been shown to be the dominant mechanism of compressive failure of aligned fibre composite materials.¹ Microbuckling is an event in which the composite suffers localized deformation within a kink band. This kink band is generally at an angle *not* normal to the fibre direction. In polymer matrix composites this deformation is associated with the non-linear plastic response of the matrix. Microbuckling is also an important failure mechanism in woods. The role played by microbuckling in the compressive failure of metal matrix and ceramic matrix composites is less clear, though microbuckling has been observed in aluminium alloy matrix composites.² In laminates microbuckling is commonly observed in plies with fibre axes that are parallel to the loading direction. Matrix cracking of off-axis plies (plies with fibre axes not in the loading direction) and interply delamination may occur concurrently, but microbuckling is thought to control failure when the proportion of off-axis plies is not large.

Early theoretical analyses by Rosen³ and others treated microbuckling as an elastic bifurcation buckling phenomenon. Results from these analyses, however, severely overestimate the critical stresses necessary for microbuckling. Here, a model is presented which includes the effects of matrix yielding and initial imperfections in the form of fibre misalignment. The kinking analysis follows the non-linear plastic collapse response of an imperfect structure and assumes that the fibres are inextensible. It is not a bifurcation analysis. Matrix non-linearity is modeled by assuming that the transverse response of the composite (shear and transverse straining) obeys plastic deformation theory. A Ramberg-Osgood hardening behaviour is adopted. The effects of fibre bending stiffness are neglected, with the result that there is no length scale in the analysis.

¹Argon, A.S. (1972). Fracture of Composites. *Treatise of Materials Science and Technology*, vol. 1. Academic Press, New York.

²Shulite, K. and Minoshima, K. (1991). *12th Risø Int. Symp. on Materials Science: Metal Matrix Composites Processing, Microstructure, and Properties*, ed. N. Hansen, et. al., 123-147.

³Rosen, B.W. (1965). *Fiber Composite Materials*, Am. Soc. Materials Seminar, Chapter 3.

Previous studies have shown that these are valid approximations.⁴ Fibres are implicitly assumed to be broken at the kink band interface, but without fibre bending stiffness this is not an issue. The kinking analysis suggests that the fibre waviness is $2^\circ - 3^\circ$.

A bifurcation analysis is performed to show that fibre extensionality combined with a non-linear matrix response is unable to account for the knockdown in compressive strength from the Rosen value. It is necessary to include fibre imperfection (in the form of waviness in order to predict compressive strength accurately. This is consistent with the experimental observation that there is a notorious scatter in compressive strength data, making safe design difficult.

The kinking model also provides an approximate solution to the microbuckling collapse response under general remote multi-axial loading. The rigid-perfectly plastic results predict a plane compressive failure surface in stress space. The model, assuming reasonable values of initial fibre misalignment, is in agreement with experimental results.

The kinking theory does not contain any material length scales and is unable to account for the kink width. Couple stress theory is used to include the effects of bending stiffness of the fibres and to predict the kink width. A predicted ratio of kink width to fibre diameter ratio of about ten is in good agreement with measurements.

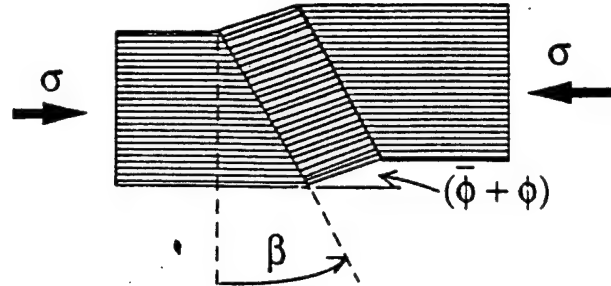
In compression-compression fatigue of aligned fibre composites, microbuckling is again the dominant failure mechanism in polymer matrix and metal matrix composites.⁵ A theoretical analysis has been developed of microbuckling under uniaxial compression - compression fatigue loading; the analysis builds upon the framework of the static model. The Mroz multi-surface model of kinematic hardening is adopted. The effect of plastic strain accumulation, or ratchetting, is considered separately using the material model first proposed by Armstrong and Frederick. Failure is determined either by an empirically based fatigue life criterion or by a plastic instability. Predictions of the model are compared to reported experimental results.

Many fibre composites are known to exhibit time dependent deformation behaviour. These include polymer matrix composites and woods. At elevated temperatures, metal matrix and ceramic matrix composites also creep. A theoretical analysis, formulated in terms of general linear viscoelastic behaviour within the kink band, is given for time dependent microbuckling of aligned fibre composites, or creep microbuckling. An alternative theoretical analysis of creep microbuckling, suitable for power-law viscous composite behaviour, is also given. Failure is due to either the attainment of a critical failure strain in the kink band or to the intervention of a different failure mechanism such as plastic microbuckling. Results indicate that the margin between static plastic microbuckling, as predicted by the first analysis above, and a no creep microbuckling threshold, below which microbuckling will not occur in a finite time period, can be small. This may help to explain the lack of experimental evidence for creep microbuckling of polymeric matrix composites. Creep microbuckling of metal matrix composites and ceramic matrix composites is to be expected, although there is a lack of experimental data.

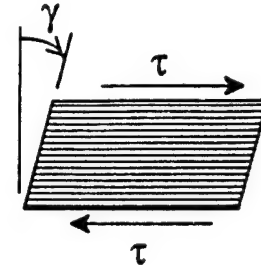
⁴Budiansky, B. (1979). Remarks on kink formation in axially compressed fiber bundles. *Preliminary Reports, Memoranda and Technical Notes of the Materials Research Council Summer Conference*, La Jolla, CA, July 1979, Sponsored by DARPA.

⁵Huang, Y.H. and Wang, S.S. (1988). Compressive fatigue damage and associated property degradation of aluminum-matrix composite. *U.S.-Japan Conf. on Composites 1988*.

Compressive Kinking of Fiber Composites



fiber volume concentration = f
 matrix shear modulus = G_m
 composite shear modulus = $\tau/\gamma = G \approx G_m/(1-f)$
 initial rotation = $\bar{\phi}$



$\beta = 0$:

Rosen (1965)

$$\sigma_c = G$$

$$(\gamma_Y = \infty)$$

Argon (1972)

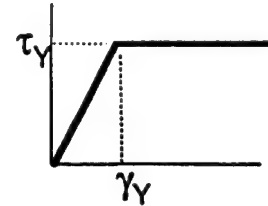
$$\sigma_c = \tau_Y / \bar{\phi}$$

$$(\gamma_Y = 0)$$

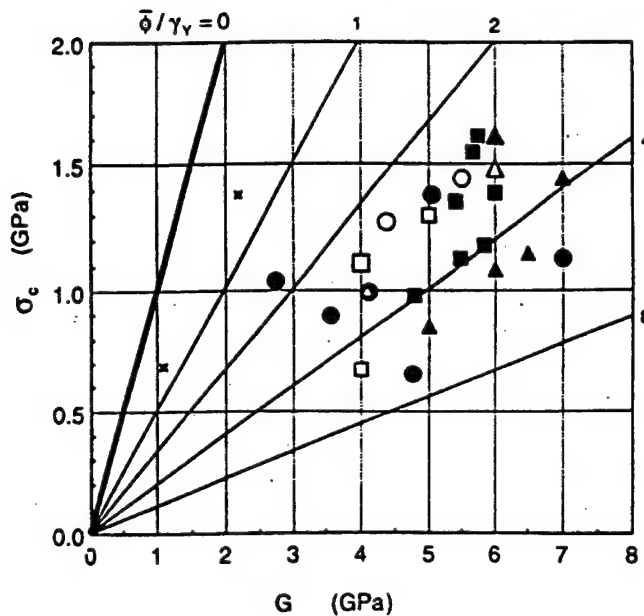
Budiansky (1983)

$$\sigma_c = \tau_Y / (\gamma_Y + \bar{\phi})$$

$$= G / (1 + \bar{\phi} / \gamma_Y)$$



Kinking Data



- ▲ Fried & Kaminsky 1964
- × Lager & June 1969
- △ Chapin 1977
- Parry & Wronski 1981
- Curtis 1985
- Hahn et al 1986
- Johnston & Hergenrother 1987
- US Polymeric 1988
- Jeff et al 1990
- △ Soutis et al 1991

$$\sigma_c = \frac{\tau_Y}{\gamma_Y + \bar{\phi}} = \frac{G}{1 + \bar{\phi} / \gamma_Y}$$

Kinking vs. Fiber Crushing

fiber crushing mechanisms

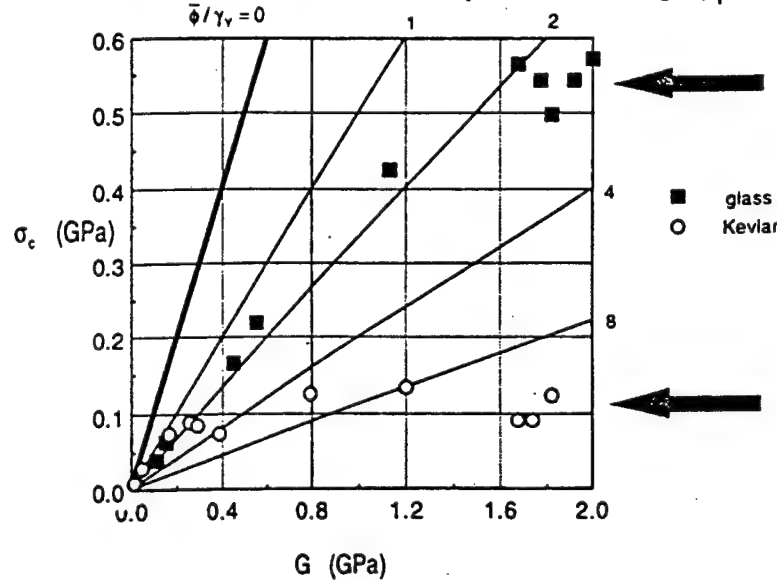
plastic yielding (steel)

longitudinal splitting (glass)

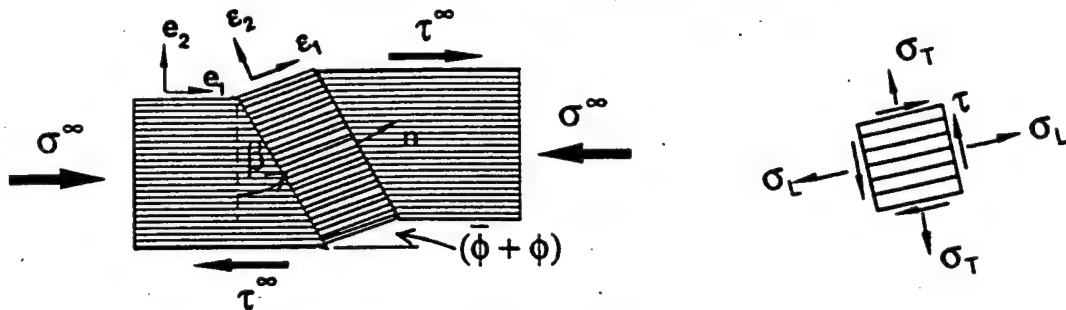
intra-fiber kinking (carbon, Kevlar, wood)

Piggott & Harris (1980); Piggott (1981)

polyester resin matrix, various G via partial curing; $\gamma_Y \approx .024$; $f=.31$



Analysis: Equilibrium



remote stress tensor: $\sigma^\infty = -\sigma^\infty \mathbf{e}_1 \mathbf{e}_1 + \tau^\infty (\mathbf{e}_1 \mathbf{e}_2 + \mathbf{e}_2 \mathbf{e}_1)$

kink stress tensor: $\sigma = \sigma_L \mathbf{e}_1 \mathbf{e}_1 + \tau (\mathbf{e}_1 \mathbf{e}_2 + \mathbf{e}_2 \mathbf{e}_1) + \sigma_T \mathbf{e}_2 \mathbf{e}_2$

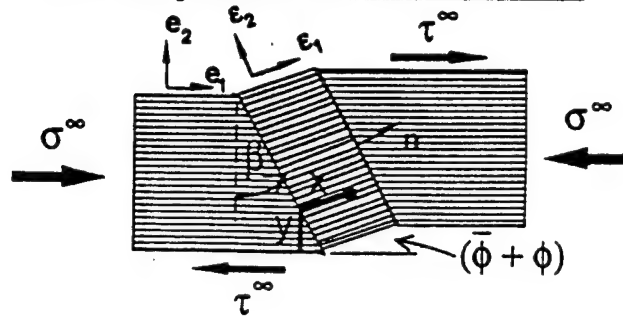
equilibrium: $\mathbf{n} \cdot \sigma^\infty = \mathbf{n} \cdot \sigma$

$$-\sigma^\infty \cos \beta \cos(\bar{\phi} + \phi) + \tau^\infty \sin(\beta + \bar{\phi} + \phi) = \tau \sin(\beta - \bar{\phi} - \phi) + \sigma_L \cos(\beta - \bar{\phi} - \phi)$$

$$\sigma^\infty \cos \beta \sin(\bar{\phi} + \phi) + \tau^\infty \cos(\beta + \bar{\phi} + \phi) = \tau \cos(\beta - \bar{\phi} - \phi) + \sigma_T \sin(\beta - \bar{\phi} - \phi)$$

$$\phi, \bar{\phi} \text{ small} \Rightarrow \sigma^\infty - 2\tau^\infty \tan \beta = \frac{\tau - \tau^\infty + \sigma_T \tan \beta}{\phi + \bar{\phi}}$$

Analysis: Kinematics



remote velocity: $\mathbf{v} = y\dot{\gamma}^\infty \mathbf{e}_1$

kink velocity: $\mathbf{v} = y\dot{\gamma}^\infty \mathbf{e}_1 + x\dot{\phi} \mathbf{e}_2$

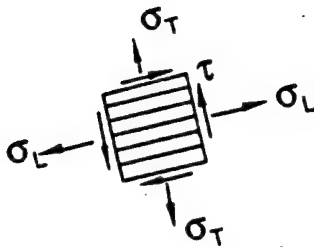
kink strain rate:

$$\begin{aligned} \dot{\boldsymbol{\epsilon}} &= \frac{1}{2} [\nabla \mathbf{v} + (\nabla \mathbf{v})^T] \equiv \frac{1}{2} \dot{\gamma} [\boldsymbol{\epsilon}_1 \boldsymbol{\epsilon}_2 + \boldsymbol{\epsilon}_2 \boldsymbol{\epsilon}_1] + \dot{\epsilon}_T \boldsymbol{\epsilon}_2 \boldsymbol{\epsilon}_2 \\ &= \frac{1}{2} [\dot{\phi} + \dot{\gamma}^\infty \cos \beta \sec(\beta - \phi - \bar{\phi}) \cos(\phi + \bar{\phi})] [\boldsymbol{\epsilon}_1 \boldsymbol{\epsilon}_2 + \boldsymbol{\epsilon}_2 \boldsymbol{\epsilon}_1] \\ &\quad + [\dot{\phi} \tan(\beta - \phi - \bar{\phi}) - \dot{\gamma}^\infty \cos \beta \sec(\beta - \phi - \bar{\phi}) \sin(\phi + \bar{\phi})] \boldsymbol{\epsilon}_2 \boldsymbol{\epsilon}_2 \end{aligned}$$

$\dot{\gamma}^\infty, \dot{\phi}, \dot{\bar{\phi}}$ small \Rightarrow

$$\begin{aligned} \gamma &= \phi + \gamma^\infty \\ \epsilon_T &= \phi \tan \beta \end{aligned}$$

Analysis: Constitutive Relations



assumed yield condition (ideal plasticity):

$$\left(\frac{\tau}{\tau_Y} \right)^2 + \left(\frac{\sigma_T}{\sigma_{TY}} \right)^2 = 1$$

strain-hardening, deformation-theory generalization:

$$\begin{aligned} \text{effective stress} &= \tau_e = \sqrt{\tau^2 + \sigma_T^2 / R^2} & R &= \frac{\sigma_{TY}}{\tau_Y} = \left(\frac{E_T}{G} \right)^{\frac{1}{2}} \\ \text{effective strain} &= \gamma_e = \sqrt{\gamma^2 + R^2 \epsilon_T^2} \end{aligned}$$

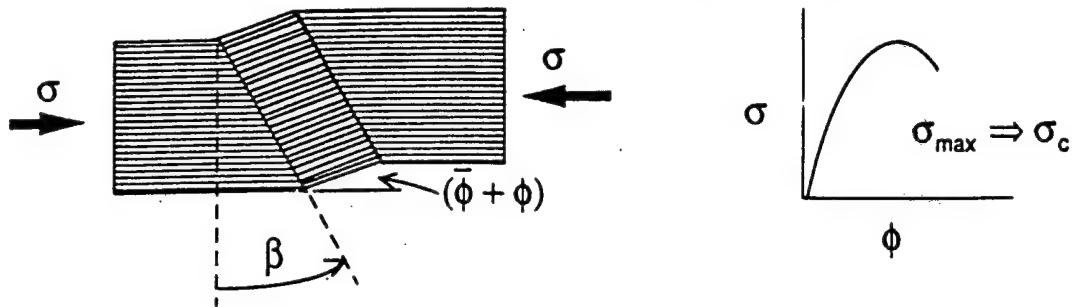
$$\begin{cases} \gamma = \left(\frac{\gamma_e}{\tau_e} \right) \tau \\ \epsilon_T = \left(\frac{\gamma_e}{\tau_e} \right) \frac{\sigma_T}{R^2} \end{cases}$$

Ramberg-Osgood

$$\frac{\gamma_e}{\tau_Y} = \frac{\tau_e}{\tau_Y} + \frac{3}{7} \left(\frac{\tau_e}{\tau_Y} \right)^n$$

$$\gamma_Y \equiv \frac{\tau_Y}{G}$$

Kinking Results: $\tau_{\infty}=0, \beta=0$

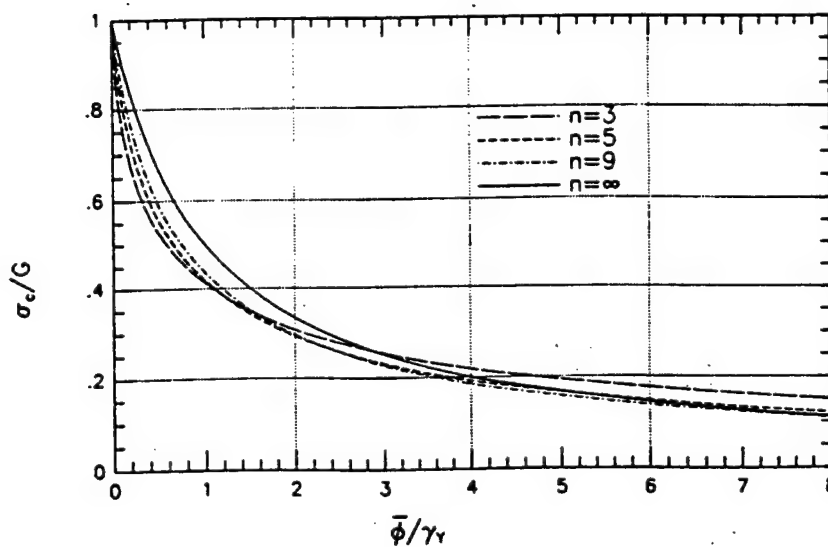
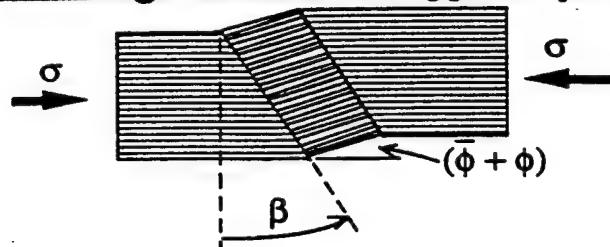


$$\frac{\sigma_c}{G} = \frac{1}{1 + n \left(\frac{3}{7} \right)^{\frac{1}{n}} \left(\frac{\bar{\phi} / \gamma_Y}{n-1} \right)^{\frac{n-1}{n}}}$$

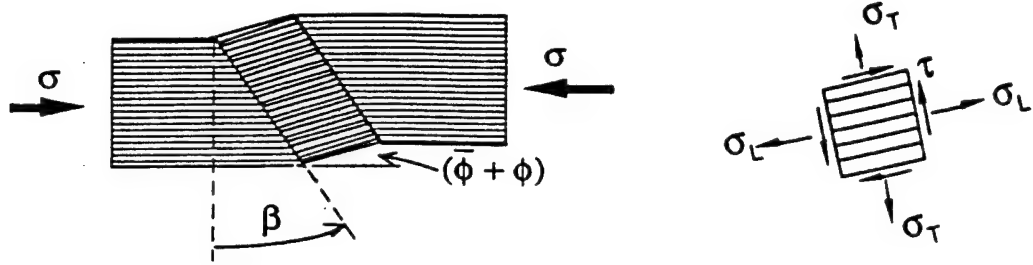
$$\bar{\phi} = 0 \text{ or } \gamma_Y = \infty \Rightarrow \sigma_c = G$$

$$n = \infty \Rightarrow \frac{\sigma_c}{G} = \frac{1}{1 + \bar{\phi} / \gamma_Y}$$

Kinking Results: $\tau_{\infty}=0, \beta=0$



Kinking Results: $\tau_{\infty}=0$, $\beta > 0$



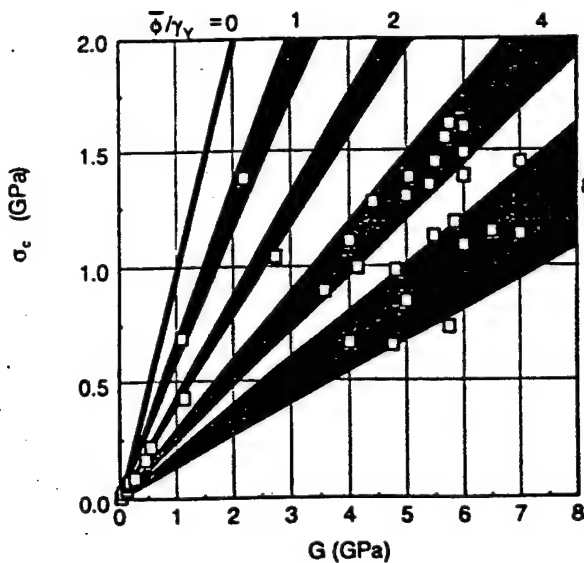
$$R = \frac{\sigma_{TY}}{\tau_Y} = \left(\frac{E_T}{G} \right)^{\frac{1}{2}} \quad \alpha = \sqrt{1 + R^2 \tan^2 \beta}$$

$$\frac{\sigma_c}{G^*} = \frac{1}{1 + n \left(\frac{3}{7} \right)^{\frac{1}{n}} \left(\frac{\bar{\phi}}{n-1} / \gamma_Y^* \right)^{\frac{n-1}{n}}} \quad G^* = \alpha^2 G$$

$$\gamma_Y^* = \gamma_Y / \alpha$$

Kinking Results: $\tau_{\infty}=0$, $\beta=20^\circ$, $R=2$

Bounds on σ_c for $3 < n < \infty$



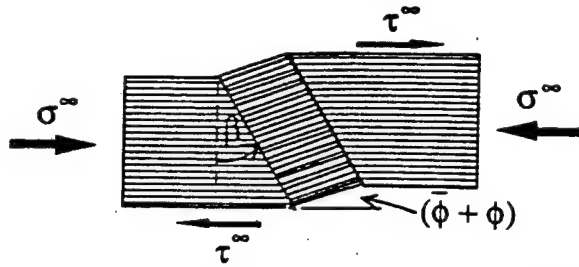
$$R = \frac{\sigma_{TY}}{\tau_Y} = \left(\frac{E_T}{G} \right)^{\frac{1}{2}}$$

$$\alpha = \sqrt{1 + R^2 \tan^2 \beta}$$

$$\left(\frac{\sigma_c}{G} \right)_{\min} = \alpha^2 \left[\frac{10}{7} + \alpha (\bar{\phi} / \gamma_Y) \right]^{-1}$$

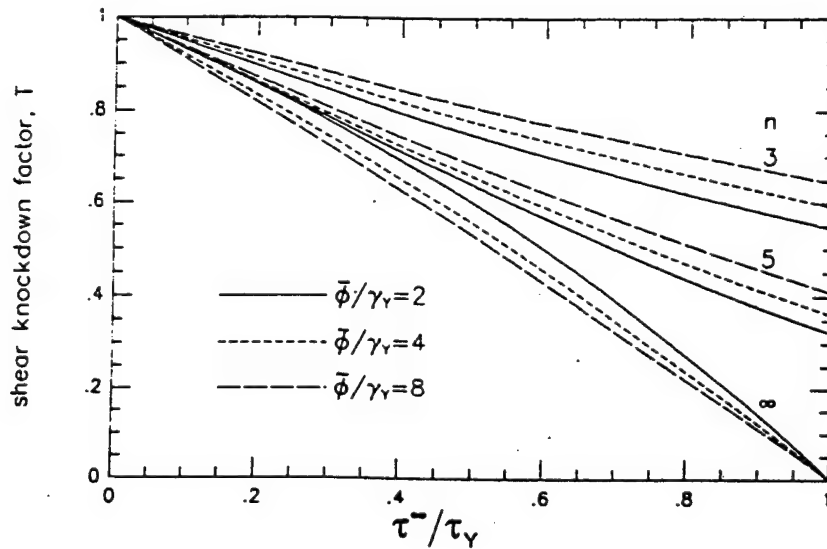
for $n = 1 + \frac{7}{3} (\bar{\phi} / \gamma_Y) \alpha$

Kinking Results: $\tau_\infty \neq 0, \beta = 0$

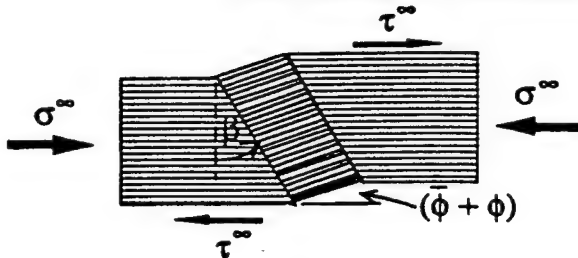


shear knockdown factor:

$$T \equiv \frac{\sigma_c}{\sigma_c|_{\tau^- = 0}}$$

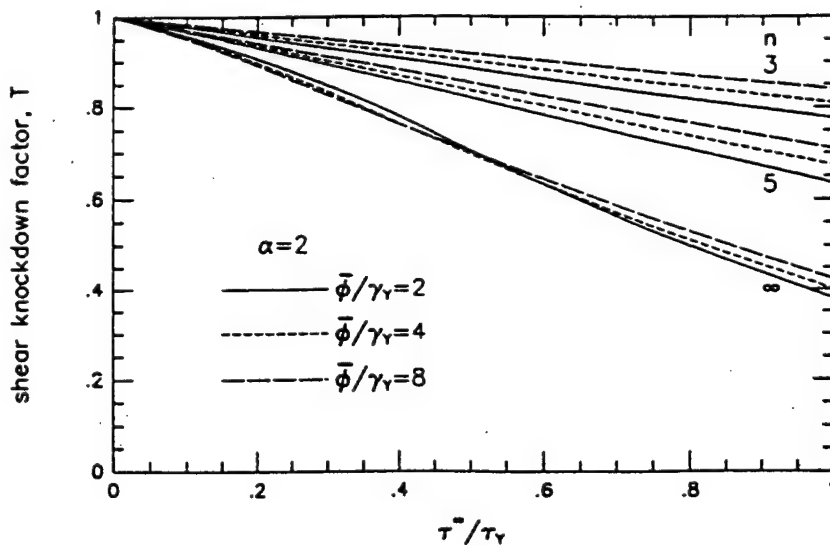


Kinking Results: $\tau_\infty \neq 0, \beta \neq 0$



shear knockdown factor:

$$T \equiv \frac{\sigma_c - 2\tau^- \tan \beta}{\sigma_c|_{\tau^- = 0}}$$



$$R = \frac{\sigma_{TY}}{\tau_Y} = \left(\frac{E_T}{G} \right)^{\frac{1}{2}}$$

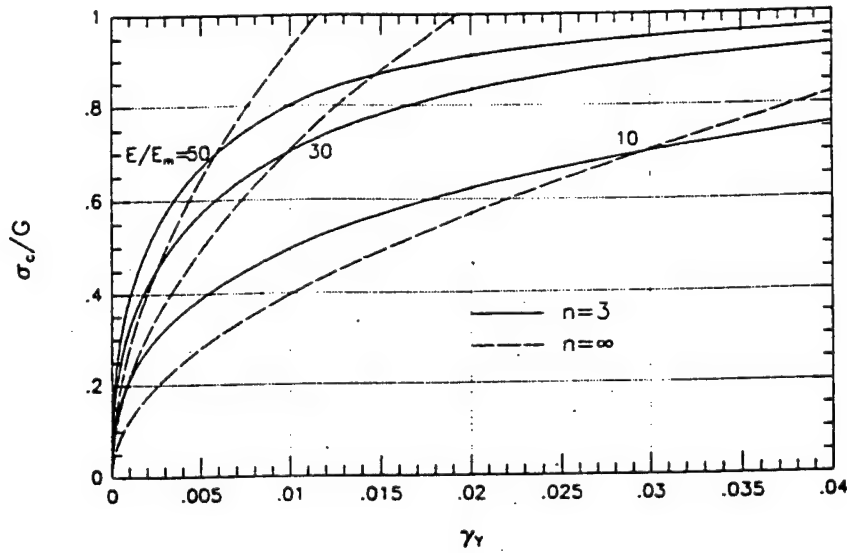
$$\alpha = \sqrt{1 + R^2 \tan^2 \beta}$$

Effect of Fiber Extensionality

Perfect fibers; $\beta=0$

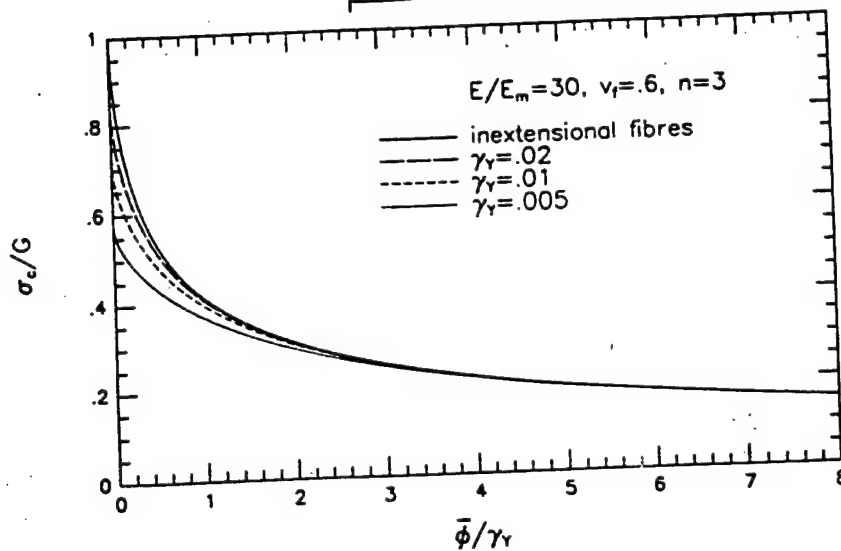
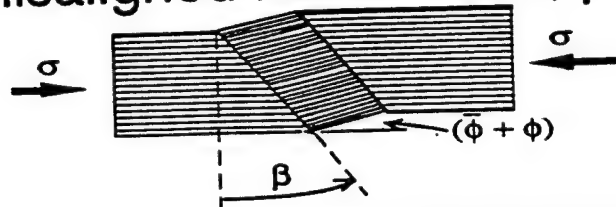
composite modulus = E
matrix modulus = E_m

composite shear yield strain = γ_y
fiber fraction $f = .6$



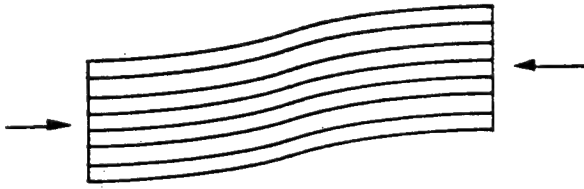
Effect of Fiber Extensionality

Misaligned fibers; $\beta=0$

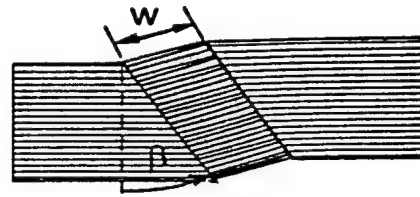
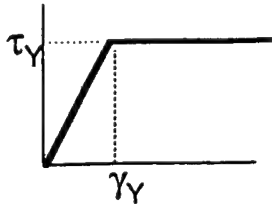


Kink-Width Analysis

Couple-stress theory



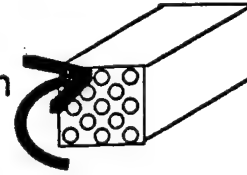
elastic-ideally plastic shear strains



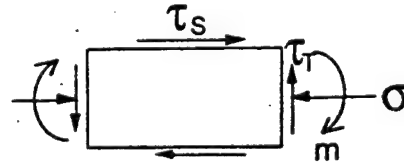
elastically bending fibers

couple stress m

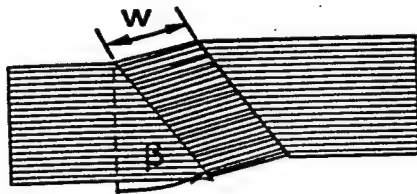
$$m = \left(\frac{f E_f d^2}{16} \right) \phi_x$$



$$\bar{\phi} = 0, \beta = 0 \Rightarrow \frac{\partial m}{\partial x} + \sigma \phi = \tau_s$$



Kink-Width Results

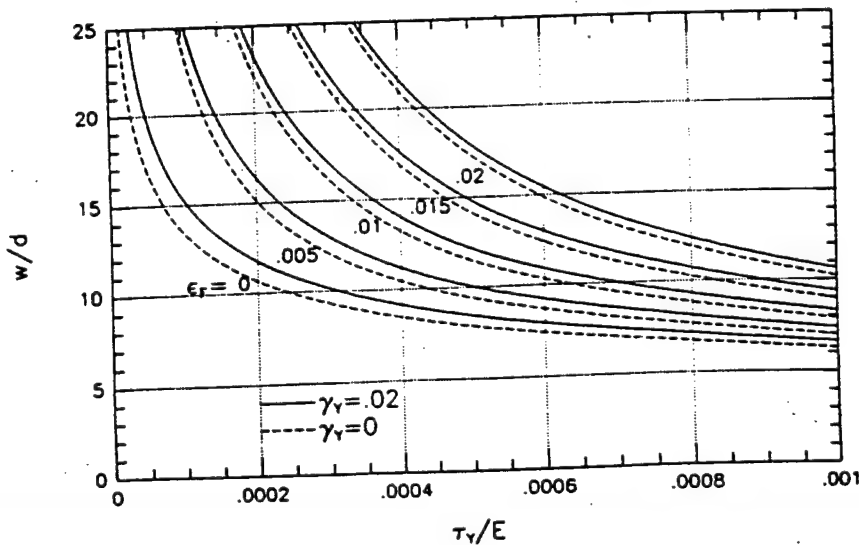


fiber diameter = d

composite shear yield stress = τ_Y

composite shear yield strain = γ_Y

composite modulus = E



$$\bar{\phi} = 0$$

$$\beta = 0$$

FIRE WRINKLING IN FILAMENT WINDING OF THICK CYLINDERS

H. Thomas Hahn
Mechanical, Aerospace and Nuclear Engineering Department
University of California, Los Angeles
Los Angeles, CA 90024-1597

Fibers in thick filament-wound cylinders are frequently found to be wrinkled. The wrinkled fibers lower the strength of the cylinder especially under external pressure and constitute one of the main strength-limiting defects. At present, the exact causes of fiber wrinkling are not well understood. Therefore, one of the main objectives of the present project is to identify when, where and how fibers wrinkle in the process of filament winding of thick cylinders.

To investigate the possibility of fiber wrinkling during winding, a special mandrel was made of an aluminum tube of 2.27 in. outside diameter and .135 in. wall thickness. The mandrel was fitted with a pair of end plates to allow monitoring of winding process at cylinder ends. Also, pressure gages were attached on the mandrel to measure pressure build-up as winding proceeded. Dry glass fiber tows were then wound in the hoop direction under different amounts of winding tension.

The winding tension had an interesting effect on the radial pressure measured at the mandrel surface and also on the compaction of the wound cylinder. When the winding tension was low, the pressure reached an equilibrium value immediately after the first few layers were wound. Winding of subsequent layers did not change the mandrel pressure even when more than 100 layers were added. When the winding tension was high, however, the pressure increased more gradually with increasing number of layers.

The winding tension had a significant effect on the cylinder thickness. The effective layer thickness in the cylinder decreased with increasing winding tension, indicating the presence of much slack between the layers. The fiber volume fraction thus depends strongly on the winding tension.

An elastic stress analysis was carried out to predict the radial pressure at mandrel surface. Since the radial modulus was not known, it was varied over an expected range. As the radial modulus was reduced to a value several orders of magnitude smaller than the hoop modulus, the predicted mandrel pressure began to behave similarly to the observed one. That is, most of the mandrel pressure was induced by the winding of the first few layers in agreement with the experimental observations. The analysis also provided a distribution of compressive hoop stress throughout most of the thickness. However, the magnitude of this compressive hoop stress was rather small, indicating that the likelihood of fiber wrinkling is rather little.

Plans for immediate future include helical winding and wet winding. Analytical correlation will continue as more experimental data becomes available.

OBJECTIVE

- To find processing conditions under which fiber wrinkling occurs in thick filament-wound cylinders

APPROACH

WINDING OF DRY FIBER TOWS

- Winding tension
- Winding angle
- Winding thickness

WINDING OF IMPREGNATED FIBER TOWS

- Winding temperature
- Winding compaction
- Cure cycle

CANDIDATE PARAMETERS

PROCESSING

- Winding tension
- Winding angle
- Winding temperature
- Winding compaction
- Winding thickness
- Mandrel diameters
- Mandrel properties

MATERIAL

- Tow size
- Tow bending stiffness
- Tow drapeability
- Resin viscosity during winding
- Cure kinetics
- Viscosity/temperature relationship

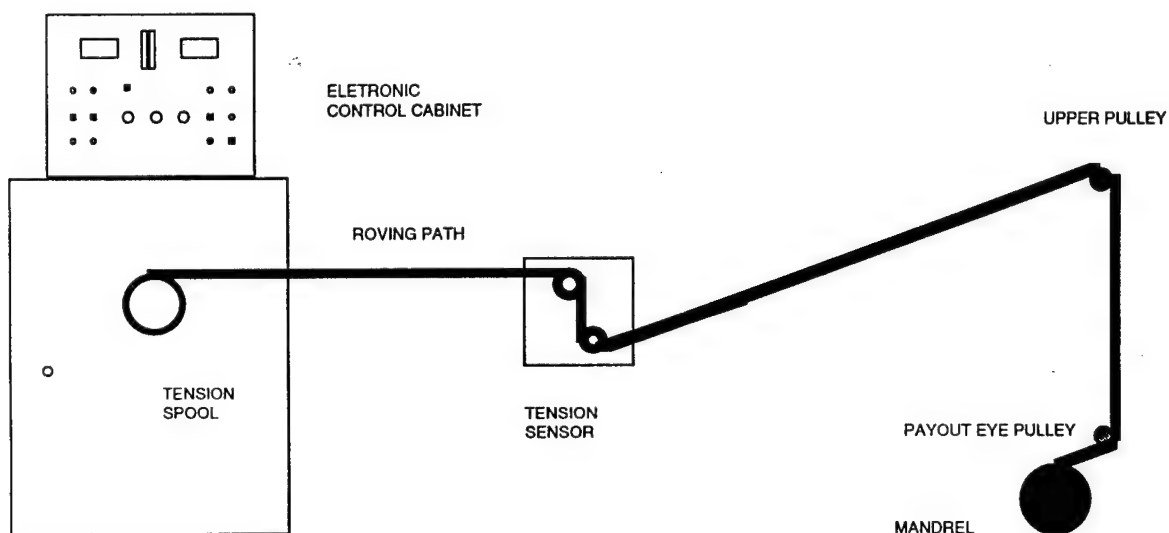
WINDING OF DRY FIBER TOWS

WINDING

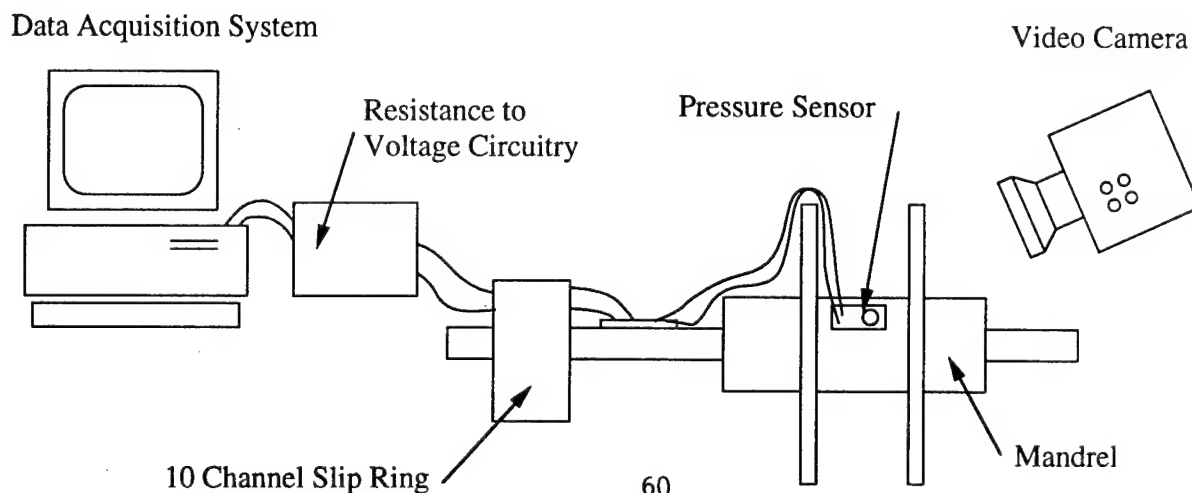
- Tension: 1 - 5 lb
- Angle: 90°
- Mandrel: 2.27 in. O.D., 0.135 in. thick, aluminum
- Length: 2 in.
- McClean Anderson winder

MATERIAL

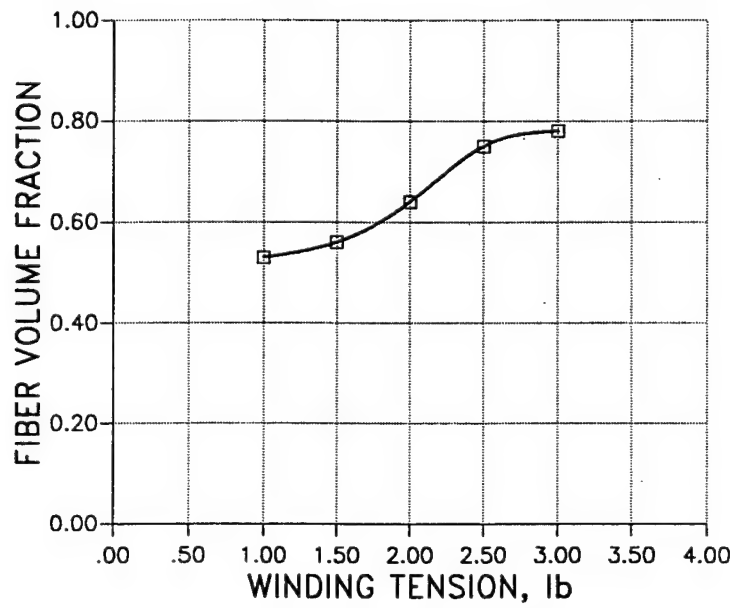
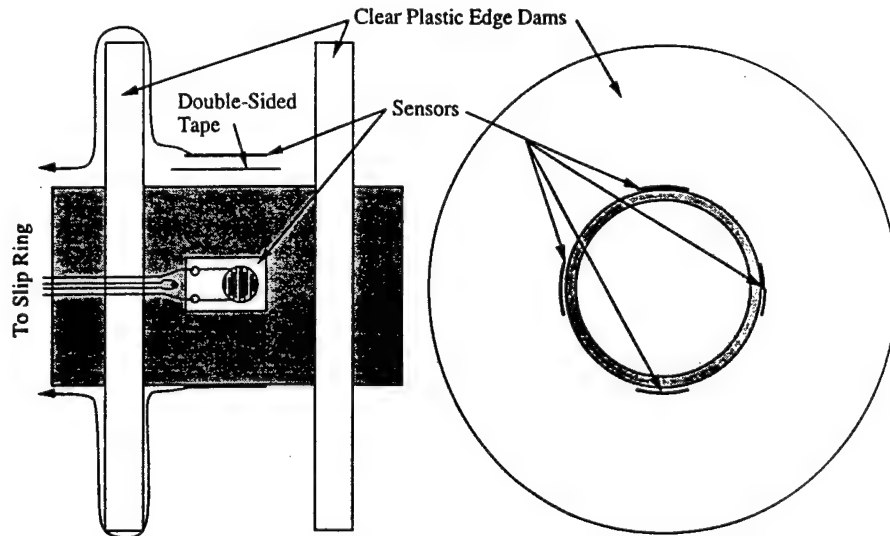
- E-glass: 13 μm diameter
- Silane sizing, uncured epoxy finish
- 5600 filaments/tow (7 groupings @ 800 ea.)
- Nominal tow dimensions: 0.13 in wide, 0.009 in. thick



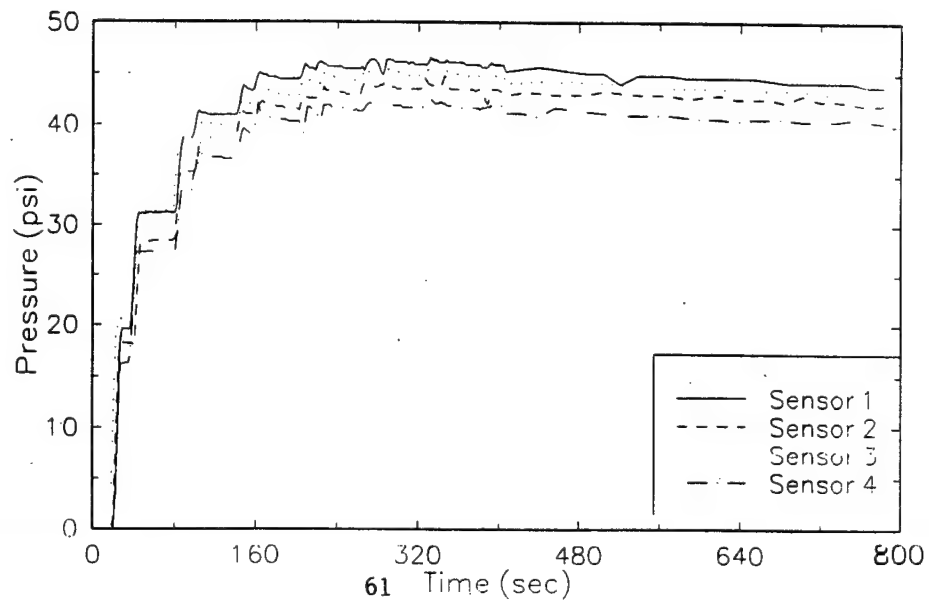
EXPERIMENTAL SETUP FOR VISUALIZING THE DEVELOPMENT OF WAVY LAYERS



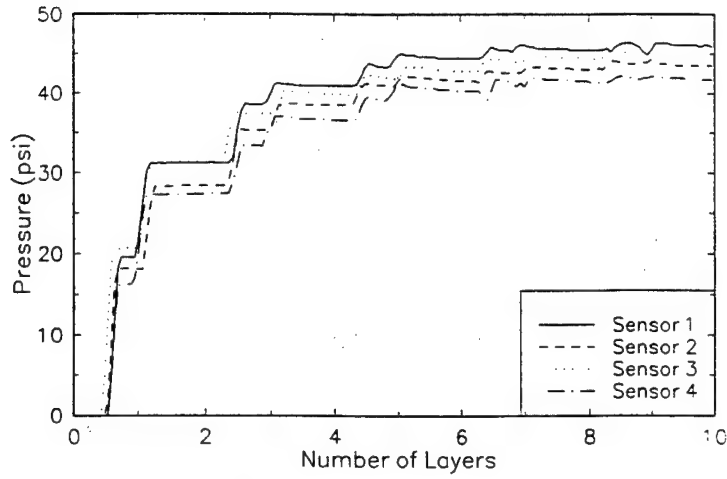
MANDREL/SENSOR ARRANGEMENT



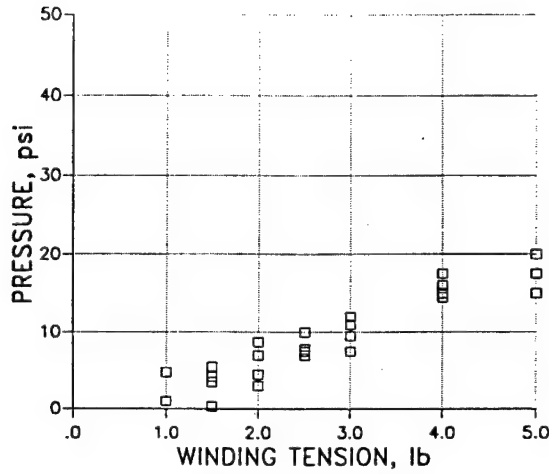
Experiment 0603921
5.0 lbs tension, dry glass



Experiment 0603921
5.0 lbs tension, dry glass



MANDREL PRESSURE AFTER FIRST LAYER



ANALYSIS

- Elastic**

- $$E_\theta = \nu_f E_r, \quad \nu_{\theta r} = \nu_f$$

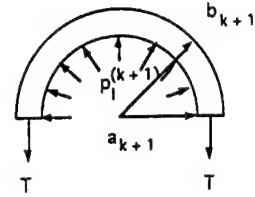
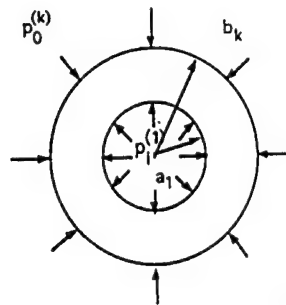
$$E_r = 0.5 - 2 \times 10^{-5} E_\theta$$

$$p_o^{(k)} = \frac{T}{b_k w}$$

$$\bar{\sigma}_\theta^{(k+1)} = \frac{T}{(b_{k+1} - a_{k+1}) w}$$

$$c_k = \frac{a_1}{b_k}$$

$$\beta = \left(\frac{E_\theta}{E_r} \right)^{\frac{1}{2}}$$



$$\Delta \sigma_r = \frac{p_o^{(1)} c_k^{\beta+1}}{1 - c_k^{2\beta}} \left[\left(\frac{r}{b_k} \right)^{\beta-1} - \left(\frac{r}{b_k} \right)^{-\beta-1} \right]$$

$$- \frac{p_o^{(k)}}{1 - c_k^{2\beta}} \left[\left(\frac{r}{b_k} \right)^{\beta-1} - c_k^{2\beta} \left(\frac{r}{b_k} \right)^{-\beta-1} \right]$$

$$\Delta \sigma_\theta = \frac{p_o^{(1)} c_k^{\beta+1} \beta}{1 - c_k^{2\beta}} \left[\left(\frac{r}{b_k} \right)^{\beta-1} + \left(\frac{r}{b_k} \right)^{-\beta-1} \right]$$

$$- \frac{p_o^{(k)} \beta}{1 - c_k^{2\beta}} \left[\left(\frac{r}{b_k} \right)^{\beta-1} + c_k^{2\beta} \left(\frac{r}{b_k} \right)^{-\beta-1} \right]$$

$$\Delta u_r = \frac{p_o^{(1)} c_k^{\beta+1} b_k}{E_\theta (1 - c_k^{2\beta})} \left[(\beta - \nu_{\theta r}) \left(\frac{r}{b_k} \right)^\beta + (\beta + \nu_{\theta r}) \left(\frac{r}{b_k} \right)^{-\beta} \right]$$

$$- \frac{p_o^{(k)} b_k}{E_\theta (1 - c_k^{2\beta})} \left[(\beta - \nu_{\theta r}) \left(\frac{r}{b_k} \right)^\beta + (\beta + \nu_{\theta r}) \left(\frac{r}{b_k} \right)^{-\beta} \right]$$

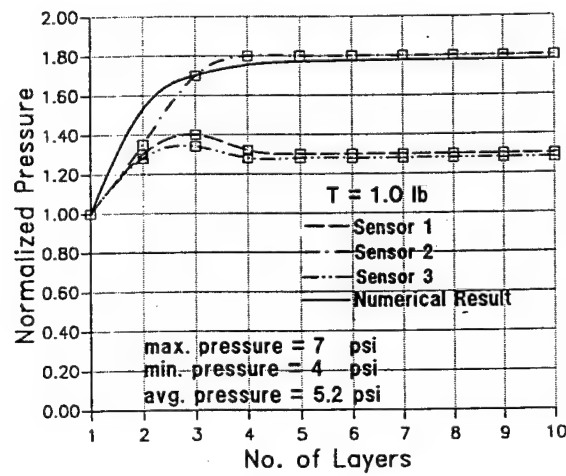
EFFECTIVE MATERIAL PROPERTIES

Properties	Winding Tension, lb				
	1	2	3	4	5
E_0, Msi	5.565	6.72	8.19	9.45	9.45
$\nu_{\theta r}$	0.22	0.22	0.22	0.22	0.22
E_r, psi	130	170	180	190	210
I'_f	0.53	0.64	0.78	0.90	0.90
Thickness, in.	0.0168	0.01392	0.0114	0.0089	0.0088

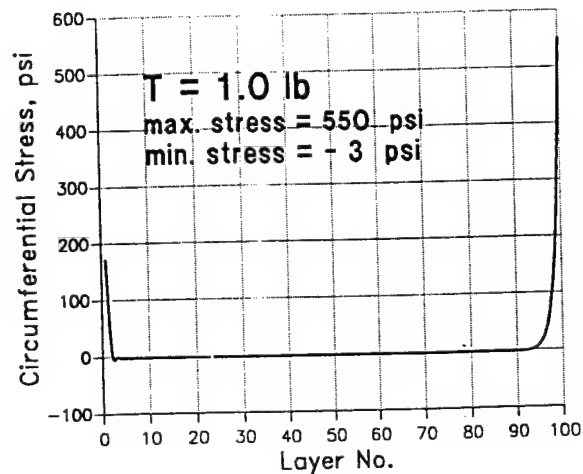
MANDREL PROPERTIES

$E_m = 10 \text{ Msi}$ $\nu_m = 0.33$
 $D_o = 2.268 \text{ in.}$ $D_i = 2.0 \text{ in.}$

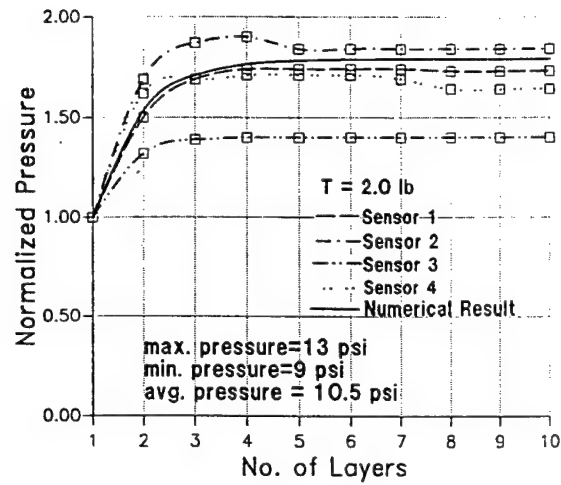
NORMALIZED MANDREL PRESSURE



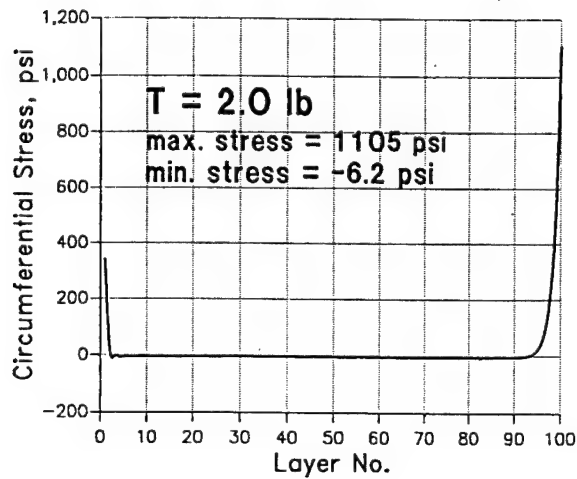
CIRCUMFERENTIAL STRESS IN CYLINDER



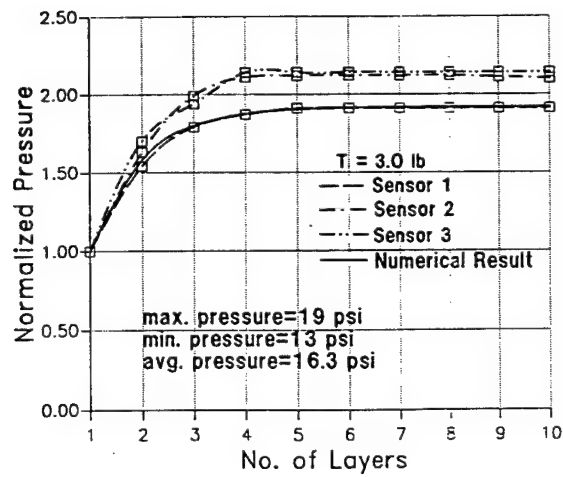
NORMALIZED MANDREL PRESSURE



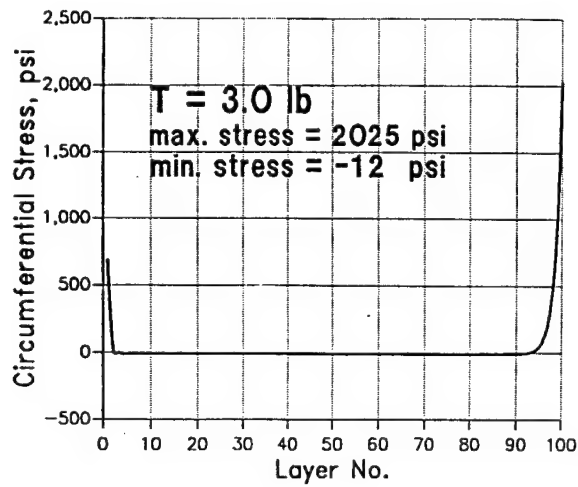
CIRCUMFERENTIAL STRESS IN CYLINDER



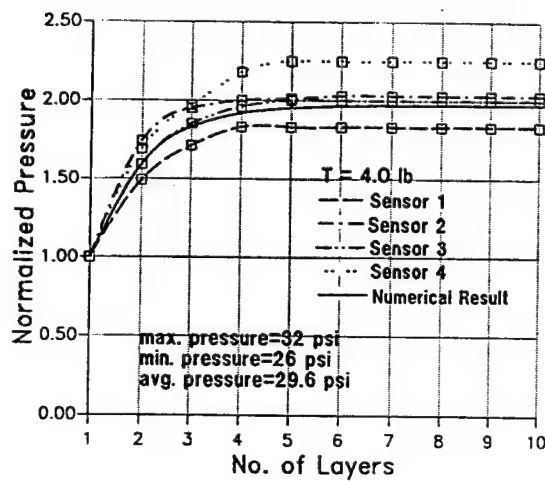
NORMALIZED MANDREL PRESSURE



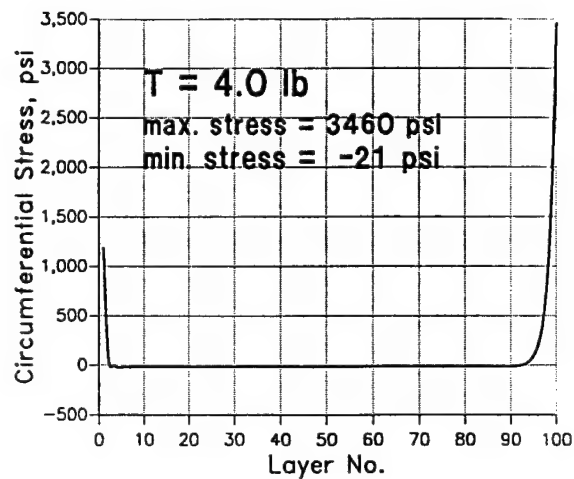
CIRCUMFERENTIAL STRESS IN CYLINDER



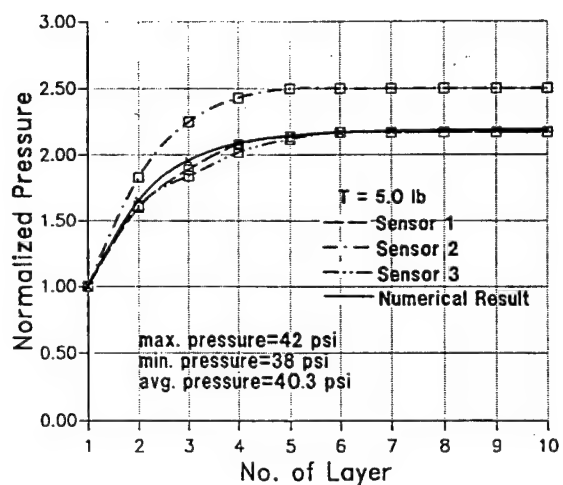
NORMALIZED MANDREL PRESSURE



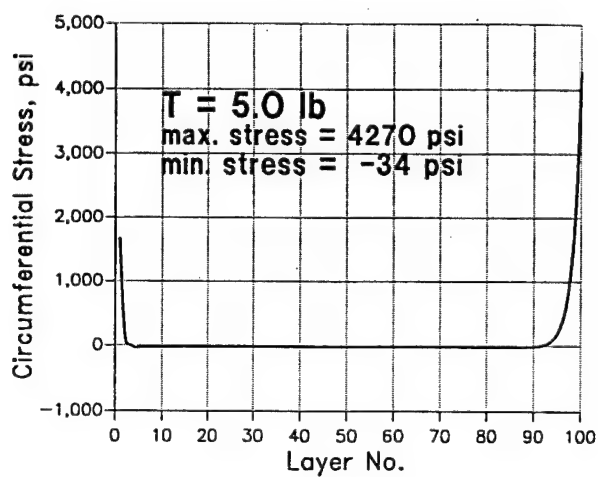
CIRCUMFERENTIAL STRESS IN CYLINDER



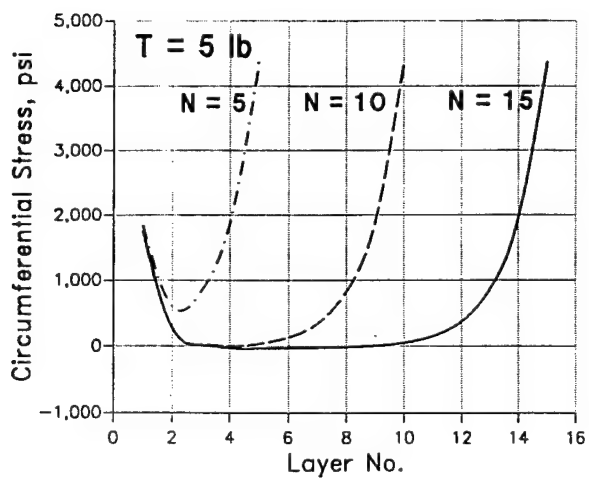
NORMALIZED MANDREL PRESSURE

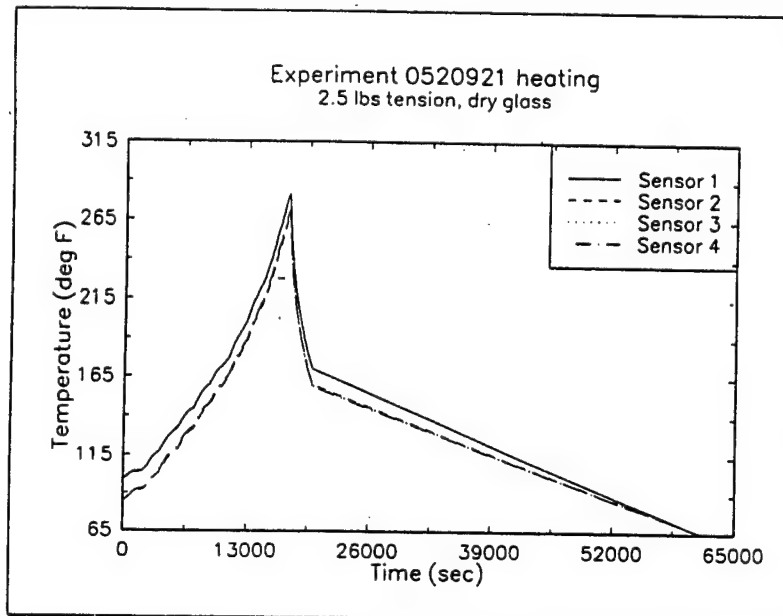
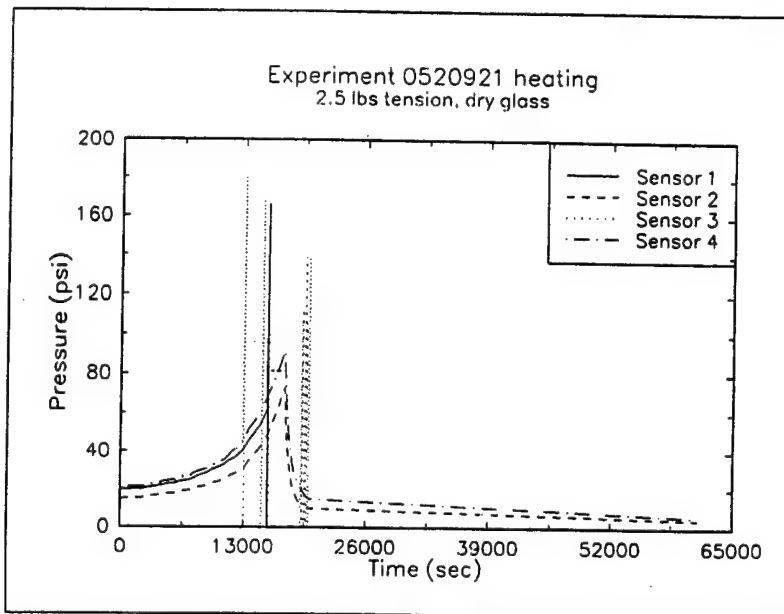


CIRCUMFERENTIAL STRESS IN CYLINDER



CIRCUMFERENTIAL STRESS VARIATION IN CYLINDER





CONCLUSIONS

- Mandrel pressure depends on winding of first few layers only.
- Effective fiber volume fraction increases with winding tension.
- Effective radial modulus increases with winding tension.
- Mandrel pressure is sensitive to effective radial modulus.
- Circumferential stress, although small, remains compressive throughout most of the inner part of the cylinder.
- Fiber wrinkling is not likely to occur because of the small circumferential stress.

PRESSURE-INDUCED NONLINEAR BEHAVIOR
OF FIBER-REINFORCED COMPOSITES

George J. Weng and Kook D. Pae
Department of Mechanical and Aerospace Engineering
Rutgers University, Piscataway, NJ 08855-0909

The objectives of the research is to determine experimentally and theoretically the effects of hydrostatic pressure on the mechanical behavior of graphite/epoxy composites. Hollow cylindrical samples with continuous and unidirectional fibers were fabricated from prepregs purchased from 3M Co. (SP-319 Scotchply) with four different fiber orientations, namely 0° , $+45^\circ$, -45° , and 90° with respect to the cylindrical axis (Fig.1). Samples of the matrix epoxy only were also fabricated and tested to established basis for comparison. The composite samples were tested in shear by applying torsion in a high pressure torsion apparatus (Fig.2-3). The apparatus is capable of containing pressure to 7 kbar and of operating at temperatures between -150 and 300°C . A low viscosity silicon oil (Dow Corning 200 Fluid) was used as the pressure transmitting fluid. The shear strain rate used was of 15%/min. The prepregs were made of 40% epoxy resin which consisted of Bisphenol A/epichlorohydrin epoxy resin (48%) and Epichlorohydrin-phenol-formaldehyde resin (40%). The curing agent was made up of polysulfone resin (4%), 3-[p-chlorophenyl]-1,1-dimethylurea (1%), and dicyandiamide (7%). The samples were coated with a rubber latex to prevent the penetration of the silicon oil.

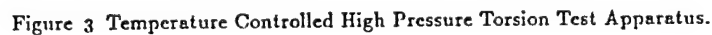
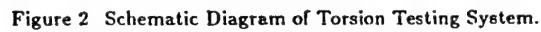
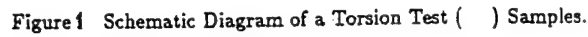
It has been determined that hydrostatic pressure induces non-linear shear stress-strain behavior in the normally linear elastic composites as well as epoxy samples. The shear stress-strain curves of the epoxy (Fig.4) and the composite samples (Fig.5-8) undergo dramatic changes. The amount of the changes in the composites depended upon pressure and fiber orientation. The in-plane shear modulus increased bilinearly with pressure with a break occurring at 2 kbar for epoxy (Fig.9) and all composites (Fig.10). The occurrence of the break has been attributed to pressure-induced shift of a secondary glass transition temperature to the ambient temperature. The secondary glass transition is believed to be due to segmental motion of molecules between the cross-links. The largest increase in the shear modulus occurred in the epoxy resin and the least in 0° samples. The yield strength (1% offset) also increased bilinearly with the break also at 2 kbar (Fig.11). The greatest increase was $+45^\circ$ and the least in 0° samples. With regard to the increase in ductility, the largest increase occurred in 0° samples from $\sim 9\%$ at atmospheric pressure to $\sim 58\%$ at 6 kbar (Fig.5). The increase in ductility was accompanied by the changes in the modes of fracture. For 0° composites, the fracture mode changed from interlaminar delamination at lower pressures to intralaminar shear at higher pressures (Fig.12); while for $+45^\circ$ composites, matrix fracture at lower pressures to fiber fracture at higher pressures (Fig.13). Mixed modes of the fracture occurred in the intermediate pressure. The changes in the modes of fracture were

often identifiable in the scanning electron micrographes (Figs. 14-15).

Theoretically, an energy approach is introduced to study the overall nonlinear behavior of fiber-reinforced composites. The theory makes use of a linear comparison composite to simulate the nonlinear deformation of the original composite (Fig.16), and it is applicable to an entire class of aligned short-fiber system. When the aspect ratio of inclusions is taken to infinity, the condition of fiber-reinforced composites is realized. The linear comparison composite is taken to possess the same microgeometry as the original one, but with a linear matrix whose elastic moduli tensor is set equal to the secant moduli tensor of the nonlinear matrix at a given stage of deformation. Since the overall elastic moduli of a linear composite are usually known, the overall secant moduli of the system is also known if the secant moduli of the matrix can be found. This was done by introducing a new definition for the effective stress of the heterogeneously deformed matrix on the basis of its average distortional energy.

The pressure-dependent constitutive equations of the epoxy matrix is then established, with its materials constants chosen to simulate the test data. With the proposed energy approach, the effective stress of the ductile matrix can be found as a function of pressure and the externally applied stress at a given concentration of fibers. The theory is then applied to predict the pressure dependence of the nonlinear behavior of the graphite/epoxy composites, and the simulated results are further compared with the experiment (Fig.17). The strength-differential effect of the composites are also studied at $p=4$ kbar, under axial tension and compression for three selected fiber concentrations (Fig.18). It is found that, at 15% of fibers, the compressive stress-strain curve is visibly higher than the tensile one. Under transverse loading, however, tensile stress-strain curves are clearly higher than the compressive ones (Fig.19). Such a strength-differential effect is also observed under plane-strain biaxial tension (Fig.20).

This combined experimental and theoretical investigation clearly points to the importance of high pressure on determining the overall nonlinear response of polymer-matrix fiber-reinforced composites. When properly utilized, high pressure can greatly enhance the overall performance of the composite systems.



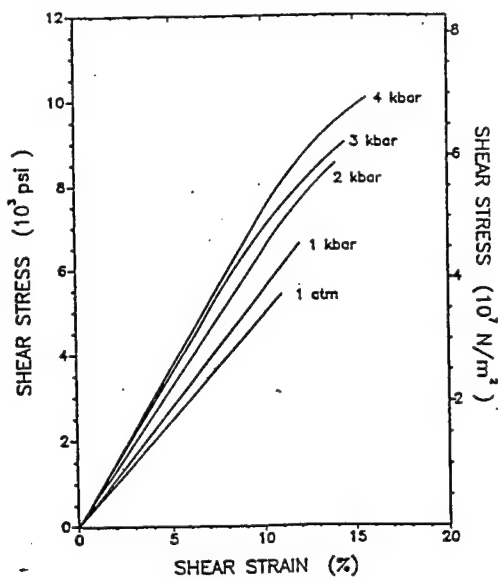


Figure 4: Some Typical Stress-Strain Curves of Matrix Material at Various Pressures in Shear.

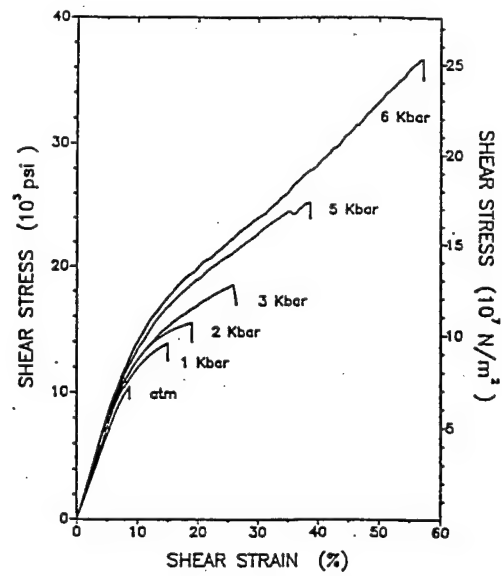


Figure 5: Typical Stress-Strain Curves of (0°) Unidirectional Composite Samples at Various Pressures in Shear.

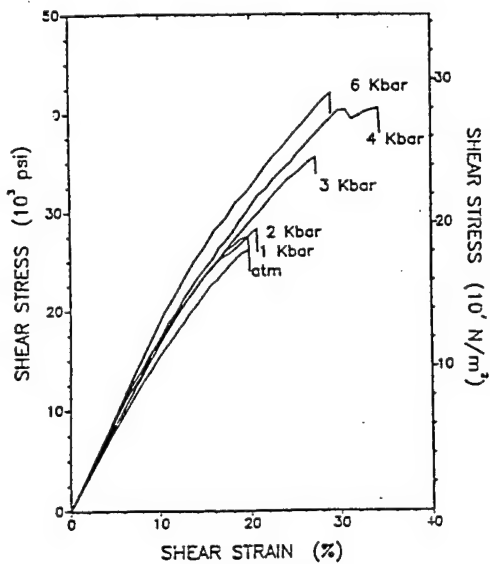


Figure 6: Typical Stress-Strain Curves of (+45°) Composite Samples at Various Pressures in Shear.

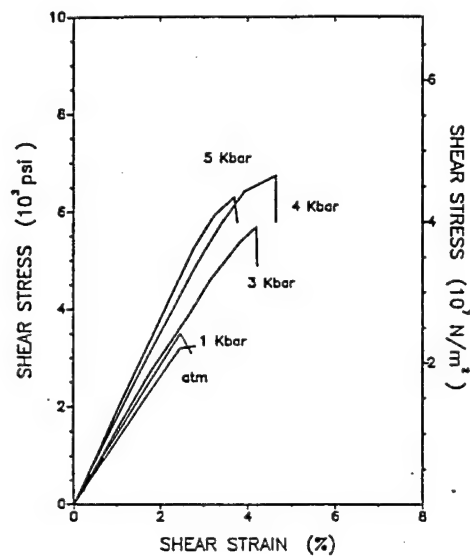


Figure 7: Some Typical Stress-Strain Curves of (-45°) Composite Samples in Shear.

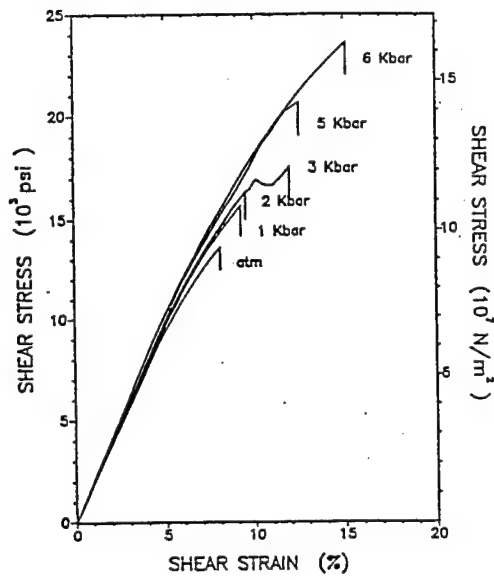


Figure 8 Typical Stress-Strain Curves of (90°) Composite Samples at Various Pressures in Shear.

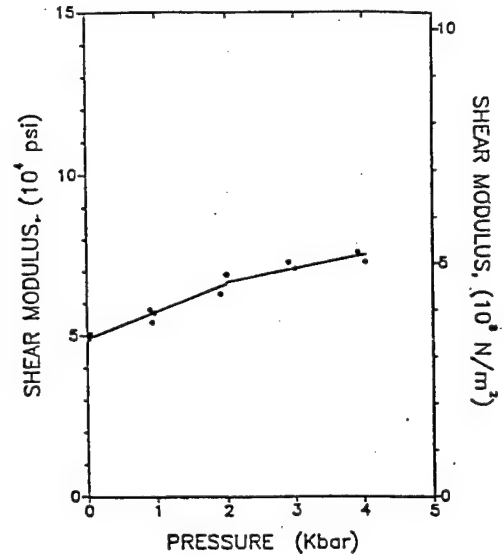


Figure 9 Torsional Shear Modulus vs. Pressure for Tubular Samples of Epoxy Matrix.

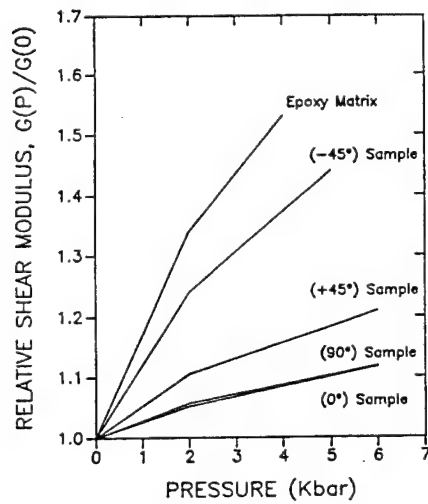


Figure 10 Relative Shear Modulus of Various Angle Composite and Epoxy Samples as a Function of Pressure in Shear.

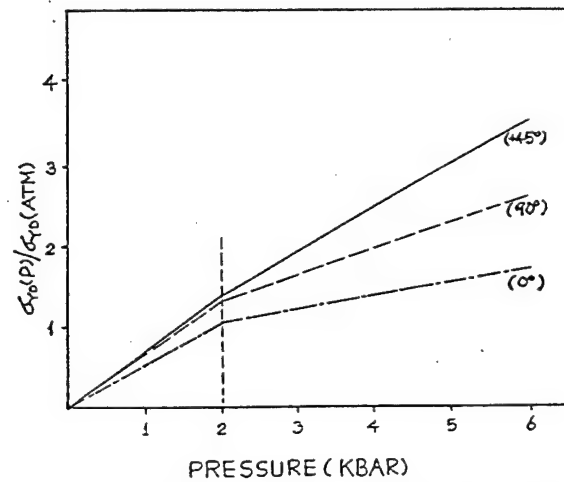


Fig. 11 Yield strength vs. pressure for (0), (90), and (45) composites

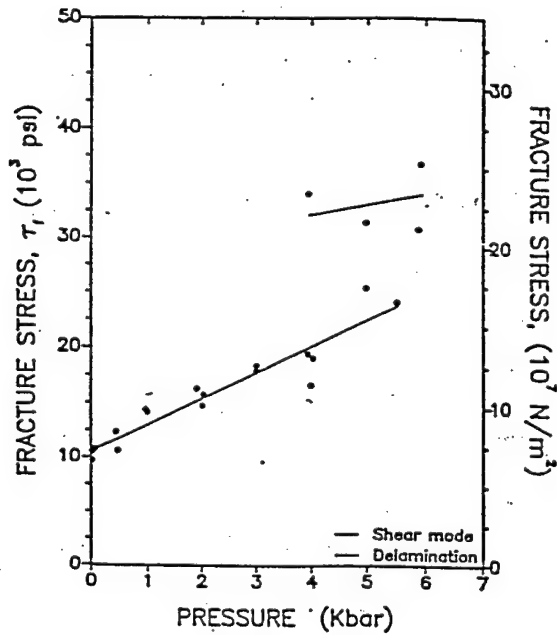


Figure 12 Fracture Strengths of (0°) Composite Samples at Various Pressures.

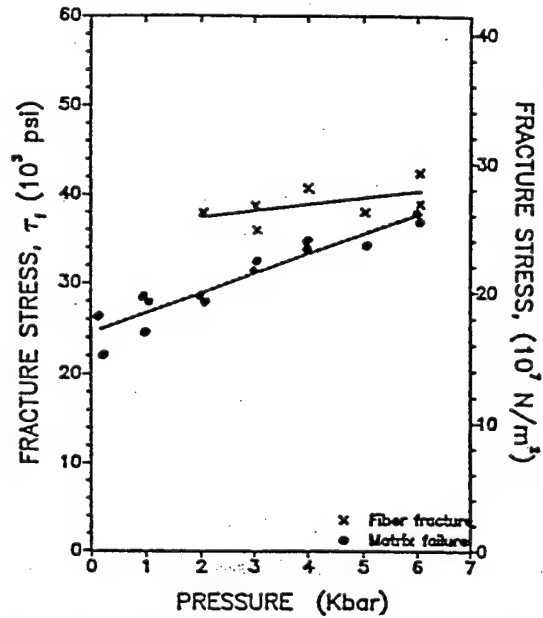


Figure 13 Fracture strengths vs. pressure for (+45°) composite samples.

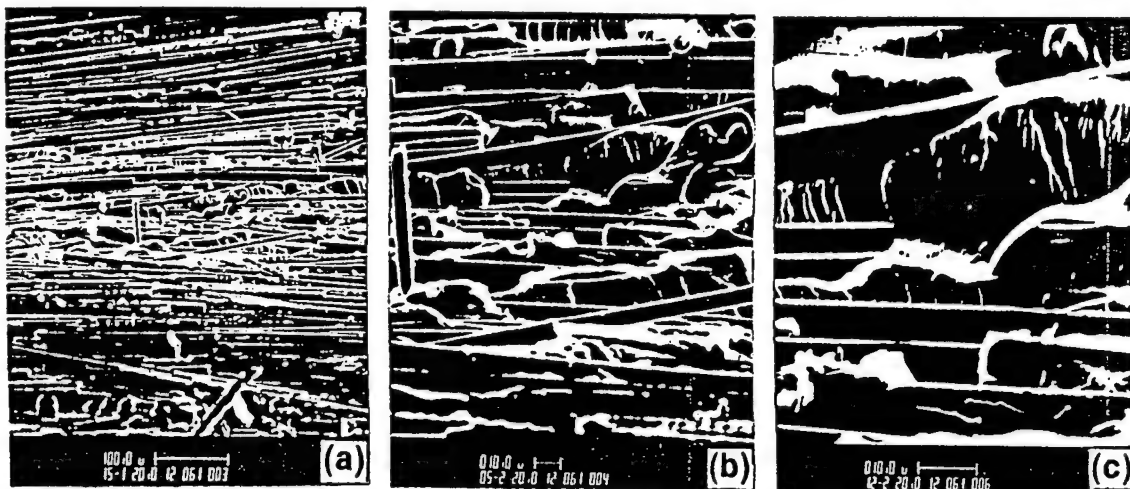


Figure 14 SEM Micrographs of Fracture Surface of a (+45°) Samples fractured in matrix failure at 4 kbar. (a) $\times 150$; (b) $\times 500$; (c) $\times 1200$.



Figure 15 SEM Micrographs of Fracture Surface of a (+45°) Samples fractured in a fiber fracture at 6 kbar. (a) $\times 250$; (b) $\times 700$; (c) $\times 1500$.

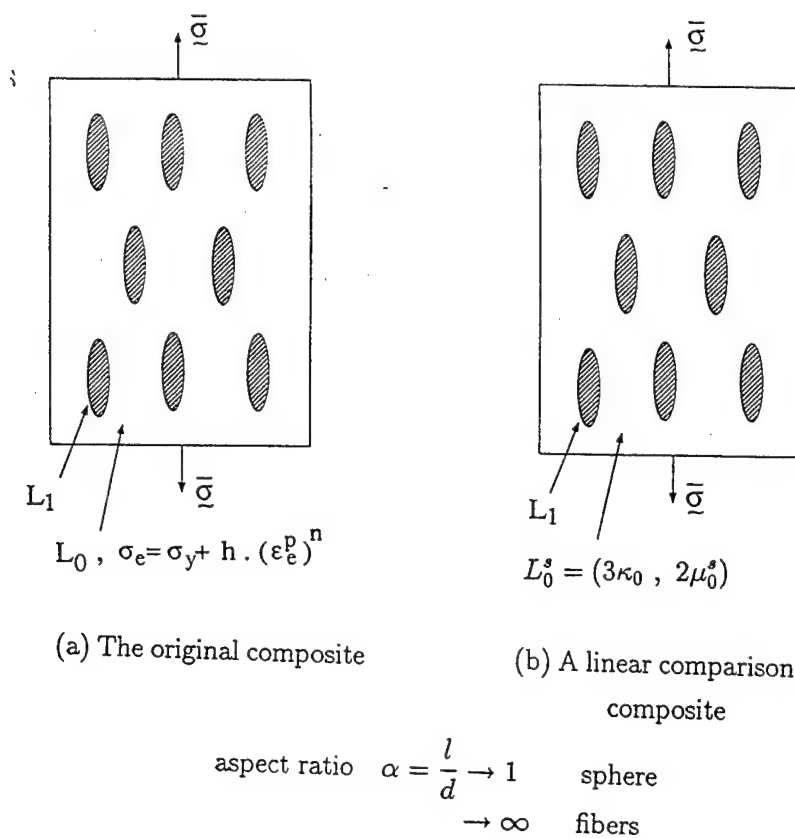


Fig.16. The original nonlinear composite (a) and the linear comparison composite (b).

For fiber-reinforced composites ($\alpha \rightarrow \infty$)

$$\begin{aligned}\frac{E_{11}^s}{E_0^s} &= c_1 E_1 + c_0 E_0^s + \frac{4c_1 c_0 (\nu_1 - \nu_0^s)^2}{\frac{c_1}{\bar{\kappa}_0^s} + \frac{c_0}{\bar{\kappa}_1} + \frac{1}{\mu_0^s}} \\ \nu_{12}^s &= c_1 \nu_1 + c_0 \nu_0^s + \frac{c_1 c_0 (\nu_1 - \nu_0^s) (\frac{1}{\bar{\kappa}_0^s} - \frac{1}{\bar{\kappa}_1})}{\frac{c_1}{\bar{\kappa}_0^s} + \frac{c_0}{\bar{\kappa}_1} + \frac{1}{\mu_0^s}} \\ \frac{\mu_{12}^s}{\mu_0^s} &= 1 + \frac{c_1}{\frac{\mu_0^s}{\mu_1 - \mu_0^s} + \frac{c_0}{2}} \\ \frac{\mu_{23}^s}{\mu_0^s} &= 1 + \frac{c_1}{\frac{\mu_0^s}{\mu_1 - \mu_0^s} + \frac{c_0}{2} \frac{(\bar{\kappa}_0^s + 2\mu_0^s)}{(\bar{\kappa}_0^s + \mu_0^s)}} \\ \bar{\kappa}_{23}^s &= \bar{\kappa}_0^s + \frac{c_1}{\frac{1}{\bar{\kappa}_1 - \bar{\kappa}_0^s} + \frac{c_0}{\bar{\kappa}_0^s + \mu_0^s}}\end{aligned}$$

$$\bar{\sigma}_{ij} = \bar{\sigma}_{ij}^{sup} - \delta_{ij} p$$

$$\begin{aligned}\frac{c_0}{3\mu_0^s} \sigma_e^{(0)2} &= \frac{1}{E_{11}^s} \bar{\sigma}_{11}^{sup2} + \frac{1}{E_{22}^s} (\bar{\sigma}_{22}^{sup2} + \bar{\sigma}_{33}^{sup2}) - \frac{2\nu_{12}^s}{E_{11}^s} \bar{\sigma}_{11}^{sup} (\bar{\sigma}_{22}^{sup} + \bar{\sigma}_{33}^{sup}) \\ &+ \left(\frac{2}{E_{22}^s} - \frac{1}{\mu_{23}^s} \right) \bar{\sigma}_{22}^{sup} \bar{\sigma}_{33}^{sup} - \frac{2}{E_{11}^s} (1 - 2\nu_{12}^s) p \bar{\sigma}_{11}^{sup} \\ &- \left(\frac{4}{E_{22}^s} - \frac{2\nu_{12}^s}{E_{11}^s} - \frac{1}{\mu_{23}^s} \right) p (\bar{\sigma}_{22}^{sup} + \bar{\sigma}_{33}^{sup}) \\ &+ \left(\frac{1}{E_{11}^s} - \frac{4\nu_{12}^s}{E_{11}^s} + \frac{4}{E_{22}^s} - \frac{1}{\mu_{23}^s} \right) p^2 + \frac{1}{\mu_{23}^s} \bar{\sigma}_{23}^{sup2} + \frac{1}{\mu_{12}^s} (\bar{\sigma}_{12}^{sup2} + \bar{\sigma}_{13}^{sup2}) \\ &- \frac{c_0}{\kappa_0} p_{(local)}^2 - \frac{c_1}{3\mu_1} \bar{\sigma}_e^{(1)2} - \frac{c_1}{9\kappa_1} \bar{\sigma}_{kk}^{(1)2}\end{aligned}$$

Under $\bar{\sigma}_{11}^{sup}$

$\bar{\sigma}_{11}^{sup} \rightarrow \text{tension}(+) , \sigma_e^{(0)} \text{ decreases}$

$\bar{\sigma}_{11}^{sup} \rightarrow \text{compression}(-) , \sigma_e^{(0)} \text{ increases}$

The amount of increase or decrease is controlled by $\frac{1}{E_{11}^s}$.

Flow Stress

$$\sigma_f = \sigma_0 + m.p + h(\epsilon_e^p)^n$$

$\bar{\sigma}_{11}^{sup} \rightarrow \text{tension}(+) , p_{(local)} \downarrow , \text{ so } \sigma_f \downarrow$

$\bar{\sigma}_{11}^{sup} \rightarrow \text{compression}(-) , p_{(local)} \uparrow , \text{ so } \sigma_f \uparrow$

But under compression, the increase in the effective stress $\sigma_e^{(0)}$ is not sufficient (to be divided by the large E_{11}^s) to offset the increase in the flow stress σ_f . So the overall response is harder in axial compression.

Under $\bar{\sigma}_{22}^{sup}$

$\bar{\sigma}_{22}^{sup} \rightarrow \text{tension}(+) , \sigma_e^{(0)} \text{ decreases}$

$\bar{\sigma}_{22}^{sup} \rightarrow \text{compression}(-) , \sigma_e^{(0)} \text{ increases}$

but the change is larger now, as E_{22}^s is much lower than E_{11}^s . So, under compression, the increase in the effective stress $\sigma_e^{(0)}$ is more than enough to offset the increase in the flow stress σ_f . So its overall response is softer in transverse compression.

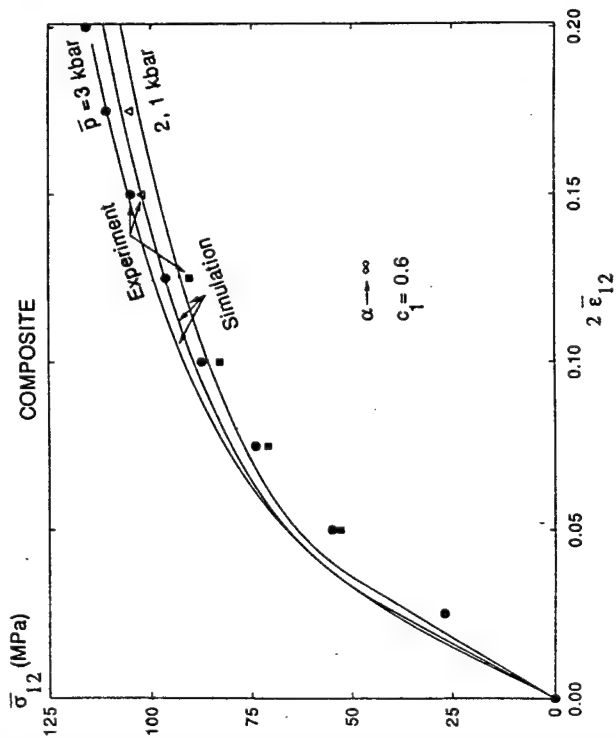


Fig. 17. Comparison between the theoretically predicted pressure dependence and the experimental one for the composite under a superimposed shear loading.

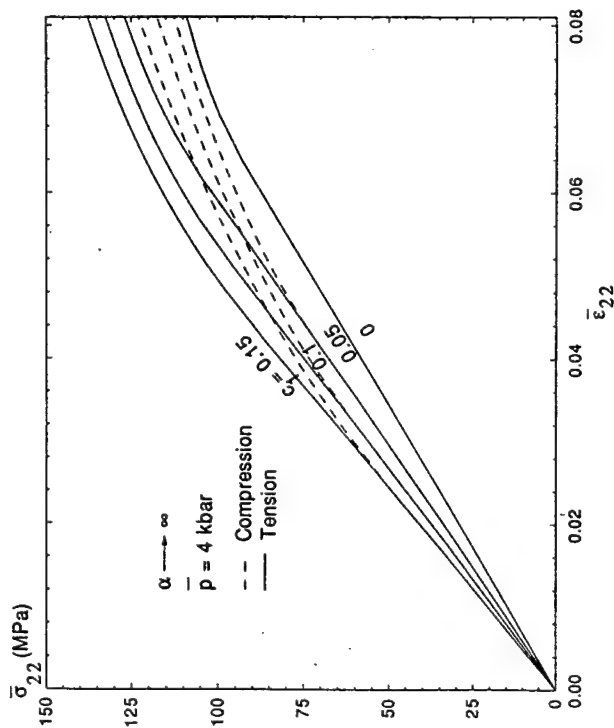


Fig. 19. Strength differential effect for the composite between transverse tension and compression under high pressures.

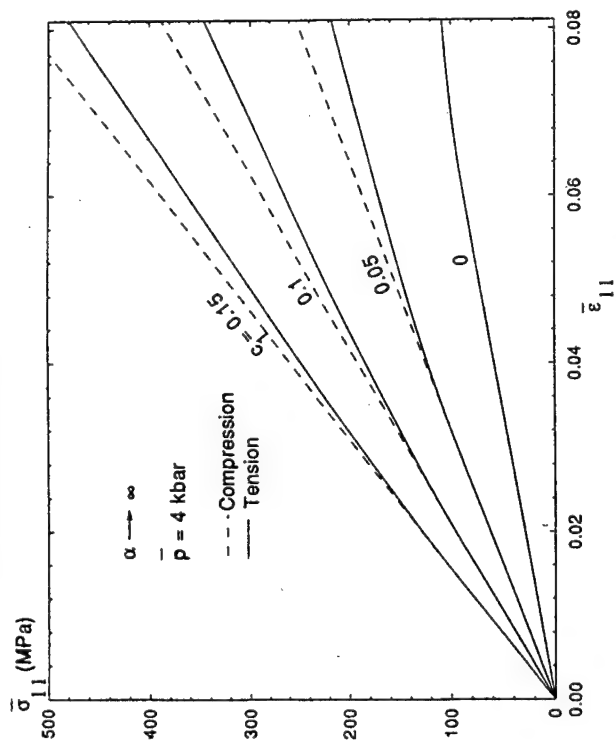


Fig. 18. Strength differential effect for the composite between axial tension and compression under high pressures.

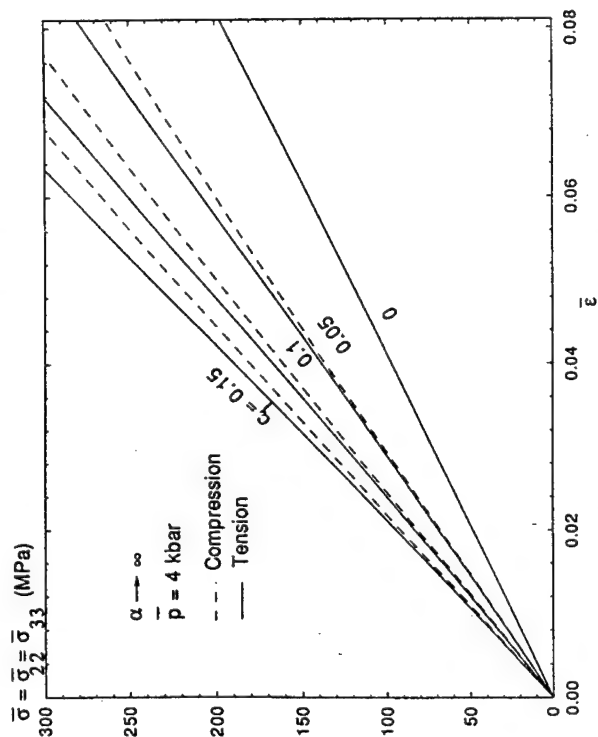


Fig. 20. Strength differential effect for the composite between biaxial tension and compression under high pressures.

INTERACTIVE BUCKLING IN RING-STIFFENED COMPOSITE SHELLS

Srinivasn Sridharan and Akihito Kasagi
Washington University in St.Louis, MO 63130

A major objective of this research effort has been to develop a novel and computationally effective procedure for the study of interaction of local and overall instabilities of composite stiffened cylindrical shells under hydrostatic pressure. The methodology must provide insights into the essential features of structural response under mode interaction and potentially facilitate optimization of design. This is sought to be achieved by a judicious combination of an asymptotic procedure for the postbuckling response in individual modes and the amplitude modulation technique in the treatment of nonlinear interaction. Computation is further simplified by the use of displacement functions which are simple trigonometric functions in the circumferential direction and p-version type polynomials in the other two orthogonal directions. A 3-D approach is used which facilitates the computation of interlaminar stresses associated with buckling. The paper presents the results of:

(i) A study of local and overall buckling using a 3-D p-version axisymmetric finite elements.

(ii) Postbuckling analyses of local and overall instabilities using Koiter's asymptotic approach; exact trigonometric variations of the displacements in the circumferential ($-\theta$) directions are employed in conjunction with p-version type polynomials in the axial (x-) and radial (z-) directions.

(iii) A preliminary study on the interaction of local and overall instabilities. As a preamble, the concept and the necessity of amplitude modulation is established. The results show severe imperfection-sensitivity associated with the interaction and underline the importance of the problem.

Buckling Problem:

The displacement functions characterizing the buckling mode are taken in the form:

$$\{\mathbf{u}^{(1)}\} = \{\mathbf{u}^c(r, x)\} \cos(n\theta) + \{\mathbf{u}^s(r, x)\} \sin(n\theta)$$

where the functions of x and r are chosen in the form of p-version type polynomials. The chosen trigonometric form provide "exact" variations and account for anisotropy. Three-dimensional nonlinear strain-displacement relations in polar coordinates are employed in the analysis. Typically for an unstiffened shell made of specially orthotropic laminate an element spans half the shell in the x-direction and one or more layers in the thickness directions. A bay of a stiffened shell is divided into four zones: two half shell skins on either side of the stiffener, the junction zone and the stiffener. Each of these zones may be further subdivided in the thickness direction as elements. Convergence studies demonstrate the effectiveness of the chosen scheme and provide a means of quantifying errors due to the neglect of shear deformation, use of simpler shell theories such as Donnell's and the influence of anisotropy.

Postbuckling Response:

Koiter's asymptotic procedure is employed in the postbuckling analysis in individual modes. First the "exact" circumferential variation of the second order displacement-field is derived. This takes the form:

$$\{u^{(2)}\} = \{u^o(r, x)\} + \{u^c(r, x)\} \cos(2n\theta) + \{u^s(r, x)\} \sin(2n\theta)$$

Once again p-version type polynomials are used in the x- and r- directions. Finally the load-displacement relationship is expressed in terms of terms of ξ , the scaling parameter of the buckling mode is expressed in the simple form:

$$\frac{\lambda}{\lambda_c} = 1 + \lambda_2 \left(\frac{\xi}{h} \right)^2$$

where λ is the loading parameter, λ_c its critical value, h the thickness of the shell and λ the index of the postbuckling response. If λ_2 is negative, the shell is imperfection-sensitive, i.e., the maximum capacity of the shell is smaller than the critical value in the presence of imperfections. The cylindrical shells under hydrostatic loading were found to be imperfection-sensitive, with longer shells (longer bays for local buckling) showing less imperfection-sensitivity in comparison to the shorter ones. Detailed convergence studies have been performed and wherever possible comparisons have been made with currently available results.

Interactive Buckling: Concept of Amplitude Modulation:

The interaction of a single local mode (wave number n) and the overall mode (wave number m) produces additional patterns of deformation, which to the first order of approximation are given by the mixed second order field that arises by the interaction. An examination of the character of the mixed second order field shows that several neighboring local modes, viz. those associated with wave numbers of .. $n-2m, n-m, n+m, n+2m...$ etc are triggered by the interaction. It is shown that these additional modes can be simply taken into account by letting the amplitude of the primary local mode (wave number n) vary according to a "slowly varying" function which is periodic with a wave length of $2\pi/m$.

Nonlinear Analysis and Imperfection-sensitivity:

A potential energy function is generated in terms of the degrees of freedom defining the amplitude modulating function, viz. ξ_i , ($i \neq 1$) and the scaling factor for the overall mode, ξ_1 and the initial imperfection parameters. It is found the most critical term that controls the interaction is the cubic term $\xi_i \xi_j \xi_1$, ($i, j \neq 1$). Complete nonlinear response characteristic is generated as the load parameter is λ is varied. It is found that the imperfection-sensitivity is severe when the two critical pressures are close to each other. For an overall imperfection of 1% of the radius and a local imperfection of 1% of the thickness, the reduction in the load carrying capacity can be of the order of the 50% from the critical values. The buckling is expected to be catastrophic as indicated by the severely reentrant postbuckling load-displacement characteristics.

BUCKLING ANALYSIS : Sample results

Material Properties: $E_{11} = 20,000$ ksi , $E_{22} = E_{33} = 2100$ ksi,
 $G_{12} = G_{13} = 850$ ksi, $\nu_{12} = \nu_{13} = \nu_{23} = 0.21$

(a) Convergence of buckling pressures q_{cr} (ksi) for a [0/90/90/0] laminate with $R/h = 10$, and $Z = 100$ ($h = 5$ in, $L/h = 31.6$)

p_r level	p_x level			
	1	2	3	4
Single element covering four layers				
2	6.810	4.031	3.993	3.992
3	6.774	3.991	3.954	3.954

3 - elements, each homogeneous				
2	6.771	3.991	3.954	3.954
3	6.758	3.977	3.941	3.941

**(b) Comparison with Jones et al. for [0/90/90/0] shell
 $R/h = 50$ ($h = 1$ in) (q_{cr} in psi)**

Z^*	Present formulation	Jones et al
10	601.3 (n=10)	634.7 (n= 10)
500	79.92 (n =4)	76.85 (n= 4)
10000	27.16 (n =3)	18.91 (n =2)

Note :

$$Z = \frac{L^2}{Rh} \sqrt{(1-\nu^2)} ; \quad Z^* = \frac{L^2}{Rh} \sqrt{(1-4\nu_{12}^2 F^2 / (1+F)^2)} \quad \text{where } F = \frac{E_{11}}{E_{22}}$$

**(c) Buckling Pressures of Shells
with differing lay-up sequences
(R/h = 10, h = 5 in.)**

Z	Buckling Pressures q_{cr} (ksi)		
	[0/90/90/0] (n)	[90/0/0/90] (n)	[0/90/0/90] (n)
10	12.421 (5)	16.253 (3)	14.033 (4)
500	2.284 (2)	6.190 (2)	3.817 (2)
10000	1.509 (2)	5.650 (2)	3.196 (2)

**(d) Comparison of Overall Buckling Pressures
Between the present and "smeared" formulations
Isotropic Material, E = 10000 ksi, ν = 0.33, R/h = 50, h = 1in.
(Shell is reinforced with six equispaced stiffeners of 2in. x 1in.)**

Buckling pressures q_{cr} in psi, (L variable)			
Z	Stiffened Shells		Unstiffened
	Present (n)	Hutchinson, et al (n)	present
50	1729 (5)	1741 (5)	564 (7)
1000	249 (3)	239 (3)	135 (3)
5000	109 (2)	81 (2)	71 (2)
10000	64 (2)	54 (2)	42 (2)

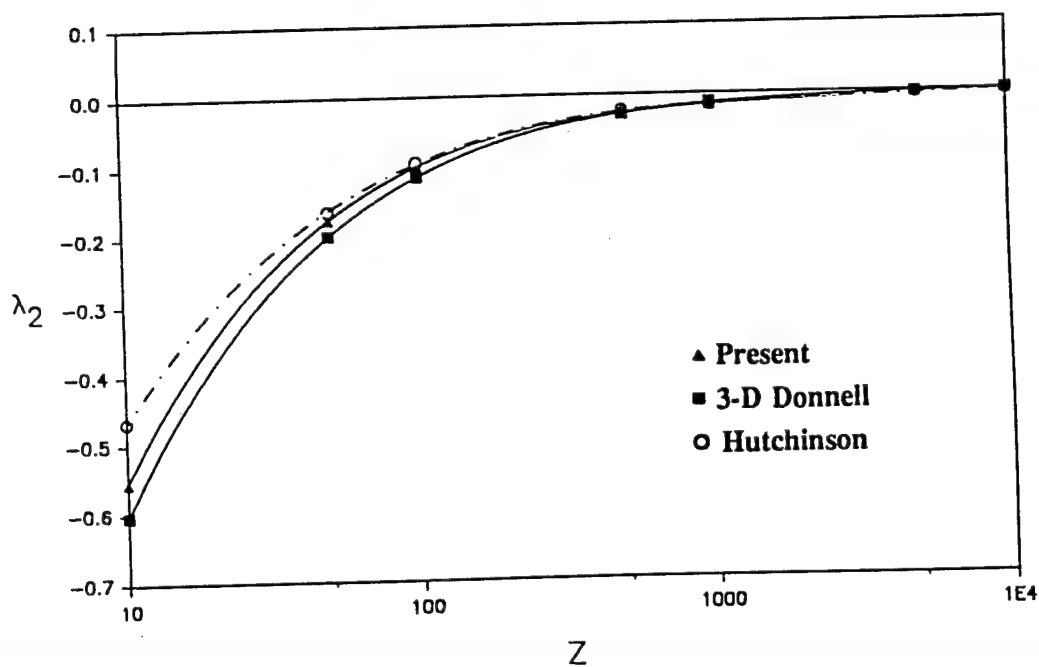
POSTBUCKLING ANALYSIS IN INDIVIDUAL MODES

(a) λ_2 for a simply supported unstiffened shell
 [0/90/90/0] laminate, $R/h = 10$, ($h = 5$ in) and $Z = 100$ ($L/h = 31.6$)
 (Buckling mode computed with 3 elements, $p_r = 3$, $p_x = 5$)

A Convergence Study

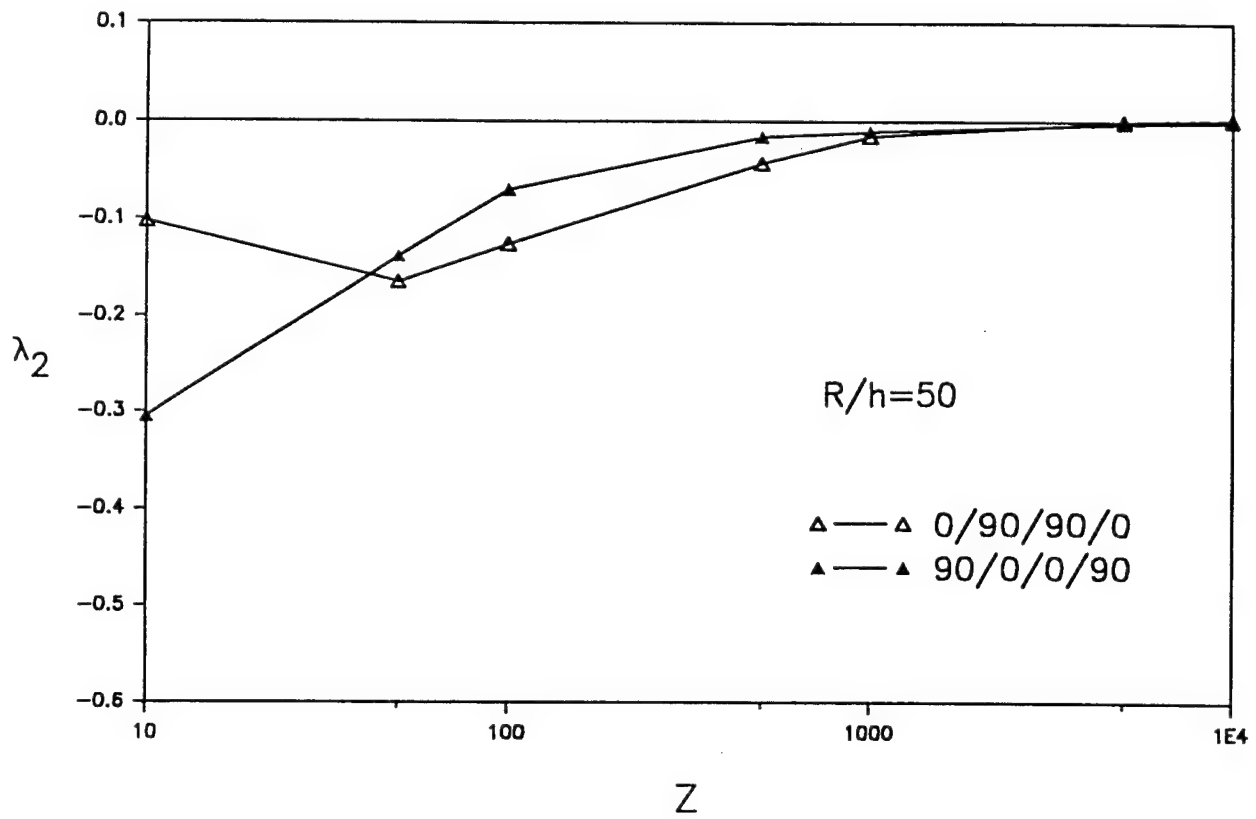
p_r level	p_x level			
	1	2	3	4
Single element covering four layers				
2	+0.054	-0.0379	-0.125	-0.127
3	+0.053	-0.0396	-0.128	-0.129
3 - elements, each homogeneous				
2	+0.053	-0.0399	-0.128	-0.130
3	+0.052	-0.0404	-0.129	-0.130

(b) Comparison with Hutchinson's results
 for unstiffened isotropic shell ($R/h = 50$)



(c) Imperfection-sensitivity of Laminated Shells

Sample results for cross-ply laminate shells.

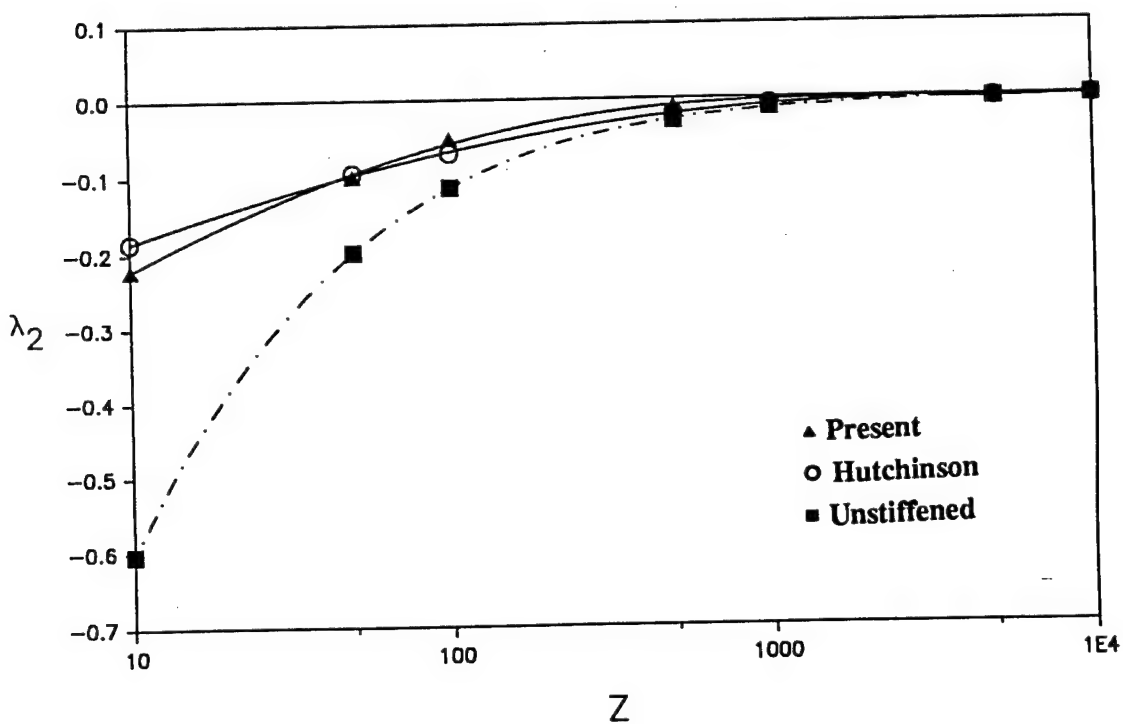


(d) Imperfection-sensitivity under Overall Buckling

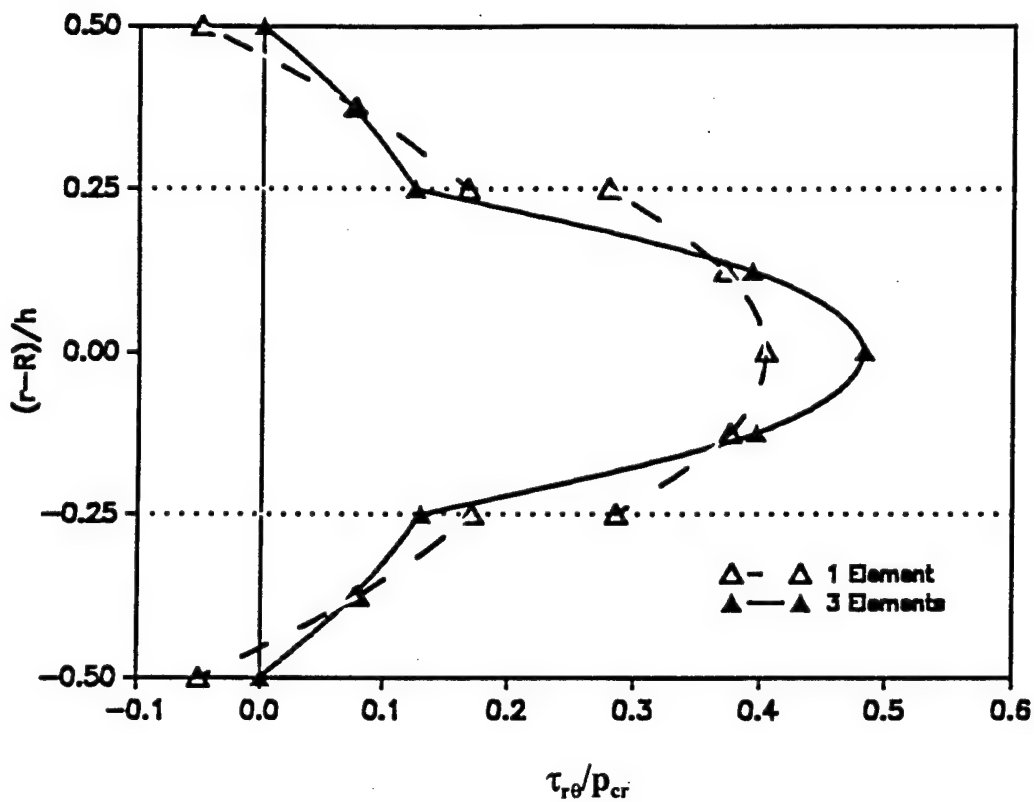
Comparison between the present and "smeared" formulations

Isotropic Material, $E = 10000$ ksi, $\nu = 0.33$, $R/h = 50$, $h = 1$ in.

(Shell is reinforced with six equispaced stiffeners of 2 in. x 1 in.)



(e) Distribution of Critical Interlaminar stress ($\tau_{r\theta}$)
 [0/90/90/0] laminate, $R/h = 10$, $Z = 100$, $h = 5$ in.



Variation of Peak shearing stress in the circumferential direction
 across the thickness, when the maximum shell deflection = $h/10$.
 ($p_{cr} = 3.941$ ksi, $n = 3$)

Interactive Buckling Example

Dimensions : $R/h = 50$

$L/h = 20$

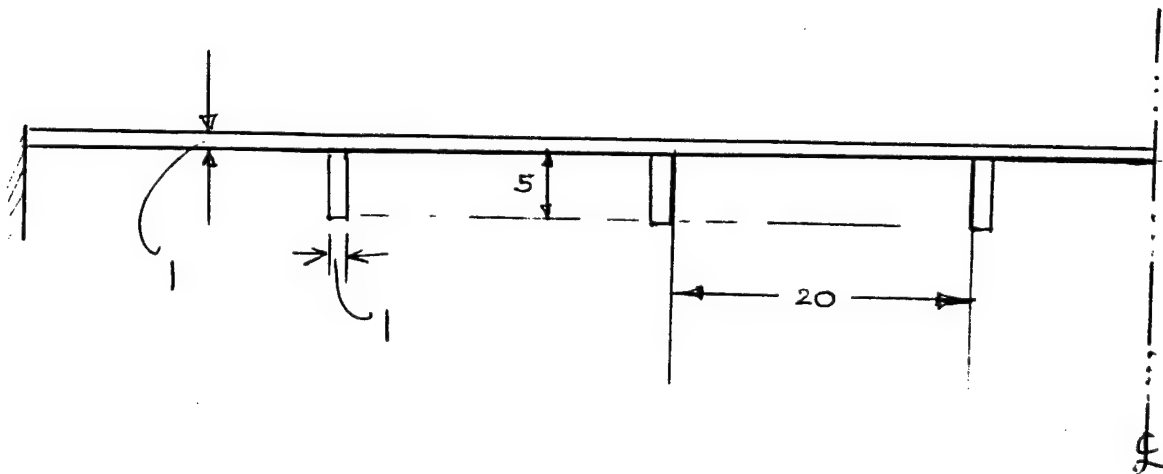
$d/h = 5$

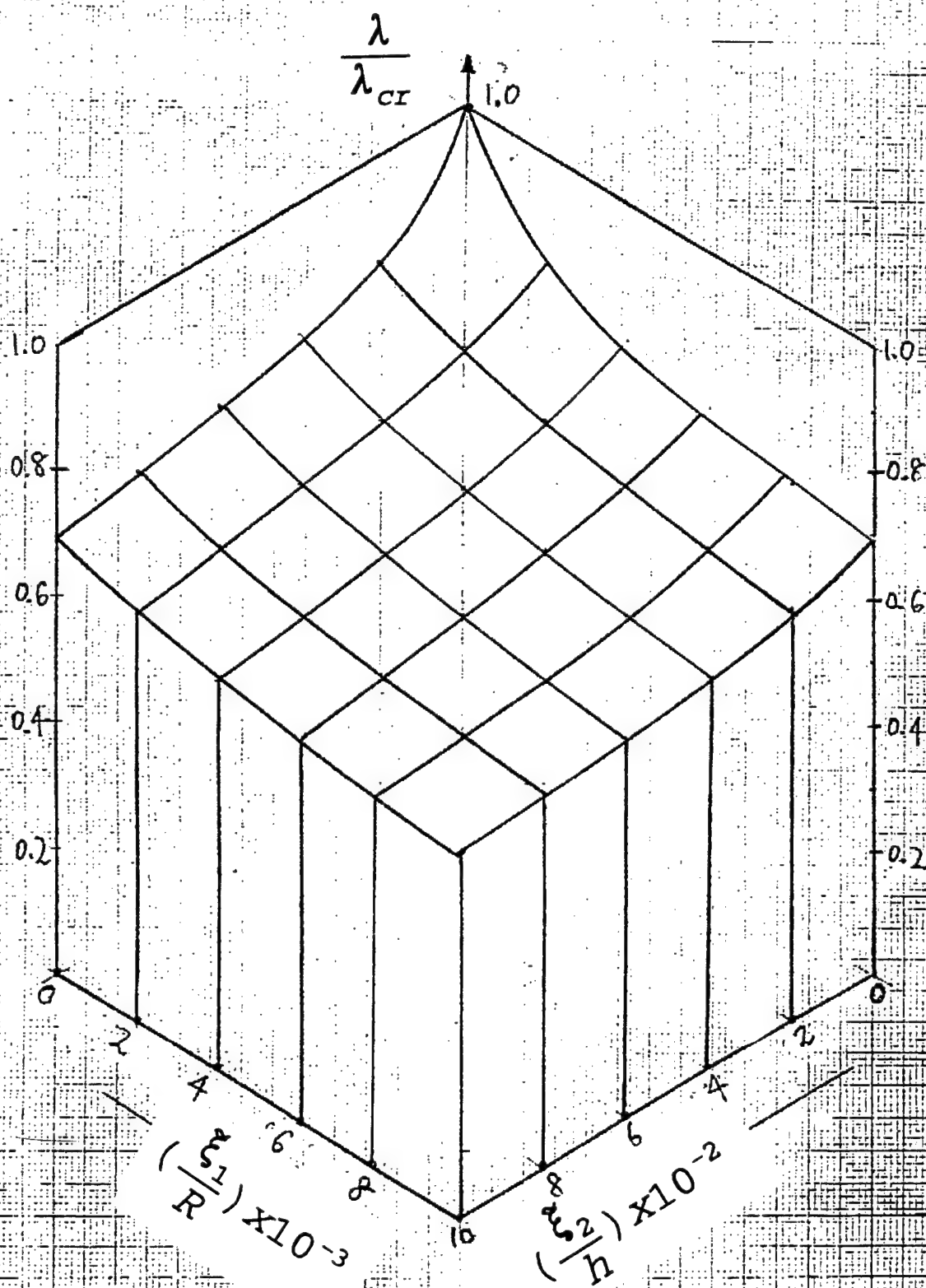
Critical Pressures : $\sigma_{cr} = p_{cr}/E$

$\sigma_{cr}^{(2)} \text{ (local)} = 1.877 \times 10^{-2} \quad (n = 9)$

$\sigma_{cr}^{(1)} \text{ (overall)} = 1.861 \times 10^{-2} \quad (m = 3)$

(Isotropic material, $\nu = 0.3$)





Imperfection-Sensitivity Surface

Behavior of Hybrid Glass/Graphite Reinforced Thick-Section Composite Cylinders under Hydrostatic Loading

Himatlal J. Garala
Carderock Division, Naval Surface Warfare Center
Bethesda, MD 20084-5000
Dr. Reaz A. Chaudhuri
University of Utah, Salt Lake City, UT 84112

Abstract

This project addresses the failure mechanisms and strength of commingled hybrid glass/graphite fiber reinforced composite cylinders subjected to bi-axial hydrostatic compressive loading. Prior investigations into the hydrostatic strength of thick-section graphite/epoxy cylinders resulted in failures which were significantly lower (50 to 70% of design pressure) than anticipated. The formation and propagation of fiber kink bands at the microscopic level, triggered by the fiber misalignment defects formed during the manufacturing process, leading to a shear crippling failure at the macroscopic level is one of the principal compressive failure modes. It is theorized that one way to improve compressive strength is through the use of a hybrid fiber system. Commingling glass fibers with graphite fibers could prevent the propagation of kink bands of the graphite fibers and provide stability to the graphite fibers. An improvement in compressive strength could lead to the use of graphite/epoxy composites more efficiently in primary and secondary naval structures where compressive strength is critical.

Parametric analyses were performed to evaluate which causes the effects of fiber orientation, fiber distribution, and ply lay-up on cylinder laminates. A new concept is introduced of micro-kinking microscopic shear damage in the advanced fiber reinforced composite specimen (containing micro-"flaws" such as fiber waviness or misalignment) under compression/shear. A mechanistic (analytical as opposed to empirical) approach is developed for derivation of constitutive relations under the framework of compression/shear damage mechanics, based on the micro-kinking concept. A Fourier series solution is derived for prediction of the nonlinear shear modulus, based on the assumption of uniform distribution of micro-kinks.

Propagation of a kink band is due to dynamic instability of the neighboring fibers, triggered by the energy released by the kinking or fracture of a defective (i.e., misaligned) fiber bundle. This explains the sudden catastrophic nature of the failure. A Griffith type fracture criterion, based on the principle of energy balance, is introduced to qualify the kink toughness and determine the required glass/graphite ratio for possible enhancement of toughness against kink band propagation. A hybrid composite cylinder will be fabricated for compression tests. The strength and failure modes observed in the ring and cylinder tests will be used to verify or modify the micro and macro-mechanics model formulation.

INTRODUCTION

Due to advantages in strength-to-weight and weight-to-displacement, composite materials have been considered for potential application in submarine pressure hulls.

Recent work at CARDEROCKDIV, NSWC (FY-83-FY86):

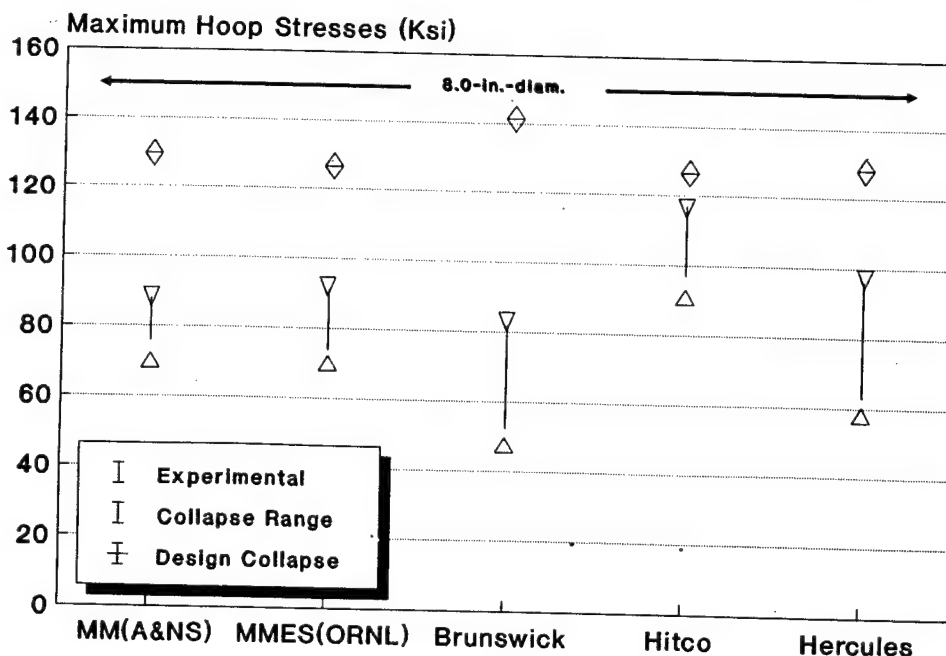
Phase 1:

- Designed 4.0-in.-diam. graphite/epoxy cylinders with $R_i/t = 6$ and $L/D = 1$ for 18,000 psi external pressure.
 - One of the models tested for 16,750 psi external pressure which resulted 122,000 psi hoop stresses.

Phase 2:

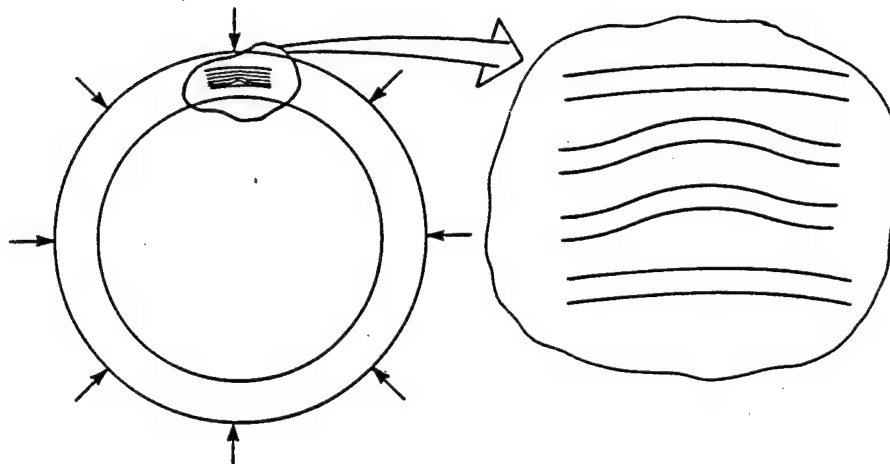
- Evaluated several (22) 8.0-in.-diam. graphite/epoxy cylinders fabricated with various processing variables and candidate fiber-resin systems (thermo-set).
 - Most cylinders failed at about 12,000 psi external pressure at hoop stress levels of apprx. 84,000 psi.
 - Failure stresses were lower than design stresses and much lower than failure stresses estimated in a flat plate laminate loaded in uni-axial compression.

DESIGN STRESS VERSUS FAILURE STRESS IN GRAPHITE-EPOXY COMPOSITE CYLINDERS



EFFECT OF FIBER WAVINESS

- Findings by Dr. Hyer (VPI)
 1. Relatively small degrees of fiber waviness will have a strong effect on stresses (shear) at ply interfaces.
 2. The location of the waviness within the laminate is important.
- Findings by Dr. Chaudhuri (Un. of Utah)
 1. Formation and propagation of fiber kink bands at the microscopic level, triggered by the fiber misalignment and other defects, leading to the shear crippling failure at the macroscopic level are identified to be the dominant compressive failure mode.
 2. Initial fiber misalignment, ultimate fiber strain and the two transverse shear moduli of the laminate are the key parameters limiting the compressive strength.
 3. Propagation of the kink band is due to dynamic instability of the neighboring fibers, triggered by the energy released by the kinking or fracture of a defective (e.g. Waviness) fiber or fiber bundle.

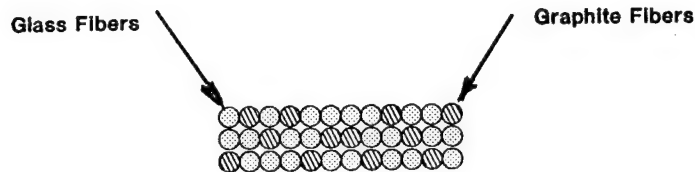


Cylinder with an Imperfection.

HYBRID GLASS/GRAPHITE COMPOSITES

ADVANTAGES OF HYBRIDIZATION

- 1. Glass have higher failure strains and failure energy**
- 2. Take larger post buckling (bending) strains**
- 3. Less sensitive to initial fiber waviness or misalignment**
- 4. Failure is expected to be gradual (not a sudden catastrophic failure like graphite)**
- 5. Will give elastic support to graphite fibers thereby increasing stability of the latter**
- 6. Will help arrest and localize any kink band type failure of graphite fibers – Design tolerance to manufacturing defects such as waviness**
- 7. Cost effective**



Commingled glass fibers within a graphite tow.

OBJECTIVE

Determine the failure mechanisms and hydrostatic strength of commingled glass/graphite fiber reinforced hybrid composite cylinders

APPROACH

(A COMBINED ANALYTICAL AND EXPERIMENTAL)

■ ANALYSES

- **Commingled Glass/Graphite Fibers Concept Formulation**
 - ✓ **Perform Stress Analysis for Baseline Configurations**
 - ✓ **Conduct a Parametric Study for Commingled Hybrid Tow**
 - ✓ **Predict Effective Material Properties for Hybrid Composites**
 - ✓ **Optimize Fiber Orientation and Stacking Sequence**
 - ✓ **Formulate Micro and Macro-Mechanics Model**

■ DESIGN

- **Design a Hybridized Cylinder Based on Optimum Parameters**
- **Predict Stresses and Strains using Linear and Non-linear Material Properties**
- **Predict Buckling Strength and Failure Mode**

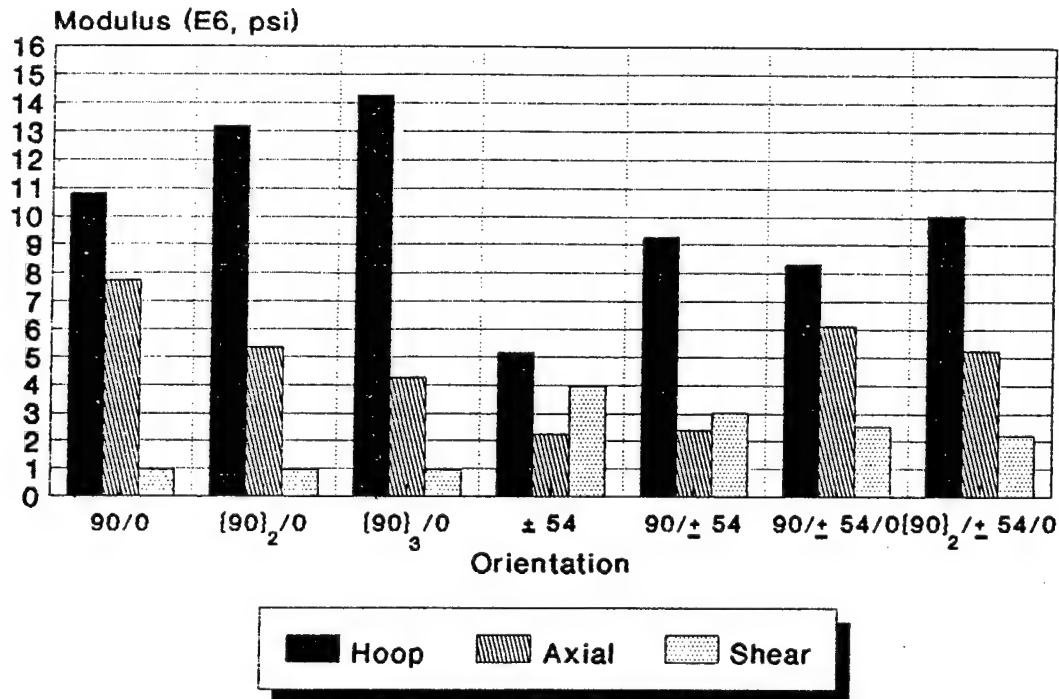
■ FABRICATION

- ✓ **Fabricate Commingled Glass/Graphite Fibers Tow**
- **Fabricate (Baseline and hybrid) flat coupons/cylinders**

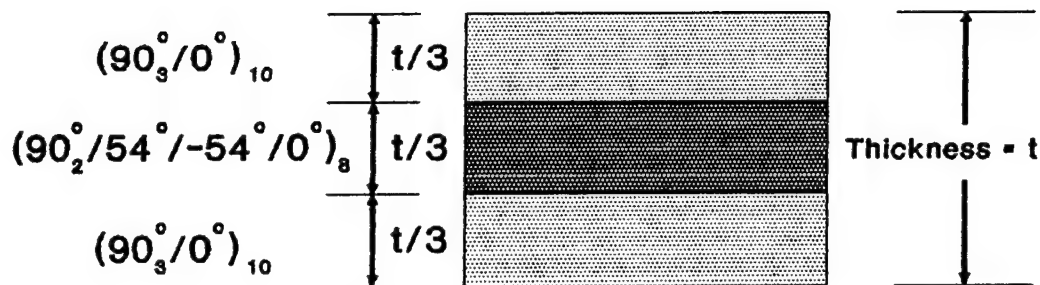
■ TEST

- **Test Rings to Study Failure Mechanisms and to Obtain Strength Data and Hoop Modulus**
- **Test Cylinders with Titanium Hemi-Heads**
- **Compare Test Results with Predictions**

Parametric Study for Fiber Orientation and Lay-up



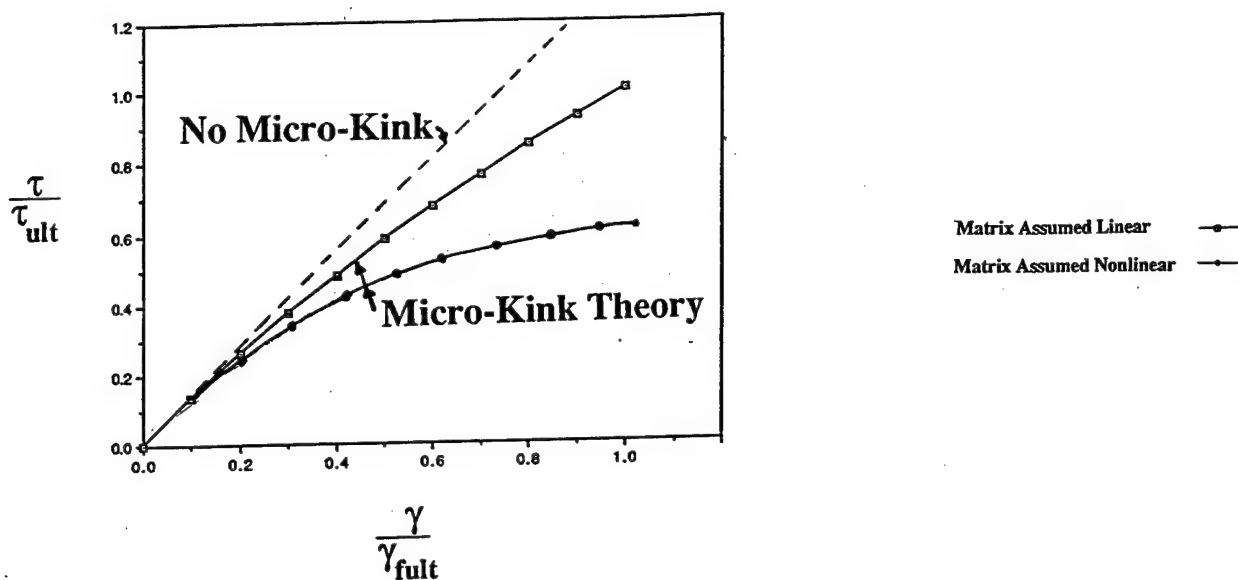
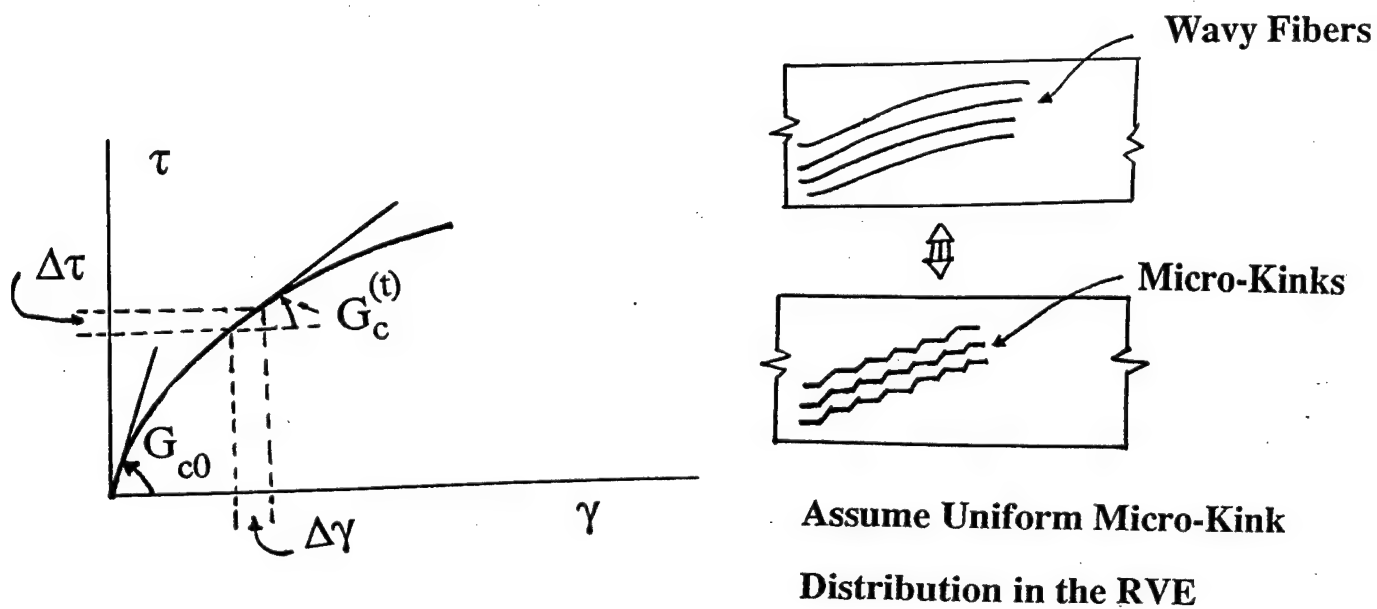
OPTIMUM FIBER ORIENTATION



FINDINGS:

1. Increase Shear Modulus, G_{12} by 122% Compared to Baseline.
2. Increase Axial Modulus, E_x by 23% Compared to Baseline.
3. An Improvement of 20% in Buckling Pressure.
4. Reduction of compressive strength due to fiber waviness caused by cross over would be minimum since off-axis fibers are located at the center of the cross section.

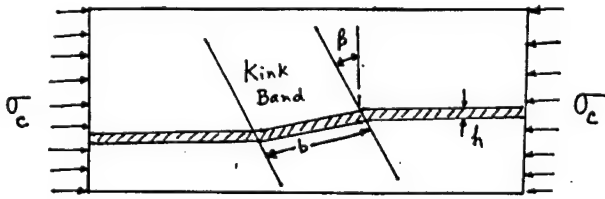
Micro-Mechanics Based Nonlinear Shear Modulus



Shear Stress vs. Shear Strain—Effect of Micro-Kinking in Graphite Fibers

Kink Toughness of Gr-Gl. Hybrid Composites

Mode II "Crack" Growth, When a Fiber Breaks in a Kink Band;



$$\tau = (1/2)\sigma_c \sin 2\beta$$

n = Ratio of Graphite to Glass Fibers in
a Tow

h = Fiber Thickness

$$\Delta U = bh \left[\frac{\tau^2}{2G_{gr}} \frac{n}{n+1} + \frac{\tau^2}{2G_{gl}} \frac{1}{n+1} \right]$$

$$W = h^2 \left[G_{gr} (\gamma_u)_{gr} \frac{n}{n+1} + G_{gl} (\gamma_u)_{gl} \frac{1}{n+1} \right]$$

Applying Griffith's Criteria:

$$\frac{\partial \Delta U}{\partial h} \geq \frac{\partial W}{\partial h} \text{ for Unstable Crack Growth}$$

$$\frac{\partial \Delta U}{\partial h} = \frac{b\sigma_c^2}{8(n+1)} \sin^2(2\beta) \left[\frac{n}{G_{gr}} + \frac{1}{G_{gl}} \right]$$

$$\frac{\partial W}{\partial h} = [G_{gr} (\gamma_{fu})_{gr} + G_{gl} (\gamma_{fu})_{gl}] \frac{2h}{(n+1)}$$

For Critical State:

$$\frac{\partial \Delta U}{\partial h} = \frac{\partial W}{\partial h}$$

$$\left(\frac{b}{h} \right)_{cr, Hybrid} = \frac{16 [n G_{gr} (\gamma_{fu})_{gr} + G_{gl} (\gamma_{fu})_{gl}]}{\sigma_c^2 \sin^2(2\beta) \left(\frac{n}{G_{gr}} + \frac{1}{G_{gl}} \right)}$$

$$\left(\frac{b}{h} \right)_{cr, Graphite} = \frac{16 G_{gr}^2 (\gamma_{fu})_{gr}}{\sigma_c^2 \sin^2(2\beta)}$$

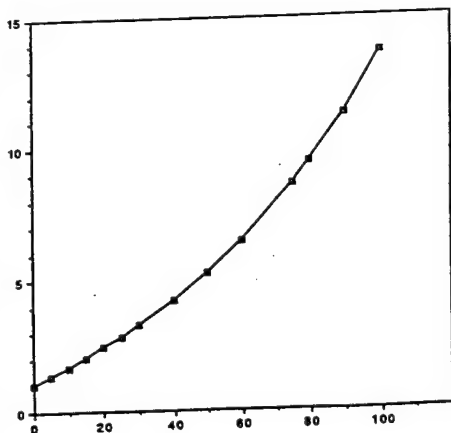
Toughness Improvement Through
Hybridization is Given by

Kink Toughness of Hybrid Composite

Kink Toughness of Graphite Composite

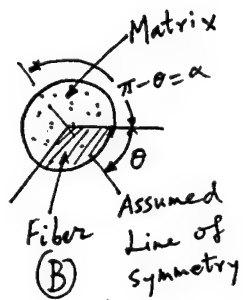
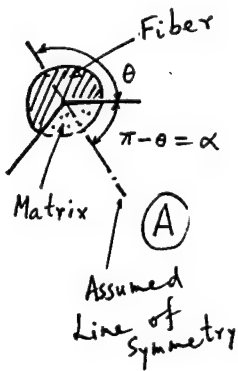
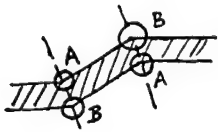
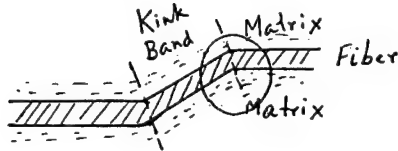
$$= \frac{(b/h)_{cr, Hybrid}}{(b/h)_{cr, Graphite}}$$

Kink Toughness of Hybrid Gr/Gl Composite
Kink Toughness of Gr. Composite



% of S-Glass Fiber Composite

Williams' Solution for Wedge Interface



$$\sigma_r = r^{\lambda-1} [F''(\theta) + (\lambda+1)F(\theta)]$$

$$\sigma_\theta = r^{\lambda-1} \lambda (\lambda+1) F(\theta)$$

$$\tau_{r\theta} = -r^{\lambda-1} \lambda F'(\theta)$$

Where Airy Stress Function $F(\theta)$ is given by

$$F(\theta) = a \sin\{(\lambda+1)\theta\} + b \cos\{(\lambda+1)\theta\} + c \sin\{(\lambda-1)\theta\} + d \cos\{(\lambda-1)\theta\}$$

λ is determined as an eigenvalue from the homogeneous equations, coming from the contact boundary conditions

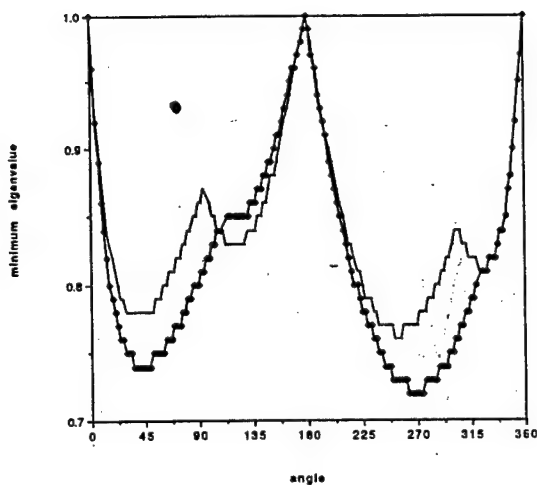


Fig. 5. $G_f/G_m=5$ $V_f=0.3$ V_m Change

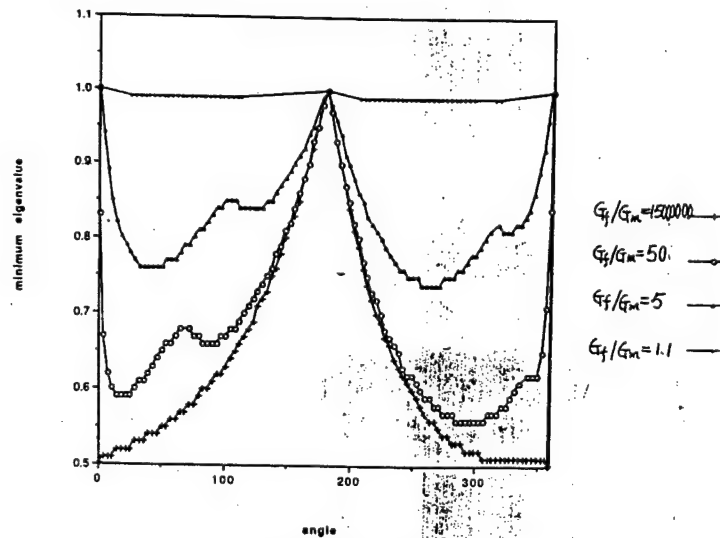


Fig. 3. $V_f=0.3$ G_f/G_m Change

MACRO-MECHANICS

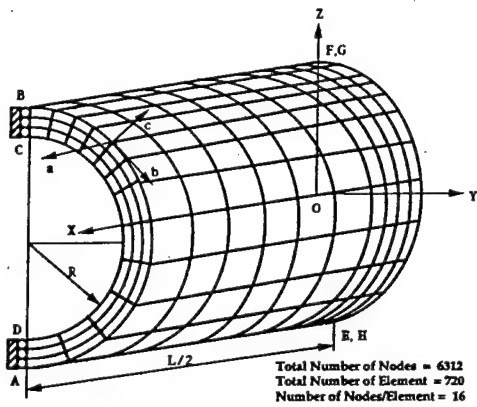


Fig. 1a Finite Element Model of Composite Cylinder

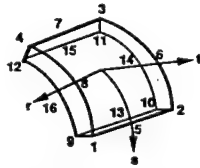


Fig. 1b 20 Node-Curvilinear Side Element on the Top and Bottom Surfaces

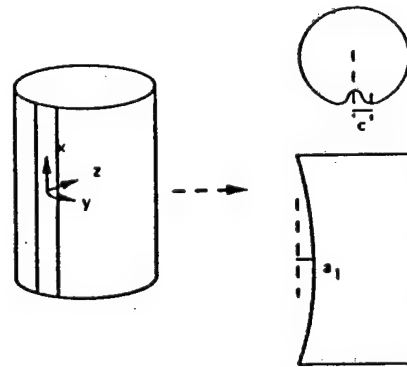


Fig. 2 Shape of the localized imperfection.

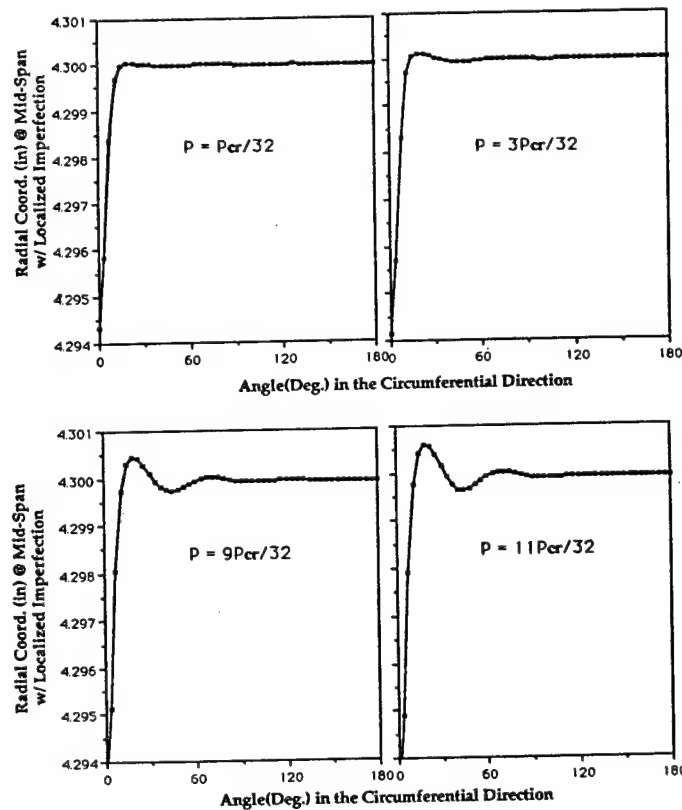


Fig. 3. Radial Coordinate vs Angle for the Localized Imperfected Cylinder

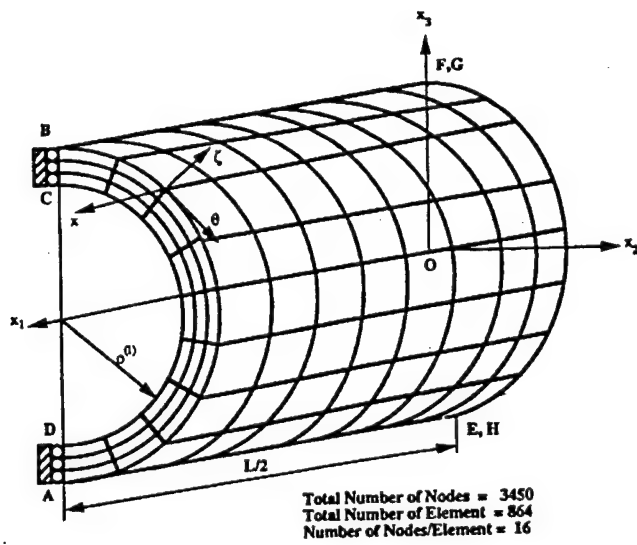


Fig. 2.1a Finite Element Model of Multilayered Composite Cylinder ($L=8.0$ in, $t=0.6048$ in, $\rho(i) = 3.4$ in, $(90/0)_2$ Layup)

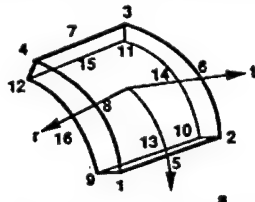
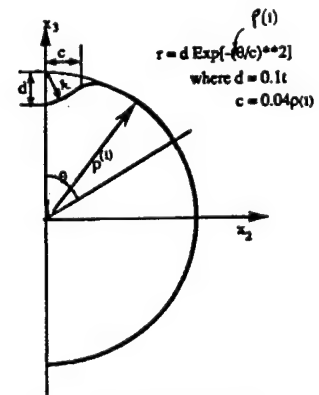
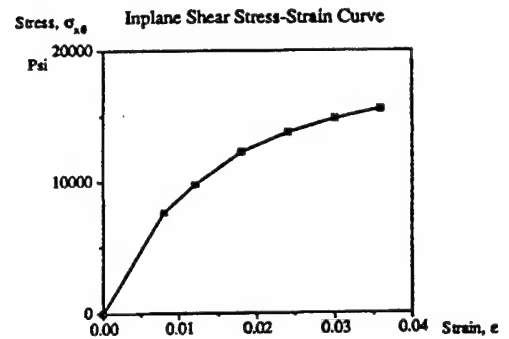
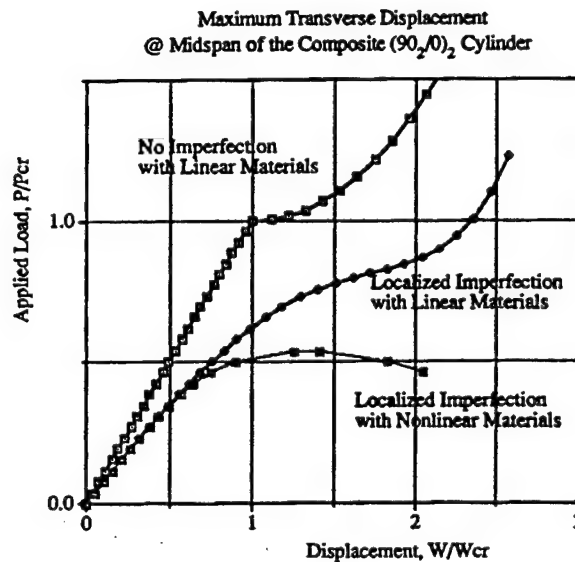


Fig. 2.1b A Curvilinear Side Element with 16 nodes on the Top and Bottom Surfaces



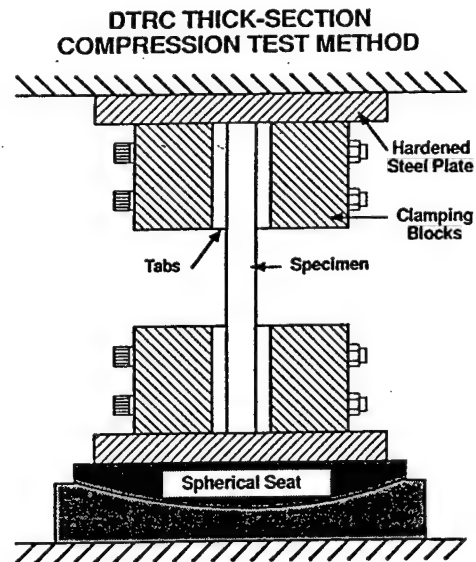
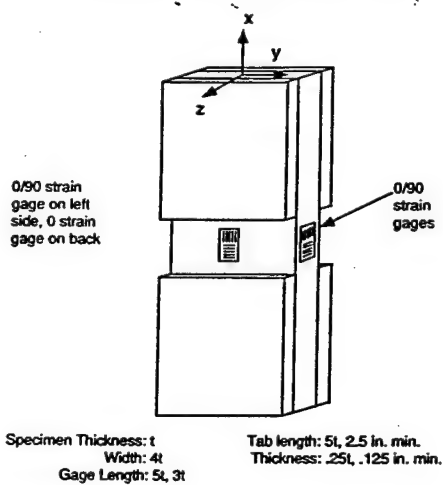
Shape of the Cylinder with Localized Imperfection



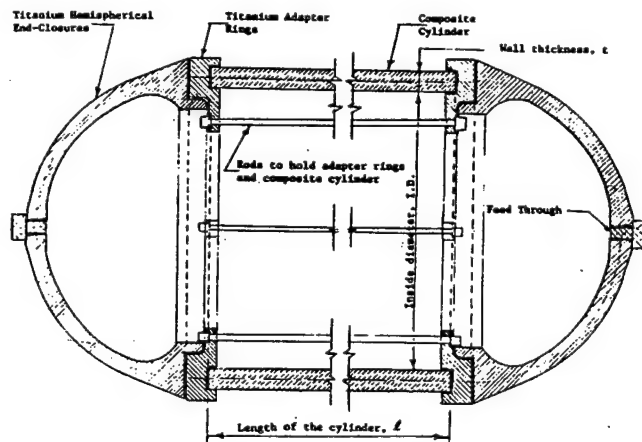
TEST PLAN

Type of Specimens	Test Fixture	Material System	No. of Spec.	Remarks	Task to be Performed in
Flat Coupon	DTRC similar to IITRI	Hybrid	10	Evaluation of Comp. Strength	FY-93
Flat Coupon	DTRC Similar to IITRI	Graphite/Epoxy	5	Comparison Test	FY-93
Rings	Hercules, Inc.	Hybrid	5	Hoop Modulus and Strength	FY-93
Cylinder	Titanium Hemi-Head	Hybrid	2	Strength and Failure Evaluation	FY-93

SPECIMEN GEOMETRY



HEMI-HEAD END-CLOSURE CONFIGURATION



Assembled test model

Analysis of Composite Aircraft Structures Containing Assembly-Induced Delaminations¹

Steven P. Wanthal
Carlos A. Fracchia

McDonnell Douglas Corporation
McDonnell Aircraft Company
St. Louis, MO 63166

ABSTRACT

Delaminations in composite structures can occur during curing, part assembly, and in the field. Delaminations which occur during the cure cycle are usually detected during quality control inspections. Assembly-induced delaminations, however, are often introduced after parts have been thoroughly inspected and can go undetected, as can delaminations introduced while the structure is in service. Assembly-induced damage is generally more severe than processing-induced damage since it usually involves multiple delaminations accompanied by matrix cracking and possible fiber damage. Once detected, the extent of damage is difficult to ascertain in great detail since the part has already been assembled with a larger structure.

A survey was conducted to determine common types of assembly-induced delaminations. The results of the survey indicate that the two most common types are impact damage due to dropped tools, etc., and delamination around fasteners attached to poorly mating substructure. The effects of impact damage have been widely studied both analytically and experimentally. Delamination around fastener holes, however, has received little attention to date. Analyses and experimental data on the effects of delaminations around fastener holes are presented herein.

Two simplified models are presented for predicting the residual strength of laminates containing impact damage and damage around fasteners. Both models are based on the assumptions that the damage area is elliptical or circular in shape and that the strength is controlled by a single delamination located at a critical ply interface. Growth of this 'critical' delamination is assumed to cause catastrophic failure of the laminate. These assumptions are shown to yield reasonable strength predictions without requiring detailed information about the actual extent of damage.

The impact damage residual strength prediction is based on an existing delamination growth model². In this model, displacement functions describing the delaminated region are assumed and the strain energy release rate around the delamination periphery is obtained. This strain energy release rate is compared to a critical value to determine when the delamination will grow. The model is shown to compare favorably with compression-after-impact tests for two material systems.

¹ The analytical work described in this presentation is being performed for the Naval Air Warfare Center and the Federal Aviation Administration under contract N62269-90-C-0281, 'Delamination Methodology for Composite Structure.'

² Flanagan, G., "Two-Dimensional Delamination Growth in Composite Laminates Under Compression Loading," *Composite Materials: Testing and Design (Eighth Conference)*, ASTM STP 972, J. D. Whitcomb, Ed., American Society for Testing and Materials, Philadelphia, 1988, pp. 180-190.

A variation of the impact damage model is also presented which includes the effects of the fastener in the delaminated region. This is accomplished by modifying the assumed displacement functions to restrict out of plane deformation around the fastener head. The strain energy release rate is then obtained and compared to a critical value to predict delamination growth. The model is validated through comparisons with experimental data for three different material systems.

ANALYSIS OF COMPOSITE AIRCRAFT STRUCTURES CONTAINING ASSEMBLY-INDUCED DELAMINATIONS

Steven P. Wanthal
Carlos A. Fracchia

McDonnell Aircraft Company
St. Louis, MO 63166

This research is being conducted under Navy/FAA contract N62269-90-C-0281, "Delamination Methodology for Composite Structure." The program monitors are Ed Kautz (Navy) and Larry Neri (FAA).

McDonnell Aircraft Company

ASSEMBLY DAMAGE SURVEY RESULTS

Assembly-Induced Damage Mainly Appears in Two Forms

- Low Velocity Impact
- Delamination Around Fastener Holes

Both types of damage include multilevel delaminations accompanied by matrix cracking and possible fiber damage

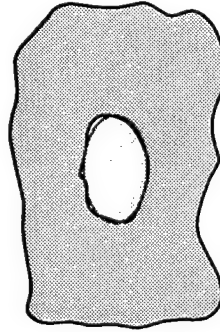
McDonnell Aircraft Company

OBJECTIVES

- Determine Common Forms of Assembly-Induced Delaminations
- Survey Existing Analytical Methods for Predicting Residual Strength
- Develop New Analytical Models for Cases Where Existing Models do not Exist
- Goal is to Develop Simplified Analytical Models, Not Intensive Numerical Solutions.
- Inputs to Models Are Limited to Damage Information Which is Easily Obtained

McDonnell Aircraft Company

MODEL IDEALIZATION

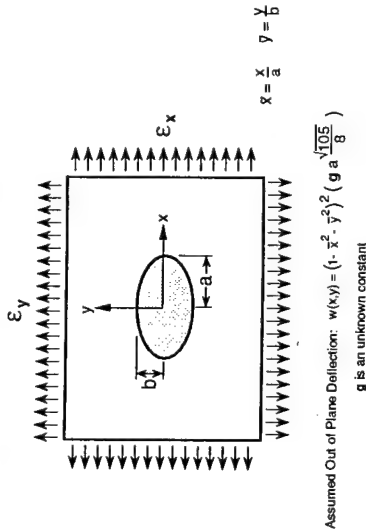


Assumptions

- Delamination is elliptical or circular in shape, clamped at the boundary
- Failure is controlled by a single delamination located at a critical ply interface
- Failure occurs when this 'critical' delamination grows

McDonnell Aircraft Company

EMBEDDED DELAMINATION GROWTH MODEL



G. Flanagan, "Two-Dimensional Delamination Growth in Composite Laminates Under Compression Loading," Composite Materials: Testing and Design (Eighty Conference), ASTM STP 972, J.D. Whitcomb, Ed., American Society for Testing and Materials, Philadelphia, 1988, pp. 180-190.

McDonnell Aircraft Company

SOLUTION PROCEDURE (Continued)

- Solve for the Unknown, g , by Minimizing Strain Energy
 $\frac{\partial U}{\partial g} = 0$
- Calculate Strain Energy Release Rate for a Change in Dimensions
 $G^a = -\frac{1}{nb} \frac{dU}{da}$ $G^b = -\frac{1}{na} \frac{dU}{db}$
- Compare to a Critical Energy Release Rate to Determine if Delamination Grows

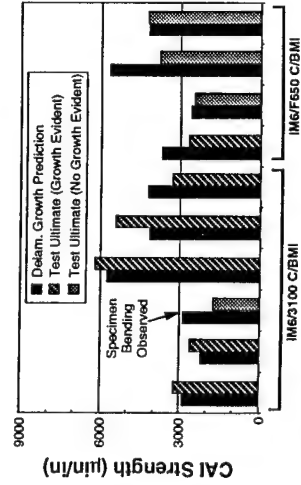
McDonnell Aircraft Company

GENERAL SOLUTION PROCEDURE

- Membrane Displacements at a Point on the Boundary:
 $u = ax^2 \epsilon_x^0 + \frac{1}{2a} \int_0^x \left(\frac{dw}{dx} \right)^2 dx$ $r = (1 - y)^{1/2}$
 $v = by^2 \epsilon_y^0 + \frac{1}{2b} \int_0^y \left(\frac{dw}{dy} \right)^2 dy$ $s = (1 - x)^{1/2}$
- Assume Linear in Plane Displacements in the Buckled Region
 $u = (\epsilon_x^0 + g^2 f^2) \bar{x} a$
 $v = (\epsilon_y^0 + g^2 s^2) \bar{y} b$
- Calculate Strain Energy in the Region, S , Containing the Sublaminar
 $U = \frac{1}{2} \iint \left\{ \epsilon' [A] \epsilon + 2 \kappa' [B] \epsilon + \kappa' [D] \kappa \right\} dA$
 $+ (S - rab) [(\epsilon_x^0)^2 A_{11} + 2 \epsilon_x^0 \epsilon_y^0 A_{12} + (\epsilon_y^0)^2 A_{22}]$

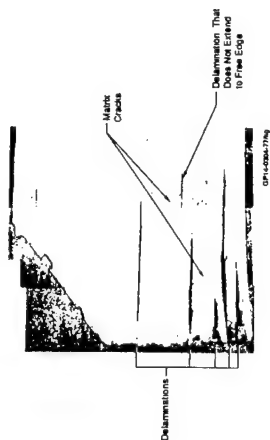
McDonnell Aircraft Company

COMPARISON WITH TEST DATA



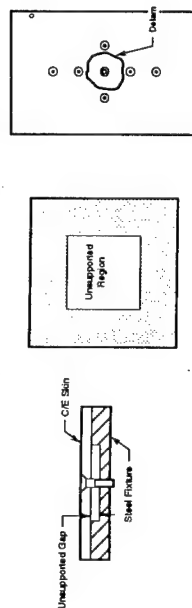
McDonnell Aircraft Company

CROSS-SECTION OF TYPICAL DAMAGE



McDonnell Aircraft Company

FASTENER HOLE DELAMINATION TEST PROGRAM



Compression Test Matrix

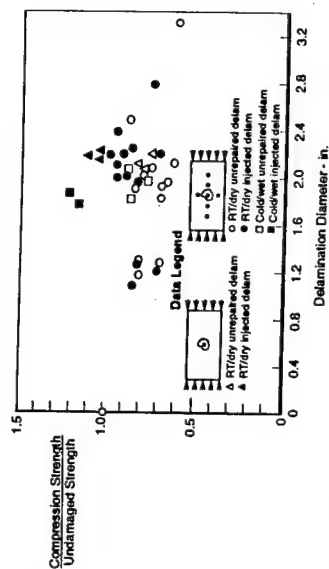
Thickness	Env	Loading		Border Fasteners		Repair Method		Delam Size		
		Static	Fatigue	Yes	No	Inject	Double	1.0	2.0	3.0
A	RTD	X	X	X	X	X	X	X	X	X
	-45 Wei	X	X	X	X	X	X	X	X	X
B	Hot Wei	X	X	X	X	X	X	X	X	X
	RTD	X	X	X	X	X	X	X	X	X
C	Hot Wei	X	X	X	X	X	X	X	X	X
	RTD	X	X	X	X	X	X	X	X	X

X: Average of 3 specimens, except double repair was 1 specimen

A.M. Rubin, "Residual Strength of Carbon/Epoxy Laminates with Induced Multilevel Delaminations," MDC Report B2179, May, 1990.

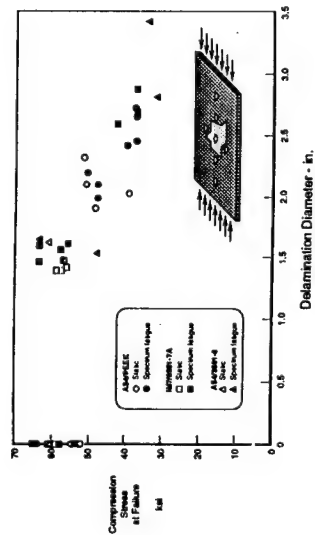
McDonnell Aircraft Company

0.104" THICK AS4/3501-6 LAMINATE



McDonnell Aircraft Company

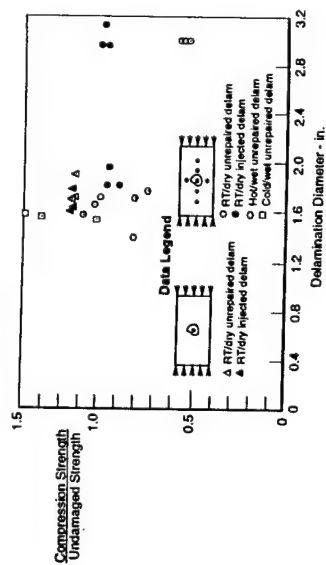
COMBINED TEST RESULTS FOR THREE MATERIALS



Source: Integrated Comprehensive Thermoplastic Composites IRAD

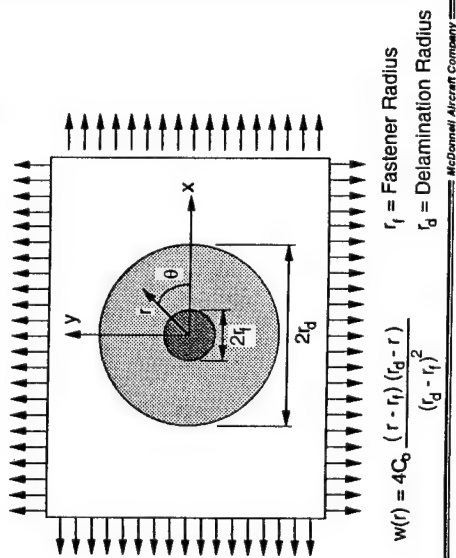
McDonnell Aircraft Company

0.224" THICK AS4/3501-6 LAMINATE



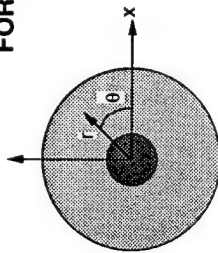
McDonnell Aircraft Company

FASTENER HOLE DELAMINATION GROWTH MODEL



McDonnell Aircraft Company

FORMULATION



r_f = Fastener Radius

r_d = Delamination Radius

C_o = Maximum Out of Plane Deflection

$$w(r) = 4C_o \frac{(r - r_f)(r_d - r)}{(r_d - r_f)^2}$$

- Displacements at the Delamination Boundary Must Match Parent Laminate:

$$d_r = (r_d - r_f) \left[\epsilon_x^o \cos^2 \theta + \epsilon_y^o \sin^2 \theta \right]$$

$$d_\theta = (r_d - r_f) \cos \theta \sin \theta \left[\epsilon_y^o - \epsilon_x^o \right]$$

FORMULATION (Continued)

- Valid roots, C_o , Must Meet Certain Criteria:

$$C_o \text{ is real and } > 0$$

$$U(C_o) > 0$$

$$\frac{\partial^2 U}{\partial C_o^2} > 0$$

- Calculate Strain Release Rate for a Change in Delamination Size:

$$G = -\frac{1}{\pi r_d} \frac{\partial U}{\partial r_d}$$

$$G = -\frac{1}{2} \left\{ \epsilon_o + \epsilon_1 C_o + \left[\epsilon_2 + \frac{(\epsilon_2^2 - \epsilon_1^2)}{2} \frac{\partial \epsilon_2}{\partial r_d} \right] C_o^2 + \left[\epsilon_3 + \frac{(\epsilon_3^2 - \epsilon_1^2)}{2} \frac{\partial \epsilon_3}{\partial r_d} \right] C_o^3 + \left[\epsilon_4 + \frac{(\epsilon_4^2 - \epsilon_1^2)}{2} \frac{\partial \epsilon_4}{\partial r_d} \right] C_o^4 - 2 \left[(\epsilon_1^2 A_{11} + 2 \epsilon_1 \epsilon_2 A_{12} + (\epsilon_2^2 A_{22})) \right] \right\}$$

- Compare to a Critical Energy Release Rate to Determine if Delamination Grows

FORMULATION (Continued)

- Add the Extra Radial Displacement Due to Buckling

$$u_r = d_r + \frac{1}{2} \int_{r_f}^r \left(\frac{dw}{dr} \right)^2 dr = d_r + \frac{C_o^2}{8} (r_d - r_f)^3$$

$$u_\theta = d_\theta$$

- Assume the In Plane Displacements Vary Linearly:

$$u_r = (r - r_f) \left[\epsilon_x^o \cos^2 \theta + \epsilon_y^o \sin^2 \theta + \frac{C_o^2}{8} (r_d - r_f)^2 \right]$$

$$u_\theta = (r - r_f) \cos \theta \sin \theta \left[\epsilon_y^o - \epsilon_x^o \right]$$

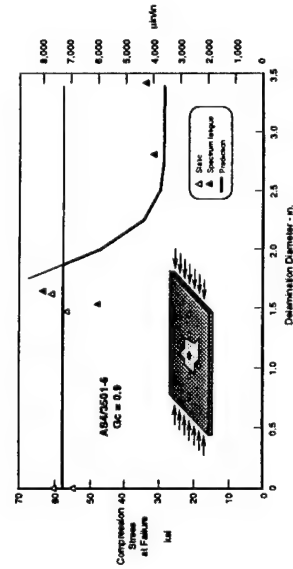
- Calculate Strain Energy in the Region, S, Containing the Sublaminate

$$U = \frac{1}{2} \iint_S \left\{ \epsilon^T [A] \epsilon + 2 \kappa^T [B] \epsilon + \kappa^T [D] \kappa \right\} dA + (S \pi C_o^2) \left[(\epsilon_x^o)^2 A_{11} + 2 \epsilon_x^o \epsilon_y^o A_{12} + (\epsilon_y^o)^2 A_{22} \right]$$

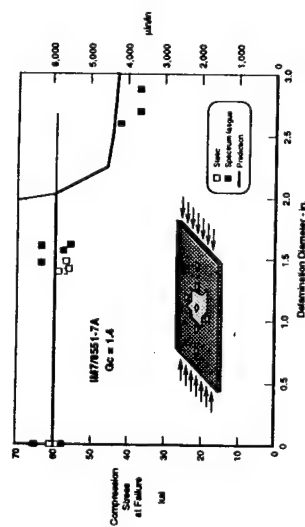
- Solve for C_o by Minimizing Strain Energy

$$\frac{dU}{dC_o} = 0 = \epsilon_1 + 2 \epsilon_2 C_o + 3 \epsilon_3 C_o^2 + 4 \epsilon_4 C_o^3$$

COMPARISON WITH AS4/3501-6 TESTS



COMPARISON WITH IM7/8551-7A TESTS



A SELF-ALIGNED TEST FIXTURE FOR INTERLAMINAR TENSILE TESTING OF TWO-DIMENSIONAL CARBON-CARBON

Ajit K. Roy
University of Dayton Research Institute
300 College Park
Dayton, OH 45469-0168

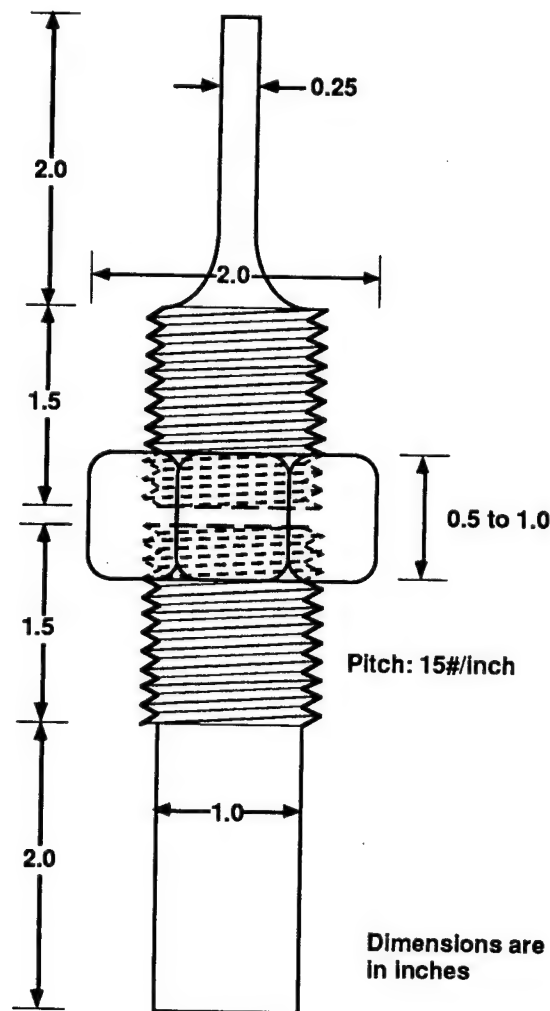
ABSTRACT

The structural application of a two-dimensional carbon-carbon composite is currently limited by its interlaminar tensile properties. To make the two-dimensional carbon-carbon composite a viable-high temperature structural composites, a great deal of improvement is needed on its interlaminar properties. At the same time we need efficient and reliable test methods to measure these properties in order to monitor the material development. The interlaminar tensile strength of two-dimensional carbon-carbon is nearly two orders of magnitude lower than its in-plane tensile properties. Thus a reliable measurement of the interlaminar tensile strength requires a careful design of the test fixture and its alignment.

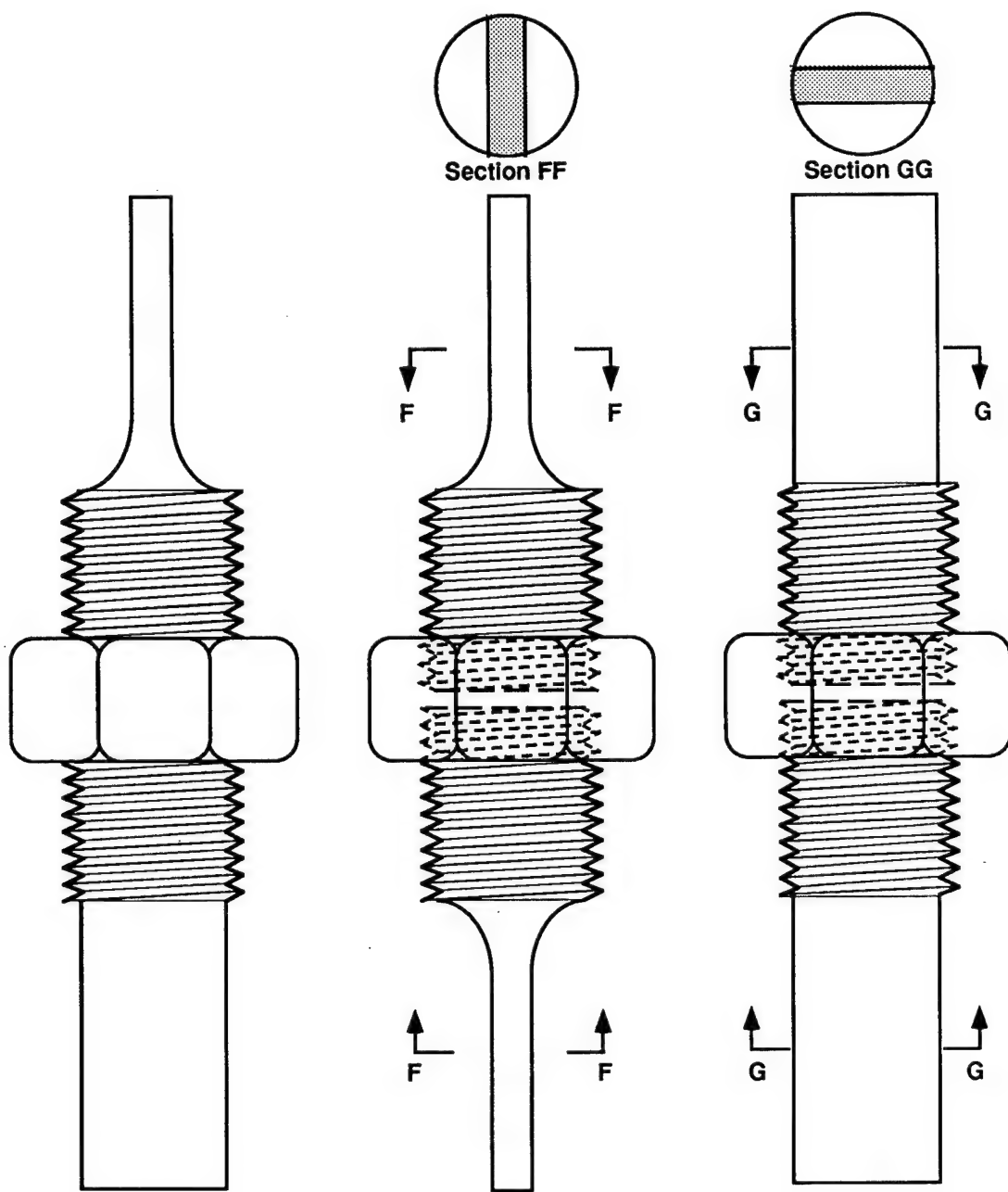
The interlaminar tensile (ILT) strength of two-dimensional carbon-carbon (whose thickness is very small, only a few plies thick) is normally measured by gluing the specimen in between two pull rods. In this type of test, the axes of the two pull rods need to be aligned with the specimen centroidal axis. To align the axes of the pull rods with that of the specimen, the normal practice is to glue the specimen in between the two pull rods first, and then machine the rods with the specimen for alignment. This alignment process is expensive and time consuming. In this work a new test fixture is designed in which the axes of the pull rods are self aligned with that of the test frame (e.g., MTS test frame), and the specimen is glued in-situ with the pull rods. The self alignment of the pull rods is achieved by holding the two threaded pull rods by means of a nut, while gripping the pull rods with the test frame. The pull rods are of circular cross-section, and its ends are gradually tapered to rectangular cross-section for direct gripping with the test frame wedge grips.

A strength analysis of the test fixture is performed for the case when the centroid of the carbon-carbon specimen is slightly misaligned with that of the test fixture. It is found that the bending of the test fixture due to a misaligned specimen is minimized by keeping the planes of the top and bottom wedge grips perpendicular to each other. The test specimens are circular in cross section with a small and gradual reduction in radius at the center. All tested specimens failed near the middle of the thickness. There was no failure at the glue

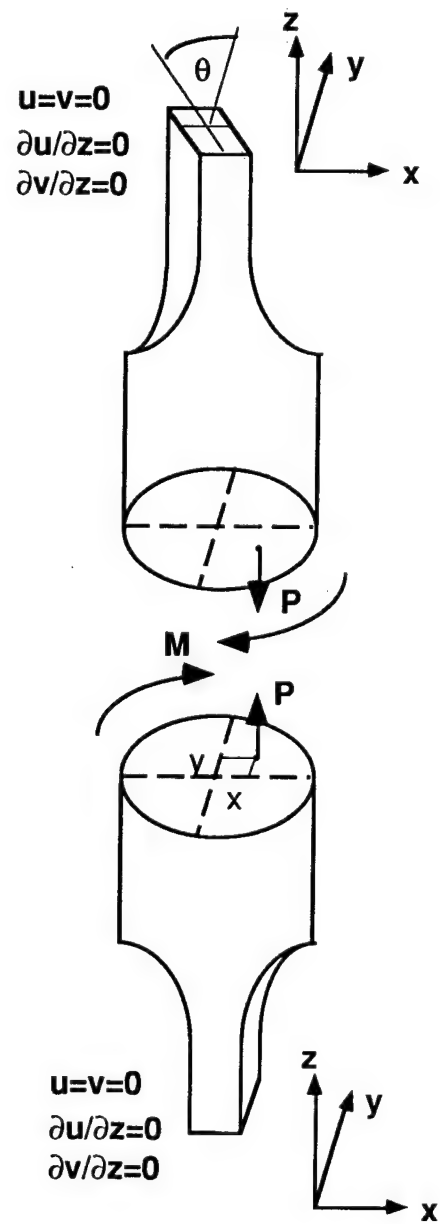
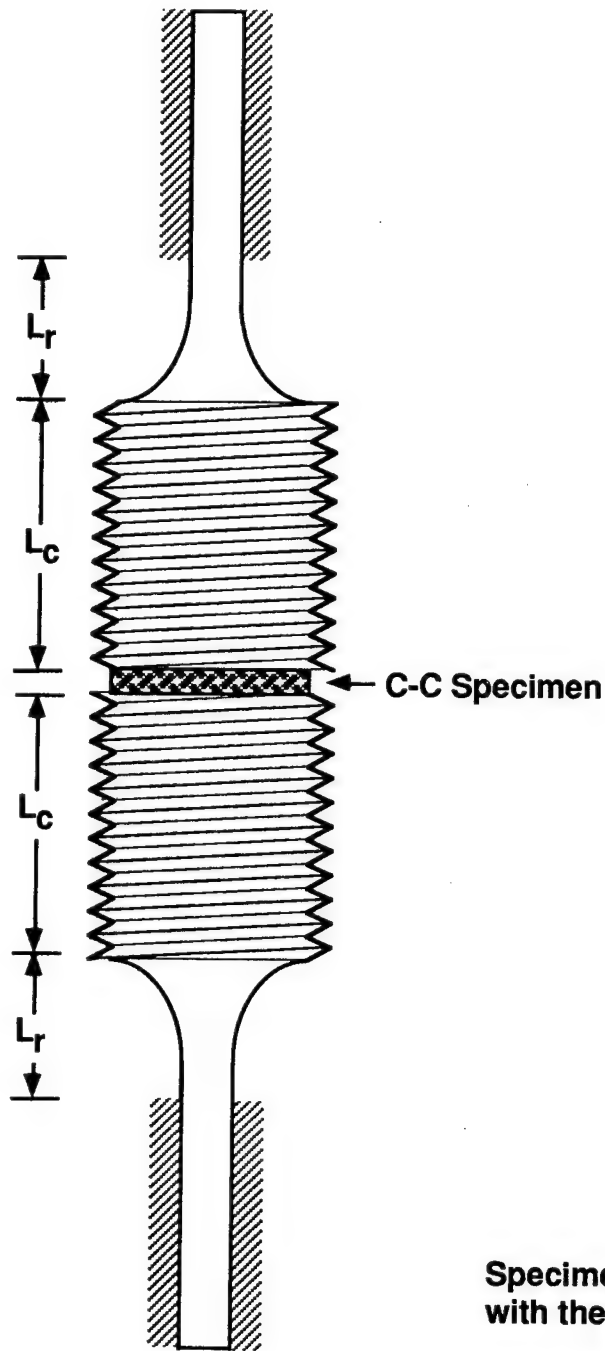
line interface between the specimen and the pull rods. To assess whether there was any effect of glue penetration to the failure surface, fluorescent optical microscopy of the specimen cross-section was performed. It was found that the penetration of the glue was limited to less than a ply thickness. All tested specimens were atleast eight plies thick. Thus it is inferred that the glue did not have any effect on specimen failure. With the same test fixture, the interlaminar tensile stiffness is also measured. The interlaminar stiffness is measured by gluing a stack of four carbon-carbon blocks together. The effect of the glue line on the stiffness measurement is found to be negligible.



Dimensions of the Test Fixture

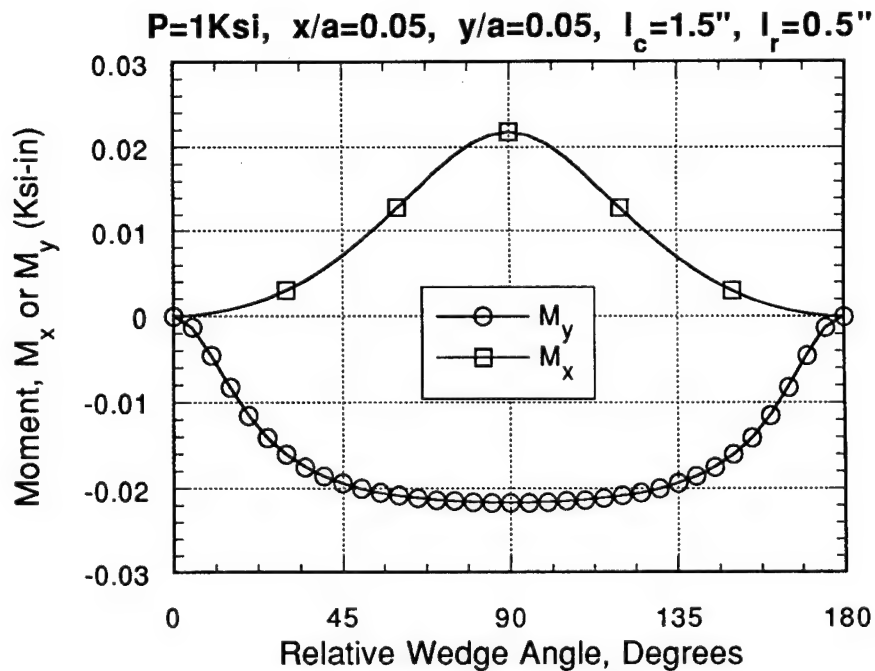


Configuration of the Test Fixture

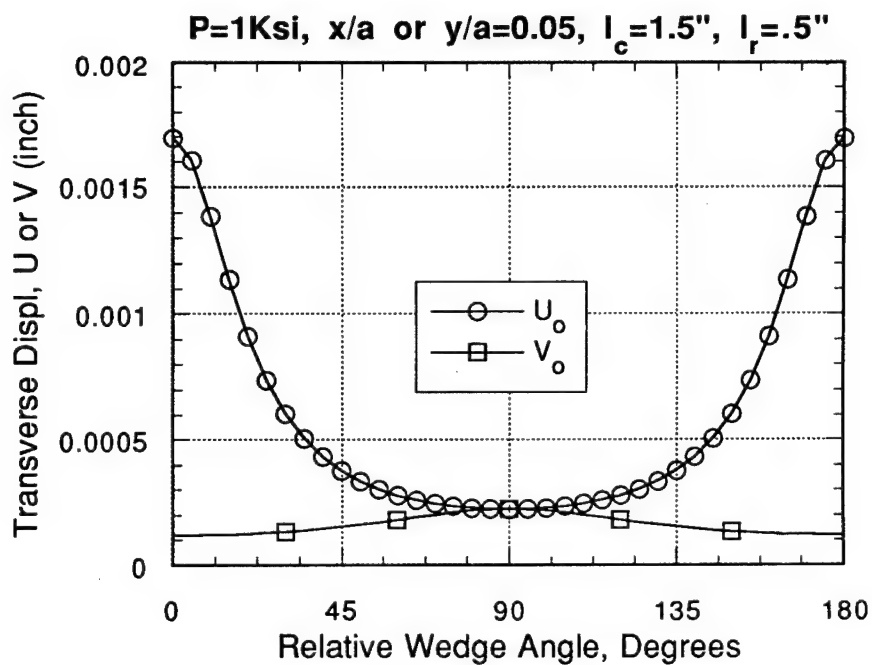


**Specimen Centroid not aligned
with the Test Fixture Axis**

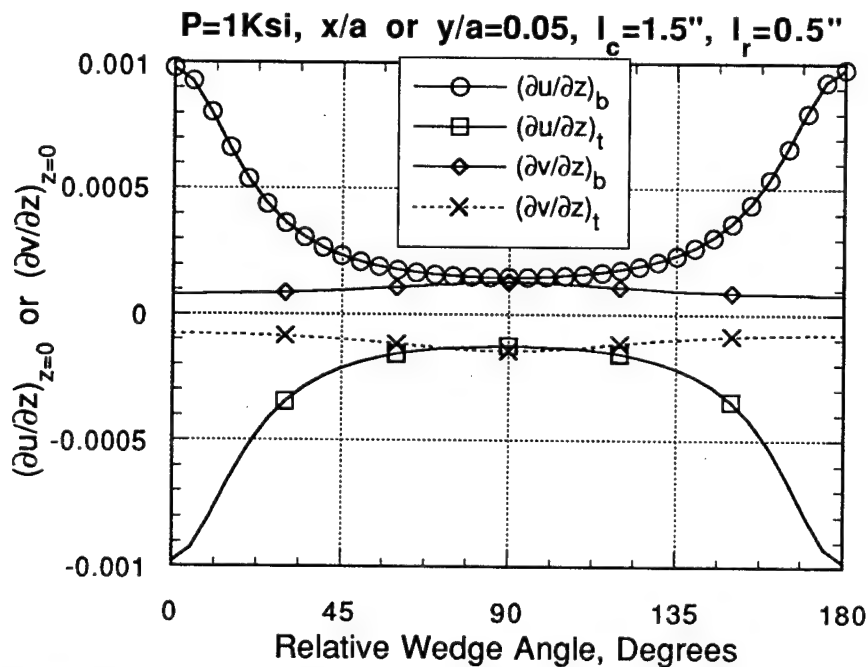
Free Body Diagram of the Induced Moment Due to Misaligned Specimen



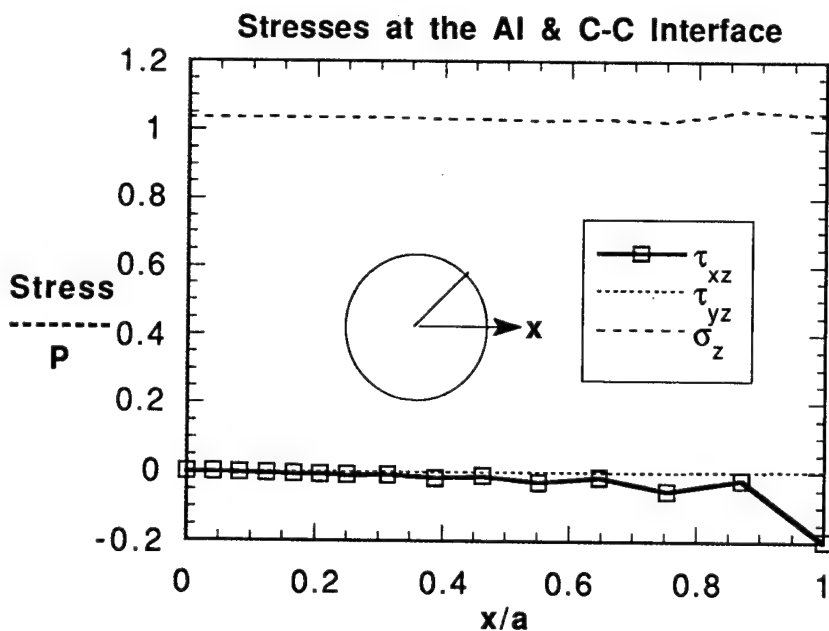
Induced Moment versus the Relative Angle between the Top and Bottom Wedges Due to Specimen Center Misaligned with the Pull Rod Axis.



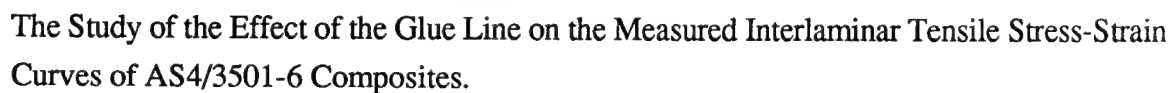
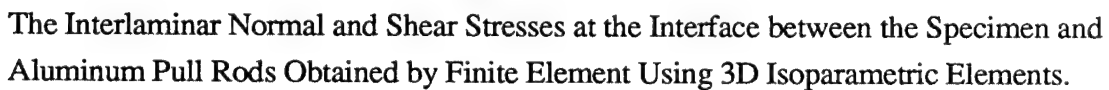
The Transverse Displacement of the Fixture Pull Rods versus the Relative Angle between the Top and Bottom Wedges Due to Specimen Center Misaligned with the Pull Rod Axis.

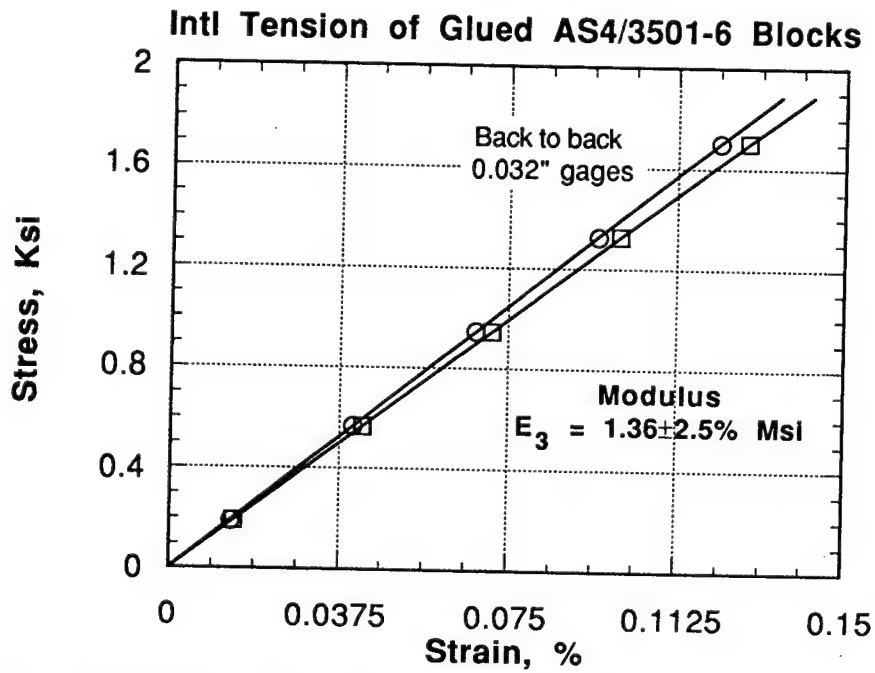


Slope of the Fixture Pull Rods versus Relative Angle between the Top and Bottom Wedges Due to Specimen Center Misaligned with the Pull Rod Axis.

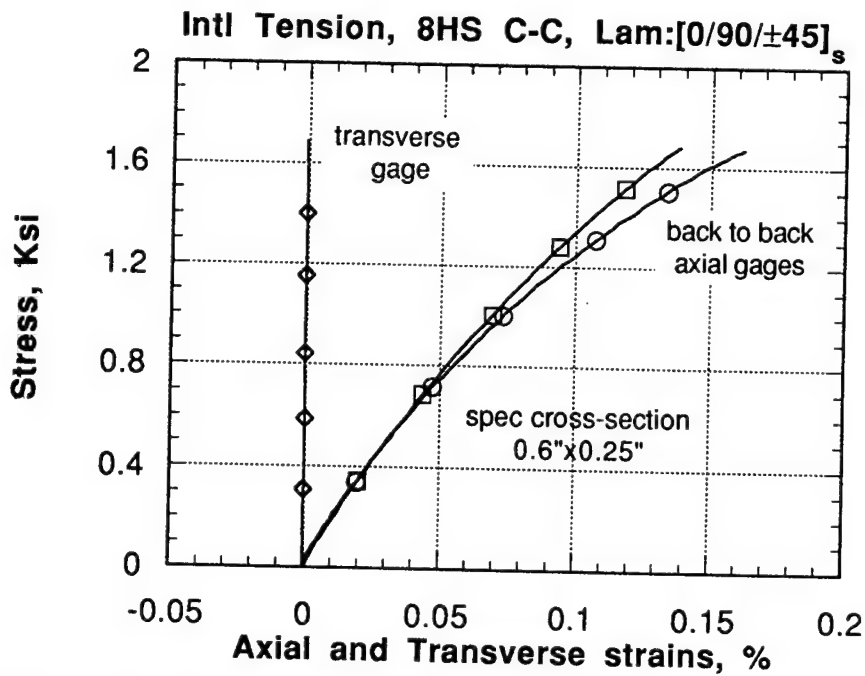


The Interlaminar Normal and Shear Stresses versus Radial Distance at the Interface between the Specimen and Aluminum Pull Rods Obtained by Finite Element using 3D Isoparametric Elements.

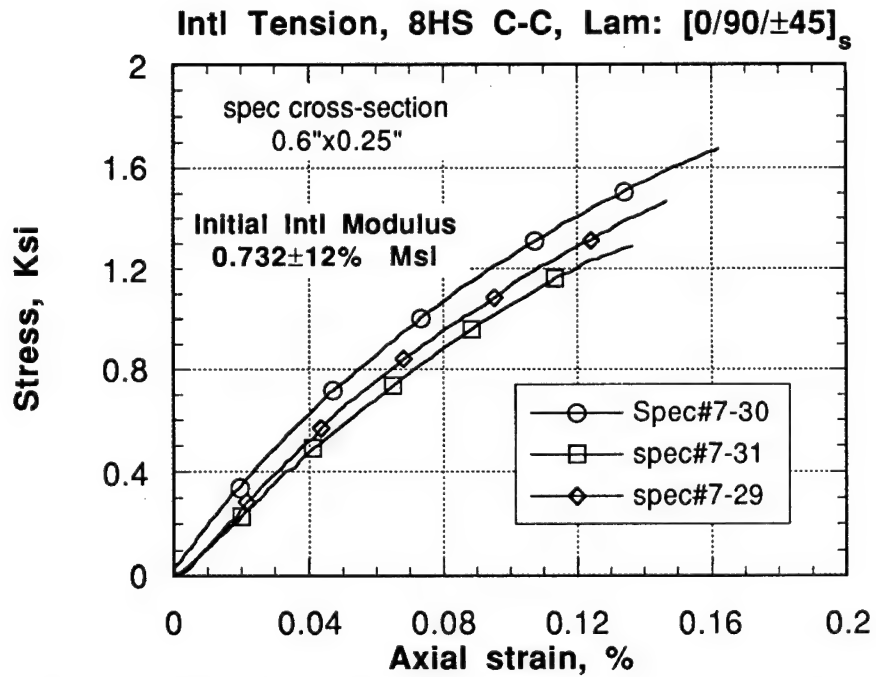




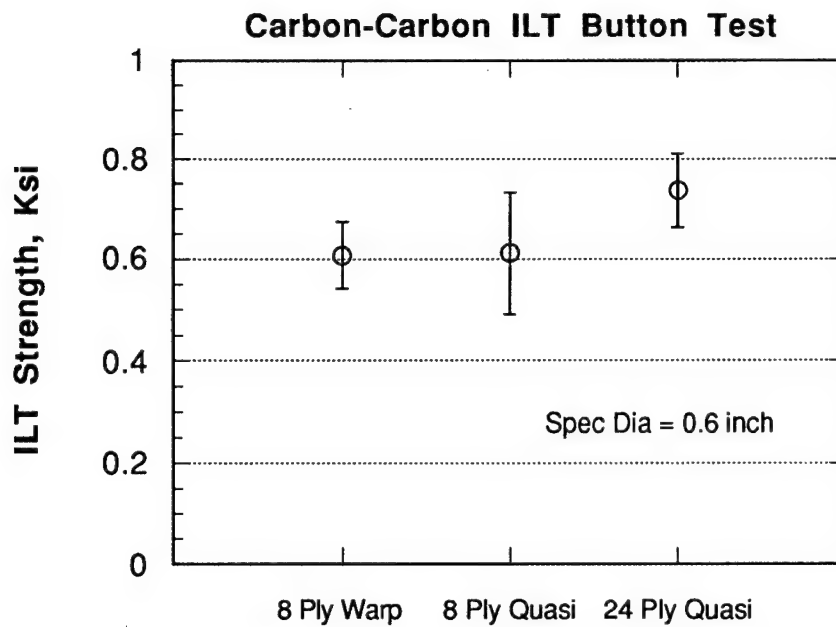
The Interlaminar Stress-Strain Curves Obtained from Two Back-to-Back Strain Gages Installed on Glued AS4/3501-6 Blocks.



The Interlaminar Stress-Strain Curves Obtained from Two Back-to-Back Strain Gages Installed on Glued 2D Carbon-Carbon Blocks.



The Interlaminar Stress-Strain Curves of Three 2D Carbon-Carbon Specimens.



The Interlaminar Tensile (ILT) Strength of Three Different Specimens of 2D Carbon-Carbon

CONCLUSIONS

- A self-aligned test fixture for interlaminar tensile test of button specimen is presented.
- The alignment of the pull rods of the fixture is simple and fast.
- The rigidity of the fixture in case of specimen misalignment is discussed.
- It is demonstrated that the ILT stiffness and strength can easily be measured with the fixture.

ACKNOWLEDGEMENT

This work is sponsored by the Air Force Wright Laboratory Materials Directorate under Contract Number F33615-91-C-5618. The finite element stress analysis performed by Ms. Diane Hageman, AFOSR Summer Student, is gratefully acknowledged.

ANALYSIS OF THERMOMECHANICAL CYCLIC BEHAVIOR OF UNIDIRECTIONAL METAL MATRIX COMPOSITES

Demirkan Coker and Noel E. Ashbaugh

University of Dayton Research Institute, Dayton, Ohio, 45469

ABSTRACT

Interest in metal matrix composites (MMC) for high-temperature aerospace applications has grown in recent years. Because of the high use temperatures envisioned, proposed applications of MMCs almost always involve both thermal and mechanical cyclic loading. Consequently, the accurate prediction of the thermomechanical fatigue (TMF) life of these components is a critical aspect of the design process. Because of the mismatch in coefficient of thermal expansion between fiber and matrix, internal thermal stresses are produced under thermal cycling. These stresses must be accounted for in analysis in addition to those produced by mechanical loading. Life prediction, therefore, requires a knowledge of the individual components of stress or strain in the fiber and/or matrix as well as the overall applied stresses.

To determine these stresses, the concentric cylinder model has been used in the literature due to its simple geometry and capability to capture the three-dimensional aspects of the stress state in a real composite. In this model a representative volume element of the composite is modeled as concentric cylinders with the core cylinder representing the fiber and the outer ring representing the matrix. The constitutive models used in the literature consist of thermo-elastic [1], elastic-plastic with deformation type theory [2,3] or elastic-perfectly plastic with Tresca's yield criterion[4].

In this investigation an analytical tool was developed to model a unidirectional composite subjected to thermomechanical cyclic loading and processing conditions. A representative volume element of the composite was modeled using concentric cylinders. The constituents were assumed to be isotropically elastic-plastic materials with von Mises yield surfaces and having temperature dependent properties. A perfect bond existed between the constituents of the composite so that there was no slippage or separation of the constituents. Finite difference method was used to solve the two ordinary differential equations of equilibrium and compatibility. An iterative technique [5] using the Prandtl-Reuss flow rule was used to determine incremental plastic strains. The analytical procedure was implemented into a PC based computer code FIDEP (Finite Difference Code for Elastic-Plastic Analysis of Composites) capable of predicting the axisymmetric triaxial stresses in a composite under thermomechanical fatigue (TMF) loading conditions [6].

Several problems were solved using FIDEP code to illustrate the capability for computing micromechanical stresses, to compare with solutions obtained by different techniques, and to analyze the stress states obtained under thermomechanical fatigue conditions. In these computations two-material concentric cylinder model consisting of SCS-6 silicon carbide fiber and Ti-24Al-11Nb matrix was used. The SCS-6 fiber was isotropic and elastic with only the coefficient of thermal expansion varying with temperature. An adequate representation of the Ti-24Al-11Nb matrix was attained using a bilinear elastic-plastic model with temperature dependent elastic and plastic moduli, yield stress and coefficient of thermal expansion.

Results for a thermal cool-down in a SCS-6/Ti-24 Al-11Nb unidirectional composite compared well with those obtained using the finite element method [7]. Several problems were solved for thermomechanical loading conditions and demonstrate the three-dimensional nature of the

stress fields in the matrix material. Predicted stress-strain behavior that stabilized after a few cycles compared favorably with experimental stress-strain curves measured after a few hundred cycles. Comparisons with one-dimensional approximations to the stress field indicate significant differences in the values of the computed axial stresses as well as the effective stresses in the matrix at the fiber-matrix interface due to significant transverse stresses predicted using the 3-D concentric cylinder model. In particular, the one-dimensional solution can show the material to behave purely elastically while the 3-D solution indicates yielding in the matrix for the same material constants and applied loading conditions. This serves to point out the importance of the 3-D nature of the stresses in a composite, particularly when stresses close to yield may be encountered.

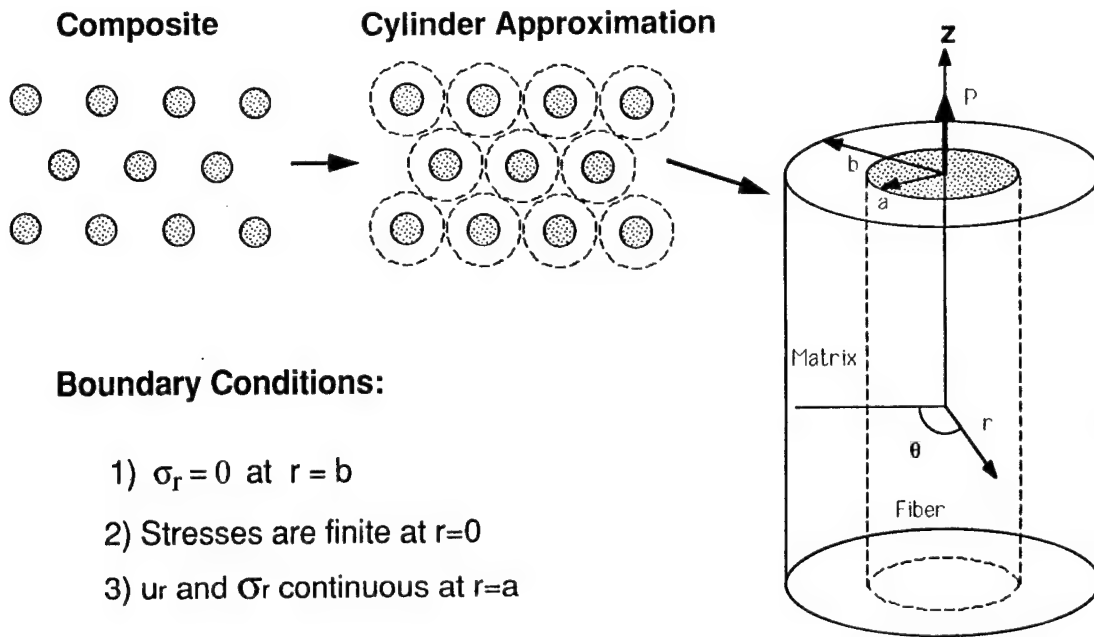
Acknowledgement

The work described here was performed at the Materials Directorate, Wright Laboratory (WL/MLLN) under Contract No. F33615-87-C-5243.

References

- [1] Pagano, N. J. and Tandon, G. P., " Elastic Response of Multi-Directional Coated-Fiber Composites," *Composites Science and Technology*, Vol. 31, 1988, pp. 273-293.
- [2] Hecker, S. S., Hamilton, C. H. and Ebert, L. J., "Elastoplastic Analysis of Residual Stresses and Axial Loading in Composite Cylinders," *Journal of Materials, JMLSA*, Vol. 5, No. 4, Dec 1970, pp. 868-900.
- [3] Gdoutos, E. E., Karalekas, D. and Daniel, I. M., "Micromechanical Analysis of Filamentary Metal Matrix Composites Under Longitudinal Loading," *Journal of Composites Technology and Research, JCTRER*, Vol. 13, No. 3, Fall 1991, pp. 168-174.
- [4] Lee, J. W. and Allen, D. H., "An Analytical Solution for the Elastoplastic Response of a Continuous Fiber Composite Under Uniaxial Loading," *Research in Structures, Structural Dynamics and Materials 1990*, NASA Conference Publication, 3064, 1990, pp. 55-65.
- [5] Mendelson, A., *Plasticity: Theory and Application*, Macmillan, New York, 1968.
- [6] Coker, D., Ashbaugh, N. E., and Nicholas, T, "Analysis of Thermomechanical Cyclic Behavior of Unidirectional Metal Matrix Composites," , to be published in ASTM STP, *Proceedings of the Symposium on Thermomechanical Fatigue Behavior of Materials*, October 16, 1991, San Diego, CA.
- [7] Kroupa, J. L., "Thermal Mechanical Fatigue Analysis of Titanium Aluminide MMC," *Fifteenth Annual Mechanics of Composites Review*, Materials Laboratory, Wright-Patterson AFB, OH, pp. 233-242.

Concentric Cylinder Model



Boundary Conditions:

- 1) $\sigma_r = 0$ at $r = b$
- 2) Stresses are finite at $r=0$
- 3) u_r and σ_r continuous at $r=a$

Theoretical Background

Equilibrium Equation:
$$\frac{d\sigma_r}{dr} + \frac{\sigma_r - \sigma_\theta}{r} = 0$$

Compatibility Equation:
$$\frac{d\varepsilon_\theta}{dr} + \frac{\varepsilon_\theta - \varepsilon_r}{r} = 0$$

Stress-Strain Equations

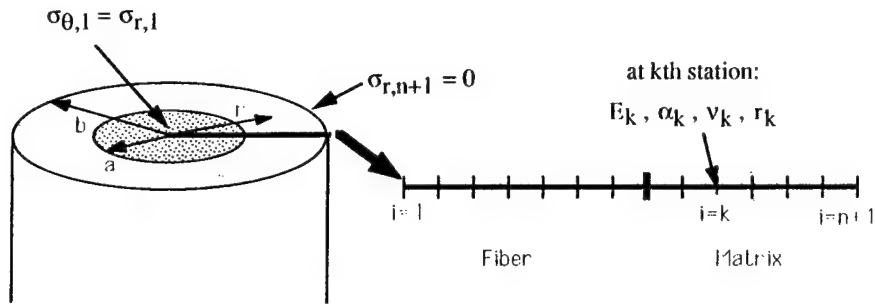
$$\varepsilon_{ij} = \varepsilon_{ij}^e + \varepsilon_{ij}^{th} + \varepsilon_{ij}^p$$

$$\varepsilon_r = \frac{1}{E} (\sigma_r - \nu(\sigma_\theta + \sigma_z)) + \alpha T + \varepsilon_r^p + \Delta\varepsilon_r^p$$

$$\varepsilon_\theta = \frac{1}{E} (\sigma_\theta - \nu(\sigma_\theta + \sigma_z)) + \alpha T + \varepsilon_\theta^p + \Delta\varepsilon_\theta^p$$

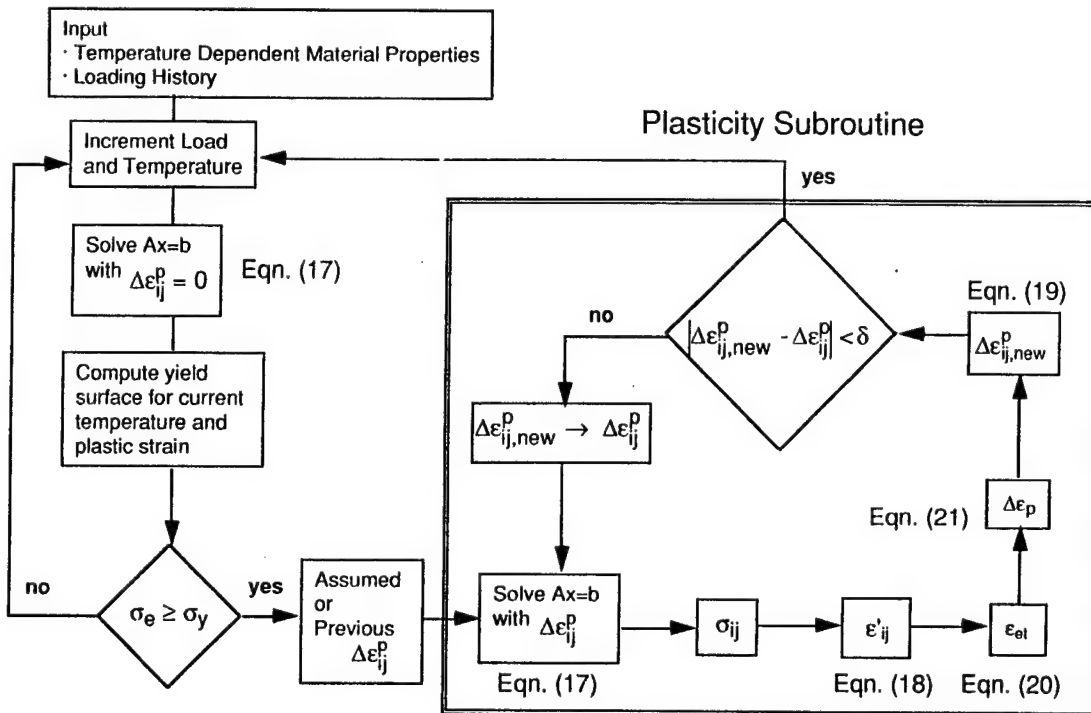
$$\varepsilon_z = \frac{1}{E} (\sigma_z - \nu(\sigma_\theta + \sigma_r)) + \alpha T + \varepsilon_z^p + \Delta\varepsilon_z^p = \text{constant}$$

Finite Difference Equations

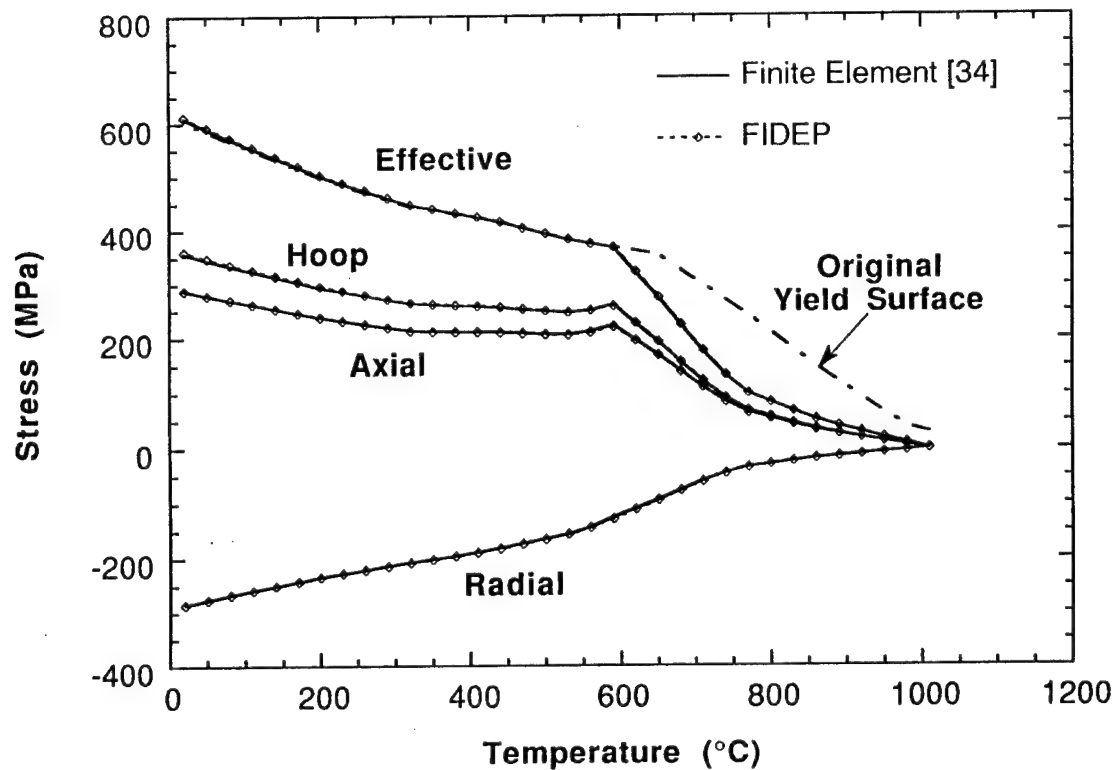


$$\left\{ \begin{array}{l} (1) \ a_i \sigma_{r,i} - \sigma_{r,i} + b_i \sigma_{\theta,i-1} + b_i \sigma_{\theta,i} = 0 \\ (2) \ c_i \sigma_{r,i-1} - d_i \sigma_{r,i} + f_i \sigma_{\theta,i-1} + g_i \sigma_{\theta,i} = q_i - E_i(P_i h_i + \epsilon_z(v_i + v_{i-1})) \end{array} \right\} \quad i = 2, \dots, n+1$$

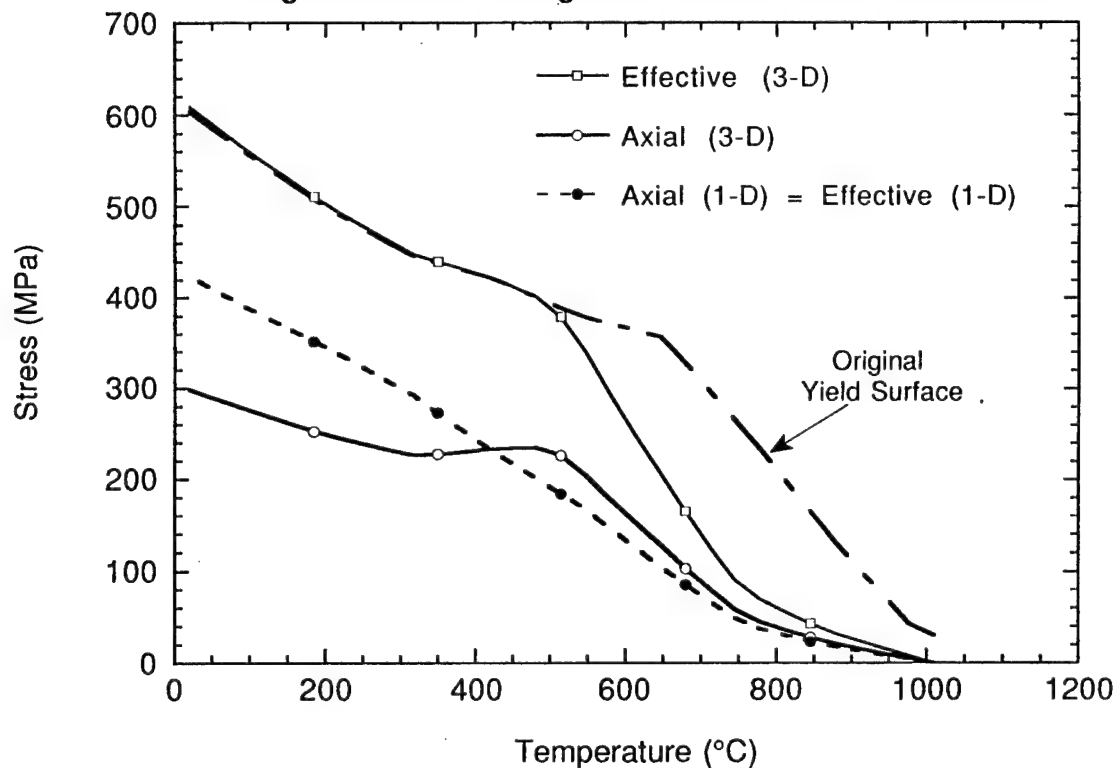
$$2n \text{ Unknowns: } \begin{bmatrix} \sigma_{r,i}, i = 1, \dots, n \\ \sigma_{\theta,i}, i = 2, \dots, n+1 \end{bmatrix} \longrightarrow [A]x = b_{2n \times 2n}$$



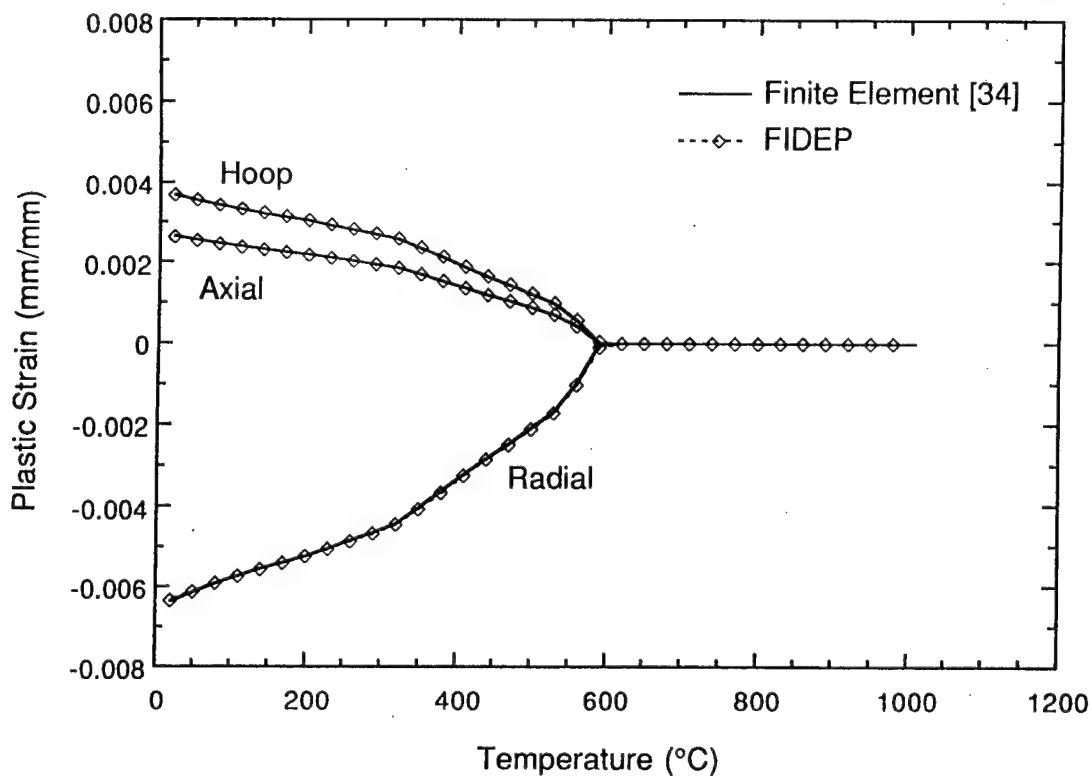
Thermally Induced Stresses in Ti-24Al-11Nb Matrix at the Fiber-Matrix Interface due to Cool-Down using FEA and FIDEP.



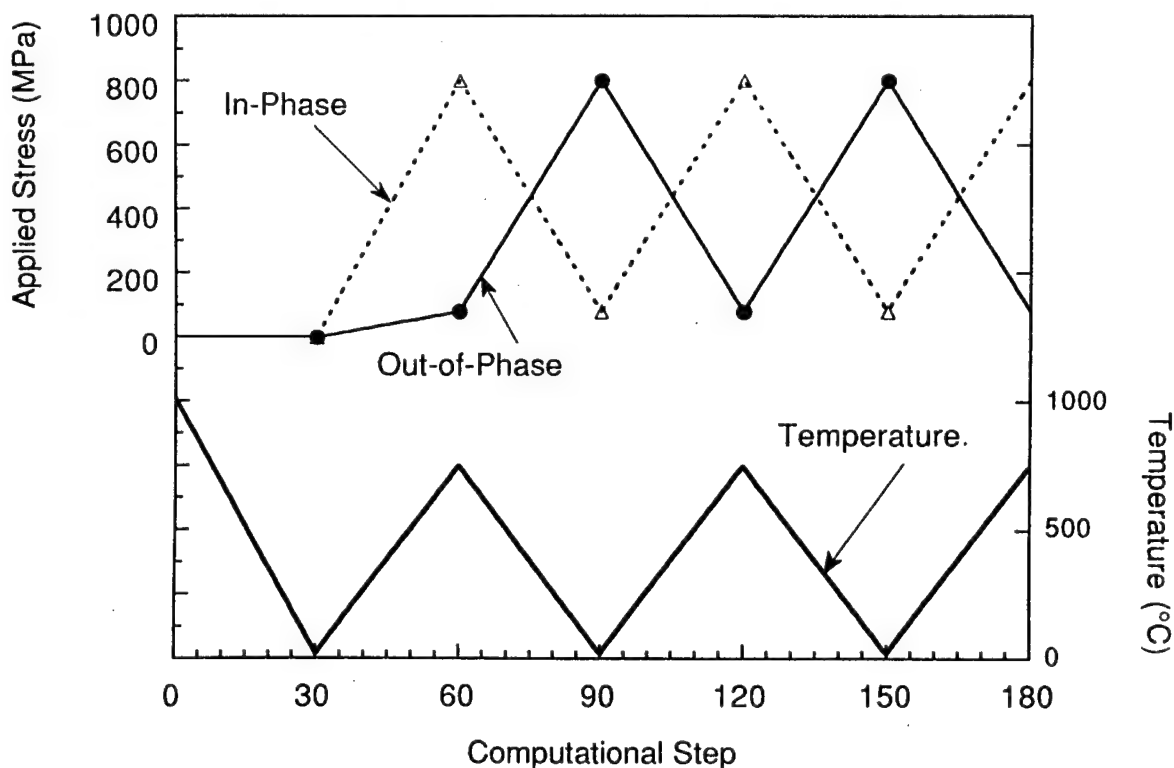
Axial Stress Predictions in Ti-24Al-11Nb Matrix during Cool-Down using the Uniaxial Model and FIDEP.



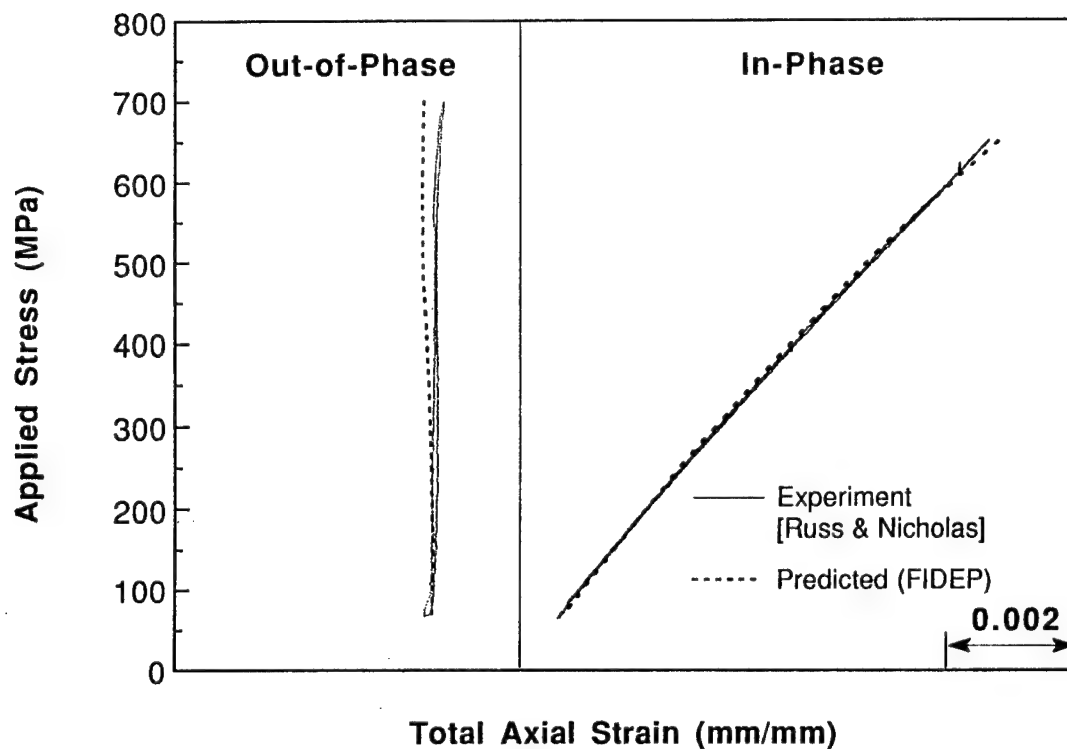
**Plastic Strain Predictions in Ti-24Al-11Nb Matrix at the
Fiber-Matrix Interface due to Cool-Down from Processing Temperature.**



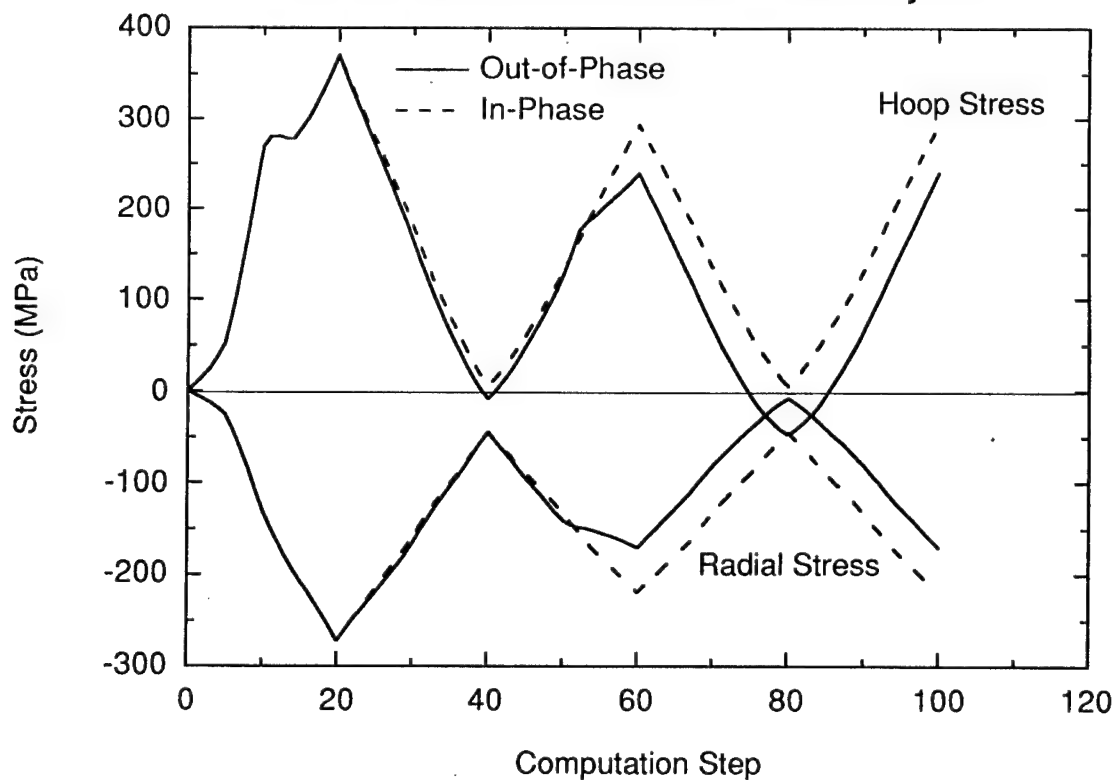
**Temperature and Stress History of a Typical
In-Phase and Out-of-Phase TMF Cycle**

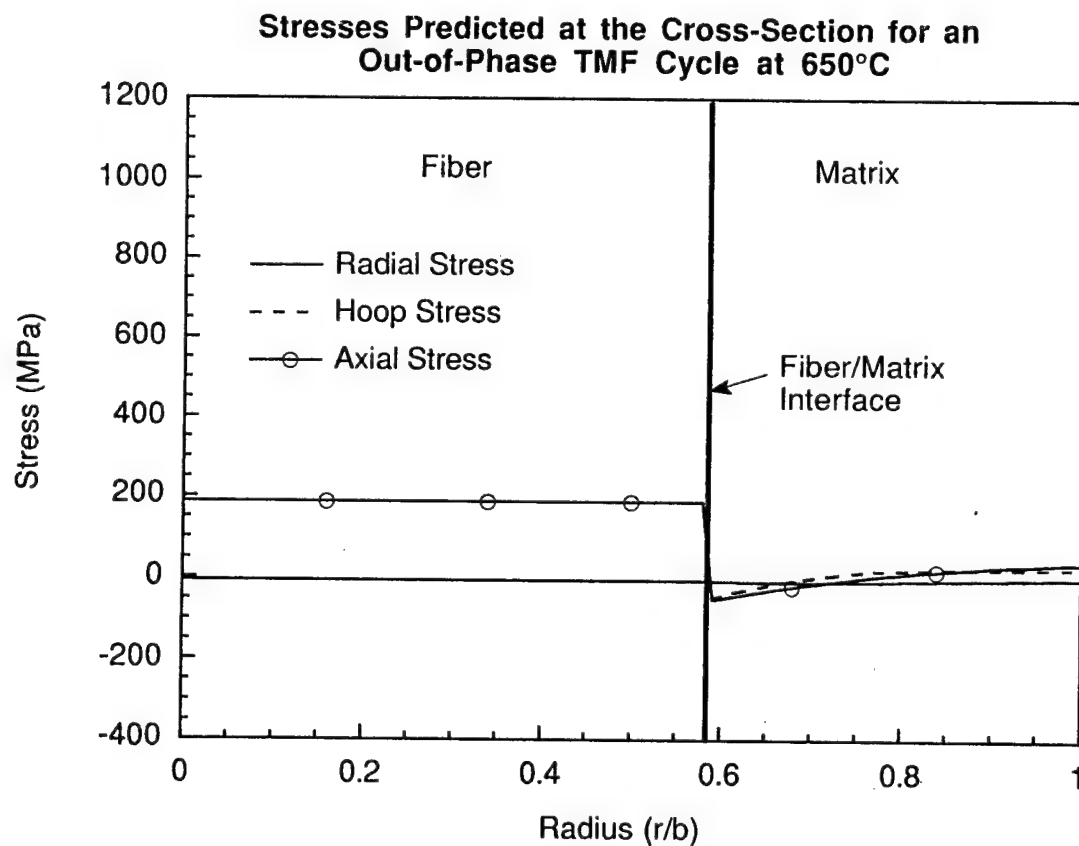
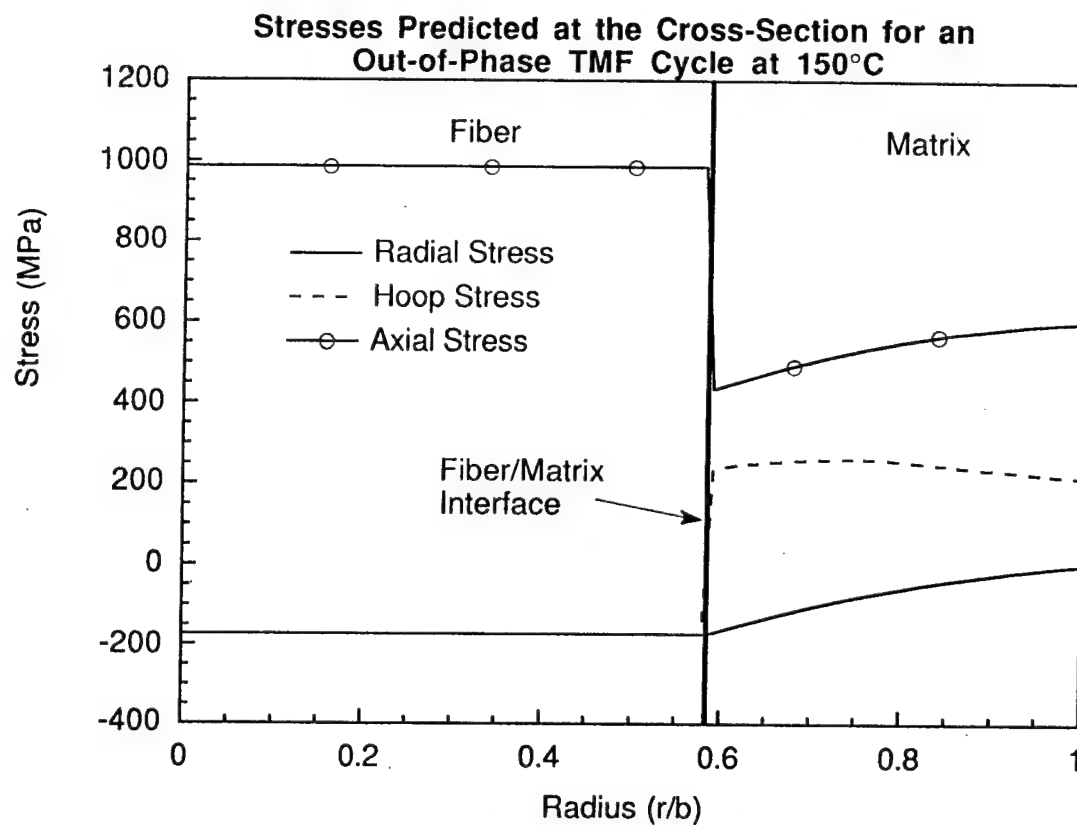


Comparison of Calculated and Experimental Stress-Strain Profiles in In-Phase and Out-of-Phase TMF Cycles

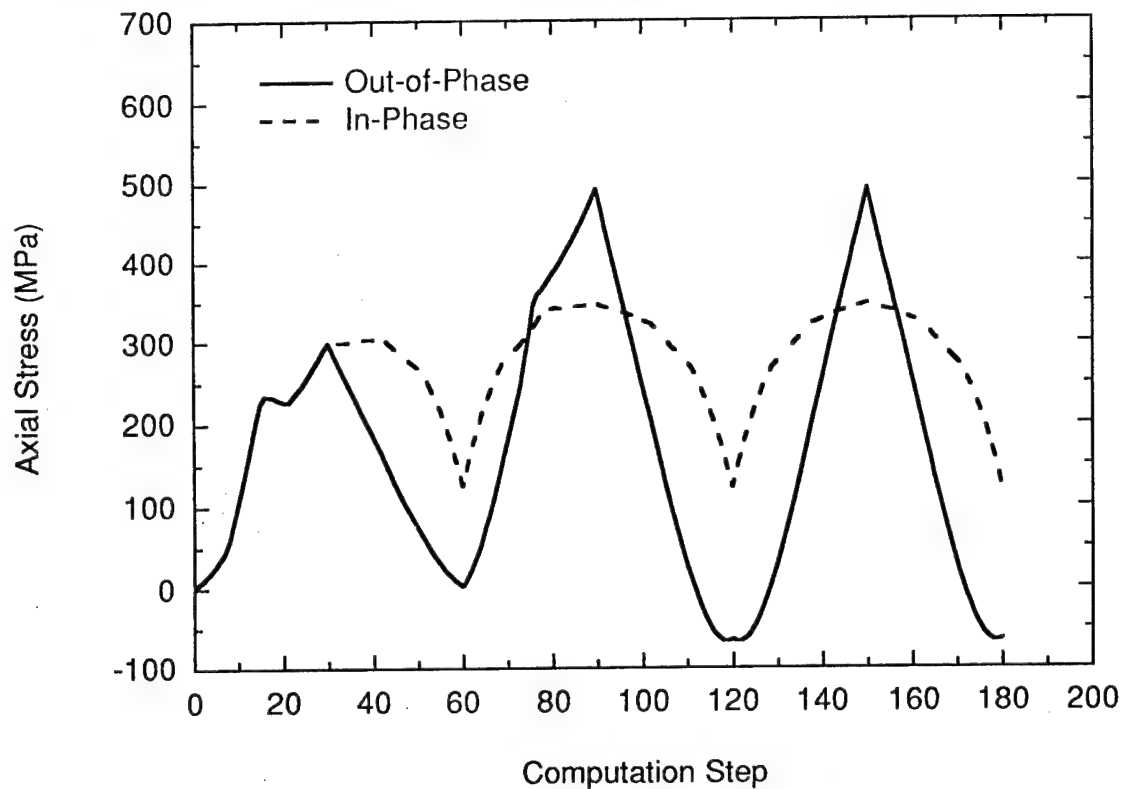


Radial and Hoop Stresses in Ti-24Al-11Nb Matrix at the Fiber-Matrix Interface in TMF Cycle

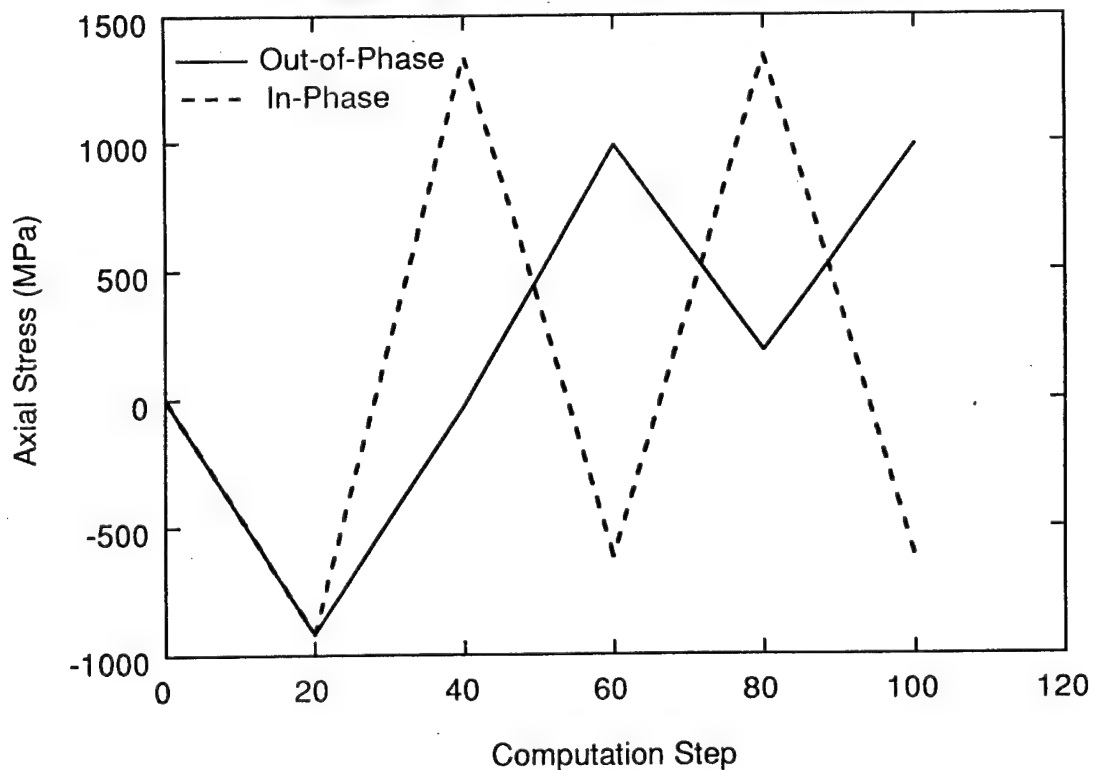




Axial Stress Predictions in the Ti-24Al-11Nb Matrix at the Fiber-Matrix Interface for In-Phase and Out-of-Phase TMF Loadings



Axial Stress Peaks in the SCS-6 Fiber for In-Phase and Out-of-Phase TMF Loadings



Summary

- An elastic-plastic code was developed to predict the triaxial stress-strain state in a unidirectional composite subjected to processing conditions and thermomechanical cycling.
- Conducted In-Phase and Out-of-Phase simulations.
- Predicted load-displacements traces showed good correlation with experimental load-displacement traces.
- Matrix maximum stress and stress range is more severe in out-of-phase. Fiber maximum stress and stress range more severe in in-phase.
- In the matrix radial and hoop stress magnitudes and ranges comparable to axial stress magnitudes and ranges.
- Bodner-Partom Unified Strain Theory with Back Stress implementation is in progress.

"Influence of Ply Waviness on Stiffness and Strength Reduction in Composite Laminates"

Travis A. Bogetti

U.S. Army Research Laboratory
ATTN: AMSRL-WT-PD
Aberdeen Proving Ground, MD 21005-5066

John W. Gillespie, Jr.

Assistant Director, Center for Composite Materials and
Associate Professor, Department of Mechanical Engineering
University of Delaware, Newark, DE 19716

Analytical models are developed to investigate the influence of ply waviness on the stiffness and strength of $[90/0]_s$ and $[90/\pm\beta]_s$ sublaminate laminate constructions commonly used in compression loaded filament wound composite cylinders. The theoretical development of the models employs a two-dimensional laminated plate theory analogy. The models predict:

- the effective (average) elastic properties (stress/strain response) and thermal expansion coefficients of sublaminates containing wavy layers.
- individual ply stresses within the sublaminate due to both prescribed mechanical and thermal loading.
- strength reduction associated with ply waviness and residual stress.

Parametric studies are conducted for AS-4 Graphite and S-2 Glass polyetherketoneketone (PEKK) thermoplastic composite laminates. Ply waviness is assumed to be in the $[0^\circ]$ ply of the $[90/0]_s$ model and the $[\pm\beta^\circ]$ ply of the $[90/\pm\beta]_s$ model. Results show that stiffness and strength reduction are significant in the direction of undulation and insignificant in the other direction. Mechanisms of stiffness reduction are attributed to out-of-plane rotation of wavy plies. The magnitude of the property reduction increases as the undulation amplitude increases and the half-wavelength of the undulation decreases. Increased material anisotropy is also shown to influence property reduction in AS-4 Graphite/PEKK much more than in S-2 Glass/PEKK laminates. Biaxial failure envelopes are derived from the application of the Maximum Stress failure criterion on the ply level. Results show that a plateau region exists at low undulation amplitudes that corresponds to compressive failure in the fiber direction. Above a critical amplitude, interlaminar shear failure modes are excited within the wavy ply and a significant reduction in laminate strength is predicted.

Model enhancement has been conducted by incorporating a three-dimensional laminated media analysis, nonlinear (incrementally piecewise linear) shear material behavior and progressive ply failure. The analytic models developed in this work can be used to generate effective property input for use in traditional structural analysis techniques to help quantify the effects of ply waviness (manufacturing defects) on the mechanical performance of realistic composite components. The models can also be useful in identifying dominant mechanisms for stiffness and strength reduction in composite laminates. Through this fundamental approach, valuable insight can be gained which could help to explain the typically observed poor translation of composite laminate (coupon) properties into realistic thick composite structures. In addition, the models can be used to establish quality control standards with respect to ply waviness that do not reduce laminate performance below design levels.

MOTIVATION:

- "Observable" Ply Waviness Found in Manufactured Components.
- Lack of Correlation Between Design/Analysis and Test Results.

GOALS:

- Quantify Effects of Ply Waviness on Stiffness and Strength Reduction in Composite Laminates.
- Explain Discrepancy Between Design/Analysis and Test Results.

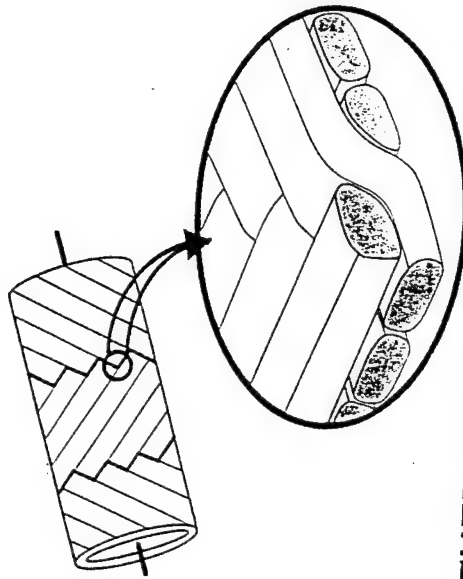
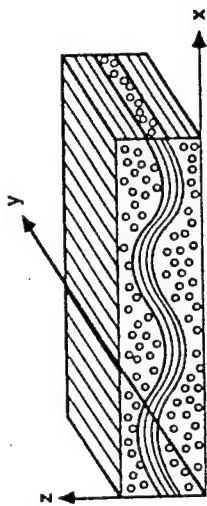
APPROACH:

- Develop an Analytic "Wavy" Model to Predict....
 - Elastic Properties.
 - Ply Level Stress and Strain.
 - Strength Reduction.
- Conduct Parametric Studies to....
 - Gain a Fundamental Understanding of the Effects of Ply Waviness on Stiffness and Strength Reduction.
 - Quantify These Effects Within Realistic Configurations.

MINI-MECHANICS MODEL DEVELOPMENT

- Microstructural Examination (Ply Level)
- Unit Cell Identification
- Mathematical Description
- Analytic Solution (CLPT Analogy)

2-DIMENSIONAL WAVY MODELS



MATHEMATICAL DESCRIPTION WITHIN UNIT CELL : [90/0/90] WAVINESS

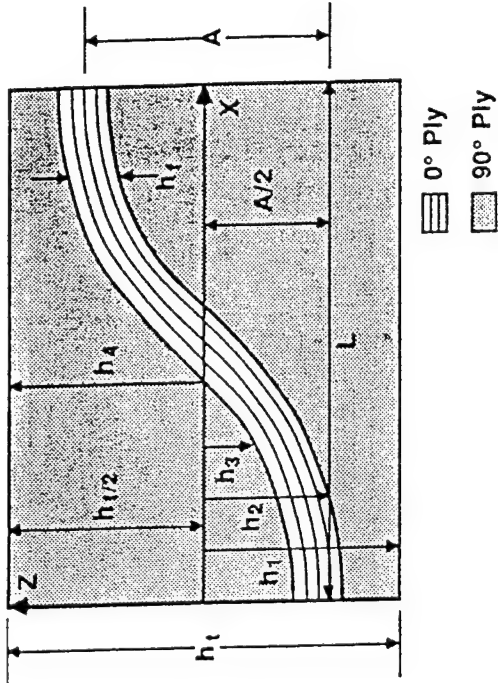
$$h_1(x) = -h_0/2$$

$$h_2(x) = -A/2 - h_0/2 + [1 + \sin(\frac{\pi}{L}(x - \frac{L}{2}))] A/2$$

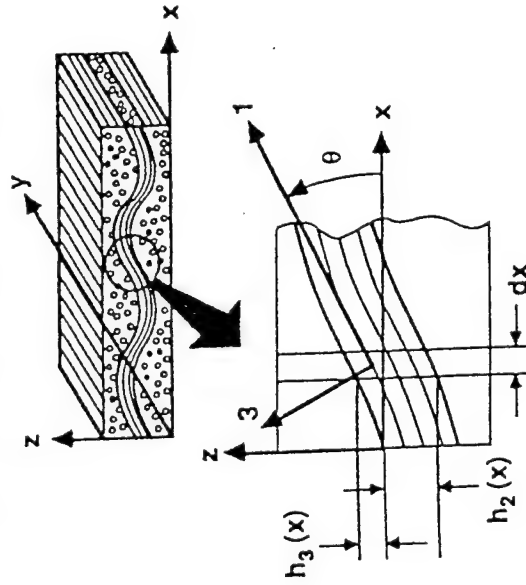
$$h_3(x) = -A/2 + h_0/2 + [1 + \sin(\frac{\pi}{L}(x - \frac{L}{2}))] A/2$$

$$h_4(x) = h_0/2$$

UNIT CELL PARAMETERS: [90/0/90] WAVINESS



LAMINATE ANALOGY FOR [90/0/90] WAVINESS



INFLUENCE OF PLY ROTATION ON IN-PLANE PROPERTIES

$$E_x(\theta) = [l\theta^4/E_1 + (1/G_{13} - 2\nu_{13}/E_1) l\theta^2 m\theta^2 + m\theta^4/E_3]^{-1}$$

$$E_y(\theta) = E_2$$

$$\nu_{xy}(\theta) = E_x(\theta) \left[\frac{l\theta^2 \nu_{12}}{E_1} + \frac{\nu_{32} m\theta^2}{E_3} \right]$$

$$G_{xy}(\theta) = \left[\frac{m\theta^2}{G_{23}} + \frac{l\theta^2}{G_{12}} \right]^{-1}$$

$$l\theta = \cos\theta$$

$$m\theta = \sin\theta$$

DEFINITION OF EFFECTIVE PROPERTIES OF THE UNIT CELL

$$\begin{aligned} E_x &= \frac{1}{h_t a_{11}^{**}} \\ E_y &= \frac{1}{h_t a_{22}^{**}} \\ \nu_{xy} &= \frac{-a_{12}^{**}}{a_{11}^{**}} \\ G_{xy} &= \frac{1}{a_{33}^{**}} \end{aligned}$$

LAMINATION THEORY APPLIED TO EACH INCREMENT (DX) WITHIN UNIT CELL

$$\left\{ \begin{matrix} N_i \\ M_i \end{matrix} \right\} = \begin{bmatrix} A_{ij} & B_{ij} \\ B_{ij} & D_{ij} \end{bmatrix} \left\{ \begin{matrix} \epsilon_j^0 \\ \kappa_j \end{matrix} \right\} \quad (i, j = 1, 2, 6)$$

$$(A_{ij}, B_{ij}, D_{ij}) = \sum_{k=1}^n \int_{h_{k-1}}^{h_k} (1, z, z^2) Q_{ij} dz$$

$$A_{ij} = \sum_{k=1}^n (Q_{ij})_k (h_k - h_{k-1})$$

$$a_{ij}^* = [a_{ij} \cdot b_{ij} d_{ij}^{-1} b_{ij}]$$

$$a_{ij}^{**} = \frac{1}{L} \int_0^L a_{ij}^*(x) dx$$

PLY STRESS WITHIN EACH SEGMENT (DX) ALONG THE UNIT CELL

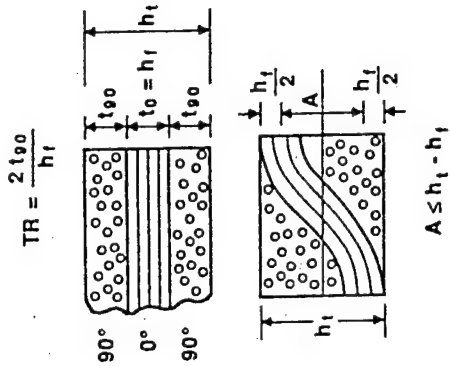
$$\{\epsilon_i^*\} = [a_{ij}^*] \{N_j\}$$

$$\{(\sigma_i^*)_k\} = [(Q_{ij})_k] \{(\epsilon_j^*)_k - (\alpha_j)(\kappa)\Delta T\}$$

GEOMETRIC CONSTRAINTS: [90/0/90] WAVINESS

Parameter Study: Geometry

TR	h_t (inches)	A_{max} (inches)
1.0	0.010	0.005
2.0	0.015	0.010
2.7	0.0185	0.0135
6.0	0.035	0.03
10.0	0.055	0.05
$\frac{L}{b_f} = 5, 20, 50$		

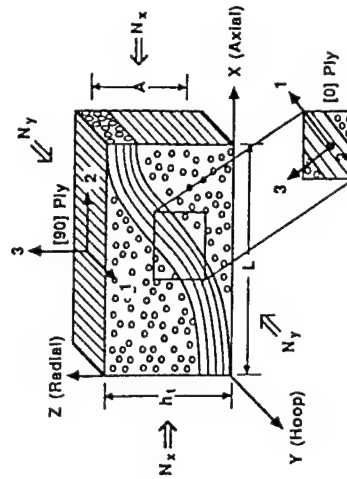


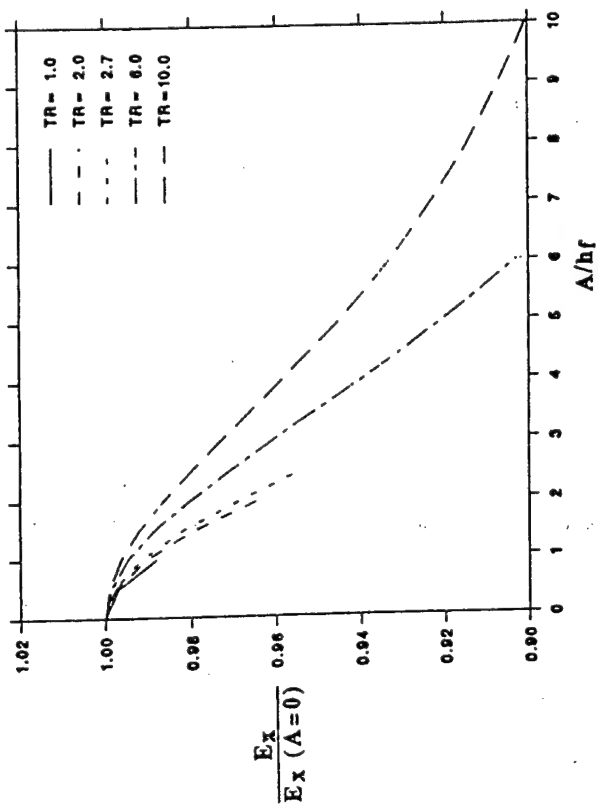
Strength Allowables

Material Properties

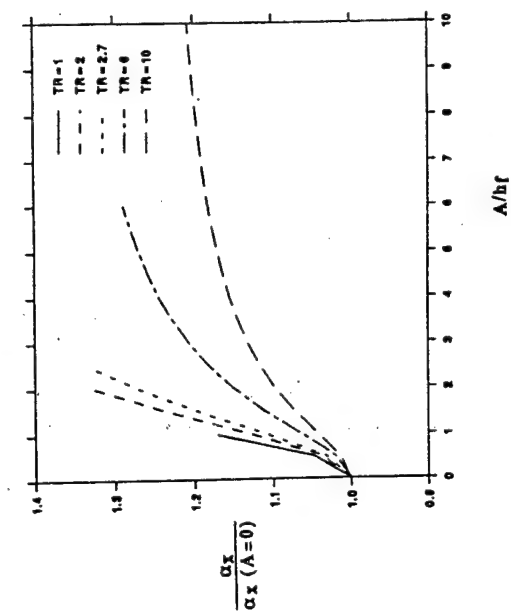
GLOBAL AND PLY COORDINATE SYSTEMS USED IN THE ANALYSIS

AS4 Graphite/PEKK		AS4 Graphite/PEKK	S2 Glass/PEKK
E_1 (Msi)	17.0	X1T (Ksi)	24.3
E_2 (Msi)	1.40	X2T (Ksi)	7.0
G_{12} (Msi)	0.98	X3T (Ksi)	8.5
G_{23} (Msi)	0.98	X1C (Ksi)	177
ν_{12}	0.36	X2C (Ksi)	30.6
ν_{23}	0.36	X3C (Ksi)	35.0
(μ_r/μ_f)	-0.5	S13 (Ksi)	17.0
(μ_z/μ_f)	15.5	S12 (Ksi)	15.7
(μ_z/μ_f)	15.5		

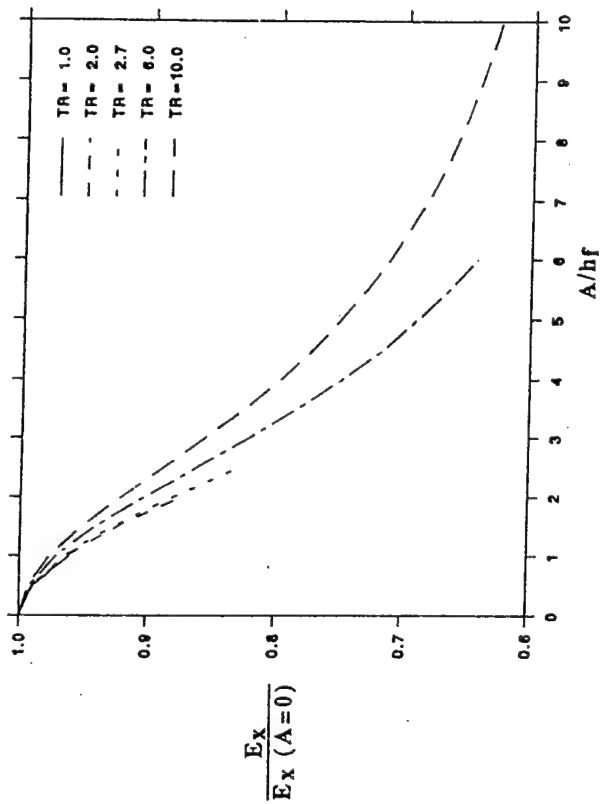




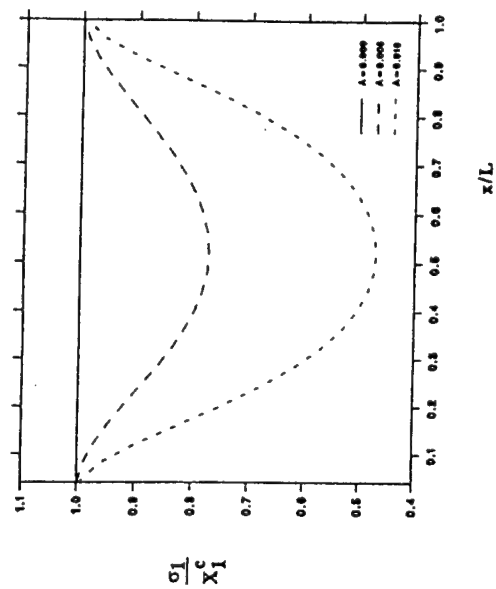
Influence of Undulation Amplitude on E_x in S2 Glass/PEKK ($L/h_f = 20$)



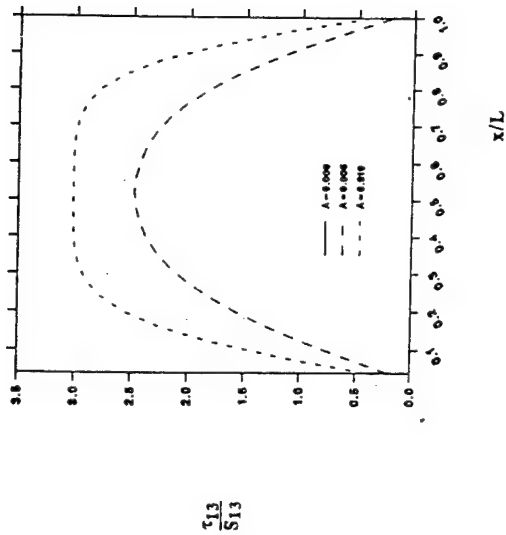
Influence of Undulation Amplitude on α_x in S2 Glass/PEKK ($L/h_f = 5$)



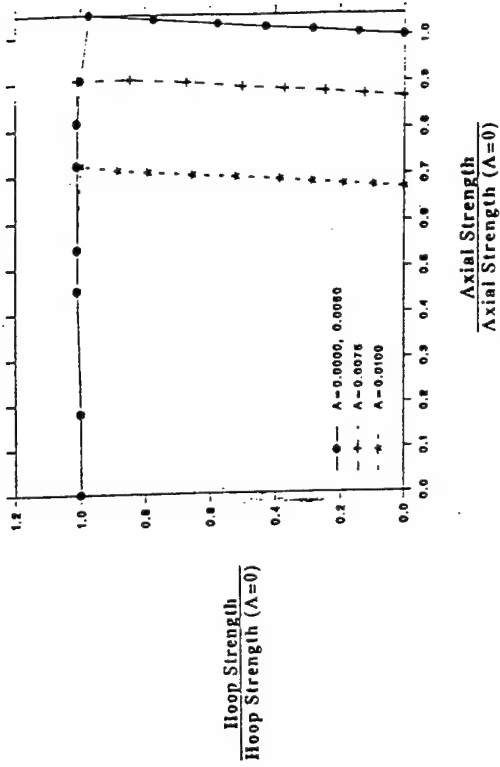
Influence of Undulation Amplitude on E_x in AS4 Graphite/PEKK ($L/h_f = 20$)



Longitudinal Stress Within a Wavy [0] Ply in AS4 Graphite/PEKK: Axial Loading (TR=2, $L/h_f = 5$, $N_x (A=0) = -901$ lbf/in at failure)



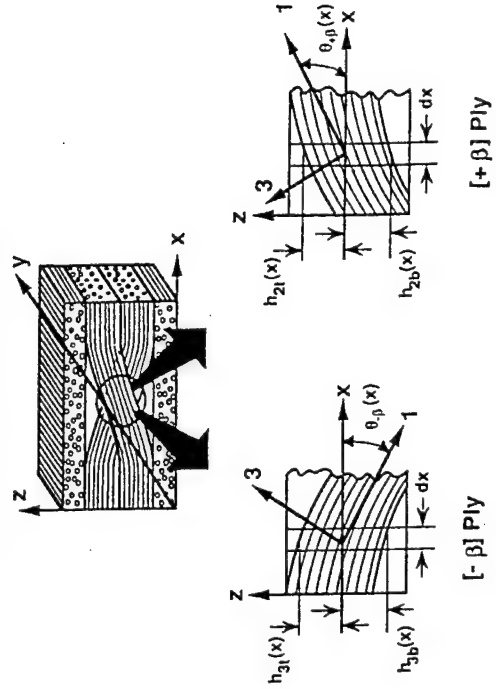
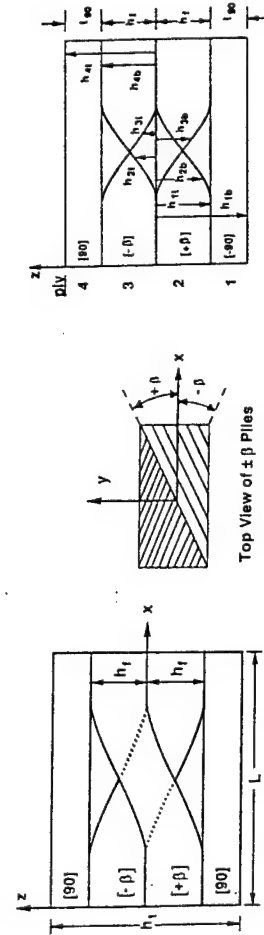
Interlaminar Shear Stress Within a Wavy [0] Ply in AS4 Graphite/PEKK: Axial Loading (TR=2, $L/h = 5$, N_1 (A=0) = -901 lb/in at failure)



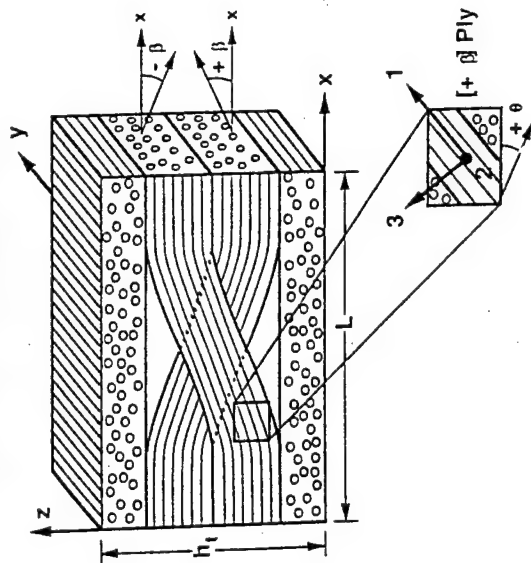
BI-Axial Compression Failure Envelopes in AS4 Graphite/PEKK (TR=2, $L/h = 20$, $\Delta T = 0^\circ F$)

UNIT CELL PARAMETERS: $[90/\pm\beta/90]$ WAVINESS

LAMINATE ANALOGY FOR $[90/\pm\beta/90]$ WAVINESS

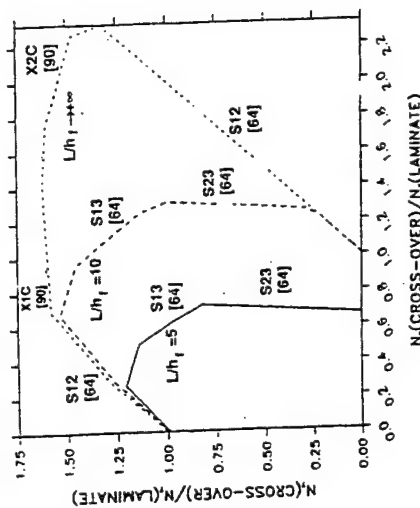


GLOBAL AND PLY COORDINATE SYSTEMS USED IN THE ANALYSIS



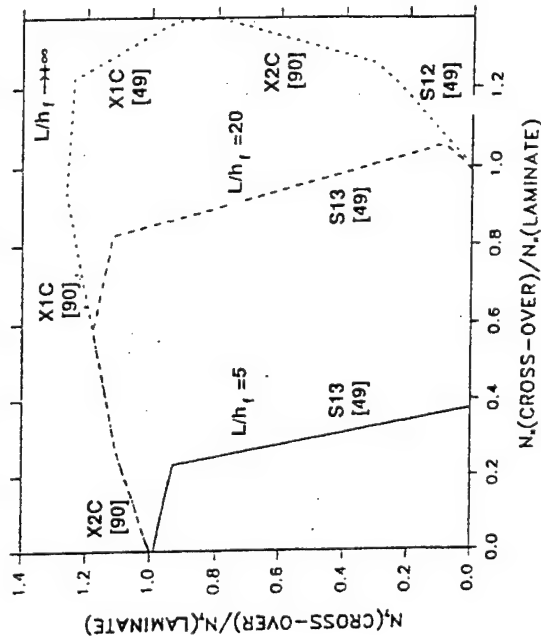
135

BI-AXIAL FAILURE COMPRESSION ENVELOPES IN S2/PEKK



Influence of Cross-Over Region Geometry on Bi-Axial Compression Failure Envelopes in S2/PEKK ($L/h_1 = 5, 10, +\infty$, $TR=2$, $\beta=64^\circ$, $S13=8$ Ksi, $\Delta T=0^\circ F$)

BI-AXIAL COMPRESSION FAILURE ENVELOPES IN AS4/PEKK

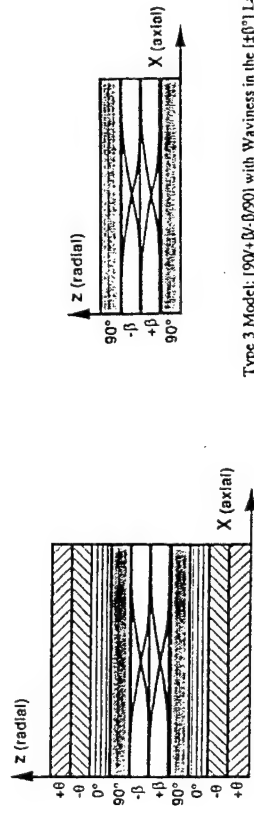
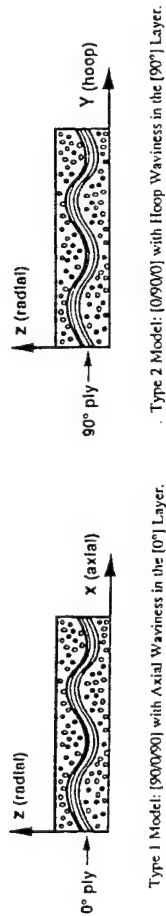


Influence of Cross-Over Region Geometry on Bi-Axial Compression Failure Envelopes in AS4/PEKK ($L/h_1 = 5, 20, +\infty$, $TR=1$, $\beta=49^\circ$, $S13=7$ Ksi, $\Delta T=0^\circ F$)

2-DIMENSIONAL WAVY MODEL CONCLUSIONS

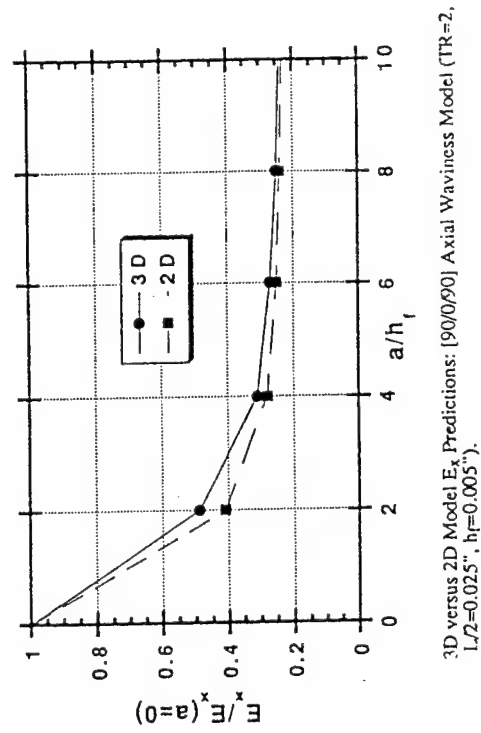
- Stiffness and Strength Reductions ...
 - Are Greatest in the Direction of Undulation.
 - Increase with Material Anisotropy (GR to 65% and GL to 8%).
 - Are Insignificant in Non-Wavy Directions.
 - Increase with the Magnitude of "Waviness".
- Strength Reduction is ...
 - Dominated by Interlaminar Shear Failure.
 - Under a Threshold Dictated by Interlaminar Shear Strength.

3-DIMENSIONAL WAVY MODELS



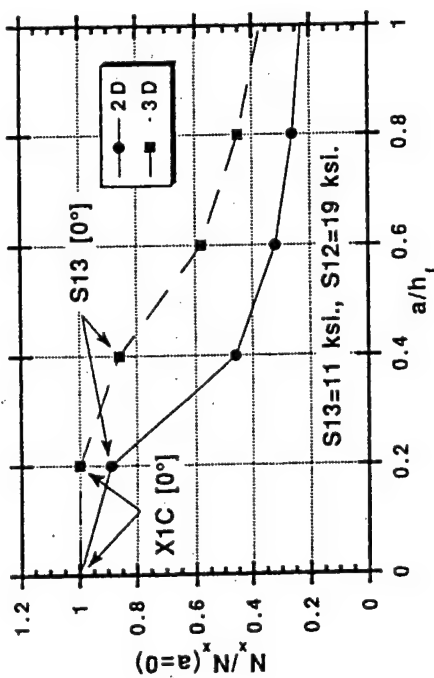
3-DIMENSIONAL ANALYSIS FEATURES

- Linear-Elastic
- Non-Linear in Shear
- Progressive Failure on Ply & Segment Level

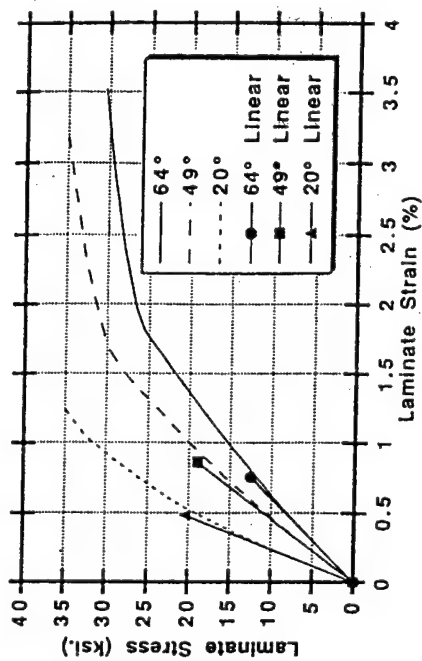


3-DIMENSIONAL WAVY MODEL ANALYSIS

- Based on 3-D Laminated Media Analysis.
- Analogous to 2-D Approach.
- "Similar" Trends Observed.



3D versus 2D Failure Predictions: [90/0/90] Axial Waviness Model (TR=2, $L/2=0.025"$, $h_1=0.005"$, $a=0.005"$) Under Uni-axial Loading.



Nonlinear Stress-Strain Response of the [90/±b/90] Cross-Over Model Under Axial Compression.

WAVY MODEL UTILITY

- Use Effective Properties as Input into Structural Analyses to Quantify the Effects of Ply Waviness on Performance.
- Conduct Tradeoff Studies Between Performance and Manufacturing Tolerances (Cost).

3-DIMENSIONAL WAVY MODEL CONCLUSIONS

- A 3-D Analysis Permits 3-D Predictions !
- Stiffness and Strength "Trends" are "Similar" to the 2-D Analysis.
 - 3-D Predictions Show Moderately Less Stiffness Reduction.
 - 3-D Predictions Show Significantly Less Strength Reduction.
- Nonlinear Analysis Predicts Significantly Higher Strengths Due to Load Redistribution Capability.

THREE-DIMENSIONAL EFFECTIVE PROPERTIES OF COMPOSITE MATERIAL FOR FINITE ELEMENT APPLICATIONS

Amos Alexander
Custom Analytical Engineering System, Inc.
Flintstone, MD 21530

Jerome T. Tzeng
U.S. Army Research Laboratory
ATTN: AMSRL-WT-PD
Aberdeen Proving Ground, MD 21005-5066

ABSTRACT

A model has been developed to compute the effective properties of an arbitrarily shaped 3D solid element with multiple anisotropic material regions. The analysis utilizes the strain energy and finite element approaches to resolve the three-dimensional complexity of composite layer geometry, anisotropy, ply orientation, and multi-material regions within an element. Accordingly, the model accounts for the effects of irregular geometry due to ply drop-offs, inhomogeneities, and variation of cross section.

The computed elastic constants are accurate, especially for the transverse shear properties. The analysis is particularly suitable for finite element applications of near-net shaped structures which, in general, contain irregular shaped elements in the finite element mesh. Based on the model, a pre-processor was developed to generate finite element models for computer codes such as DYNA, NIKE, and ABAQUS. The FEM results are finally recovered and ply-by-ply results are obtained by the developed post-processor.

OBJECTIVES

- Develop a model which accurately calculates the effective properties for an 3D arbitrarily shaped multi-material solid element.
- Accurate transverse shear properties
- Finite element applications for near-net shaped thick-section composites
- Develop pre- and post- processors to be used for NIKE, DYNA, ABAQUS computer codes.
- Automatic mesh generator
- Layer response recovery and ply-by ply stress and strain results

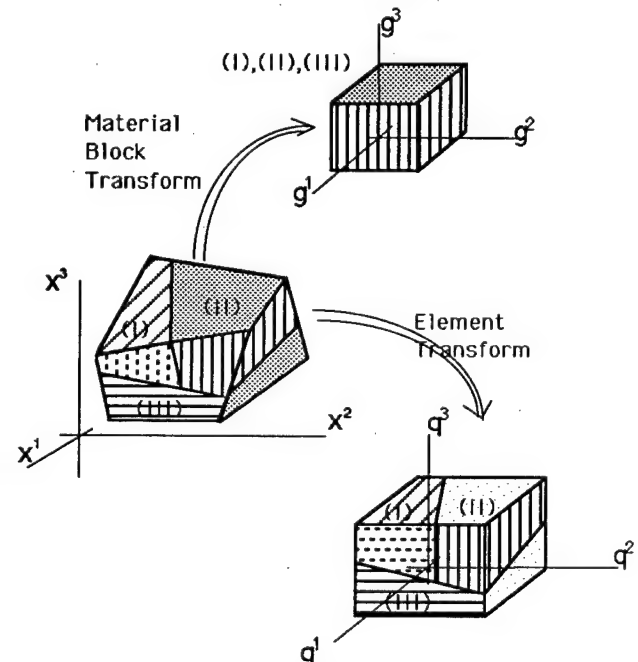


Figure 1. Coordinates Transformations of Material Blocks and Element

MODEL DEVELOPMENT

Consider a material block contained within some internal region of an element (Figure 1). Relative to the global coordinates (X^1 , X^2 , and X^3), the generalized elastic constitutive behavior of the material block is described as follows:

$$\sigma_i^j = C_{ik}^{jl} \varepsilon_l^k \quad (1)$$

where σ_i^j is the stress tensor, ε_l^k is the strain tensor, and C_{ik}^{jl} represents the material stiffness tensor relative to the global frame.

The total strain energy of the material block, E can be derived from the strain energy density, E_0 and expressed in terms of the displacements, u^i as the following expression.

$$\begin{aligned} E &= \int_M E_0 dv \\ &= \int_M \left[\int_0^{\varepsilon_i^j} \sigma_i^j d\varepsilon_i^j \right] dv \\ &= \int_M \frac{1}{2} C_{ik}^{jl} \frac{\partial u^i}{\partial X^j} \frac{\partial u^k}{\partial X^l} dv \end{aligned} \quad (2)$$

Since the displacements within the volume are continuous, they can be approximated by interpolation functions. Let's introduce an isoparametric element in local coordinates (g^1 , g^2 , and g^3). With the conformal mapping, the displacement fields and the coordinates can be expressed in terms of the local coordinates as follows :

$$\begin{aligned} u^i &= N^\alpha U_\alpha^i \\ X^i &= N^\alpha X_\alpha^i \end{aligned} \quad (3)$$

where the U_α^i represents the displacement components of the corner or nodal points, the X_α^i are the global coordinates of the corner or nodal points, and $N^\alpha = N^\alpha(g^1, g^2, g^3)$ represents the interpolation functions. The interpolation functions may be an 8 node linear formulation or a 20 node quadratic formulation. For the linear formulation, the interpolation functions are as follows:

$$\begin{aligned} N^1 &= \frac{1}{8} (1 - g^1) (1 - g^2) (1 - g^3) & N^5 &= \frac{1}{8} (1 - g^1) (1 - g^2) (1 + g^3) \\ N^2 &= \frac{1}{8} (1 + g^1) (1 - g^2) (1 - g^3) & N^6 &= \frac{1}{8} (1 + g^1) (1 - g^2) (1 + g^3) \\ N^3 &= \frac{1}{8} (1 + g^1) (1 + g^2) (1 - g^3) & N^7 &= \frac{1}{8} (1 + g^1) (1 + g^2) (1 + g^3) \\ N^4 &= \frac{1}{8} (1 - g^1) (1 + g^2) (1 - g^3) & N^8 &= \frac{1}{8} (1 - g^1) (1 + g^2) (1 + g^3) \end{aligned} \quad (4)$$

The strain energy of the material block can be therefore rewritten in terms of the nodal displacements and interpolation functions as the following expression.

$$E_{(M)} = \frac{1}{2} [C_{ik}^{jl}]_{(M)} \left[\int \frac{\partial N^\alpha}{\partial g^m} \frac{\partial N^\beta}{\partial g^n} \frac{\partial g^m}{\partial X^j} \frac{\partial g^n}{\partial X^l} dv \right]_{(M)} U_\alpha^j U_\beta^k \quad (5)$$

The force components contributed by the material block M at corner point α can be obtained from

$$\begin{aligned} \frac{\partial E_{(M)}}{\partial U_\alpha^j} &= [F_i^\alpha]_{(M)} \\ &= [K_{ik}^{\alpha\beta}]_{(M)} U_\beta^k \quad \text{where} \end{aligned}$$

$$[K_{ik}^{\alpha\beta}]_{(M)} = \frac{1}{2} [C_{ik}^{jl}]_{(M)} \left[\int \frac{\partial N^\alpha}{\partial g^m} \frac{\partial N^\beta}{\partial g^n} \frac{\partial g^m}{\partial X^j} \frac{\partial g^n}{\partial X^l} dv \right]_{(M)} \quad (6)$$

Summing over all material blocks that are common to corner point α results in an expression for the net external applied force on that point:

$$F_i^\alpha = \sum_M [K_{ik}^{\alpha\beta}]_{(M)} U_\beta^k \quad (7)$$

Assuming there are a total of Γ corner points of material blocks contained within the element, there will be 3Γ equations of the form (7). Let the first Ω represents points corresponding to the nodes of the element ($\Omega < \Gamma$). The next Δ points correspond to the corner points lying on the surface of the element at locations other than the element nodes ($0 < \Delta < (\Gamma - \Omega)$) and the last $(\Gamma - \Omega - \Delta)$ points correspond to points falling within the interior of the element boundary.

A similar approach can be applied to the entire element. If the material stiffness of the overall element is represented by an equivalent homogeneous anisotropic material

with stiffness tensor \bar{C}_{ik}^{jl} then the total strain energy for the element is given by

$$\bar{E} = \frac{1}{2} \left[\bar{C}_{ik}^{jl} \left[\int \frac{\partial S^\gamma}{\partial q^m} \frac{\partial S^\rho}{\partial q^n} \frac{\partial q^m}{\partial X^j} \frac{\partial q^n}{\partial X^l} dv \right]_{\bar{V}} U_\gamma^j U_\rho^k \right]_{\bar{V}} \quad (\gamma, \rho = 1, \dots, \Omega) \quad (8)$$

where the integration is over the entire volume of the element, U_γ^j and U_ρ^j are the displacements at the node points γ and ρ , S_γ represent the element deformation shape

functions, and q^m are the isoparametric coordinates of the transformation. Accordingly, the relationship of coordinate transform can be expressed as follows:

$$\begin{aligned} x^i &= S^\gamma x_\gamma^i \quad \text{and} \\ S^\gamma &= S^\gamma(q_1, q_2, q_3) \end{aligned} \quad (9)$$

where x_γ^i corresponding to the global coordinates of the node point γ .

The force applied at node γ is thus given by

$$F_\gamma^j = \frac{\partial \bar{E}}{\partial U_\gamma^j} = \bar{C}_{ik}^{jl} \left[\int \frac{\partial S^\gamma}{\partial q^m} \frac{\partial S^\rho}{\partial q^n} \frac{\partial q^m}{\partial X^j} \frac{\partial q^n}{\partial X^l} dv \right]_{\bar{V}} U_\rho^k \quad (\gamma, \rho = 1, \dots, \Omega) \quad (10)$$

From Eq.7 and Eq.10, the following expression can be concluded from equivalent forces for each node γ

$$\bar{C}_{ik}^{jl} \left[\int \frac{\partial S^\gamma}{\partial q^m} \frac{\partial S^\rho}{\partial q^n} \frac{\partial q^m}{\partial X^j} \frac{\partial q^n}{\partial X^l} dv \right]_{\bar{V}} U_\rho^k = \sum_M \{ [K_{ik}^{\gamma\rho}] U_\rho^k + [K_{ik}^{\gamma\beta}] U_\beta^k \} \quad (\gamma, \rho = 1, \dots, \Omega) \quad (\beta = (\Omega+1), \dots, \Gamma) \quad (11)$$

For notation convenience, we define

$$\begin{aligned} A_{jl}^{\gamma\rho} &= \left[\int \frac{\partial S^\gamma}{\partial q^m} \frac{\partial S^\rho}{\partial q^n} \frac{\partial q^m}{\partial X^j} \frac{\partial q^n}{\partial X^l} dv \right]_{\bar{V}} \quad \text{and} \\ B_{ik}^{\gamma\rho} &= \sum_M [K_{ik}^{\gamma\rho}] \end{aligned} \quad (12)$$

Totally, there are 3Ω equations at the Ω nodes of the element ready to be solved and they are expressed as follows:

$$\bar{C}_{ik}^{jl} A_{jl}^{\gamma\rho} U_\rho^k = B_{ik}^{\gamma\rho} U_\rho^k + B_{ik}^{\gamma\beta} U_\beta^k \quad (\gamma, \rho = 1, \dots, \Omega) \quad (\beta = (\Omega+1), \dots, \Gamma) \quad (13)$$

The displacements of corner points ($\beta = (\Omega+1), \dots, \Gamma$) can be expressed as a linear combination of the element nodal displacements in the form :

$$U_{\beta}^k = Q_{\beta l}^{k\gamma} U_{\gamma}^l \quad \begin{array}{l} (\gamma = 1, \dots, \Omega) \\ (\beta = (\Omega+1), \dots, \Gamma) \end{array} \quad (14)$$

The coefficients $Q_{\beta l}^{k\gamma}$ are obtained from constraints that must be imposed on the $(\Omega+1)$ through Γ corner points contained in the element volume. For the Δ corner points lying on the surface of the element, we require that the net force on these points in any direction tangent to the surface be set to zero, and also that the points remain on the surface as the element deforms. For the remaining $(\Omega+\Delta+1)$ through Γ corner points that are located internally within the volume, we require that the net external force be zero. These constraints are applied with the aid of expressions of (3) and (7), resulting in a system of $3(\Gamma-\Omega)$ equations which relate the displacements of the $(\Omega+1)$ through Γ corner points to the displacements of the Ω element node points. Solution of this system of equations results in the coefficients $Q_{\beta l}^{k\gamma}$. Substitution of (14) into (13) results in the expression

$$\bar{C}_{ik}^{jl} A_{jl}^{\gamma p} U_p^k = B_{ik}^{\gamma p} U_p^k + B_{im}^{\gamma \beta} Q_{\beta k}^{mp} U_p^k \quad \begin{array}{l} (\gamma, p = 1, \dots, \Omega) \\ (\beta = (\Omega+1), \dots, \Gamma) \end{array} \quad (15)$$

or, since the order of the summation is not important

$$\bar{C}_{ik}^{jl} A_{jl}^{\gamma p} U_p^k = (B_{ik}^{\gamma p} + B_{im}^{\gamma \beta} Q_{\beta k}^{mp}) U_p^k \quad \begin{array}{l} (\gamma, p = 1, \dots, \Omega) \\ (\beta = (\Omega+1), \dots, \Gamma) \end{array} \quad (16)$$

Since the nodal displacement is independent to each other, the following expression is obtained

$$\bar{C}_{ik}^{jl} A_{jl}^{\gamma p} = B_{ik}^{\gamma p} + B_{im}^{\gamma \beta} Q_{\beta k}^{mp} \quad \begin{array}{l} (\gamma, p = 1, \dots, \Omega) \\ (\beta = (\Omega+1), \dots, \Gamma) \end{array} \quad (17)$$

Recalling the transform in Eq.9, $X^i = S^{\gamma} X_{\gamma}^i$, and taking the derivative with respect to q^m , we have

$$\frac{\partial X^i}{\partial q^m} = \frac{\partial S^{\gamma}}{\partial q^m} X_{\gamma}^i$$

From the chain rule for partial differentiation, the following expression is obtained

$$\frac{\partial X^i}{\partial q^m} \frac{\partial q^m}{\partial X^j} = \frac{\partial S^{\gamma}}{\partial q^m} \frac{\partial q^m}{\partial X^j} X_{\gamma}^i = \delta_j^i \quad (18)$$

Multiplying the expression in Eq.12 by $X_{\gamma}^i X_{\rho}^k$, we obtain

$$A_{jl}^{\gamma p} X_{\gamma}^j X_p^k = \int_V \frac{\partial S^{\gamma}}{\partial q^m} \frac{\partial S^p}{\partial q^n} \frac{\partial q^m}{\partial X^j} \frac{\partial q^n}{\partial X^l} X_{\gamma}^j X_p^k dv = \bar{V} \delta_j^i \delta_l^k \quad (19)$$

where the V is the total volume of the element.

Accordingly, the following expression can be derived from Eq.18 and Eq.19

$$\begin{aligned} \bar{C}_{ik}^{jl} A_{jl}^{\gamma p} X_{\gamma}^r X_p^s &= \bar{C}_{ik}^{rs} \bar{V} \\ &= [B_{ik}^{\gamma p} + B_{im}^{\gamma \beta} Q_{\beta k}^{mp}] X_{\gamma}^r X_p^s \\ &\quad \begin{matrix} (\gamma, \rho = 1, \dots, \Omega) \\ (\beta = (\Omega+1), \dots, \Gamma) \end{matrix} \end{aligned} \quad (20)$$

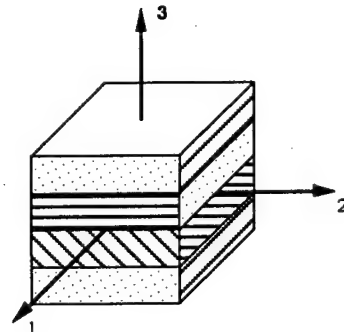
Finally, the equivalent element material stiffness tensor can be obtained by rearranging Eq.22 and has the following expression :

$$\begin{aligned} \bar{C}_{ik}^{jl} &= \frac{1}{\bar{V}} [B_{ik}^{\gamma p} + B_{im}^{\gamma \beta} Q_{\beta k}^{mp}] X_{\gamma}^j X_p^l \\ &\quad \begin{matrix} (\gamma, \rho = 1, \dots, \Omega) \\ (\beta = (\Omega+1), \dots, \Gamma) \end{matrix} \end{aligned} \quad (21)$$

CONSTITUTIVE RELATION OF LAMINATED MATERIAL

EFFECTIVE PROPERTY MODELS

- Enie, R. B. and Rizzo, R. R., 1970.
- Chou, P. C., Carleone, J., and Hsu, C. M., 1972.
- Pagano, N. J., 1974.
- Sun, C. T. and Li, S., 1988.
- Christensen, R. M. and Zywicz, E., 1989.
- Roy A. K. and Tsai S. W., 1992



$$\begin{Bmatrix} \sigma_{11} \\ \sigma_{22} \\ \sigma_{33} \\ \tau_{23} \\ \tau_{31} \\ \tau_{12} \end{Bmatrix} = \begin{bmatrix} C_{11} & C_{12} & C_{13} & C_{14} & C_{15} & C_{16} \\ C_{21} & C_{22} & C_{23} & C_{24} & C_{25} & C_{26} \\ C_{31} & C_{32} & C_{33} & C_{34} & C_{35} & C_{36} \\ C_{41} & C_{42} & C_{43} & C_{44} & C_{45} & C_{46} \\ C_{51} & C_{52} & C_{53} & C_{54} & C_{55} & C_{56} \\ C_{61} & C_{62} & C_{63} & C_{64} & C_{65} & C_{66} \end{bmatrix} \begin{Bmatrix} \epsilon_{11} \\ \epsilon_{22} \\ \epsilon_{33} \\ \gamma_{23} \\ \gamma_{31} \\ \gamma_{12} \end{Bmatrix}$$

COMPARISON OF TRANSVERSE SHEAR PROPERTIES

Chou's Model [0/0/90/90]					
0.1211E+08	0.5883E+06	0.5051E+06	0	0	0
0.5883E+06	0.1211E+08	0.5051E+06	0	0	0
0.5051E+06	0.5051E+06	0.1342E+07	0	0	0
0	0	0	<u>0.6033E+06</u>	0	0
0	0	0	0	<u>0.6033E+06</u>	0
0	0	0	0	0	0.7000E+06

3D Solid Element Model [0/0/90/90]					
0.1211E+08	0.5883E+06	0.5051E+06	0	0	0
0.5883E+06	0.1211E+08	0.5051E+06	0	0	0
0.5051E+06	0.5051E+06	0.1342E+07	0	0	0
0	0	0	<u>0.5531E+06</u>	0	0
0	0	0	0	<u>0.5531E+06</u>	0
0	0	0	0	0	0.7000E+06

Chou's Model [0/0/45/45]					
0.1497E+08	0.3117E+07	0.5444E+06	0	0	0.2694E+07
0.3117E+07	0.4194E+07	0.4658E+06	0	0	0.2692E+07
0.5444E+06	0.4658E+06	0.1342E+07	0	0	0.3933E+05
0	0	0	<u>0.5670E+06</u>	<u>0.4209E+05</u>	0
0	0	0	<u>0.4209E+05</u>	<u>0.6512E+06</u>	0
0.2694E+07	0.2692E+07	0.3933E+05	0	0	0.3231E+07

3D Solid Element Model [0/0/45/45]					
0.1497E+08	0.3117E+07	0.5444E+06	0	0	0.2694E+07
0.3117E+07	0.4194E+07	0.4658E+06	0	0	0.2692E+07
0.5444E+06	0.4658E+06	0.1342E+07	0	0	0.3933E+05
0	0	0	<u>0.5167E+06</u>	<u>0.3441E+05</u>	0
0	0	0	<u>0.3441E+05</u>	<u>0.5881E+06</u>	0
0.2694E+07	0.2692E+07	0.3933E+05	0	0	0.3231E+07

DEPENDENCE OF STACKING SEQUENCE ON TRANSVERSE SHEAR PROPERTIES

[0 / 45 / 45 / 0]					
0.1497E+08	0.3117E+07	0.5444E+06	0	0	0.2694E+07
0.3117E+07	0.4194E+07	0.4658E+06	0	0	0.2692E+07
0.5444E+06	0.4658E+06	0.1342E+07	0	0	0.3933E+05
0	0	0	<u>0.5128E+06</u>	<u>0.3138E+05</u>	0
0	0	0	<u>0.3138E+05</u>	<u>0.5925E+06</u>	0
0.2694E+07	0.2692E+07	0.3933E+05	0	0	0.3231E+07

[0 / 0 / 45 / 45]					
0.1497E+08	0.3117E+07	0.5444E+06	0	0	0.2694E+07
0.3117E+07	0.4194E+07	0.4658E+06	0	0	0.2692E+07
0.5444E+06	0.4658E+06	0.1342E+07	0	0	0.3933E+05
0	0	0	<u>0.5167E+06</u>	<u>0.3441E+05</u>	0
0	0	0	<u>0.3441E+05</u>	<u>0.5881E+06</u>	0
0.2694E+07	0.2692E+07	0.3933E+05	0	0	0.3231E+07

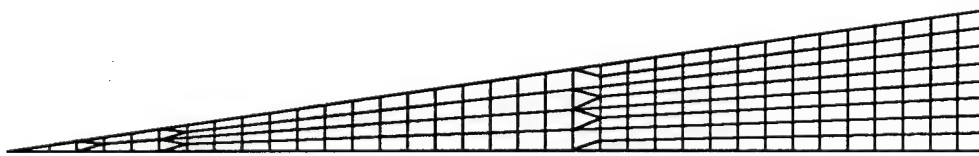
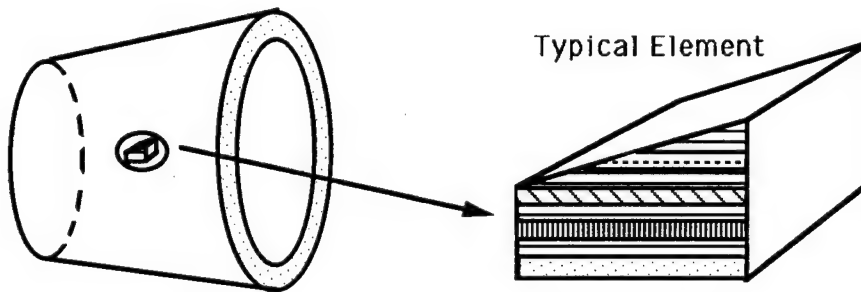
[45 / 0 / 0 / 45]					
0.1497E+08	0.3117E+07	0.5444E+06	0	0	0.2694E+07
0.3117E+07	0.4194E+07	0.4658E+06	0	0	0.2692E+07
0.5444E+06	0.4658E+06	0.1342E+07	0	0	0.3933E+05
0	0	0	<u>0.5204E+06</u>	<u>0.3746E+05</u>	0
0	0	0	<u>0.3746E+05</u>	<u>0.5835E+06</u>	0
0.2694E+07	0.2692E+07	0.3933E+05	0	0	0.3231E+07

[0 / 90 / 90 / 0]					
0.1211E+08	0.5883E+06	0.5051E+06	0	0	0
0.5883E+06	0.1211E+08	0.5051E+06	0	0	0
0.5051E+06	0.5051E+06	0.1342E+07	0	0	0
0	0	0	<u>0.5446E+06</u>	0	0
0	0	0	0	<u>0.5611E+06</u>	0
0	0	0	0	0	0.7000E+06

[0 / 0 / 90 / 90]					
0.1211E+08	0.5883E+06	0.5051E+06	0	0	0
0.5883E+06	0.1211E+08	0.5051E+06	0	0	0
0.5051E+06	0.5051E+06	0.1342E+07	0	0	0
0	0	0	<u>0.5531E+06</u>	0	0
0	0	0	0	<u>0.5531E+06</u>	0
0	0	0	0	0	0.7000E+06

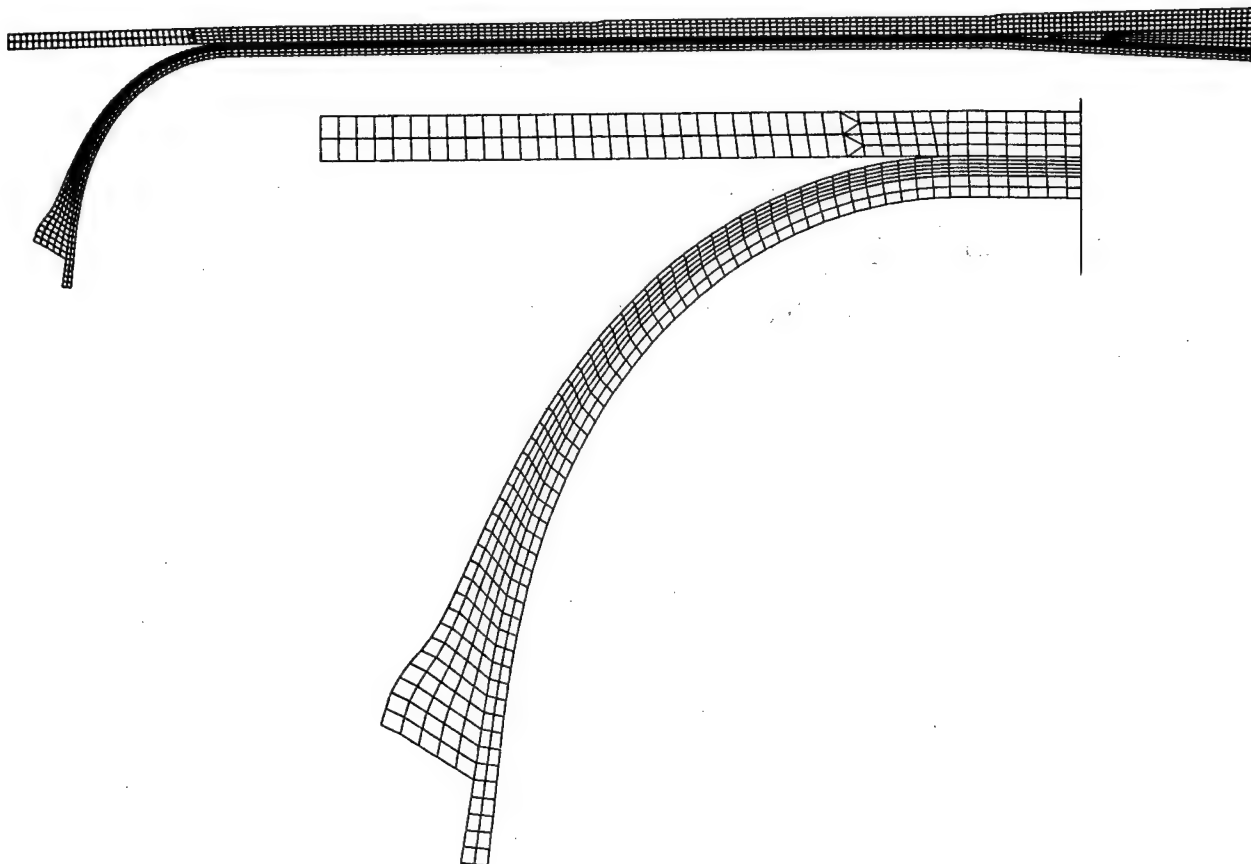
[90 / 0 / 0 / 90]					
0.1211E+08	0.5883E+06	0.5051E+06	0	0	0
0.5883E+06	0.1211E+08	0.5051E+06	0	0	0
0.5051E+06	0.5051E+06	0.1342E+07	0	0	0
0	0	0	<u>0.5611E+06</u>	0	0
0	0	0	0	<u>0.5446E+06</u>	0
0	0	0	0	0	0.7000E+06

COMPOSITE CONE

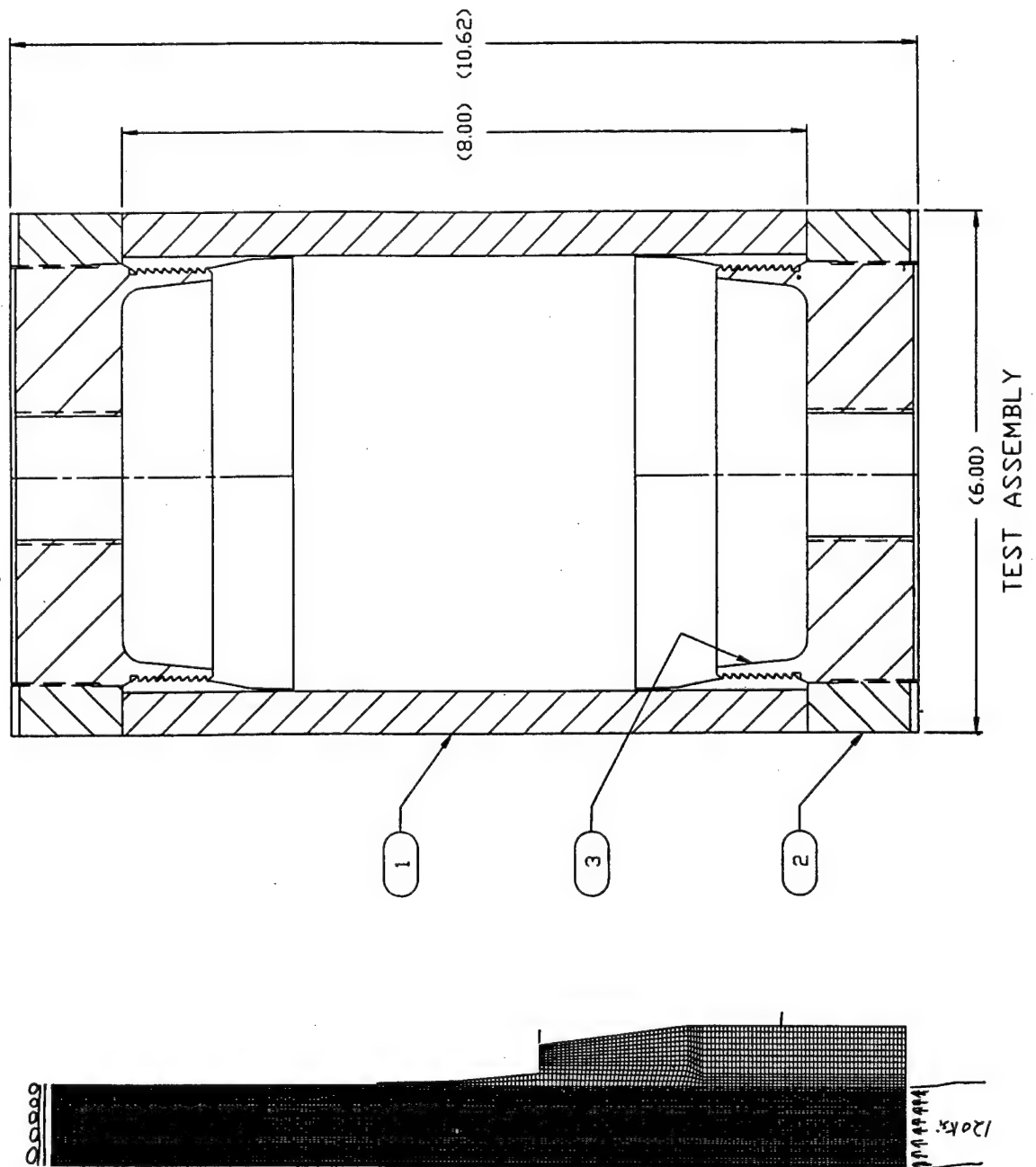


Finite Element Model

COMPOSITE ROCKET MOTOR CASE



COMPOSITE CYLINDER SUBJECTED TO AXIAL COMPRESSION



SUMMARY

- **Material Constitutive Model**
 - 3D formulation
 - Arbitrarily shaped element geometry
 - Multi-material regions within the element
 - Accurate transverse shear properties
 - Dependence of stacking sequence
- **Finite element applications**
 - I) **Pre-processor**
 - Account for element layer content and geometry
 - Automatic mesh generation
 - Effective properties for each individual element
 - II) **Post-processor**
 - Element deformation recovery
 - Layer response recovery
 - Failure criteria
- **Validation of the computer code**

A {1,2}-ORDER THEORY FOR THE ANALYSIS OF THICK COMPOSITE SHELLS

T. Tsui and E. Saether
Mechanics and Structures Branch
U.S. Army Materials Technology Laboratory
Watertown, MA 02172-0001

Abstract

The superior material efficiency of composite materials systems, afforded by the increase in inplane strength and stiffness to weight ratios and anisotropic tailoring capabilities, has motivated designers towards an ever expanding use of these materials in design concepts. Of current interest is the application of composites to thick-section plate and shell type structures which necessitates an accurate analytical methodology to predict static and dynamic behaviour. Unlike materials, the lower stiffness and strength of laminates in the transverse normal material direction can contribute to potential failure modes involving delaminations and matrix cracking. As the sectional thickness or gradients in applied loading increase, the effects of transverse shear and transverse normal deformation modes become more pronounced in the total response of the laminate. Therefore, a simple and accurate theory accounting for the effects of transverse shear and transverse normal deformation is needed for predicting structural response and failure. An additional requirement of the theory, for practical use, is that it be amenable for finite element approximations within the conventional 'h-version' framework of finite element formulations.

Current analysis capabilities available in most finite element codes incorporate laminate plate and shell theories of order {1,0} commonly referred to as 1st-order theories. These type of theories account in an average sense for transverse shear but neglect the effects of transverse normal deformations. The accuracy of these theories is limited to the case of thin laminates; the static and dynamic response predictions obtained from this order of approximation is inadequate for thick laminates. The use of three-dimensional elements are computationally expensive in the analysis of large-scale structures - often prohibitively so - unless employed in a global-local fashion in which accurate stress predictions are required for only a relatively small domain of interest.

In recent years, various higher-order theories have been proposed for the analysis of thick composites by including the effect of transverse normal deformations. However, they have either failed to produce sufficiently accurate predictions or are unsuitable for implementation in standard finite element computer codes because these theories require various higher-order displacement variables and associated stress resultants on the element boundaries that are not supported within the conventional 'h-version' framework of these finite element programs. Recently, Tessler[1] proposed a homogeneous plate theory of order {1,2}. The theory is based on the assumption that the inplane displacements are linear functions while the transverse displacement is a parabolic function of the thickness coordinate of the plate. In addition, independent expansions are assumed for the transverse shear and transverse normal strains. The coefficients of the expansions are determined by requiring the stress field to satisfy the physical conditions at the top and bottom shell surfaces and a weak transverse strain compatibility. An important feature of the theory is the requirement of only C^0 and C^{-1} continuity for the shell kinematic variables, thus allowing the development of efficient shell finite elements with exclusively Poisson type boundary conditions. An extension of this theory to laminated composite plates was later advanced by Tessler and Saether[2] and to thick-section orthotropic shells by Tsui and Tessler[3].

This paper discusses the formulation of a general {1,2}-order theory for thick composite shells by following the basic methodology established in [1,2]. Equations of motion and associated Poisson boundary conditions are derived from Hamilton's variational principle. Analytical solutions for the problem of vibration of composite cylinders are obtained and compared with exact solutions of three-dimensional elasticity and other higher-order theories. The present theory is shown to provide improved accuracy over other higher-order shell theories and is ideally suited for finite element applications.

References

- [1] Tessler, A. "A Higher-Order Plate Theory with Ideal Finite Element Suitability", *Comput. Meths. Appl. Mech. Eng.* v. 85, No. 2 1991 p. 183-205.
- [2] Tessler, A. and Saether, E. "A Computationally Viable Higher-Order Theory for Laminated Composite Plates", *Int. J. Num. Meth. Eng.*, v. 31, 1991 p. 1069-1086.
- [3] Tsui, T. and Tessler, A. "An Improved Theory of Order {1,2} for Stress Analysis of Thick Orthotropic Shells", MTL TR 92-, (To appear), U.S. Army Materials Technology Laboratory, Watertown, Mass.



ANALYSIS OF THICK COMPOSITE SHELLS



MATERIALS TECHNOLOGY LABORATORY

TECHNICAL OBJECTIVE

- TO DEVELOP IMPROVED ANALYTICAL AND COMPUTATIONAL METHODS FOR PREDICTING MECHANICAL RESPONSE AND FAILURE OF THICK-SECTION COMPOSITE SHELLS

DEFINITION OF THICK-SECTION STRUCTURES

- A STRUCTURE IS CONSIDERED AS A THICK-SECTION STRUCTURE WHEN DEFORMATIONS DUE TO TRANSVERSE SHEAR AND TRANSVERSE NORMAL STRAINS AND STRESSES CAN SIGNIFICANTLY CONTRIBUTE TO THE THREE DIMENSIONAL STRESS STATE. IN OTHER WORDS, THE EFFECT OF TRANSVERSE SHEAR AND TRANSVERSE NORMAL STRESSES CAN NOT BE NEGLECTED

CRITERIA FOR DETERMINING THICK-SECTION SHELLS

1. H/a or $H/R > 0.1$ (H = Thickness, a = Length of Panel side, R = Radius)
2. $E_3 \ll E_1$ or E_2 , G_{13} or $G_{23} \ll E_1$ or E_2
3. SHELL IS SUBJECTED A RAPIDLY FLUCTUATING LOAD WITH A WAVELENGTH OF THE ORDER OF THE SHELL THICKNESS



ANALYSIS OF THICK COMPOSITE SHELLS

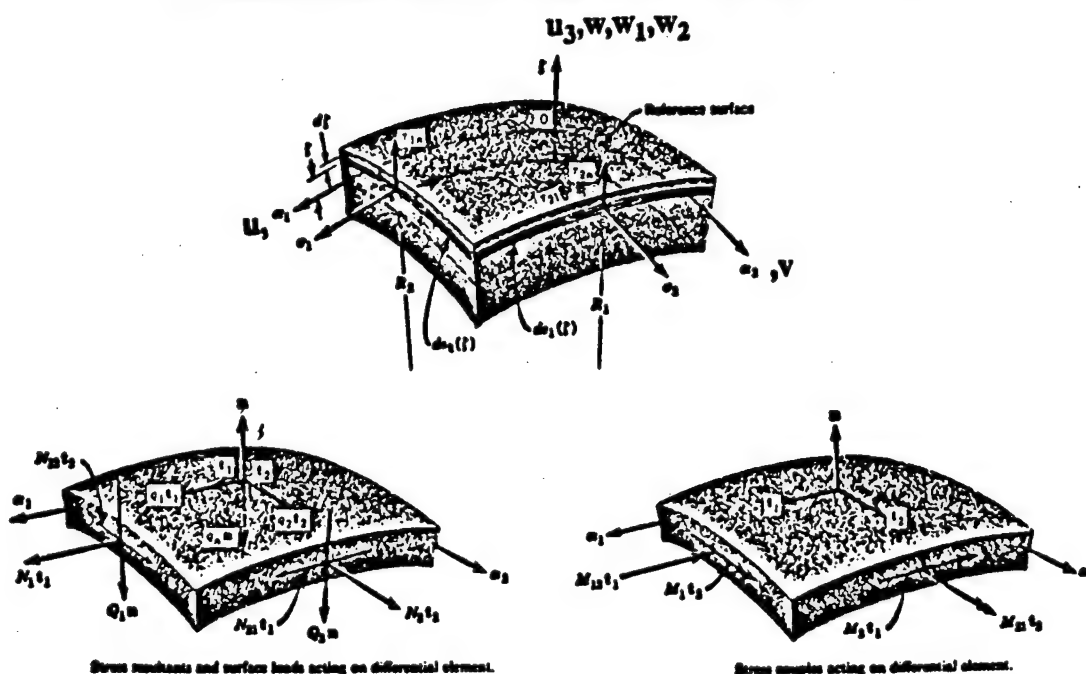


MATERIALS TECHNOLOGY LABORATORY

ANALYSIS OF THICK-SECTION SHELL STRUCTURES

- EXACT SOLUTIONS USING THREE DIMENSIONAL THEORY OF ELASTICITY
 - LIMITED TO SIMPLE GEOMETRIES AND BOUNDARY CONDITIONS
- ANALYTICAL SOLUTIONS USING SHELL THEORIES
 - CLASSICAL SHELL THEORY RARELY PROVIDES ACCURATE SOLUTIONS IN THE THICK REGIME
 - FIRST-ORDER SHELL THEORIES NEGLECT TRANSVERSE NORMAL DEFORMATION MODES
 - HIGHER-ORDER SHELL THEORIES ARE NOT AMENABLE TO FINITE ELEMENT APPLICATIONS
- NUMERICAL SOLUTIONS USING FINITE ELEMENTS
 - ONLY SHELL ELEMENTS BASED ON CLASSICAL AND FIRST-ORDER SHELL THEORY ARE CURRENTLY AVAILABLE IN STANDARD FINITE ELEMENT CODES
 - 3-D ELEMENTS INCUR HIGH COMPUTATIONAL COST IN MODELLING GENERAL SHELL STRUCTURES

COORDINATE SYSTEM AND STRESS RESULTANTS





ANALYSIS OF THICK COMPOSITE SHELLS



MATERIALS TECHNOLOGY LABORATORY

HIGHER-ORDER (M,N) SHELL THEORIES

“M” - ORDER OF EXPANSION OF INPLANE DISPLACEMENTS
WITH RESPECT TO THICKNESS COORDINATE

“N” - ORDER OF EXPANSION OF TRANSVERSE DISPLACEMENTS
WITH RESPECT TO THICKNESS COORDINATE

HIGHER-ORDER SHELL THEORY:

$$u_1 = u + \xi\theta_1 + \xi^2\phi_1 + \xi^3\phi_1$$

$$u_2 = v + \xi\theta_2 + \xi^2\phi_2 + \xi^3\phi_2$$

$$u_3 = w + \xi\theta_3 + \xi^2\phi_3 + \xi^3\phi_3$$

CLASSICAL SHELL THEORY:

$$u_1 = u + \xi\theta_1$$

$$u_2 = v + \xi\theta_2$$

$$u_3 = w$$

LIMITATIONS OF CURRENT THEORIES FOR THE ANALYSIS OF THICK-SECTION COMPOSITES

1. 1ST-ORDER (1,0) AND HIGHER-ORDER (M>1,0) SHEAR DEFORMABLE THEORIES WHICH INCLUDE TRANSVERSE SHEAR BUT DO NOT CONSIDER THE EFFECT OF TRANSVERSE NORMAL DEFORMATIONS.
2. OTHER HIGHER-ORDER THEORIES (M>=1, N>=2) INCLUDE BOTH TRANSVERSE SHEAR AND TRANSVERSE NORMAL DEFORMATION BUT ARE NOT SUITABLE FOR FINITE ELEMENT APPROXIMATIONS BECAUSE THEY:
 - a) INCORPORATE A LARGE NUMBER OF KINEMATIC VARIABLES REQUIRING C⁰ OR HIGHER CONTINUITY
 - b) IMPOSE NATURAL BOUNDARY CONDITIONS THAT INVOLVE SUCH NON-CLASSICAL QUANTITIES AS HIGHER-ORDER STRESS RESULTANTS
 - c) ARE UNABLE TO MODEL APPROPRIATE TRANSVERSE STRESS BOUNDARY CONDITIONS AT TOP AND BOTTOM LAMINATE SURFACES
 - d) REQUIRE SHEAR CORRECTION FACTOR THAT TUNES THE TRANSVERSE SHEAR PROPERTIES



ANALYSIS OF THICK COMPOSITE SHELLS



MATERIALS TECHNOLOGY LABORATORY

FEATURES OF TESSLER'S HIGHER-ORDER THEORY

1. ASSUMED DISPLACEMENT FIELDS:

$$\begin{aligned}u_1(\alpha_1, \alpha_2, \zeta, t) &= u(\alpha_1, \alpha_2, t) + h\xi\theta_1(\alpha_1, \alpha_2, t) \\u_2(\alpha_1, \alpha_2, \zeta, t) &= v(\alpha_1, \alpha_2, t) + h\xi\theta_2(\alpha_1, \alpha_2, t) \\u_3(\alpha_1, \alpha_2, \zeta, t) &= w(\alpha_1, \alpha_2, t) + \xi w_1(\alpha_1, \alpha_2, t) \\&\quad + (\xi^2 - 1/5)w_2(\alpha_1, \alpha_2, t)\end{aligned} \quad (\xi = \zeta/h \in [-1, 1])$$

$u, v, w, \theta_1, \theta_2$ are defined as weighted-average kinematic variables

$$\begin{aligned}u &= \frac{1}{2h} \int_{-h}^h u_1 d\zeta, \quad v = \frac{1}{2h} \int_{-h}^h u_2 d\zeta \\ \theta_1 &= \frac{3}{2h^3} \int_{-h}^h u_1 \zeta d\zeta, \quad \theta_2 = \frac{3}{2h^3} \int_{-h}^h u_2 \zeta d\zeta \\ w &= \frac{3}{4h} \int_{-h}^h u_3 (1 - \xi^2) d\zeta\end{aligned}$$

2. INDEPENDENT EXPANSIONS OF TRANSVERSE STRAINS:

$$\epsilon_n = \sum_{n=0}^3 \xi^n a_n, \quad \gamma_{in} = \sum_{n=0}^2 \xi^n b_{in} \quad (i = 1, 2)$$

3. THE EXPANSION COEFFICIENTS ARE OBTAINED BY REQUIRING THE ASSUMED TRANSVERSE STRAINS TO MAKE INTEGRALS I_1 AND I_2 A MINIMUM

$$I_1 = \int_{-h}^h \left\{ \gamma_{in} - [\mu_i^0 + \xi w_{1,i} + (\xi^2 - 1/5)w_{2,i}] \right\}^2 L_i^2 d\zeta$$

$$I_2 = \int_{-h}^h \left[\epsilon_n - (\epsilon_n^0 + 2\xi\kappa_n^0) \right]^2 d\zeta, \quad L_i = 1 + h\xi/R_i \quad (i = 1, 2).$$



ANALYSIS OF THICK COMPOSITE SHELLS



MATERIALS TECHNOLOGY LABORATORY

$$\begin{aligned}\mu_1^0 &= -u/R_1 + \theta_1 + w_{,1}/A_1, & \epsilon_n^0 &= w_1/h \\ \mu_2^0 &= -v/R_2 + \theta_2 + w_{,2}/A_2, & \kappa_n^0 &= w_2/h^2\end{aligned}$$

$$A_1, A_2 : \text{surface metrics} \quad A_1^2 = r_{,1} \cdot r_{,1}, \quad A_2^2 = r_{,2} \cdot r_{,2}$$

r : position vector

4. THE EXACT PHYSICAL BOUNDARY CONDITIONS AT THE TOP AND BOTTOM SHELL SURFACES ARE SATISFIED

$$\tau_{in}(\alpha_1, \alpha_2, \pm h, t) = \sigma_{n,\xi}(\alpha_1, \alpha_2, \pm h, t) = 0 \quad (i = 1, 2)$$

5. FIELD CONSISTENT TRANSVERSE STRAINS

$$\begin{aligned}\gamma_{in} &= \frac{5}{4}(1 - \xi^2)\mu_i^0/L_i \quad (i = 1, 2) \\ \epsilon_n &= s_1\epsilon_1^0 + s_2\epsilon_2^0 + s_3\epsilon_n^0 + s_4\beta_1^0 + s_5\beta_2^0 + \\ &\quad s_6\kappa_1^0 + s_7\kappa_2^0 + s_8\kappa_n^0 + s_9\beta_1' + s_{10}\beta_2'\end{aligned}$$

DERIVATION OF EQUATIONS OF MOTION

The equations of motion together with the natural boundary conditions are derived via Hamilton's variational principle:

$$\begin{aligned}&\delta \int_{t_0}^{t_1} \left[\int_{\alpha_1} \int_{\alpha_2} \int_{-h}^h (\sigma_1\epsilon_1 + \sigma_2\epsilon_2 + \sigma_n\epsilon_n + \tau_{12}\gamma_{12} \right. \\ &\quad \left. + \tau_{1n}\gamma_{1n} + \tau_{2n}\gamma_{2n}) A_1 A_2 L_1 L_2 d\alpha_1 d\alpha_2 d\zeta \right. \\ &\quad - \rho/2 \int_{\alpha_1} \int_{\alpha_2} \int_{-h}^h (\dot{u}_1^2 + \dot{u}_2^2 + \dot{u}_3^2) A_1 A_2 L_1 L_2 d\alpha_1 d\alpha_2 d\zeta \\ &\quad - \int_{\alpha_1} \int_{\alpha_2} (q_n^+ u_3^+ L_1^+ L_2^+ - q_n^- u_3^- L_1^- L_2^-) A_1 A_2 d\alpha_1 d\alpha_2 \\ &\quad - \int_{\alpha_2} \int_{-h}^h (\bar{\sigma}_1 u_1 + \bar{\tau}_{12} u_2 + \bar{\tau}_{1n} u_3) A_2 L_2 d\alpha_2 d\zeta \\ &\quad \left. - \int_{\alpha_1} \int_{-h}^h (\bar{\tau}_{21} u_1 + \bar{\sigma}_2 u_2 + \bar{\tau}_{2n} u_3) A_1 L_1 d\alpha_1 d\zeta \right] dt = 0\end{aligned}$$



ANALYSIS OF THICK COMPOSITE SHELLS



MATERIALS TECHNOLOGY LABORATORY

EQUATIONS OF MOTION FOR CYLINDRICAL SHELLS

$$\begin{aligned} &A_{11}u_{,xx} + A_{55}u_{,\theta\theta}/a^2 + (A_{12} + A_{54})v_{,x\theta}/a + B_{11}\theta_{,xx} \\ &B_{55}\theta_{,\theta\theta}/a^2 + (B_{12} + B_{54})\theta_{,x\theta}/a + A_{12}w_{,x}/a + \\ &A_{13}w_{1,x}/h + B_{13}w_{2,x}/h^2 = \rho h(I_0\ddot{u} + I_1h\ddot{\theta}_\theta) \end{aligned}$$

$$\begin{aligned} &(B_{54} + B_{12})u_{,x\theta}/a + B_{44}v_{,xx} + B_{22}v_{,\theta\theta}/a^2 + (D_{45} + D_{21})\theta_{,x\theta}/a + \\ &D_{44}\theta_{,xx} + D_{22}\theta_{,\theta\theta}/a^2 + (B_{22} - aG_{44})w_{,\theta}/a^2 + B_{32}w_{1,\theta}/ha + \\ &D_{23}w_{2,\theta}/h^2a + G_{44}(v - a\theta_x)/a = \rho h(hI_1\ddot{v} + hI_2\ddot{\theta}_x) \end{aligned}$$

$$\begin{aligned} &G_{55}w_{,xx} + G_{44}w_{,\theta\theta}/a^2 - A_{21}u_{,x}/a - (A_{22} + G_{44})v_{,\theta}/a^2 - \\ &(B_{21} - aG_{55})\theta_{,x}/a - (B_{22} - aG_{44})\theta_{,x\theta}/a^2 - A_{22}w/a^2 - A_{23}w_1/ah \\ &- B_{23}w_2/ah^2 = \rho h[I_0\ddot{w} + I_1\ddot{w}_1 + (-I_0/5 + I_2)\ddot{w}_2] \end{aligned}$$

$$\begin{aligned} &(A_{45} + A_{21})u_{,x\theta}/a + A_{44}v_{,xx} + A_{22}v_{,\theta\theta}/a^2 + (B_{45} + B_{21})\theta_{,x\theta}/a + \\ &B_{44}\theta_{,xx} + B_{22}\theta_{,\theta\theta}/a^2 + (A_{22} + G_{44})w_{,\theta}/a^2 + A_{23}w_{1,\theta}/ha + \\ &B_{23}w_{2,\theta}/h^2a - G_{44}(v - a\theta_x)/a^2 = \rho h(I_0\ddot{v} + I_1h\ddot{\theta}_x) \end{aligned}$$

$$\begin{aligned} &B_{11}u_{,xx} + B_{55}u_{,\theta\theta}/a^2 + (B_{21} + B_{45})v_{,x\theta}/a + D_{11}\theta_{,xx} + \\ &D_{55}\theta_{,\theta\theta}/a^2 + (D_{12} + D_{54})\theta_{,x\theta}/a + (B_{21} - aG_{55})w_{,x}/a + \\ &B_{31}w_{1,x}/h + D_{13}w_{2,x}/h^2 - G_{55}\theta_\theta = \rho h(hI_1\ddot{u} + h^2I_2\ddot{\theta}_\theta) \end{aligned}$$

$$\begin{aligned} &-[A_{31}u_{,x} + A_{32}(v_{,\theta} + w)/a + A_{33}w_1/h + B_{31}\theta_{,x} + B_{32}\theta_{,x\theta}/a + \\ &B_{33}w_2/h^2]/h = \rho h[I_1\ddot{w} + I_2\ddot{w}_1 + (-I_1/5 + I_3)\ddot{w}_2] \end{aligned}$$

$$\begin{aligned} &-[B_{13}u_{,x} + B_{23}(v_{,\theta} + w)/a + B_{33}w_1/h + D_{31}\theta_{,x} + D_{32}\theta_{,x\theta}/a + \\ &D_{33}w_2/h^2]/h^2 = \rho h[(-I_0/5 + I_2)\ddot{w} + \\ &(-I_1/5 + I_3)\ddot{w}_2 + (I_0/25 - 2I_2/5 + I_4)\ddot{w}_2] \end{aligned}$$



ANALYSIS OF THICK COMPOSITE SHELLS



MATERIALS TECHNOLOGY LABORATORY

ASSUMED DISPLACEMENT SOLUTIONS

$$\begin{aligned}u(x, \theta, t) &= \sum_{m=n=1}^{\infty} U_{mn} \sin \alpha x \cos n\theta e^{i\omega_{mn}t} \\v(x, \theta, t) &= \sum_{m=n=1}^{\infty} V_{mn} \cos \alpha x \sin n\theta e^{i\omega_{mn}t} \\w(x, \theta, t) &= \sum_{m=n=1}^{\infty} W_{mn} \cos \alpha x \cos n\theta e^{i\omega_{mn}t} \\\theta_x(x, \theta, t) &= \sum_{m=n=1}^{\infty} \phi_{mn} \cos \alpha x \sin n\theta e^{i\omega_{mn}t} \\\theta_\theta(x, \theta, t) &= \sum_{m=n=1}^{\infty} \psi_{mn} \sin \alpha x \cos n\theta e^{i\omega_{mn}t} \\w_1(x, \theta, t) &= \sum_{m=n=1}^{\infty} W_{mn}^1 \cos \alpha x \cos n\theta e^{i\omega_{mn}t} \\w_2(x, \theta, t) &= \sum_{m=n=1}^{\infty} W_{mn}^2 \cos \alpha x \cos n\theta e^{i\omega_{mn}t}\end{aligned}$$

COMPARISONS OF NATURAL FREQUENCIES

Table 1: Normalized Natural Frequencies for Homogeneous Isotropic Cylinders
 $2h/a = .01, m = 1, n = 1$ (Ref. [4])

$2h/L$	Ω_1		Ω_2		Ω_3		Ω_4	
	Exact	Present	Exact	Present	Exact	Present	Exact	Present
.01	.0046	.0046	.01069	.01069	1.0001	1.0001	1.8706	1.8708
.10	.0160	.0159	.1001	.1001	1.0050	1.0050	1.8498	1.8726
.20	.0577	.0576	.2000	.2000	1.0198	1.0198	1.8121	1.8779
.40	.1989	.1973	.4000	.4000	1.0771	1.0771	1.7520	1.9020

Table 2: Normalized Natural Frequencies for Homogeneous Isotropic Cylinders
 $2h/a = .01, m = 1, n = 3$ (Ref. [4])

$2h/L$	Ω_1		Ω_2		Ω_3		Ω_4	
	Exact	Present	Exact	Present	Exact	Present	Exact	Present
.01	.0026	.0026	.0142	.0142	1.0001	1.0001	1.8704	1.8709
.10	.0160	.0160	.1005	.1005	1.005	1.005	1.8496	1.8726
.20	.0579	.0577	.2002	.2002	1.0199	1.0199	1.8120	1.8779
.40	.1990	.1974	.4001	.4001	1.0771	1.0771	1.7520	1.9021

Table 3: Normalized Natural Frequencies for Homogeneous Isotropic Cylinders
 $2h/a = .3, m = 1, n = 1$ (Ref. [4])

$2h/L$	Ω_1		Ω_2		Ω_3		Ω_4	
	Exact	Present	Exact	Present	Exact	Present	Exact	Present
.01	.0012	.0012	.0972	.0972	1.0083	1.0086	1.8583	1.8676
.10	.0616	.0616	.1648	.1648	1.0183	1.0185	1.8423	1.8693
.20	.1266	.1269	.2375	.2375	1.0383	1.0381	1.8100	1.8747
.40	.2440	.2440	.4142	.4142	1.0970	1.0965	1.7551	1.8992



ANALYSIS OF THICK COMPOSITE SHELLS



MATERIALS TECHNOLOGY LABORATORY

Table 4: Normalized Natural Frequencies for Homogeneous Isotropic Cylinders
 $2h/a = .3$, $m = 1$, $n = 3$ (Ref. [4])

$2h/L$	Ω_1		Ω_2		Ω_3		Ω_4	
	Exact	Present	Exact	Present	Exact	Present	Exact	Present
.01	.0957	.0951	.2875	.2875	1.0455	1.0458	1.7865	1.8814
.10	.1064	1.060	.3095	.3095	1.0517	1.0519	1.7812	1.8833
.20	.1455	.1451	.3613	.3612	1.0692	1.0693	1.7681	1.8895
.40	.2792	.2772	.5018	.5017	1.1303	1.1305	1.7439	1.9171

$$\Omega = \omega_1 2h(\rho/G)^{1/2}/\pi \quad (i = 1, 2, 3, 4)$$

Table 5: Normalized Natural Frequencies for [90/0]₅ Laminated, Simply Supported Cylindrical Shell with $E_L/E_T = 15$.

N	$2h/R = 0.05$ ($M = 1$)		$2h/R = 0.2$ ($M = 1$)	
	EXACT	PRESENT	EXACT	PRESENT
0	1.234	1.234	19.74	19.74
1	0.5447	0.5448	11.77	11.89
2	0.2557	0.2559	8.933	9.114
3	0.1753	0.1755	10.84	11.15
4	0.1938	0.1945	16.65	17.26
5	0.2987	0.3008	26.06	27.19
6	0.5036	0.5089	38.88	40.69
7	0.8288	0.8404	54.94	57.55
8	1.295	1.317	74.18	77.61

$$\Omega = 100\omega^2 \rho h^2/E_T \quad (\text{Ref. [5]})$$

Table 7: Normalized Natural Frequencies for [0/90/0] Laminated, Simply Supported Cylindrical Shell with $E_L/E_T = 25$. (Ref. [6])

A/R	$R/2h = 50$			
	CLT	FSDT	ZIG-ZAG	PRESENT
0.10	1120.50	815.53	715.25	714.25
0.25	233.17	205.48	194.86	195.73
0.5	70.07	68.04	67.15	66.04
1	27.31	27.18	27.14	27.14
2.5	11.49	11.48	11.48	11.48
5	6.28	6.28	6.28	6.28
10	3.53	3.53	3.53	3.53
25	1.27	1.27	1.27	1.27
50	0.54	0.54	0.54	0.54
100	0.14	0.14	0.14	0.14

$$\Omega = \omega R^2(\rho/E_T)^{1/2}/4h^2$$

Table 6: Normalized Natural Frequencies for [0/90/0] Laminated, Simply Supported Cylindrical Shell with $E_L/E_T = 25$. (Ref. [6])

A/R	$R/2h = 100$			
	CLT	FSDT	ZIG-ZAG	PRESENT
0.10	1409.90	1160.00	1075.00	1073.59
0.25	248.06	240.75	236.20	230.14
0.5	83.45	82.96	82.74	79.21
1	38.72	38.72	38.72	37.62
2.5	17.52	17.51	17.51	17.39
5	9.37	9.37	9.37	9.37
10	4.76	4.76	4.76	4.78
25	1.74	1.74	1.74	1.74
50	1.08	1.08	1.08	1.08
100	0.28	0.28	0.28	0.28

Table 8: Normalized Natural Frequencies for [0/90/0] Laminated, Simply Supported Cylindrical Shell with $E_L/E_T = 25$. (Ref. [6])

A/R	$R/2h = 20$			
	CLT	FSDT	ZIG-ZAG	PRESENT
0.10	448.31	384.29	352.93	322.49
0.25	220.01	132.46	116.98	116.87
0.5	59.24	50.02	46.96	47.01
1	18.82	18.15	17.87	17.90
2.5	6.55	6.53	6.52	6.52
5	3.70	3.70	3.70	3.70
10	1.73	1.73	1.73	1.73
25	0.74	0.74	0.74	0.74
50	0.22	0.22	0.22	0.22
100	0.06	0.06	0.06	0.06

$$\Omega = \omega R^2(\rho/E_T)^{1/2}/4h^2$$

REFERENCES

- [4] A.E. Armenakas, D.C. Gazis and G. Herrmann, Vibrations of Circular Cylindrical Shells (Pergamon Press, 1969).
- [5] A. K. Noor, et. al., Assessment of Computational Models for Multilayered Composite Cylinders, Int. J. Solids and Struct., 27 (10), 1269-1286.
- [6] M. D. Sciuva and E. Carrera, Elastodynamic Behavior of Relatively Thick, Symmetrically Laminated, Anisotropic Circular Cylindrical Shells, J. Appl. Mech. 59 (3), 222-223.

DYNAMIC TESTING OF COMPOSITE CYLINDERS

Aileen M. Voltmer

Bob Neugebauer

AAI Corporation

P.O. Box 126, Hunt Valley, Maryland

As part of the continuing research for characterizing the behavior of composite materials under dynamic loading, AAI Corporation has developed a test fixture which is capable of applying triaxial dynamic loads to cylindrical composite specimens. The test facility, which is fully housed within a temperature and humidity controlled environment, generates pressures of up to 60 ksi within a working fluid via dropped weights. Loading rates of 2 ksi/msec to 20 ksi/msec are capable. Maximum energy input is achieved with a 14 foot drop height of 2000 lbs. Axial tension or compression, radial/circumferential tension or compression, or any combination can be applied to the specimens. Up to 8 channels of pressure, strain, and load head acceleration data are recorded at a speed of 1 MHz. Testing can be conducted over a temperature range of -25°F to $120^{\circ}\text{F} \pm 5^{\circ}\text{F}$. The test fixture accepts cylindrical test specimens which are fabricated in the same manner as actual parts. It also serves as a tool for the verification of three dimensional failure criteria for composite materials subjected to triaxial loads. Successful demonstration of axial tension, axial compression, and radial compression tests at room temperature have been completed. Dynamic properties such as transverse tensile and compressive strength, transverse modulus, and poisson's ratio have been determined for S-2 glass/epoxy and graphite/epoxy filament wound specimens.

DYNAMIC TESTING OF COMPOSITE CYLINDERS

Aileen M. Voltmer

Bob Neugebauer

AAI Corporation

P.O. Box 126, Hunt Valley, Maryland

CAPABILITIES: DYNAMIC TEST FACILITY

GENERAL

- . IMPACT LOADING USING 2000 LBS DROPPED FROM APPROXIMATELY 14 FEET(28,000 FT-LB)
- . LOADING RATES FROM 2 KSI/MSEC TO 20 KSI/MSEC
- . SPECIMENS HYDROSTATICALLY PRESSURIZED BY EITHER WATER OR ETHYLENE GLYCOL
- . CHAMBER DESIGNED TO WITHSTAND 60,000 PSI

CLIMATE CONTROL

- . TEMPERATURE CONTROLLED (-25°F TO 120°F ± 5°F)
- . HUMIDITY CONTROLLED (45% RH ± 5%)

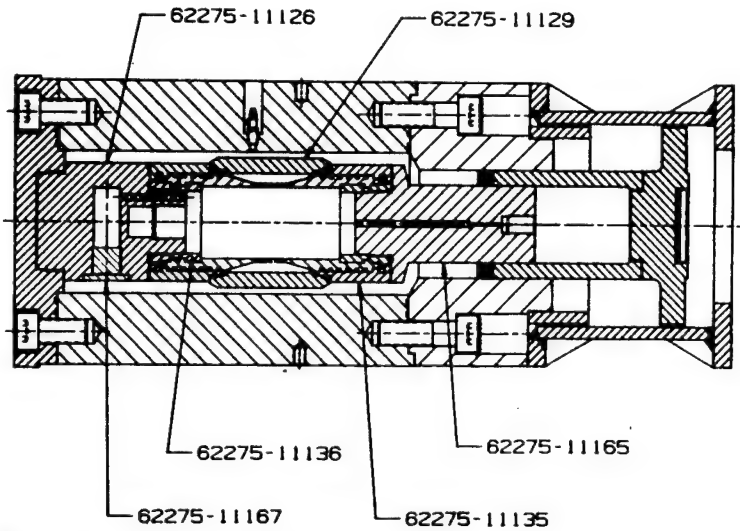
DATA ACQUISITION

- . MAXIMUM OF EIGHT DATA CHANNELS RECORDED AT 1 MHZ
- . PRESSURE, STRAIN GAGE, AND ARBOR TOP ACCELERATION MEASURED



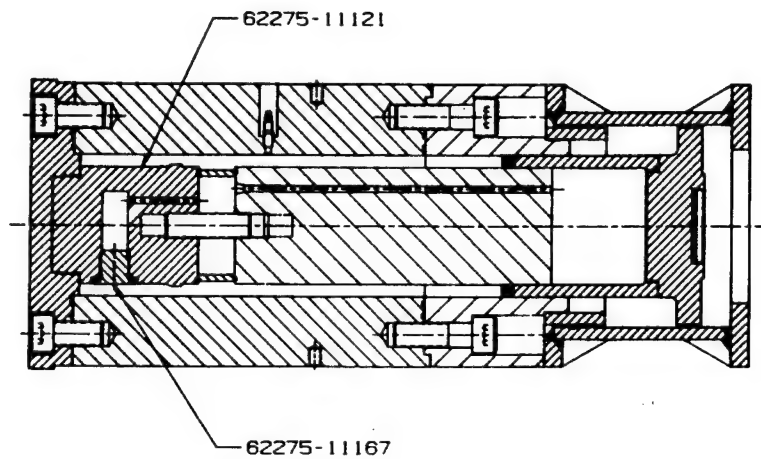
AAI 111 807

TRANSVERSE COMPRESSION TEST FIXTURE



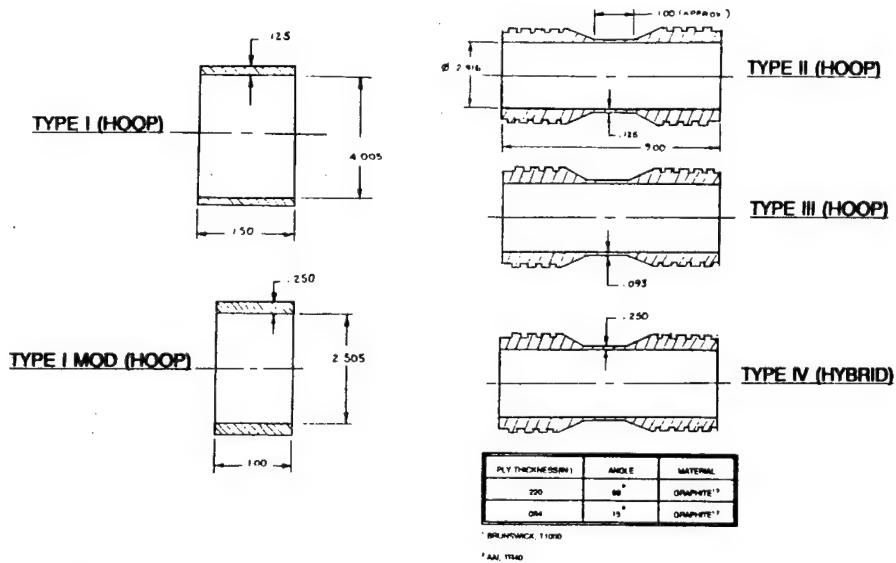
AA103125402

FIBER COMPRESSION TEST FIXTURE



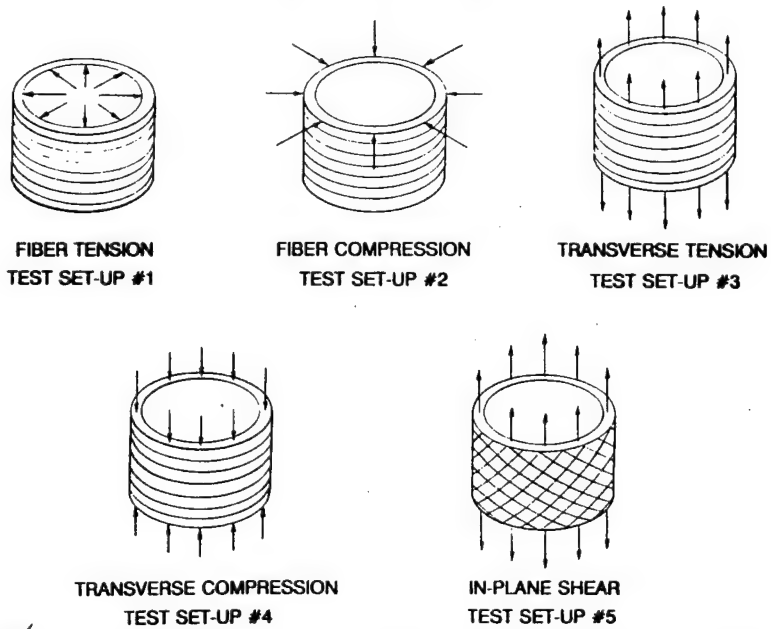
AA103125402

MATERIAL CHARACTERIZATION SPECIMEN DESCRIPTION

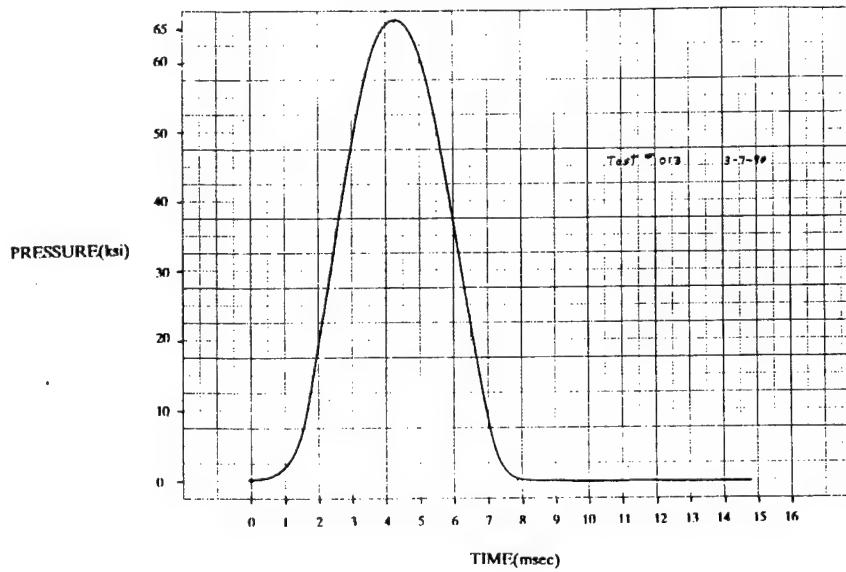


AAE 1112-1/82

BASIC LOADING CONDITIONS

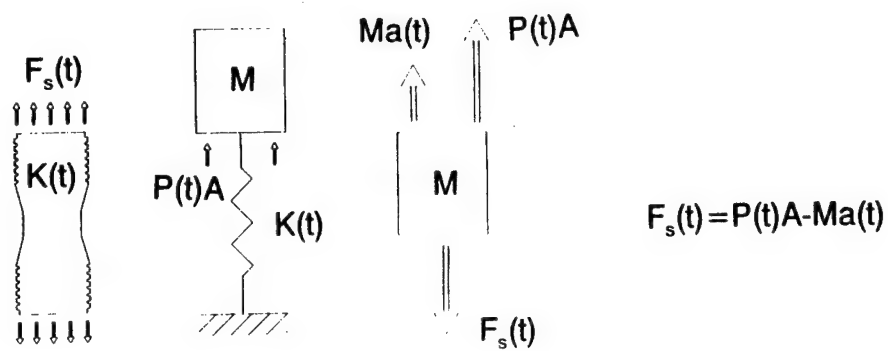


90 MM PRESSURE PULSE



AMT 112 4.87

INSTANTANEOUS LOAD DETERMINATION



$F_s(t)$ = time-varying force on the specimen.
 $P(t)A$ = time-varying force applied to the arbor top by the pressurized fluid.
 M = mass of the arbor top.
 $a(t)$ = time-varying acceleration of the arbor top.
 $K(t)$ = time-varying spring stiffness of the specimen



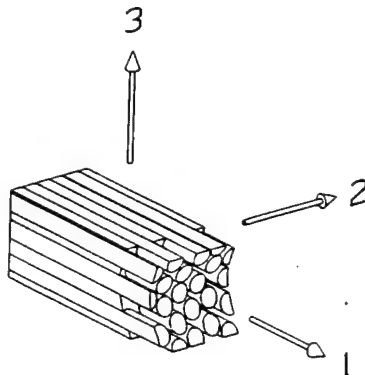
AMT 112 4.87

MATERIAL CHARACTERIZATION TEST SETUP

SPECIMEN TYPE	PLY ANGLE	TEST TYPE NO.	TYPE OF TEST	SPECIMEN LOADING CONDITIONS
1	89°	1	FIBER TENSION	INTERNAL 50 KSI
1	89°	2	FIBER COMPRESSION	EXTERNAL 50 KSI
2	89°	3	TRANSVERSE TENSION	AXIAL TENSION
2	89°	4	TRANSVERSE COMPRESSION	AXIAL COMPRESSION
3	45° HELIX	5	IN-PLANE SHEAR	AXIAL TENSION
2	89°	6	FIBER TEN/TRANS COMP/ T.T.T. COMP	EXTERNAL 30 KSI INTERNAL 40.7 KSI
2	89°	7	FIBER COMP/TRANS COMP/ T.T.T. COMP	EXTERNAL 50 KSI INTERNAL 25 KSI
4	HYBRID	8	FIBER COMP/TRANS TEN/ T.T.T. COMP	EXTERNAL 50 KSI INTERNAL 20 KSI



FIVE INDEPENDENT STRENGTHS FOR TRANSVERSELY ISENTROPIC MATERIALS



F_{T1} = FIBER TENSION

F_{T2} = TRANSVERSE TENSION

F_{C1} = FIBER COMPRESSION

F_{C2} = TRANSVERSE COMPRESSION

F_s = 1-2 PLANE SHEAR



UNIDIRECTIONALLY LOADED TESTS

DETERMINATION OF F_{T2} , F_{C2} AND F_S

TEST SET-UP 3 - TRANSVERSE TENSION

TEST SET-UP 4 - TRANSVERSE COMPRESSION

TEST SET-UP 5 - IN-PLANE SHEAR

ALL OF THE ABOVE TESTS CONTAIN SLIGHT DEGREES OF
BENDING AND STRESS CONCENTRATION AT THE GAGE
TRANSITION ZONE, THEREFORE, THE RESULTS ARE
SLIGHTLY CONSERVATIVE.



AAE/T1174/87

DETERMINATION OF F_{T1} , F_{C1} , F_{12} AND F_{23}

F_{T1} , F_{C1} , F_{12} AND F_{23} WILL BE FOUND VIA SIMULTANEOUS EQUATION
SOLUTION OF ...

$$F_{11}\sigma_1^2 + F_{22}(\sigma_2^2 + \sigma_3^2 + 3\sigma_{23}^2) + F_S(\sigma_{13}^2 + \sigma_{12}^2) + 2F_{12}\sigma_1(\sigma_2 + \sigma_3) + 2F_{23}\sigma_2\sigma_3 \\ + F_1\sigma_1 + F_2(\sigma_2 + \sigma_3) = 1$$

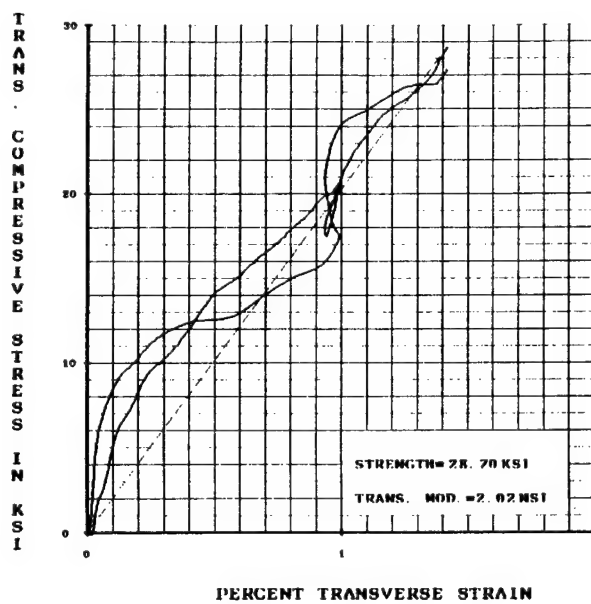
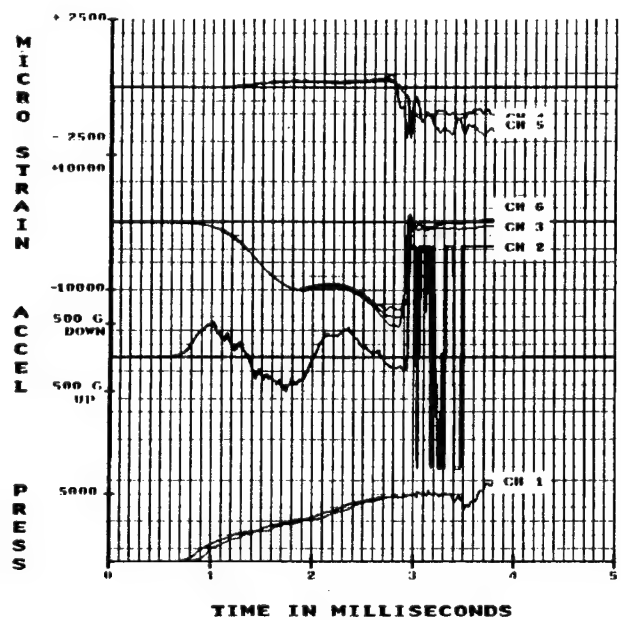
$$\text{WHERE: } F_{11} = 1/(F_{T1}F_{C1}) \qquad F_1 = 1/F_{T1} - 1/F_{C1}$$

$$F_{22} = 1/(F_{T2}F_{C2}) \qquad F_2 = 1/F_{T2} - 1/F_{C2}$$

$$F_{12} = F_{12}^*(F_{11}F_{22})^{\frac{1}{2}} \qquad -1 \leq F_{12}^* \leq 1$$

$$F_{23} = F_{23}^*F_{22}$$





PRELIMINARY RESULTS

MATERIAL	TEST TYPE	STATIC STRENGTH (PSI)	DYNAMIC STRENGTH (PSI)	DYNAMIC TO STATIC RATIO
S-2 GLASS/862 RESIN	TRANSVERSE TENSION	4707	8634	1.8
S-2 GLASS/862 RESIN	TRANSVERSE COMPRESSION	17,260	28,700	1.7
T-1000 GRAPHITE/862 RESIN	TRANSVERSE TENSION	3508 ¹	3849 ²	1.1
T-1000 GRAPHITE/828 RESIN	FIBER COMPRESSION	223,000 ³	132,000 ⁴	.59

¹DATA FROM HR40 GRAPHITE FIBER WITH EPON 862 RESIN

²GRAPHITE SPECIMENS UNDER DYNAMIC LOADING DID NOT SHOW A DISTINCT FAILURE POINT AS DID THE GLASS SPECIMENS

³ESTIMATED FIBER ALLOWABLE

⁴FIBER DIRECTION COMPONENT OF STRESS FOR TRIAXIALLY LOADED SPECIMEN



AMF 312-4-82

APPENDIX A: PROGRAM LISTINGS

AIR FORCE OFFICE OF SCIENTIFIC RESEARCH

IN-HOUSE

NONE

GRANTS AND CONTRACTS

EXPERIMENTAL AND THEORETICAL INVESTIGATIONS IN NANOSTRUCTURAL MATERIALS AND COMPOSITES

AFOSR-91-0421

15 Sep 91 - 14 Sep 94

Principal Investigator: Prof Elias C Aifantis
Department of Mechanical Engineering and Engineering Mechanics
Michigan Technological University
Houghton MI 49931
(906) 487-2518

Program Manager: Dr Walter F Jones
AFOSR/NA
Bolling AFB DC 20332-6448
(202) 767-0470

Objective: The objective of this effort is to gain fundamental insight into the mechanical behavior of nanostructural materials and to use this insight to design and manufacture novel composites which outperform currently available materials.

SITE SPECIFIC REACTIONS OF CARBON WITH OXYGEN AND SILICON IN GRAPHITE, CARBON FIBERS AND CARBON-CARBON COMPOSITES

AFOSR-91-0103

1 Dec 90 - 30 Nov 93

Principal Investigator: Prof Dawn A Bonnell
Dept of Materials Science and Engineering
University of Pennsylvania
Philadelphia PA 19104-3246
(215) 898-8337

Program Manager: Lt Col Larry W Burggraf
AFOSR/NC
Bolling AFB DC 20332-6448
(202) 767-4960

Objective: The objective of this research is to investigate the reactions of carbon with oxygen, boron and silicon at a fundamental level by direct observation (imaging) and spectroscopic analysis that exploits the spatial localization of information obtained by scanning tunneling microscopy (STM).

INTERFACIAL STUDIES OF COATED FIBER/GLASS CERAMIC MATRIX COMPOSITES

F49620-92-C-0001

1 Nov 91 - 31 Oct 94

Principal Investigator: Dr John J Brennan
United Technologies Research Center
400 Main Street
East Hartford CT 06108
(203) 727-7220

Program Manager: Lt Col Larry W Burggraf
AFOSR/NC
Bolling AFB DC 20332-6448
(202) 767-4960

Objective: The objective of this program is to develop an understanding of the relationships between the fiber, the fiber coating, and the glass-ceramic matrix that will lead to a composite system exhibiting high strength, high toughness, and high thermal and environmental stability to temperatures of 1200°C.

MICROSTRUCTURAL DESIGN FOR TOUGH CERAMICS

F49620-92-J-0039

1 Nov 91 - 31 Oct 94

Principal Investigators: Prof Helen M Chan
Prof Brian R Lawn
Department of Materials Science and Engineering
Lehigh University
Bethlehem PA 18015
(215) 758-5554

Program Manager: Lt Col Larry W Burggraf
AFOSR/NC
Bolling AFB DC 20332-6448
(202) 767-4960

Objective: The objective of this research is to understand the role of the microstructure in the strength, fatigue, and wear properties of monolithic ceramics, in particular ceramics that are characterized by "R-curve behavior" wherein the toughness increases with increasing flaw size up to a plateau where the toughness (and thus the strength) is insensitive to the flaw size.

DAMAGE TOLERANCE OF LAMINATED COMPOSITES TO IMPACT

AFOSR-89-0554

1 Sep 89 - 31 Aug 92

Principal Investigator: Prof Fu-Kuo Chang
Dept of Aeronautics and Astronautics
Stanford University
Stanford CA 94305-4125
(415) 723-3466

Program Manager: Dr Walter F Jones
AFOSR/NA
Bolling AFB DC 20332-6448
(202) 767-0470

Objective: The objectives of this program are (1) to identify and describe the fundamental damage mechanisms induced by impact in composite laminates, (2) to predict the extent of damage as a function of impact momentum, material properties, etc., and (3) to predict the residual strength and stiffness in the laminate after impact.

ORIGINS OF IMPERFECTIONS IN COMPOSITE MATERIALS

AFOSR-91-0437
30 Sep 91 - 29 Sep 94

Principal Investigator: Prof Dale E Chimenti
Department of Materials Science and Engineering
Johns Hopkins University
102 Maryland Hall
Baltimore MD 21218-2689
(410) 338-5215

Program Manager: Dr Jim C I Chang
AFOSR/NA
Bolling AFB DC 20332-6448
(202) 767-4987

Objective: The objective of this research is to characterize the damage characteristics, and to determine the deformation and fracture characteristics of composite structures, using complementary nondestructive techniques (NDT).

3-D ANALYSIS AND VERIFICATION OF FRACTURE GROWTH MECHANISMS IN FIBER-REINFORCED CERAMIC COMPOSITES

F49620-92-J-0220
1 Sep 88 - 31 Dec 92

Principal Investigator: Prof Michael P Cleary
Department of Mechanical Engineering
Massachusetts Institute of Technology
Cambridge MA 02139
(617) 253-2308

Program Manager: Dr Walter F Jones
AFOSR/NA
Bolling AFB DC 20332-6448
(202) 767-0470

Objective: The objective of this program is to model the fracture mechanisms in mechanical systems representative of existing and proposed ceramic composites. Emphasis is placed on the roles of the fibers and the interface in generating, arresting, or retarding the growth of fractures.

CHARACTERIZATION OF DEFORMATION AND DAMAGE IN BRITTLE-MATRIX COMPOSITE MATERIALS

F49620-92-J-0423

1 Aug 92 - 31 Jul 95

Principal Investigator: Prof Isaac Daniel
Dept of Civil Engineering
Northwestern University
Evanston IL 60208
(409) 491-5649

Program Manager: Dr Walter F Jones
AFOSR/NA
Bolling AFB DC 20332-6448
(202) 767-0470

Objective: The objective of this research is to understand the failure processes that occur in ceramic-matrix composite materials under various types of loadings. This study will include characterization of the fiber/matrix interphase region and its effect on the toughness and failure of unidirectional composites under longitudinal and transverse tensile loading.

MICROMECHANICAL PREDICTION OF TENSILE DAMAGE FOR CERAMIC-MATRIX COMPOSITES UNDER HIGH TEMPERATURE

AFOSR-90-0341 (URI)

15 Aug 90 - 14 Aug 93

Principal Investigator: Professor Feridun Delale
Department of Mechanical Engineering
City College - CUNY
New York NY 10031
(212) 650-5224

Program Manager: Lt Col Larry W Burggraf
AFOSR/NC
Bolling AFB DC 20332-6448
(202) 767-4960

Objective: The aim of the research is to generate a model to predict the non-linear behavior of ceramic-matrix composites at high temperatures. The experiments are designed to observe and record in situ the progression of tensile damage at high temperature. An analytical model based on micromechanics will be developed to predict the expected non-linear damage behavior.

NONLINEAR AEROELASTIC ANALYSIS FOR STALL FLUTTER OF AIRCRAFT

FY 1992 NEW START

15 Sep 92 - 30 Jun 93

Principal Investigator: Prof John Dugundji
Department of Aeronautics and Astronautics
Massachusetts Institute of Technology
Cambridge MA 02139

(617) 253-3758

Program Manager: Dr Spencer Wu
AFOSR/NA
Bolling AFB DC 20332-6448
(202) 767-6962

Objective: The objective of this research is to investigate the nonlinear aeroelastic analysis methodology and the control of aeroelastic response of composite wings with actuators on the structural surface. The aims are not only to increase the flutter stability but to decrease the turbulence response.

STATIC AND FATIGUE DAMAGE IN HIGH-TEMPERATURE COMPOSITES

F49620-92-J-0391

15 Jul 92 - 14 Jul 95

Principal Investigator: Prof George J Dvorak
Department of Civil and Environmental Engineering
Rensselaer Polytechnic Institute
Troy NY 12180-3590
(518) 276-6940

Program Manager: Dr Walter F Jones
AFOSR/NA
Bolling AFB DC 20332-6448
(202) 767-0470

Objective: The objectives of this study are to examine damage initiation mechanisms associated with inelastic deformations in high-temperature metal-matrix composite material systems, to develop predictive techniques for characterization of damage evolution in these systems, and to evaluate residual stiffness and strength of damaged composite systems.

FAILURE CRITERIA IN LAMINATES BASED ON A 3-D MICROMECHANICS CONSIDERATION

AFOSR-90-0351

15 Jun 90 - 31 Oct 92

Principal Investigator: Prof E S Folias
Department of Mathematics
The University of Utah
Salt Lake City UT 84112
(801) 581-6931

Program Manager: Dr Walter F Jones
AFOSR/NA
Bolling AFB DC 20332-6448
(202) 767-0470

Objective: The objective of this study is to use analytically determined three-dimensional stress fields derived for laminated composites to establish failure criteria based on micromechanics considerations.

DEVELOPMENT OF AN ADVANCED CONTINUUM THEORY FOR COMPOSITE LAMINATES

F49620-91-C-0019 (SBIR)

30 Sep 90 - 31 Aug 92

Principal Investigator: Dr G R Ghanimati
Berkeley Applied Science and Engineering
P. O. Box 10104
Berkeley CA 94709-0104
(415) 653-2323

Program Manager: Dr Walter F Jones
AFOSR/NA
Bolling AFB DC 20332-6448
(202) 767-0470

Objective: The objective of this research program is the development of a continuum model for laminated composite materials which is physically and mathematically accurate and accounts for the effects of the microstructure, both geometric and material nonlinearities, and curved geometry. The model will consist of a set of constraint equations, a set of global/local equations of motion, and response functions (constitutive equations). The model will be applied to composites with flat and curved layers and the predictions will be compared with those of existing models. The specific objectives of the current effort are (1) explicit derivation of constitutive relations, (2) application of the theory to practical problems, (3) further development of the theory, and (4) finite element formulation and development of a computer code.

THERMOMECHANICAL ENVIRONMENTAL DAMAGE IN THE FIBER-REINFORCED β 21S/SIGMA 1240 TITANIUM-BASED METAL-MATRIX COMPOSITES

F49620-92-J-0291

15 May 92 - 14 May 95

Principal Investigator: Prof Hamouda Ghonem
Department of Mechanical Engineering
University of Rhode Island
Kingston RI 02881
(401) 792-2909

Program Manager: Dr Walter F Jones
AFOSR/NA
Bolling AFB DC 20332-6448
(202) 767-0470

Objective: The objectives of this effort are to develop a mechanistic predictive model describing the role of time-dependent environmental effects on the evolution of localized damage in the fiber/matrix interface region in β 21S/Sigma 1240 Ti-based metal-matrix composite, and to study this damage evolution through appropriate thermomechanical testing.

MULTIPHASE CERAMICS FOR MECHANICAL AND STRUCTURAL RELIABILITY AT LOW AND ELEVATED TEMPERATURES

AFOSR-91-0126

15 Dec 90 - 14 Dec 93

Principal Investigators: Prof Martin P Harmer
Prof Helen M Chan
Department of Materials Science and Engineering
Lehigh University
Bethlehem PA 18015
(215) 758-4227

Program Manager: Lt Col Larry W Burggraf
AFOSR/NC
Bolling AFB DC 20332-6448
(202) 767-4960

Objective: The objective of this program is the development and testing of simple analytical and physical models to describe the coarsening mechanism in multiphase ceramics and a study of the high-temperature properties of multi-phase interpenetrating materials systems.

MECHANISMS OF ELEVATED TEMPERATURE FATIGUE DAMAGE IN FIBER-REINFORCED CERAMIC-MATRIX COMPOSITES

AFOSR-91-0106

1 Dec 90 - 30 Nov 92

Principal Investigator: Prof John W Holmes
University of Michigan
1065 G.G. Brown Laboratory
Ann Arbor MI 48109-2125
(313) 763-5969

Program Manager: Dr Walter F Jones
AFOSR/NA
Bolling AFB DC 20332-6448
(202) 767-0470

Objective: The objective of this research is to explore and identify the microstructural damage mechanisms that occur during high temperature fatigue and creep loading of fiber reinforced ceramic-matrix composite materials.

FRACTURE MECHANICS OF BRITTLE-MATRIX COMPOSITES WITH IMPERFECT INTERFACES

FY 1992 NEW START

15 Sep 92 - 14 Sep 95

Principal Investigator: Prof Autar K Kaw
Department of Mechanical Engineering
University of South Florida
4202 East Fowler Avenue
Tampa FL 33620-5350
(813) 974-5626

Program Manager: Dr Walter F Jones
AFOSR/NA
Bolling AFB DC 20332-6448
(202) 767-0470

Objective: The objective of this research project is to develop basic mathematical models of the damage growth and fracture behavior of brittle-matrix composites. The goal is to understand the influence of the constituent elastic moduli, fiber volume fraction, crack geometry, and interface conditions on the initiation and progression of damage.

HIGH TEMPERATURE HETEROGENEOUS MATERIALS
AFOSR-90-0237 (URI)
1 Dec 89 - 30 Nov 92

Principal Investigator: Prof Leon M Keer
Department of Civil Engineering
Northwestern University
Evanston IL 60208
(708) 491-4046

Program Manager: Dr Walter F Jones
AFOSR/NA
Bolling AFB DC 20332-6448
(202) 767-0470

Objective: The objective of this program is to study the high-temperature behavior of ceramic fiber-reinforced, ceramic-matrix composites. The types, severity, and growth of damage mechanisms under various loading conditions will be experimentally established and analytically described.

MECHANICS OF FAILURE OF HIGH TEMPERATURE METAL-MATRIX COMPOSITES
AFOSR-89-424 (URI)
15 Mar 90 - 14 Mar 93

Principal Investigator: Prof D A Kouris
Department of Mechanical and Aerospace Engineering
Arizona State University
Tempe AZ 85287
(602) 965-4977

Program Manager: Dr Walter F Jones
AFOSR/NA
Bolling AFB DC 20332-6448
(202) 767-0470

Objective: The objectives of this research are to establish the damage mechanisms mainly responsible for the degradation of metal-matrix composite materials under high-temperature fatigue conditions and to describe those mechanisms analytically so that predictions of the expected behavior can be made. Experimental work (to be carried out by Rockwell International Science

Center) will establish physical damage mechanisms by direct observation and will also verify analytical damage-growth rate predictions.

HIGH PERFORMANCE LAMINATED COMPOSITES

AFOSR-90-0132 (URI)

1 Jan 90 - 31 Dec 92

Principal Investigator: Prof F A Leckie
Department of Mechanical Engineering
University of California
Santa Barbara CA 93106
(805) 961-2652

Program Manager: Dr Walter F Jones
AFOSR/NA
Bolling AFB DC 20332-6448
(202) 767-0470

Objective: The objective of this study is to establish the mechanics framework which will allow the analysis and interpretation of the mechanical behavior of laminated systems consisting of thin alternating layers of brittle and ductile materials.

TRANSFORMATION TOUGHENING OF CERAMICS

F49620-92-C-0028

1 Apr 92 - 31 Mar 95

Principal Investigator: Dr David B Marshall
Rockwell International Science Center
1049 Camino Dos Rios
Thousand Oaks CA 91360
(805) 373-4170

Program Manager: Lt Col Larry W Burggraf
AFOSR/NC
Bolling AFB DC 20332-6448
(202) 767-4960

Objective: The objectives of this research are to provide a basic understanding of the factors that dictate toughening of ceramic materials by displacive transformation and to provide the background of theoretical modeling and critical measurements that will allow design of optimum microstructures.

INTERFACES IN INORGANIC-MATRIX COMPOSITES: EXPERIMENT AND ATOMISTIC SIMULATION

AFOSR-91-0285

15 May 92 - 14 May 96

Principal Investigator: Dr Janez Megusar
Materials Processing Center
Massachusetts Institute of Technology
Cambridge MA 02139
(617) 253-6917

Program Manager: Lt Col Larry W Burggraf
AFOSR/NC
Bolling AFB DC 20332-6448
(202) 767-4960

Objective: The objective of this research is to advance the understanding of interfacial phenomena in ceramic-matrix composite materials by a combination of atomistic simulation, experimental study of interfaces, and ceramic-matrix composite processing in an interdisciplinary research program. A graphic fiber/silicon carbide bi-material is proposed as the model system. Specimens will be fabricated by coating graphite fibers with a layer of silicon carbide using plasma enhanced chemical vapor deposition. The specimens will be subjected to a series of heat treatments in which the annealing time and temperature will be systemically varied in order to establish a basis for studying the kinetics of the interface reactions and a detailed characterization of interface structures. The characterization of the graphite/SiC interfaces will include high-resolution transmission electron microscopy and analytical electron microscopy. Limited testing of the interface strength and toughness will be performed for the purpose of verifying the predictions of the atomistic simulation. The experiments will contribute toward optimizing interface structure and properties of the proposed model system and will furthermore ensure that the parallel atomistic simulation will relate to real systems.

PERFORMANCE IMPROVEMENT OF COMPOSITE AIRCRAFT WINGS THROUGH AEROELASTIC
TAILORING AND MODERN CONTROL
AFOSR-91-0351
1 Sep 91 - 31 Aug 94

Principal Investigator: Prof Leonard Meirovitch
Department of Engineering Science and Mechanics
Virginia Polytechnic Institute and State University
Blacksburg VA 24061-4899
(703) 231-5146

Program Manager: Dr Jim C I Chang
AFOSR/NA
Bolling AFB DC 20332-6448
(202) 767-4987

Objective: The objective of this research is to investigate the dynamic response of active structural systems complete with actuator dynamics and piezoactive system components. The study will develop methodology capable of improving aerodynamic characteristics of the composite wing structures with active control feedback design.

REVISIT INHOMOGENEITY PROBLEM VIA MODULUS PERTURBATION AND USE OF THE INVERSE
METHOD OF MICROMECHANICS
F49620-92-J-0319
1 May 92 - 30 Apr 95

Principal Investigator: Prof Toshio Mura
Department of Civil Engineering
Northwestern University
Evanston IL 60208
(312) 491-4003

Program Manager: Dr Walter F Jones
AFOSR/NA
Bolling AFB DC 20332-6448
(202) 767-0470

Objective: The objective of this study is to investigate the effects of inhomogeneities on structural response. The primary area of study will be the relationship between surface displacements and subsurface damage elements in aerospace structural components.

STRUCTURAL RESPONSE OF OXIDATION-RESISTANT CARBON/CARBON UNDER CYCLIC LOADING

FY 1992 NEW START

1 Aug 92 - 31 Jul 95

Principal Investigator: Prof Ozden O Ochoa
Mechanical Engineering Department
Texas A & M University
College Station TX 77843-3123
(409) 845-2022

Program Manager: Dr Walter F Jones
AFOSR/NA
Bolling AFB DC 20332-6448
(202) 767-0470

Objective: The objective of this research is to characterize the initiation and growth of damage in carbon/carbon (C/C) composite laminates fabricated with woven cloth, coated with an external ceramic oxidation-protective coating, with and without internal oxidation inhibitors, and subjected to realistic mission cycles.

THE OVERALL RESPONSE OF COMPOSITE MATERIALS UNDERGOING LARGE ELASTIC DEFORMATIONS

AFOSR-91-0161

1 Jan 91 - 31 Aug 92

Principal Investigator: Prof Pedro Ponte-Castaneda
Department of Mechanical Engineering and Applied Mechanics
University of Pennsylvania
208 Towne Building
Philadelphia PA 19104-6315
(215) 898-5046

Program Manager: Dr Walter F Jones
AFOSR/NA
Bolling AFB DC 20332-6448
(202) 767-0470

Objective: The objective of this research effort is to establish the limits of the overall constitutive behavior starting with limited statistical information about the distribution of phases in the composite.

PRESSURELESS DENSIFICATION OF CERAMIC-MATRIX COMPOSITES

AFOSR-90-0267 (URI)

1 Mar 90 - 28 Feb 93

Principal Investigator: Professor Mohamed N Rahaman
Department of Ceramic Engineering
University of Missouri
Rolla MO 65401-0249
(314) 341-4406

Program Manager: Lt Col Larry W Burggraf
AFOSR/NC
Bolling AFB DC 20332-6448
(202) 767-4960

Objective: The objective of this research is to study and model the sintering of ceramic particles around hard inclusions. The limits for pressureless sintering will be evaluated and the responsible impediments will be identified through model theoretical studies. It is also proposed to study the in situ formation of reinforcements during reaction sintering.

THERMOMECHANICAL ANALYSIS OF OXYGEN PROTECTED CARBON-CARBON COMPOSITES

F49620-92-C-0024

24 Feb 92 - 23 Feb 95

Principal Investigator: Dr B Walter Rosen
Materials Sciences Corporation
930 Harvest Drive, Suite 300
Blue Bell PA 19422
(215) 542-8400

Program Manager: Dr Walter F Jones
AFOSR/NA
Bolling AFB DC 20332-6448
(202) 767-0470

Objective: The objectives of this effort are to develop and verify mathematical models for predicting the thermo-mechanical properties of oxidation resistant carbon-carbon composites and to utilize these models to make judgments on the merits of both current and future materials concepts for oxidation resistance. Effort will be focused on the understanding of the formation and growth of damage within these materials, and on the analysis of oxidation protection mechanisms for carbon-carbon material systems.

MECHANICS OF COMPOSITE MATERIALS

AFOSR-MIPR-92-0026

1 Jul 92 - 30 Jun 93

Principal Investigator: Dr S Carlos Sanday
Naval Research Laboratory, Code 6370
Washington DC 20375-5320
(202) 767-2264

Program Manager: Dr Jim C I Chang
AFOSR/NA
Bolling AFB DC 20332-6448
(202) 767-4987

Objective: The objective of this study is to develop mathematical models for various problems in the mechanics of solids. Nonhomogeneous, anisotropic, and inelastic material behavior is included in the study. Particular effort will be focused on the development of general solutions which can be specialized to study a variety of relevant problems.

MICROSTRUCTURE/PROPERTY RELATIONSHIPS FOR METAL-MATRIX COMPOSITES
FY 1992 NEW START
1 Sep 92 - 31 Aug 95

Principal Investigator: Dr Donald A Shockey
SRI International
333 Ravenswood Avenue
Menlo Park CA 94025
(415) 859-2587

Program Manager: Dr Walter F Jones
AFOSR/NA
Bolling AFB DC 20332-6448
(202) 767-0470

Objective: The objectives of this research are to establish microstructure-property relationships for metal-matrix composites based on principles of mechanics, and to develop a computational failure model based on these relationships that can be applied to predict failure behavior. This research will develop guidelines for the specification of processing and composition routes to microstructures that have improved failure resistance over existing materials.

FLAW SENSITIVITY IN CERAMIC-MATRIX COMPOSITES
AFOSR-89-0548
1 Sep 89 - 28 Feb 93

Principal Investigator: Prof Paul Steif
Department of Mechanical Engineering
Carnegie-Mellon University
Pittsburgh PA 15213-3890
(412) 268-3507

Program Manager: Dr Walter F Jones
AFOSR/NA
Bolling AFB DC 20332-6448
(202) 767-0470

Objective: The objective of this research project is to develop an analytical model which will predict whether or not cracks propagating in the matrix will spare or break the fibers as they approach. The model will be developed in terms of physical parameters such as the crack geometry, the strength and moduli of fibers and matrix, and in particular, the character of the fiber-matrix interface.

A STUDY OF THE CRITICAL FACTORS CONTROLLING THE SYNTHESIS OF CERAMIC-MATRIX COMPOSITES FROM PRECERAMIC POLYMERS

F49620-91-C-0017

15 Dec 90 - 14 Dec 93

Principal Investigator: Dr James R Strife
United Technologies Research Center
400 Main Street
East Hartford CT 06108
(203) 727-7270

Program Manager: Lt Col Larry W Burggraf
AFOSR/NC
Bolling AFB DC 20332-6448
(202) 767-4960

Objective: The objective of this research is to investigate the critical factors which determine the mechanical properties of composites synthesized from a preceramic polymer matrix and carbon or ceramic fibers.

DAMAGE ACCUMULATION IN ADVANCED METAL-MATRIX COMPOSITES UNDER THERMAL CYCLING

FY 1993 NEW START

15 Oct 92 - 14 Oct 95

Principal Investigator: Prof Minoru Taya
Department of Mechanical Engineering, FU-10
University of Washington
Seattle WA 98195
(206) 685-2850

Program Manager: Dr Walter F Jones
AFOSR/NA
Bolling AFB DC 20332-6448
(202) 767-0470

Objective: The objectives of this research are to characterize the mechanisms of the damage accumulation process in metal-matrix composites subjected to creep and/or thermal cycling, including the nucleation and growth of interface damage. An analytical/experimental procedure will be developed to assess the durability of metal-matrix composites subjected to thermal cycling and combined thermal cycling/creep loadings.

ANISOTROPIC ELASTIC MATERIALS AND COMPOSITES WITH THE EFFECT OF TEMPERATURE AND
PIEZOELECTRICITY

F49620-92-J-0087

1 Nov 91 - 31 Oct 94

Principal Investigator: Prof T C T Ting
Department of Civil Engineering, Mechanics, and Metallurgy
University of Illinois at Chicago
Chicago IL 60680
(312) 996-2429

Program Manager: Dr Jim C I Chang
AFOSR/NA
Bolling AFB DC 20332-6448
(202) 767-4987

Objective: The objective of this research is to develop a rational approach for predicting the anisotropic behavior of composites subjected to thermal and piezoelectric loadings. Local physical phenomena including debonding and crack branching at the interfaces will all be included in the mathematical (nonlinear) analysis.

ANISOTROPIC DAMAGE MECHANICS MODELING IN METAL-MATRIX COMPOSITES

AFOSR-90-0227 (URI)

1 Apr 90 - 31 Mar 93

Principal Investigator: Prof George Z Voyiadjis
Department of Civil Engineering
Louisiana State University
Baton Rouge LA 70803
(504) 388-8668

Program Manager: Dr Walter F Jones
AFOSR/NA
Bolling AFB DC 20332-6448
(202) 767-0470

Objective: The objective of this program is to formulate a constitutive model for ductile fracture and finite strains in metal-matrix composites, using the anisotropic theory of continuum damage mechanics. A damage tensor derived with respect to the unstressed damaged state will be utilized.

A COMPREHENSIVE STUDY OF MATRIX FRACTURE MECHANISMS IN FIBER-REINFORCED
CERAMIC-MATRIX COMPOSITES

AFOSR-90-0172 (URI)

15 Feb 90 - 14 Feb 93

Principal Investigator: Prof Albert S D Wang
Department of Mechanical Engineering and Mechanics
Drexel University
Philadelphia PA 19104
(215) 895-2297

Program Manager: Dr Walter F Jones
AFOSR/NA
Bolling AFB DC 20332-6448
(202) 767-0470

Objective: The objective of this study is to establish both a fabrication and a material characterization capability for a class of high-temperature ceramic-matrix composites as an integrated effort.

PRESSURELESS SINTERING OF CERAMIC COMPOSITES
AFOSR-90-0265 (URI)
1 Apr 90 - 31 Mar 93

Principal Investigator: Professor Martin W Weiser
Department of Mechanical Engineering
University of New Mexico
Albuquerque NM 87131
(505) 277-2831

Program Manager: Lt Col Larry W Burggraf
AFOSR/NC
Bolling AFB DC 20332-6448
(202) 767-4960

Objective: The objective of this research is to study and model the sintering of ceramic-matrix composites. This work intends to examine the pressureless sintering and densification of two sequences of model ceramic composites in order to determine the range of suitability of each of the two current theories and to allow the formulation of a theory to describe the densification of real short fiber composites.

OFFICE OF NAVAL RESEARCH
MECHANICS DIVISION
ARLINGTON VA 22217-5000

GRANTS AND CONTRACTS

FAILURE OF THICK COMPOSITE LAMINATES

N00014-90-F-0060

February 90 - January 93

Scientific Officer: Dr. Yapa D. S. Rajapakse
Office of Naval Research
Mechanics Division, Code 1132SM
Arlington, VA 22217-5000
(703) 696-4405, Autocon 226-4405

Principal Investigator: Dr. R. M. Christensen
Lawrence Livermore National Laboratory
P. O. Box 808
Livermore, CA 94550
(415) 422-7136

Objective: Research will be conducted into the mechanics of failure of composite materials, with emphasis on physically-based failure criteria for thick composites laminates.

NONDESTRUCTIVE EVALUATION AND DAMAGE ACCUMULATION OF COMPOSITES

N00014-90-J-1724

April 90 - September 92

Scientific Officer: Dr. Yapa D. S. Rajapakse
Office of Naval Research
Mechanics Division, Code 1132SM
Arlington, VA 22217-5000
(703) 696-4405, Autocon 226-4405

Principal Investigator: Prof. I. M. Daniel
Northwestern University
Department of Civil Engineering
Evanston, IL 60201
(708) 491-5649

Objective: Research will be conducted to understand the process of damage growth in thick composite laminates subjected to complex loading states and fatigue. Nondestructive evaluation methods for damage characterization will be developed.

ENVIRONMENTAL EFFECTS AND ENVIRONMENTAL DAMAGE IN THERMOPLASTIC COMPOSITES

N00014-90-J-1556

January 90 - December 92

Scientific Officer: Dr. Yapa D. S. Rajapakse
Office of Naval Research
Mechanics Division, Code 1132SM
Arlington, VA 22217-5000
(703) 696-4405, Autovon 226-4405

Principal Investigator: Prof. Y. Weitsman
University of Tennessee
Dept. of Engineering Science & Mechanics
Knoxville, TN 37996-2030
(615) 974-5460

Objective: Research will be conducted into the effects of constant and cyclic pressure on moisture absorption and moisture-induced damage in thermoplastic composites. The development of residual stresses during processing will be investigated.

DYNAMIC MATRIX CRACKING AND DELAMINATION IN COMPOSITE LAMINATES SUBJECTED TO IMPACT LOADING

N00014-90-J-1666

July 90 - November 92

Scientific Officer: Dr. Yapa D. S. Rajapakse
Office of Naval Research
Mechanics Division, Code 1132SM
Arlington, VA 22217-5000
(703) 696-4405, Autovon 226-440S

Principal Investigator: Prof. C. T. Sun
Purdue University
School of Aeronautics and Astronautics
West Lafayette, IN 47907
(317) 494-5130

Objective: The propagation of damage in composite laminates due to impact loading conditions will be investigated using theoretical and experimental techniques. Dynamic delamination models will be established. Concepts for controlling impact damage will be explored, including the use of soft adhesive strips. Compression failure of thick composites will be investigated.

THERMOMECHANICAL BEHAVIOR OF HIGH TEMPERATURE COMPOSITES

N00014-89-J-3107

March 89 - December 94

Scientific Officer: Dr. Yapa D. S. Rajapakse
Office of Naval Research
Mechanics Division, Code 1132SM
Arlington, VA 22217-5000
(703) 696-4405, Autovon 226-4405

Principal Investigator: Prof. G. J. Dvorak
Rensselaer Polytechnic Institute
Department of Civil Engineering
Troy, NY 12181
(518) 276-6943

Objective: Investigations of the thermomechanical response, damage growth and fracture in metal matrix composites and intermetallic matrix composites will be conducted using analytical and experimental techniques. Local stress states caused during fabrication and by thermal changes in service, inelastic time-dependent behavior, and static and fatigue damage will be explored. Fundamental theories and applications of micromechanical analysis of composite materials and structures subjected to transformation fields will be investigated.

QUANTITATIVE ULTRASONICS MEASUREMENTS IN COMPOSITES
N00014-90-J-1273
July 90 - September 92

Scientific Officer: Dr. Yapa D. S. Rajapakse
Office of Naval Research
Mechanics Division, Code 1132SM
Arlington, VA 22217-5000
(703) 696-4405

Principal Investigator: Prof. W. Sachse
Cornell University
Dept. of Theoretical and Applied Mechanics
Ithaca, NY 14853
(607) 255-5065

Objective: Research will be conducted to establish quantitative active and passive ultrasonic measurement techniques for characterizing the microstructure and mechanical properties as well as the dynamics of deformation processes in composite materials.

IMPACT RESPONSE AND QNDE OF COMPOSITE LAMINATES
N00014-90-J-1857
April 90 - April 92

Scientific Officer: Dr. Yapa D. S. Rajapakse
Office of Naval Research
Mechanics Division, Code 1132SM
Arlington, VA 22217-5000
(703) 696-4405, Autovon 226-4405

Principal Investigator: Prof. A. K. Mal
University of California, Los Angeles
Dept. of Mechanical, Aerospace & Nuclear
Engineering
Los Angeles, CA 90024
(310) 825-5481

Objective: Research will be conducted into wave propagation in composite laminates. The Leaky Lamb Wave technique will be utilized for the characterization of elastic properties and defects in composites. The use of ultrasonic techniques for interfaces and interfacial regions will be explored.

MICROMECHANICS OF COMPOSITES
N00014-90-J-1377
October 90 - August 92

Scientific Officer: Dr. Yapa D.S. Rajapakse
Office of Naval Research
Mechanics Division, Code 1132SM
Arlington, VA 22217-5000
(703) 696-4405, Autocon 226-4405

Principal Investigator: Prof. B. Budiansky
Harvard University
Division of Applied Science
Cambridge, MA 02138
(617) 495-2849

Objective: Research will be conducted into the enhancement of the fracture toughness of ceramics and intermetallics by the incorporation of toughening agents such as fibers, whiskers, ductile particles and phase-transforming particles. Models will be established for the compression failure of polymer matrix composites. Microbuckling and kink band models will be established.

MECHANICS OF INTERFACE CRACKS AND COMPOSITES
N00014-90-J-1380
November 90 - November 93

Scientific Officer: Dr. Yapa D. S. Rajapakse
Office of Naval Research
Mechanics Division, Code 1132SM
Arlington, VA 22217-5000
(703) 696-4405, Autocon 226-4405

Principal Investigator: Prof. C. F. Shih
Brown University
Division of Engineering
Providence, RI 02912
(401) 863-2868

Objective: Research will be conducted to provide a fundamental understanding of the behavior of interface cracks in bimaterial elastic-plastic systems. The stress and strain fields around such cracks will be studied at both the continuum and polycrystalline slip theory levels. The effects of mode mixity and stress triaxiality will be investigated. Compression failure in thick composites will be investigated.

FRACTURE MECHANICS OF INTERFACIAL ZONES IN BONDED MATERIALS

N00014-89-J-3188

September 89 - August 92

Scientific Officer: Dr. Yapa D. S. Rajapakse
Office of Naval Research
Mechanics Division, Code 1132SM
Arlington, VA 22217-5000
(703) 696-4405, Autovon 226-4405

Principal Investigator: Prof. F. Erdogan
Lehigh University
Dept. of Mechanical Engineering & Mechanics
Bethlehem, PA 18015
(215) 758-4099

Objective: Research will be conducted into the micromechanics aspects of failure of composites, accounting for realistic interfacial zones. Models will be established for crack propagation in interfacial regions with continuously varying mechanical properties.

FAILURE MECHANICS OF THICK COMPOSITES

N00014-91-J-1173

October 90 - September 93

Scientific Officer: Dr. Yapa D. S. Rajapakse
Office of Naval Research
Mechanics Division, Code 1132SM
Arlington, VA 22217-5000
(703) 696-4405, Autovon 226-4405

Principal Investigator: Prof. S. N. Atluri
Georgia Institute of Technology
Dept. of Civil Engineering
Atlanta, GA 30332
(404) 894-2758

Objective: Research will be conducted into three-dimensional aspects of deformation, damage and failure in composites. Compression failure in thick composites will be investigated, and efficient computational models will be established.

OPTICAL MAPPING OF DEFORMATION FIELDS AROUND INTERFACE CRACKS
N00014-91-J-1380
January 90 - December 93

Scientific Officer: Dr. Yapa D. S. Rajapakse
Office of Naval Research
Mechanics Division, Code 1132SM
Arlington, VA 22217-5000
(703) 696-4405, Autovon 226-4405

Principal Investigator: Prof. F. P. Chiang
State University of New York
Dept. of Mechanical Engineering
Stony Brook, NY 11794-2300
(516) 632-8311

Objective: The optical techniques of moire interferometry and laser speckle interferometry will be used to determine two-dimensional and three-dimensional deformations in the vicinity of interface cracks. Optical techniques will be used in the investigation of failure in composites.

INVESTIGATION OF THE COMPRESSIVE FAILURE OF LONG FIBER COMPOSITES DUE TO MICROBUCKLING
N00014-91-J-1916
June 91 - May 94

Scientific Officer: Dr. Yapa D. S. Rajapakse
Office of Naval Research
Mechanics Division, Code 1132SM
Arlington, VA 22217-5000
(703) 696-4405, Autovon 226-4405

Principal Investigator: Dr. N. A. Fleck
University of Cambridge
Department of Engineering
Cambridge, U.K.

Objective: Research will be conducted into the mechanisms of compression failure in polymer matrix composites. The effects of fiber misalignment, material nonlinearity, multiaxial stress states, and specimen thickness will be investigated.

COMPRESSIVE RESPONSE OF DEBONDED THICK COMPOSITE SHELLS INCLUDING THE EFFECTS OF TRANSIENT MOISTURE SORPTION
N00014-91-J-1892
April 91 - March 93

Scientific Officer: Dr. Yapa D. S. Rajapakse
Office of Naval Research
Mechanics Division, Code 1132SM
Arlington, VA 22217-5000
(703) 696-4405, Autovon 226-4405

Principal Investigator: Prof. G. A. Kardomateas
Georgia Institute of Technology
Dept. of Aerospace Engineering
Atlanta, GA 30332
(404) 894-8198

Objective: Research will be conducted into the effect of local delaminations on the stability of thick composite shells under external pressure. The influence of moisture on stress fields at the boundaries of debonded regions will be explored.

THE INFLUENCE OF HIGH PRESSURE AND STRAIN RATE ON THE MECHANICAL BEHAVIOR OF
FIBER-REINFORCED COMPOSITES
N00014-91-J-1937
June 91 - May 93

Scientific Officer: Dr. Yapa D. S. Rajapakse
Office of Naval Research
Mechanics Division, Code 1132SM
Arlington, VA 22217-5000
(703) 696-4405, Autovon 226-4405

Principal Investigator: Prof. G. J. Weng
Rutgers University
Dept. of Mechanics and Materials Science
Piscataway, NJ 08855
(908) 932-2223

Objective: The effects of high hydrostatic pressure states on the constitutive properties and compression failure of thick composites will be investigated. The effects of strain-rate on the mechanical properties will be investigated.

COMPRESSION FAILURE OF THICK FIBROUS COMPOSITES
N00014-91-J-1705
March 91 - March 93

Scientific Officer: Dr. Yapa D. S. Rajapakse
Office of Naval Research
Mechanics Division, Code 1132SM
Arlington, VA 22217-5000
(703) 696-4405, Autovon 226-4405

Principal Investigator: Prof. A. M. Waas
University of Michigan
Dept. of Aerospace Engineering
Ann Arbor, MI 48109
(313) 764-8227

Objective: Compression failure mechanisms in composite laminates will be investigated using moire interferometry and holographic interferometry. Failure under uniaxial compression and under combined loading states will be investigated. The failure of cylindrical composite shells subjected to external hydrostatic pressure will be explored.

VISCOELASTIC BEHAVIOR OF THICK COMPOSITE LAMINATES
N00014-91-J-4091
April 91 - May 94

Scientific Officer: Dr. Yapa D. S. Rajapakse
Office of Naval Research
Mechanics Division, Code 1132SM
Arlington, VA 22217-5000
(703) 696-4405, Autovon 226-4405

Principal Investigator: Prof. R. A. Schapery
University of Texas at Austin
Dept. of Aerospace Engineering and Engineering
Mechanics
Austin, TX 78712
(512) 471-3924

Objective: Research will be conducted into the time-dependent behavior of composites subjected to compressive static and fatigue loading. The effects of initial ply waviness on the response of composite laminates will be established.

THE EFFECTS OF PROCESSING AND CONSTITUENT MATERIALS ON COMPRESSIVE STRENGTH OF THICK COMPOSITE LAMINATES
N00014-92-J-1846
August 92 - July 94

Scientific Officer: Dr. Yapa D. S. Rajapakse
Office of Naval Research
Mechanics Division, Code 1132SM
Arlington, VA 22217-5000
(703) 696-4405, Autovon 226-4405

Principal Investigator: Prof. H. Thomas Hahn
University of California
Dept. of Mechanical, Aerospace
and Nuclear Engineering
Los Angeles, CA 90024
(310) 825-2383

Objective: The objective of this research effort is to understand the dependence of the compression strength of thick composites on fiber microstructure, fiber mechanical properties and processing conditions.

PROCESS-INDUCED FIBER/PLY WAVINESS IN THICK SECTION COMPOSITE LAMINATES
N00014-92-J-1470
March 92 - February 95

Scientific Officer: Dr. Yapa D. S. Rajapakse
Office of Naval Research
Mechanics Division, Code 1132SM
Arlington, VA 22217-5000
(703) 696-4405, Autocon 226-4405

Principal Investigator: Prof. Tess J. Moon
University of Texas at Austin
Department of Mechanical Engineering
Austin, TX 78712
(512) 471-0094

Objective: Research will be conducted into the development of fiber-waviness and ply-waviness in continuous fiber polymeric composites during processing.

BUCKLING, POSTBUCKLING AND MODE INTERACTION IN THICK COMPOSITE STIFFENED
CYLINDRICAL SHELLS
N00014-91-J-1637
January 91 - December 92

Scientific Officer: Dr. Yapa D. S. Rajapakse
Office of Naval Research
Mechanics Division, Code 1132SM
Arlington, VA 22217-5000
(703) 696-4405, Autocon 226-4405

Principal Investigator: Prof. S. Sridharan
Washington University
Department of Civil Engineering
St. Louis, MO 6310
(314) 889-6348

Objective: Postbuckling behavior of anisotropic composite ring stiffened cylindrical shells will be investigated. Modal interactions and mechanisms of material damage will also be explored.

NAVAL RESEARCH LABORATORY
WASHINGTON, DC 20375-5000

IN-HOUSE

SIMULATION OF STRUCTURAL RESPONSE OF DAMAGED COMPOSITE SHIP COMPONENTS
October 86 - September 93

Principal Investigator: Dr. Phillip Mast
Naval Research Laboratory
Code 6383
Washington, DC 20375-5000
(202) 767-2165, Autovon 297-2165

Objective: Develop and apply an advanced simulation capability for predicting the effect of damage on the structural response of naval components made with fiber reinforced composites.

CONTRACTS

DYNAMIC BEHAVIOR OF COMPOSITES
N00014-86-C-2580
October 86 - March 93

Scientific Officer: Mr. Irvin Wolock
Naval Research Laboratory
Washington, DC 20375-5000
(202) 767-2567, Autovon 297-3567

Principal Investigator: Dr. Longin B. Greszczuk
McDonnell Douglas Astronautics Company
5301 Bolsa Avenue
Huntington Beach, CA 92647
(714) 896-3810

Objective: Develop a capability to predict the effects of large area dynamic loading, such as that due to an underwater explosion, on the mechanical response of composite materials and structures.

NAVAL AIR WARFARE CENTER
WARMINSTER, PA 19874-5000

IN-HOUSE

INVESTIGATION OF ADVANCED LIGHT-WEIGHT SANDWICH STRUCTURAL CONCEPTS
October 90 - September 92

Project Engineer: Dr. H. Ray
Naval Air Warfare Center, ADW
AVCSTD/6043
Warmister, PA 18974-5000
(215) 441-1149, Autovon 441-1149

Objective: To investigate advanced light-weight sandwich structures fabricated of composite materials, retaining no moisture and eliminating corrosion with improved damage tolerance.

EFFECTS OF FIBER/MATRIX INTERFACE ON TRANSVERSE TENSILE STRENGTH AND FRACTURE
RESISTANCE OF ORGANIC COMPOSITE MATERIALS
October 91 - September 92

Project Engineer: Dr. H. C. Tsai
Naval Air Warfare Center, ADW
AVCSTD/6043
Warminster, PA 18974-5000
(215) 441-2871, Autovon 441-2871

Objective: To develop analytical methods which predict the transverse tensile failures of composite materials and to examine how various micromechanical parameters influence the transverse tensile strength and failure modes.

MICROMECHANICS OF SHAPE MEMORY COMPOSITES
October 91 - September 94

Project Engineer: Dr. David Barrett
Naval Air Warfare Center, ADW
AVCSTD/6043
Warminster, PA 18974-5000
(215) 441-3770, Autovon 441-3770

Objective: To establish models to investigate the shape memory effect inside a composite system.

CONTRACTS

DELAMINATION METHODOLOGY FOR COMPOSITE STRUCTURES

N62269-90-C-0282

September 90 - September 92

Project Engineer: Dr. E. Kautz
Naval Air Warfare Center
Warminster, PA 18974-5000
(215) 441-1561, Autovon 441-1561

Principal Investigator: Dr. H. P. Han
Northrop Corporation
One Northrop Avenue
Hawthorne, CA 90250
(213) 332-5285

Objective: To develop a methodology to evaluate the significance of delaminations that occur during assembly of composite structures and to establish criteria for acceptance, rejection, or repair of the delaminated structure.

ASSEMBLY INDUCED DELAMINATIONS IN COMPOSITE STRUCTURES

N62269-90-C-0281

September 90 - March 93

Project Engineer: Dr. E. Kautz
Naval Air Warfare Center
Warminster, PA 18974-5000
(213) 441-1561, Autovon 441-1561

Principal Investigator: Mr. J. Goering
McDonnell Aircraft Co.
Box 518
St. Louis, MO 63166
(314) 233-9622

Objective: To analytically predict and experimentally verify the initiation/resistance of delaminations around fastener holes during mechanical assembly due to poorly mating skins to substructure.

NAVAL SURFACE WARFARE CENTER/CARDEROCK DIVISION
BETHESDA, MD 20084-5000
ANNAPOLIS, MD 21842

IN-HOUSE

COMPRESSION RESPONSE OF THICK-SECTION COMPOSITE MATERIALS
October 86 - September 93

Principal Investigator: Dr. E. T. Camponeschi, Jr.
CD/NSWC, Annapolis Division, Code 2802
Annapolis, MD 21842
(410) 267-2165, Autovon 281-2165

Objective: Develop an understanding of the mechanics of thick composites including compression response and in-plane/out-of-plane shear response.

NONLINEAR MECHANICS FOR THICK SECTION COMPOSITES
October 89 - September 92

Principal Investigator: Ms. K. Gipple
CD/NSWC, Annapolis Division, Code 2844
Annapolis, MD 21842
(301) 267-5218, Autovon 281-5218

Objective: Develop three-dimensional nonlinear material models for thick section composites.

COMPOSITE STRUCTURES FOR SUBMARINES
October 85 - September 95

Principal Investigator: Dr. W. Phyllaier
CD/NSWC, Code 1720
Bethesda, MD 20084-5000
(301) 227-1707, Autovon 287-1707

Objective: Develop the basic technology to support the applications of composites to submarine structures including methods of analysis and design for thick composite structures, design concepts for joints and penetrations in thick section composites, and failure prediction and residual strength after damage due to impact. Demonstrate the feasibility of using FRP composites for submarine applications such as control surfaces, air flasks, foundations, and ballast tank structures.

COMPOSITE STRUCTURES FOR SURFACE SHIPS
October 85 - September 95

Principal Investigator: Dr. M. Critchfield
CD/NSWC, Code 1720
Bethesda, MD 20084-5000
(301) 227-1769, Autovon 287-1769

Objective: Develop the basic technology to support the applications of composites to naval ship structures including static and dynamic analysis of hybrid fiber reinforced laminates, joints and attachments, failure prediction and residual strength after damage due to fire insult. Demonstrate the feasibility of using FRP composites for surface ship structural applications such as deckhouses, stacks and masts, and secondary structures.

BEHAVIOR OF HYBRID GLASS/GRAPHITE REINFORCED THICK-SECTION COMPOSITE CYLINDERS
UNDER HYDROSTATIC LOADING
October 89 - September 92

Principal Investigator: Dr. H. Garala
CD/NSWC, Code 1720
Bethesda, MD 20084-5000
(301) 227-1706, Autovon 287-1706

Objective: Determine the failure mechanisms and hydrostatic strength of commingled glass/graphite reinforced composite cylinders.

FEDERAL AVIATION ADMINISTRATION
FAA TECHNICAL CENTER

IN-HOUSE

SUPPORT TO MIL-HDBK-17

88-May - 95 September

Project Engineer: D. W. Oplinger
Propulsion and Structures Branch
Code ACD-210
FAA Technical Center
Atlantic City International Airport NJ 08405
(609) 484-4914

Objective: The FAA has been an active participant in the development of MIL-HD'BK-17B since this effort began in 1978. The FAA objective in this activity is to obtain a document with wide Government and Industry acceptance providing a data basis of structural and material properties, together with procedures for their usage, which satisfy the needs of Government representatives responsible for certification and related activities. In addition to providing support for various mechanics-of-materials related issues incorporated in MIL-HD'BK-17, the in house activity at the FAA Tech Center includes preparation of a chapter on structural joints for incorporation into Vol. III of the Handbook.

CONTRACTS

COMPOSITE FAILURE ANALYSIS HANDBOOK
(FAA Tech Center/Wright Laboratory Materials Directorate)
F33615-87-C-5212/F33615-86-c-5071
86 September - 93 June

Project Engineer:

(FAA) D. W. Oplinger
Propulsion and Structures Branch
Code ACD-210
FAA Technical Center
Atlantic City International Airport NJ 08405
(609) 484-4914

(USAF) P. Stumpf
Wright Aeronautical Laboratories
Materials directorate WL-MLSA
Wright Paterson Air Force Base OH 45433
(513) 255-3623

FEDERAL AVIATION ADMINISTRATION
FAA TECHNICAL CENTER

Program Manager:

R. Kar
Northrop Corporation
Aircraft division
One Northrop Avenue
Hawthorne CA 90250-3277

G. Walker MS 4H-98
Boeing Defense & Space Group
Material Processes and Physics Technology
PO Box 3703
Seattle WA
(206) 393-5534

Objective: The objective of this effort is to provide a handbook for FAA, National Transportation Safety Board and DoD accident investigators for determining the causes and progression of failures in composite aircraft structures. The program involved: 1) development of systematized procedures for evaluating causes of structural failures in composite components; 2) development of an extensive catalog of macroscopic/microscopic optical photography,, scanning electron microscopy, transmission electron microscopy and related techniques, and ; 3)case studies on failed aircraft components to evaluate the validity of the failure analysis procedures reported in the Handbook. The first release of the Handbook was issued in Feb. 92 as USAF/FAA Reports WL-TR-91-4032 and DoT/FAA/CT-91/23.

EVALUATION OF IMPACT DAMAGE IN COMPOSITE STRUCTURES
(FAA Tech Center/Naval Air Development Center)
N00019-89-C-0058
84 September - 92 September

Project Engineer: D. W. Oplinger
Propulsion and Structures Branch
Code ACD-210
FAA Technical Center
Atlantic City International Airport NJ 08405
(609) 484-4914

FEDERAL AVIATION ADMINISTRATION
FAA TECHNICAL CENTER

Principal Investigator:

P. Lagace
Department of Aeronautics and Astronautics
Massachusetts Institute of Technology
Cambridge MA 02139
(617) 253-3628

Objective: The objective of this effort is to develop improved concepts for characterizing the nature and consequences of impact damage in composite structures. The effort emphasizes the distinction between damage resistance -- i.e. the geometric nature of the damage produced by a given impact event -- and damage tolerance -- the residual strength of the structure after a given damage has been sustained. Experimental and analytical efforts on cylindrical specimens as well as flat panels are included.

MECHANICAL PROPERTY TEST METHODS FOR COMPOSITE MATERIALS

(FAA Tech Center/ Army Materials Technology Laboratory)

DAAL04-89-C-0023

90 September-93 February

Project Engineer: D. W. Oplinger
Propulsion and Structures Branch
Code ACD-210
FAA Technical Center
Atlantic City International Airport NJ 08405
(609) 484-4914

Principal Investigator:

S. Chatterjee
Materials Sciences Corporation
Fort Washington PA 19034
(215) 542-8400

Objective: The objective of this effort is to provide FAA representatives with an up-to-date knowledge of appropriate test methods for composite materials, as well as to provide improvements in test methods where appropriate. Results sought include a state-of-the art review of mechanical property tests together with a program of experimental and analytical efforts on selected test methods as needed.

FEDERAL AVIATION ADMINISTRATION
FAA TECHNICAL CENTER

COMPOSITE CONCEPTS FOR TURBINE ENGINE FAILURE CONTAINMENT
(FAA Tech Center/Army Materials Technology Laboratory)

DTFA03-88-A-00029

88 September - 92 December

Project Engineer: B. Fenton
Propulsion and Structures Branch
Code ACD-210
FAA Technical Center
Atlantic City International Airport NJ 08405
(609) 484-5158

Principal Investigator:
S. Petrie
Code SLCMT-MEC
Army Materials Technology Laboratory
Watertown MA 02172
(617) 923-5174

Objective: The objective of this effort is to evaluate the effectiveness of aramid and glass reinforced containment rings for protection of aircraft from blade and disk failures in small turbine engines.

DELAMINATION METHODOLOGY FOR COMPOSITE STRUCTURES

(FAA Tech Center/ Naval Air Development Center)

N62269-90-C-028 (MacAir)

N62261-90-C-0282 (Northrop)

90 December - 92 december

Project Engineer:
(FAA)D. W. Oplinger
Propulsion and Structures Branch
Code ACD-210
FAA Technical Center
Atlantic City International Airport NJ 08405
(609) 484-5158

FEDERAL AVIATION ADMINISTRATION
FAA TECHNICAL CENTER

(NADC) E. W. Kautz
Naval Air Development Center
Warminster, PA
(215) 441-1561

Principal Investigators

(Northrop): H. P. Kan
Department 3853
Aircraft Division
Northrop Corporation
Hawthorne CA 90250-3277
310-332-2134

(MacAir): J. Goering
MS 1021322
McDonnell Aircraft Corp.
PO Box 516
St Louis MO 63166-0516

Objective: The objective of this joint contractual effort is to develop a methodology for evaluating the significance of manufacturing-induced delaminations related to inadequate assembly procedures for composite structures, and to establish criteria for acceptance, rejection and/or repair of the affected components.

CERTIFICATION METHODOLOGY FOR STIFFENER TERMINATIONS
(FAA Tech Center/NASA Langley Research Center)
NAS1-19347
92 May - 93 December

Project Engineer

(FAA) D. W. Oplinger
Propulsion and Structures Branch
Code ACD-210
FAA Technical Center
Atlantic City International Airport NJ 08405
(609) 484-5158

(NASA) M. Rouse
NASA Langley Research Center
Hampton VA
(804) 864-3182

FEDERAL AVIATION ADMINISTRATION
FAA TECHNICAL CENTER

Principal Investigator:

H. P. Kan
Department 3853
Aircraft Division
Northrop Corporation
Hawthorne CA 90250-3277
310-332-2134

Objective: The objective of this effort is to establish certification methodology for structural details in composite structures such as stiffener terminations or interruptions, which may be subject to special problems due to out-of-plane loading. Effort will include : (1) generation of experimental data on stiffener termination configurations; (2) verification of failure analysis methods developed in earlier Navy-funded efforts ; (3) estimation of static strength and fatigue life scatter at this type of structural detail; (4) establish guidelines for certification of cocured composite structures with stiffener terminations present.

EFFECT OF SPECTRUM LOADING ON LIFETIME OF COMPOSITE STRUCTURES
(FAA Tech Center/ Naval Space and Warfare Systems Command)
N00039-92-C-0100
92 March - 95 March

Project Engineer

D. W. Oplinger
Propulsion and Structures Branch
Code ACD-210
FAA Technical Center
Atlantic City International Airport NJ 08405
(609) 484-5158

Principal Investigator:

H. T. Hahn
Department of Mechanical Engineering
UCLA
(310) 825-2383

Objective: The objective of this effort is to evaluate spectrum loading effects in fatigue testing of composite structures to establish characteristics which are relevant to lifetime assessment. Effects of load sequencing, cycling rate, defects, environmental degradation and stress concentrations on fatigue life of composite coupon specimens will be assessed.

WRIGHT LABORATORY
MATERIALS DIRECTORATE

IN-HOUSE

ADVANCED COMPOSITES
WORK UNIT DIRECTIVE (WUD) NUMBER 45
92 October - 93 October

WUD Leader: Steven L. Donaldson
Materials Directorate
Wright Laboratories
WL/MLBM
Wright-Patterson AFB OH 45433-6533
(513) 255-9096, DSN: 785-9096

Objective: The long-term objective for the in-house research effort is to develop an understanding of deformation and failure in composite materials. The short-term objectives include the following: (a) understanding of failure mechanisms in polymer matrix composites, particularly under compression loading; (b) intelligent on-line processing of composites, including sensor development; (c) the development of advanced carbon-carbon materials; (d) failure of brittle matrix ceramic composites; (e) an investigation of biological composites in nature.

CONTRACTS

IMPROVED COMPOSITE MATERIALS
F33615-91-C-5618
16 Sep 91 - 15 Sep 95

Project Engineer: Ken Johnson
Materials Directorate
Wright Laboratory
WL/MLBC
Wright-Patterson AFB OH 45433-6533
(513) 255-6981, DSN: 785-6981

Principal Investigator: Allan Crasto
University of Dayton Research Institute
300 College Park Avenue
Dayton OH 45469

Objective: The objective of this program is to investigate from both an experimental and an analytical standpoint the potential of new and/or modifications of existing matrix materials and reinforcements/product forms for use in advanced composite materials, including processing/mechanical property relationships. Such materials are subsequent candidates for use in advanced aircraft and aerospace structural applications. This on-site contract assists in accomplishing the research objectives outlined under WUD 45 along with the investigation of biotechnology approaches to advanced composite fabrication and design.

MICROMECHANICS OF COMPOSITE FAILURE

F33615-88-C-5420

1 Oct 88 - 30 Sep 92

Project Engineer: Capt David Rose
Materials Directorate
Wright Laboratory
WL/MLBM
Wright-Patterson AFB OH 45433-6533
(513) 255-9097, DSN 785-9097

Principal Investigator: Som R. Soni
AdTech Systems Research Inc
1342 N Fairfield Road
Dayton OH 45432

Objective: The objective of this program is to provide exploratory development in thermomechanical response, model material system development composite processing, and failure mechanism investigations of composite and related constituent materials.

MECHANICS OF ADVANCED COMPOSITE

F33615-91-C-5600

1 Mar 91 - 1 Aug 95

Project Engineer: Capt David Rose
Materials Directorate
Wright Laboratory
WL/MLBM
Wright-Patterson AFB OH 45433-6533
(513) 255-9097, DSN 785-9097

Principal Investigator: Som R. Soni
AdTech Systems Research Inc
1342 N Fairfield Road
Dayton OH 45432

Objective: The objective of this program is to develop mathematical models which describe the behavior of advanced composite materials with emphasis on micromechanics and to transition the models to industry through the development of a series of user friendly computer programs.

ULTRA-LIGHTWEIGHT MATERIALS AND PROCESS DEVELOPMENT

F33615-91-C-5617

16 Sep 91 - 16 Jan 95

Project Engineer: Keith Bowman
Materials Directorate
Wright Laboratory
WL/MLBC
Wright-Patterson AFB OH 45433-6533
(513) 255-9076, DSN: 785-9076

Principal Investigator: Dr Anna Yen
Northrop Corporation
Aircraft Division
One Northrop Avenue
Hawthorne CA 90250

Objective: To develop advanced ultra-lightweight (ULW) materials and processes which will enable innovative approaches to design ULW aircraft structures that are at least 50% lighter and offer reduced life cycle costs and improved system performance when compared with current state-of-the-art (SOTA) aircraft structures utilizing up to 10% advanced composite materials in their structures.

ARMY PROGRAM INPUT

**Seventeenth Annual Mechanics of Composites Review
Dayton, Ohio
27-28 October 1992**

**Submitted By
Dr. Bruce P. Burns
U.S. Army Research Laboratory
ATTN: AMSRL-WT-PD
Aberdeen Proving Ground, MD 21005-5066**

**U.S. ARMY
ARMY RESEARCH OFFICE**

CONTRACTS

TITLE: Large-Amplitude Forced Response of Dynamic Systems

**RESPONSIBLE INDIVIDUAL: Dr. Anderson
U.S. Army Research Office
P.O. Box 12211
Research Triangle Park, NC 27790-2211
(919) 549-4317**

**PRINCIPAL INVESTIGATOR: Ali H. Nayfeh
Department of Engineering Science & Mechanics
Virginia Polytechnic Institute and State University
Blacksburg, VA 24061**

OBJECTIVE: To investigate the response and stability of non-linear dynamical systems in the presence of both parametric and external excitations. RELEVANCE: Non-linear effects are known to influence hingeless and bearingless rotor stability. The non-linear response of rotorcraft in forward flight may be of particular importance. The proposed investigation could be highly relevant in studying changes of dynamic response of components, such as rotor blades, whose stiffness and inertial parameters vary with time as a result of environmental and/or ballistic effects.

TITLE: Stability of Elastically Tailored Rotor Systems

RESPONSIBLE INDIVIDUAL: Dr. Anderson
U.S. Army Research Office
P.O. Box 12211
Research Triangle Park, NC 27790-2211
(919) 549-4317

PRINCIPAL INVESTIGATOR: D. H. Hodges and L. W. Rehfield
Department of Aerospace Engineering
Georgia Institute of Technology
Atlanta, GA 30332

OBJECTIVE: To develop mathematical modeling and analysis procedures to determine the aeroelastic stability characteristics of bearingless helicopter rotors on elastic supports in axial flow and tilt rotor aircraft with elastic wings in axial flight in the helicopter mode and in the airplane mode. **RELEVANCE:** The investigation is a necessary step in the design of tailored composite rotors.

TITLE: Severe Edge Effects & Simple Complimentary Interior Solutions for Anisotropic & Composite Structures

RESPONSIBLE INDIVIDUAL: Dr. Anderson
U.S. Army Research Office
P.O. Box 12211
Research Triangle Park, NC 27709-2211
(919) 549-4317

PRINCIPAL INVESTIGATOR: C. O. Horgan and J. G. Simmonds
Applied Mathematics
University of Virginia
Charlottesville, VA 22904

OBJECTIVE: To investigate the deformation, stability, and vibration characteristics of thin-walled structures, namely, (1) the interior where there are no steep stress gradients; and (2) the edge zones, where stress gradients are high. **Relevance:** This research of severe edge effects could be very significant in stress-based designs of composite structures. It is relevant to the missions of several Army laboratories since high stress levels can occur near the edges of structures such as gun barrels, rocket motor casings, helicopter rotor blades, and containment vessels which must remain elastic when subjected to mechanical, inertial, or thermal loads. In particular, end effects in composite structures have direct bearing on helicopter rotor blades, with such effects being important near the rotor hub.

TITLE: Smart Materials & Structures Incorporating Electro-rheological Fluids Analytical & Experimental Investigation

RESPONSIBLE INDIVIDUAL: Dr. Anderson
U.S. Army Research Office
P.O. Box 12211
Research Triangle Park, NC 27709-2211
(919) 549-4317

PRINCIPAL INVESTIGATOR: Mukesh V. Gandhi and Brian S. Thompson
Department of Mechanical Engineering
Michigan State University
East Lansing, MI 48823

OBJECTIVE: To develop the ability to change in a rapid and significant manner the vibrational characteristics of structures fabricated from advanced smart composite materials in which electro-rheological materials are embedded by changing in a controlled fashion the electrical field imposed upon the fluid domains. **RELEVANCE:** The generic research program offers the potential of accelerating the development of a new generation of advanced helicopter and rotorcraft systems, battlefield robotic and ammunition supply systems, and vehicular suspensions and materiel handling systems.

TITLE: Damage-Survivable & Damage-Tolerant Laminated Composite with Optimally Placed Piezoelectric Layers

RESPONSIBLE INDIVIDUAL: Dr. Anderson
U.S. Army Research Office
P.O. Box 12211
Research Triangle Park, NC 27790-2211
(919) 549-4317

PRINCIPAL INVESTIGATOR: Shiv P. Joshi
Department of Aerospace Engineering
University of Texas at Arlington
Arlington, TX 76010

OBJECTIVE: To produce a smart laminated composite structure by embedding piezoelectric sensors and actuators in it, determining the optimal placement of piezoelectric layers in a laminated composite and the durability (fatigue loading) and survivability (impact loading) of embedded sensors and actuators. Devise means of estimating the extent of damage, locating impact damage, actively suppressing damage survivability of composite structures, and to suppress structural damage in an active manner has considerable potential application to the design of various helicopter components.

TITLE: Active Control of NITINOL-reinforced Smart Structural Composites

RESPONSIBLE INDIVIDUAL: Dr. Anderson
U.S. Army Research Office
P.O. Box 12211
Research Triangle Park, NC 27790-2211
(919) 549-4317

PRINCIPAL INVESTIGATOR: Amr M. Baz
Department of Mechanical Engineering
Catholic University of America
Washington DC 20017-1575

OBJECTIVE: To develop the ability to change the vibrational characteristics of structures fabricated from advanced composite materials in which shape memory nickel-titanium alloy (nitinol) wires are embedded to sense and control the static and dynamic characteristics of the composite structure. **RELEVANCE:** The generic research program offers the potential of accelerating the development of a new generation of advanced helicopter and rotorcraft systems, battlefield robotic and ammunition supply systems, and vehicular suspensions and materiel handling systems.

TITLE: Use of Shape Memory Alloys in the Robust Control of Smart Structures

RESPONSIBLE INDIVIDUAL: Dr. Anderson
U.S. Army Research Office
P.O. Box 12211
Research Triangle Park, NC 27790-2211
(919) 549-4317

PRINCIPAL INVESTIGATOR: Vittal S. Rao and Thomas J. O'Keefe
Electrical Engineering
University of Missouri at Rolla
Rolla, MO 65401

OBJECTIVE: To develop appropriate electro-deposition techniques for the processing of shape memory alloys characterized by ultra-fine sizes that are amenable to manufacturing processes (the preparation of layered smart structures is foreseen). Identify optimum deposition parameters for the best properties of the electro-deposited film. Establish mathematical models for phase transitions (constitutive relations). Develop robust controller design methodology for smart structures with rigid and flexible models through the use of reduced order models. **RELEVANCE:** The research program offers the potential of accelerating the development of a new generation of advanced rotorcraft systems, battlefield robotic and ammunition supply systems, and vehicular suspension and materiel handling systems. The shape-memory-alloys-based smart structures with robust control systems form the basis of effective vibration suppression systems.

TITLE: Smart Composite Structures Featuring Embedded Hybrid Actuation and Sensing Capabilities

RESPONSIBLE INDIVIDUAL: Dr. Anderson
U.S. Army Research Office
P.O. Box 12211
Research Triangle Park, NC 27790-2211
(919) 549-4317

PRINCIPAL INVESTIGATOR: Mukesh V. Gandhi and Brian S. Thompson
Department of Mechanical Engineering
Michigan State University
East Lansing, MI 48823

OBJECTIVE: To investigate the possibility of applying a hybridization of electro-rheological fluid and piezoelectric actuator systems to accomplish in real time with minimal energy consumption the vibration tailoring and control of beam and plate structures fabricated from composite materials. **RELEVANCE:** The generic research program offers the potential of accelerating the development of a new generation of advanced rotorcraft systems, battlefield robotic and ammunition supply systems, and vehicular suspension and materiel handling systems. Some national defense programs that may also benefit from the proposed research include the Strategic Defense Initiative, the National Aerospace Plane, NASA Space Stations, the B-2 Bomber, and various weapons systems.

TITLE: Development of "Smart" Piezothermo-Elastic Laminae: Theory and Applications

RESPONSIBLE INDIVIDUAL: Dr. Anderson
U.S. Army Research Office
P.O. Box 12211
Research Triangle Park, NC 27790-2211
(919) 549-4317

PRINCIPAL INVESTIGATOR: Horn S. Tzou
Department of Mechanical Engineering
University of Kentucky
Lexington, KY 40506-0999

OBJECTIVE: (1) Develop a piezothermoelastic lamination theory for multilayered composite shells (each layer of which can be either elastic, piezoelectric, thermoelastic, or piezothermoelastic); (2) devise a new finite element to analyze a distributed modal sensor actuator theory; and (3) conduct a theoretical and experimental validation of prototype structures, with one or more piezoelectric layers serving as a distributed actuator.

RELEVANCE: The development of smart structures that consist of multilayered composite shells with embedded piezoelectric sensors and actuators offers the potential of suppressing structural vibrations and reducing the noise occurring inside rotorcraft constructed with these materials. The results of this research are relevant to the mission of the Aerostructures Directorate.

TITLE: Control of Sandwich and Composite Plates Using Piezoelectric Stiffeners

RESPONSIBLE INDIVIDUAL: Dr. Gary L. Anderson
U.S. Army Research Office
P.O. Box 12211
Research Triangle Park, NC 27790-2211
(919) 549-4317

PRINCIPAL INVESTIGATOR: Prof. Victor Birman
Engineering Education Center
University of Missouri
8001 Natural Bridge Road
St. Louis, Missouri 63121

OBJECTIVE: Develop a comprehensive theory of sandwich and composite plates reinforced by beam-type piezoelectric stiffeners bonded to the structure. Take into account in the theory large deformations by means of a Von Karman-type theory of elastic plates. Derive the exact solution of active control problems of certain piezoelectrically stiffened sandwich and composite plates.

TITLE: Smart Materials, Structures, and Mathematical Issues for Active Damage Control

RESPONSIBLE INDIVIDUAL: Dr. Gary L. Anderson
U.S. Army Research Office
P.O. Box 12211
Research Triangle Park, NC 27790-2211
(919) 549-4317

PRINCIPAL INVESTIGATOR: Prof. Craig A. Rogers
Department of Mechanical Engineering
Virginia Polytechnic Institute & State University
Blacksburg, Virginia 24061-0261

OBJECTIVE: Develop active damage control techniques for modifying the three-dimensional strain fields in composite structures to improve the performance of structural systems, with the specific goals of reducing stress concentrations, preventing delaminations, reducing the effects of impact, modifying the buckling behavior, and increasing the fatigue life of structures. Develop constitutive models appropriate for macroscopic design of actuators and sensors for potential sensor and actuator materials such as shape memory alloys, piezoelectric ceramics, electrostrictors, and magnetostrictors. Perform detailed constitutive characterization tests to aid in the understanding of the control possibilities of new actuator and sensor materials and the design of new material devices. Perform aging and extended life cycle tests to understand the control implications of realistic implementation of induced strain actuators and sensors and the adaptability needed to account for extended use and aging non-linearities. Refine the existing polarization fatigue model to account for high electric fields and relatively thick actuators.

TITLE: Interdisciplinary Basic Research in Smart Materials and Structures

RESPONSIBLE INDIVIDUAL: Dr. Gary L. Anderson
U.S. Army Research Office
P.O. Box 12211
Research Triangle Park, NC 27790-2211
(919) 549-4317

PRINCIPAL INVESTIGATOR: Prof. Iradj G. Tadjbakhsh
Department of Civil Engineering
Rensselaer Polytechnic Institute
Troy, New York 12180-3590

OBJECTIVE: Model the non-linear coupling of the electric and/or thermal fields with the deformation fields of electrostatic materials, shape memory alloys, and electro-rheological fluids in combination with homogeneous and composite materials. Concentrate on the development of a consistent, accurate, and tractable description of the descriptive field equations when active material elements are embedded in a host medium to form active structural systems. Investigate hysteresis effects in piezoceramics, electro-viscoelasticity, and depolarizing effects, deriving equations of motion for a small field superimposed on a bias. Develop methodologies for vibration suppression, shape control, trajectory tracking, and damage detection. Incorporate the derived non-linear constitutive relations for electro-elasticity, shape memory alloys, and electro-rheological fluids into approximate theories for flexible structures. Combine the direct theories for flexible structures and the inverse problem of calculating the actuation strains for prescribed geometric configuration changes. Devise control strategies for optimum actuation strain distribution to achieve desired shapes. Modify the theory of layered structures to include microcracks in the composite laminae and their interactions with piezoelectric sensors. Apply sensitivity analyses for the optimum placement of sensors and actuators suited for self-damage diagnosis and damage mitigation. Conduct experimental investigations of flexible smart cylindrical rods with shape memory alloy fibers, layered structures with piezoelectric sensors and actuators, composite plates containing electro-rheological fluids, and control procedures as applied to a robot arm with embedded piezoelectric actuators.

TITLE: Smart Structures Technology: Innovations and Applications to Rotorcraft Systems

RESPONSIBLE INDIVIDUAL: Dr. Gary L. Anderson
U.S. Army Research Office
P.O. Box 12211
Research Triangle Park, NC 27790-2211
(919) 549-4317

PRINCIPAL INVESTIGATOR: Prof. Inderjit Chopra
Department of Aerospace Engineering
University of Maryland
College Park, Maryland 20742-3015

OBJECTIVE: Investigate the application of sensors, actuators, distributed controls, and micromechanics to rotorcraft, exploring the potential of smart structures to reduce vibration, minimize rotor blade dynamic stresses, ensure aeromechanical stability, reduce acoustic levels, increase life of structural components, enhance handling qualities, and detect and suppress incipient damage. Conduct fundamental studies of novel hybrid and magnetostrictive actuators, optical fiber strain sensors, structural integrity of smart structures, innovative feedback and distributed controller systems and model identification schemes. Build in-house and test dynamically scaled models in university laboratories, in a vacuum chamber, and in a wind tunnel (for example, rotor blades with directionally attached piezoelectric crystals that will permit the local control of the blade lift and pitching moments through changes in the airfoil contour and local twist for the purpose of reducing rotor noise levels). Modify existing comprehensive rotorcraft analyses such as UMARC (a software code for performing numerical calculations), adding feedback control and piezoelectric technologies, to include the modeling of smart structures and validate the resulting code through the use of experimental test data. Exploit the properties of electro-rheological fluids embedded in composite rotor blades to change dramatically their viscous characteristics when subjected to an electric potential with the goal of augmenting rotor blade lag mode damping.

TITLE: Programmable Materials and Structures

RESPONSIBLE INDIVIDUAL: Dr. Gary L. Anderson
U.S. Army Research Office
P.O. Box 12211
Research Triangle Park, NC 27790-2211
(919) 549-4317

PRINCIPAL INVESTIGATOR: Prof. Daniel J. Inman
Department of Engineering Science & Mechanics
Virginia Polytechnic Institute & State University
Blacksburg, Virginia 24061-0219

OBJECTIVE: Examine the possibility of using microprocessors embedded in composite beam and plate structures combined with embedded sensors and actuators for both vibration suppression and damage detection, addressing issues of structural modeling, experimental verification, optimal design of various layers, mathematical modeling, and control.

TITLE: Inelastic Deformation & Failure Analysis of Filament-Wound Composite Structures

RESPONSIBLE INDIVIDUAL: Dr. Iyer
U.S. Army Research Office
P.O. Box 12211
Research Triangle Park, NC 27709-2211
(919) 549-4258

PRINCIPAL INVESTIGATOR: Gerald A. Wempner and Wan-Lee Yin
Department of Civil Engineering
Georgia Institute of Technology
Atlanta, GA 30332

OBJECTIVE: To develop analytical models for describing inelastic deformations and failure behavior of filament-wound composite structures. **RELEVANCE:** There are several critical applications of this technology needed today (e.g., the analysis and evaluation of rocket motor casings and launch tubes).

TITLE: Wave Propagation & Dynamic Response of Laminated Structures

RESPONSIBLE INDIVIDUAL: Dr. Iyer
U.S. Army Research Office
P.O. Box 12211
Research Triangle Park, NC 27790-2211
(919) 549-4258

PRINCIPAL INVESTIGATOR: R. K. Kapania and J. N. Reddy
Department of Aerospace & Ocean Engineering
Virginia Polytechnic Institute and State University
Blacksburg, VA 24061

OBJECTIVE: To investigate wave propagation and nonlinear dynamic response of laminated structures under impact and other short duration (transient) loads, placing special emphasis on transient wave propagation in the presence of residual stresses. **RELEVANCE:** This research has been identified as being quite relevant to work conducted by the Applied Technology Director in the area of composite structures and weapons interfacing. The development of a space-time finite-element which would account for unsymmetric laminates and nonlinear response is particularly relevant to the noise transmission, stress analysis, fatigue, and dynamic response activities of the aerostructures directorate.

TITLE: Effect of Nose Shape & Mass of the Impactor on Impact Damage of Laminated Composite Shells

RESPONSIBLE INDIVIDUAL: Dr. Iyer
U.S. Army Research Office
P.O. Box 12211
Research Triangle Park, NC 27709-2211
(919) 549-4258

PRINCIPAL INVESTIGATOR: Fu-Kuo Chang
Department of Aeronautics & Astronautics Engineering
Stanford University
Stanford, CA 94305

OBJECTIVE: To investigate impact damage in thin to thick shells fabricated from fiber-reinforced, polymer-based matrix composites subjected to low-velocity impact under different types of impactors. Determine the effect of the impactor's mass and nose shape on impact damage in laminated composites as a function of ply orientation, thickness, and laminate curvature. **RELEVANCE:** Strength degradation of carbon-reinforced composites due to low-speed impact continues to be a problem area. This research addresses particular aspects of the problem that are important but that have not been addressed elsewhere.

TITLE: High-Velocity Impact of Composite Laminates

RESPONSIBLE INDIVIDUAL: Dr. Iyer
U.S. Army Research Office
P.O. Box 12211
Research Triangle Park, NC 27790-2211
(919) 549-4258

PRINCIPAL INVESTIGATOR: C. T. Sun
Department of Aerospace and
Astronautical Engineering
Purdue University
Lafayette, IN 47907

OBJECTIVE: To conduct theoretical and experimental studies to contribute to the understanding of the key elements in high-velocity impact of composite laminates and to model the penetration, perforation, and delamination processes during impact. **RELEVANCE:** This research has direct implications on mission objectives in the Terminal Ballistics Division at BRL. Technological development in high-velocity impact of composites is needed and would represent a significant contribution to many ballistic armor programs. Some of the basic issues addressed in the proposed project are important to programs at the ASTD, particularly the modeling of the contact-penetration problem and analysis of the progressive failure through the thickness of composite laminates.

TITLE: Assessment of Damage in Composite Materials by a Real-time Nondestructive Laser Technique

RESPONSIBLE INDIVIDUAL: Dr. Iyer
U.S. Army Research Office
P.O. Box 12211
Research Triangle Park, NC 27709-2211
(919) 549-4258

PRINCIPAL INVESTIGATOR: M. A. Seif
Department of Mechanical Engineering
Tuskegee University
Tuskegee, AL 36083

OBJECTIVE: To develop a laser speckle shearing interferometry technique for the characterization of nucleation and propagation of microcracks in composites. **RELEVANCE:** Laser speckle shearing interferometry offers the potential for dynamically characterizing the formation and subsequent propagation of microcracks under specific load environments. When correlation with defect characteristics are established, load-carrying capacity and remaining service life of components could be assessed nondestructively. The technique could also be a powerful tool in the development of composites for specific applications.

MATERIALS SCIENCE - COMPOSITE MECHANICS

TITLE: Mismatched Induced Superplasticity in Metal Matrix Composites

RESPONSIBLE INDIVIDUAL: Dr. Simmons
U.S. Army Research Office
P.O. Box 12211
Research Triangle Park, NC 27709-2211
(919) 549-4329

PRINCIPAL INVESTIGATOR: Professor Glen Daehn
Department Materials Science and Engineering
Ohio State University
Columbus, OH 43210-1179

OBJECTIVE: To study the Mismatched Induced Superplasticity (MISP) of Metal Matrix Composites (MMCs) induced by pressure or temperature cycles. **RELEVANCE:** Many Army systems require components having high strength, toughness and resistance to ballistic projectiles. MMCs are desirable for these applications and this research will aid in the superplastic-forming of complex shapes of MMCs. Superior performance at a minimum fabrication cost.

TITLE: Measurement of Interface Strength, Intrinsic Toughness and Their Dependence on Interfacial Segregants

RESPONSIBLE INDIVIDUAL: Dr. Simmons
U.S. Army Research Office
P.O. Box 12211
Research Triangle Park, NC 27790-2211
(919) 549-4329

PRINCIPAL INVESTIGATOR: Vijay Gupta
Thayer School of Engineering
Dartmouth College
Hanover, NH 03755

OBJECTIVE: To develop and implement a laser spallation technique to investigate the mechanical properties of selected interface systems. **RELEVANCE:** The determination and control of interfacial strength is of great importance to the development of coatings and composites needed in the design and protection of Army weapons and vehicles.

TITLE: Effect of Processing Parameters on the High-Temperature Creep of SiC Whisker-Reinforced Alumina

RESPONSIBLE INDIVIDUAL: Dr. Simmons
U.S. Army Research Office
P.O. Box 12211
Research Triangle Park, NC 27790-2211
(919) 549-4329

PRINCIPAL INVESTIGATOR: Terence G. Langdon
Department of Materials Science
University of Southern California
Los Angeles, CA 90089-1452

OBJECTIVE: To determine the influence of processing parameters on the high-temperature creep behavior of silicon carbide whisker-reinforced alumina composites. **RELEVANCE:** The research will contribute to the understanding of high-temperature creep in ceramic and ceramic composites and provide guidelines for process control for optimum properties. Advanced ceramic composites are needed in high-temperature applications such as thermal barriers for pistons in adiabatic engines, turbine blades, and missile parts.

TITLE: Manufacturing Science, Reliability and Maintainability Technology

RESPONSIBLE INDIVIDUAL: A. Crowson
U.S. Army Research Office
P.O. Box 12211
Research Triangle Park, NC 27790-2211
(919) 549-0641

PRINCIPAL INVESTIGATOR: T. W. Chou and R. L. McCullough
Center For Composite Materials
University of Delaware
Newark, DE 19716

OBJECTIVE: This university research initiative program consists of the following elements: cure characterization and monitoring, on-line intelligent, non-destructive evaluation for in-process control of manufacturing, process simulation, computer-aided manufacturing by filament winding, structural property relationships, mechanics of thick-section composite laminates, structure performance and durability, and integrated engineering for durable structures.

**U.S. ARMY LABORATORY COMMAND
MATERIALS TECHNOLOGY LABORATORY**

TITLE: Composite Hull Program

**PROJECT MANAGER: Mr. Wm. E. Haskell III
U.S. Army Materials Technology Laboratory
ATTN: SLCMT-MEC
Watertown, MA 02172-0001
DSN 955-5172 COMM (617) 923-5172**

**MTL CONTRACT DAALO4-86-C-0079
PROJECT MANAGER: Mr. Paul R. Para
FMC Corporation
Ground Systems Division
Santa Clara, CA 95108**

OBJECTIVE: Develop and demonstrate the benefits of composite hull technology for combat vehicle hull applications. Primary payoffs are weight reduction, survivability enhancement, corrosion resistance, signature reduction, and reduced manufacturing and life-cycle costs.

PROGRESS: During Phase I and II of this multiyear effort, the 30-ton Composite Infantry Fighting Vehicle (CIFV) was designed, fabricated, and field tested. Deliverables included manufacturing process procedures, quality assurance procedures, structural analysis report, economic analysis, and detailed technical drawing package. Based on the success of the CIFV, the Army will further develop composite hull technology under the TACOM Composite Armored Vehicle (CAV) program. CAV design contracts have been awarded to General Dynamics Land Systems Division and FMC Corporation.

The ongoing Phase III effort is developing composite hull technology for future main battle tank (FMBT) and advanced field artillery systems applications. The 50-ton composite hull structure has been designed, and fabrication is 85% complete. Weight studies indicate that this heavy composite hull could save up to 4 tons compared to an RHA steel heavy chassis. Outfitting and field testing of the heavy composite hull is currently not funded. It is MTL's goal to obtain support and funding for this effort.

U.S. ARMY MATERIALS TECHNOLOGY LABORATORY

TITLE: Lightweight Hull Floor Program

ARMY PROGRAM MANAGER: Mr. Wm. E. Haskell III
U.S. Army Materials Technology Laboratory
ATTN: SLCMT-MEC
DSN 955-5172
COMM: 617-923-5172

MTL CONTRACT DAALO4-92-C-0014

PROJECT MANAGER: Mr. Henry Catherino
General Dynamics Land Systems Division
Warren, MI 48090

OBJECTIVE: There is currently no formal blast test procedure for evaluating combat vehicle floor plate configurations. This contract will develop a standardized test procedure for evaluating current and future floor plate configurations. The goal is to realistically simulate an actual mine blast at minimal cost. The test specimen and fixture design should constrain an unfailed specimen in the fixture. Floor plate boundary conditions typical of a future composite hulled 30-ton armored vehicle will be incorporated. Baseline blast test will be run on aluminum specimens prior to testing S-2 glass/polyester laminates. The areal density of the test specimens will be held constant, and the explosive charge weight will be increased.

TITLE: Analytic Methodology for Adhesive Joints and Thick Composites

RESPONSIBLE INDIVIDUAL: S. C. Chou
U.S. Army Laboratory Command
Materials Technology Laboratory
Watertown, MA 02172-0001
(617) 923-5427

PRINCIPLE INVESTIGATOR: E. Seather, T. Y. Tsui
U.S. Army Laboratory Command
Materials Technology Laboratory
Watertown, MA 02172-0001

OBJECTIVE: The program objective is to develop improved analytical and numerical methods for analyzing adhesively bonded joints and thick composites.

Research of bonded joints focus on the development of special finite element formulations to accurately and efficiently model bonded joints of arbitrary 3-D geometry. Efforts in this area include: (1) the investigation of novel displacement-based and hybrid stress-based finite element formulations to best simulate adhesive layer stresses; and (2) research of appropriate material models to represent nonlinear adhesive response.

Efforts directed towards developing analytical methodology for thick composites include: (1) development of higher-order plate and shell theories for static and dynamic analysis of thick composite laminates; and (2) formulation of finite plate and shell elements based on developed higher-order theories.

U.S. ARMY MISSILE COMMAND

TITLE: Determination of Mechanical Material Properties for Filament Wound Structures

RESPONSIBLE INDIVIDUAL: Dr. Larry C. Mixon
Army Missile Command

PRINCIPAL INVESTIGATOR: Terry L. Vandiver
Army Missile Command
(205) 876-1015

OBJECTIVE: The objective of this task is to develop test standards for the determination of mechanical material properties for filament-wound composite structures. The initial task is to develop uniaxial material properties. Future plans include biaxial and triaxial material property determination. This effort is being performed by the joint-Army-Navy-NASA-Air Force (JANNAF) composite motor case subcommittee through a round robin test effort. This task is coordinated with MIL-HDBK-17, ASTM, National Bureau of Standards, and DOD CMPS Composites Technology Program. Three military standards have been developed and are currently being reviewed and undergoing balloting for ASTM.

TITLE: Composite Materials Evaluation for Filament Winding

RESPONSIBLE INDIVIDUAL: Lawrence W. Howard
Army Missile Command

PRINCIPAL INVESTIGATOR: Terry L. Vandiver
Army Missile Command
(205) 876-1015

OBJECTIVE: The object of this task is to evaluate new fibers for filament winding. Delivered strengths are determined via strand tests and 3-inch-diameter filament-wound pressure vessels with different stress ratios. The experimental data is used in the design of composite rocket motor cases, launchers, pressure vessels, and other filament-wound structures.

**U.S. ARMY RESEARCH LABORATORY
WEAPONS TECHNOLOGY DIRECTORATE**

TITLE: Lightweight Structures for Interior Ballistics

**PRINCIPAL INVESTIGATOR: W. H. Drysdale
U.S. Army Research Laboratory
ATTN: AMSRL-WT-PD
Aberdeen Proving Ground, MD 21005-5066
(410) 278-6123**

OBJECTIVE: Composite materials represent a portion of this effort. The objective of this project is to develop failure criteria, architecture transition technology, and optimum design technology for thick ballistic structures. Rate of loading and layup transition studies are being addressed at BRL. A special high-rate, propellant-driven test apparatus is under development to generate uniaxial or triaxial stress states at strain rates of up to 200 per second. Three-dimensional failure criteria and other constitutive effects are being studied and hypothesized by Lawrence Livermore National Lab (LLNL). They are also sponsoring studies at the University of Utah and Pennsylvania State University. Experimental activities to develop failure data are being conducted at both the LLNL and the University of Utah. Additional failure criteria work and extensions to optimal notions for relatively simple structures and layup.

TITLE: Composite Hull Technology

**PRINCIPAL INVESTIGATOR: B. Moore
U.S. Army Research Laboratory
ATTN: AMSRL-WT-WA
Aberdeen Proving Ground, MD 21005-5066
(410) 278-8688**

OBJECTIVE: Develop evaluation tools for composite technology, especially that related to providing ballistic protection for ground vehicles. Perform baseline testing of various threats (KE, CE, EFP blast) against composite structures and advanced armors; develop related empirically based models; choose code for KE simulations. Perform engineering analysis of the application of composite materials to ground vehicles, with due consideration of other advanced technologies.

VEHICLE STRUCTURES DIRECTORATE
U.S. ARMY RESEARCH LABORATORY
NASA LANGLEY RESEARCH CENTER

TITLE: Basic Research in Structures

RESPONSIBLE INDIVIDUAL: Dr. F. D. Bartlett, Jr.
U.S. Army Research Laboratory
NASA Langley Research Center (MS 266)
Hampton, VA 23665-5225
(804) 864-3960

PRINCIPAL INVESTIGATORS: Dr. T. K. O'Brien, G. B. Murri,
Dr. R. L. Boitnott, Dr. K. E. Jackson,
Dr. G. L. Farley, V. L. Metcalf, M. Nixon

OBJECTIVE: The focus of the Army Basic Research in composites is to investigate and explore structure technologies which improve structural integrity of rotorcraft composite structures, develop superior analyses for composites design, exploit structural tailoring and smart structures potential to improve structural performance, and develop more effective nondestructive evaluation sciences for inspecting composite structures. The Army Basic Research is conducted jointly with NASA to provide the fundamental mechanics of composites knowledge needed to transition these technology developments to military and civil advanced rotorcraft applications.

TITLE: Structures Technology Applications

RESPONSIBLE INDIVIDUAL: Dr. F. D. Bartlett, Jr.
U.S. Army Research Laboratory
NASA Langley Research Center (MS 266)
Hampton, VA 23665-5225
(804) 864-3960

PRINCIPAL INVESTIGATORS: Dr. R. L. Boitnott, Dr. K. E. Jackson,
Dr. G. L. Farley, V. L. Metcalf,
M. W. Nixon, D. J. Baker, J. N. Zalameda

OBJECTIVE: The goals of this applied research are to explore and demonstrate innovative structural concepts and design methodologies for composite structures so that U.S. industries can build safe, durable, and affordable rotorcraft structures. The ultimate goal is to develop mature composites technology that can compete with metals in providing more durable structures at a lower cost and save weight. This research is conducted through jointly sponsored Army/NASA investigations which establish reliable composite structures, validate new and improved analytical capabilities, and demonstrate faster and more effective field and manufacturing inspection methods for complex composite structures. The benefits of this research will provide proven technology to the rotorcraft industry and the U.S. Army for applications to future air vehicle systems.

**U.S. ARMY AVIATIONS SYSTEMS COMMAND
FT. EUSTIS**

TITLE: Ballistic Survivability of Generic Composite Main Rotor Hub Flexbeams

RESPONSIBLE INDIVIDUAL: Dan Good
U.S. Army ARTA (AVSCOM)
Aviation Applied Technology Directorate
SAVRT-TV-ATS
Ft. Eustis, VA 23604-5577
(804) 878-5921

PRINCIPAL INVESTIGATOR: E. Robeson

OBJECTIVE: The goal of this effort is to quantify the ballistic survivability of typical composite main rotor hub flexbeams. Two different flexbeam designs will be impacted with various ballistic threats. One design will be tested under simulated centrifugal load while the other will be fatigue tested following ballistic impact in a no load condition. Fatigue testing of the first design will be considered after a damage assessment is made.

TITLE:

RESPONSIBLE INDIVIDUAL: Dan Good
U.S. Army ARTA (AVSCOM)
Aviation Applied Technology Directorate
SAVRT-TV-ATS
Ft. Eustis, VA 23604-5577
(804) 878-5921

PRINCIPAL INVESTIGATOR: N. Calapodas and D. Kinney
U.S. Army ARTA (AVSCOM)
Aviation Applied Technology Directorate
SAVRT-TV-ATS
Ft. Eustis, VA 23604-5577
(804) 878-3303

OBJECTIVE: A joint program among Army/NASA/contractor is planned to conduct detail correlation of the finite element (FE) dynamic models of both ACAP airframes. AATD will perform all shake testing and the contractors will be responsible for analytical changes to the FE models. The FE dynamic models, generated under Army funding during the developmental phases of the ACAP Program, were further improved under funding of the NASA DAMVIBS Program. However, the thrust of shake testing performed during the developmental phase was oriented towards the usefulness of the models to 15 Hz and below. In the correlation to be performed, the test vehicles will be stripped down to the basic structure. The inertia of the components removed will be substituted with concentrated masses. Upon successful correlation of the basic configuration, components will be installed and correlation efforts repeated. The goal is to achieve satisfactory correlation at modal and force response frequencies up to 40 Hz.

TITLE: Composite Airframe Design for Weapons Interface

RESPONSIBLE INDIVIDUAL: Dan Good
U.S. Army ARTA (AVSCOM)
Aviation Applied Technology Directorate
SAVRT-TV-ATS
Ft. Eustis, VA 23604-5577
(804) 878-5921

PRINCIPAL INVESTIGATOR: J. Moffatt
U.S. Army ARTA (AVSCOM)
Aviation Applied Technology Directorate
SAVRT-TV-ATS
Ft. Eustis, VA 23604-5577
(804) 878-2377

OBJECTIVE: The effect of 20–30-mm weapon firing in close proximity to composite airframe is investigated. Effects of weapon-induced pressure and thermal environments on weight tradeoffs for structural design are investigated. This program has been completed and the results documented in USA AVSCOM TR91-D-S.

NASA LANGLEY RESEARCH CENTER
IN-HOUSE

ADVANCED CONCEPTS FOR COMPOSITE HELICOPTER STRUCTURES

89 April 1 - 96 January 1

Project Engineer: Mr. Donald J. Baker
Mail Stop 190
Aerostructures Directorate, USAARTA (AVSCOM)
NASA Langley Research Center
Hampton, VA 23665-5225
(804) 864-3171

Objective: To investigate new design concepts using composite materials for helicopter and tilt-rotor structures. Trade studies are performed using the various computer codes. Task assignment contracts are used to complement in-house activities to evaluate advanced designs.

POSTBUCKLING AND CRIPPLING OF COMPRESSION-LOADED COMPOSITE STRUCTURAL COMPONENTS

79 March 1 - 94 September 30

Project Engineer: Dr. James H. Starnes, Jr.
Mail Stop 190
NASA Langley Research Center
Hampton, VA 23665-5225
(804) 864-3168

Objective: To study the postbuckling and crippling of compression-loaded composite components and to determine the limitations of postbuckling design concepts in structural applications.

DESIGN TECHNOLOGY FOR STIFFENED CURVED COMPOSITE PANELS AND SHELLS

79 October 1 - 94 September 30

Project Engineer: Dr. James H. Starnes, Jr.
Mail Stop 190
NASA Langley Research Center
Hampton, VA 23665-5225
(804) 864-3168

Objective: To develop verified design technology for generic advanced-composite stiffened curved panels.

POSTBUCKLING OF FLAT STIFFENED COMPOSITE SHEAR WEBS
81 July 1 - 92 September 30

Project Engineer: Mr. Marshall Rouse
Mail Stop 190
NASA Langley Research Center
Hampton, VA 23665-5225
(804) 864-3182

Objective: To study the postbuckling response and failure characteristics of flat stiffened composite webs.

BUCKLING, DAMAGE TOLERANCE, AND STRENGTH OF COMPOSITE CYLINDERS
86 October 1 - 94 September 30

Project Engineer: Ms. Dawn C. Jegley
Mail Stop 190
NASA Langley Research Center
Hampton, VA 23665-5225
(804) 864-3185

Objective: To develop accurate analyses for predicting the behavior of composite cylinders and to verify the analytical results by test.

ADVANCED COMPOSITE STRUCTURAL CONCEPTS
84 October 1 - 94 September 30

Project Engineer: Dr. James H. Starnes, Jr.
Mail Stop 190
NASA Langley Research Center
Hampton, VA 23665-5225
(804) 864-3168

Objective: To develop composite structural concepts and design technology needed to realized the improved performance, structural efficiency, and lower-cost advantage offered by new material systems and manufacturing methods for advanced aircraft structures.

FAILURE MECHANISMS FOR COMPOSITE LAMINATES WITH DAMAGE AND LOCAL DISCONTINUITIES

81 October 1 - 94 September 30

Project Engineer: Dr. Mark J. Stuart
Mail Stop 190
NASA Langley Research Center
Hampton, VA 23665-5225
(804) 864-3170

Objective: To study the effects of impact damage and local discontinuities on the strength of composite structural components, to identify the failure modes that govern the behavior of components subjected to low-velocity impact damage, and to analytically predict failure and structural response.

MECHANICS OF ANISOTROPIC COMPOSITE STRUCTURES

86 October 1 - 93 September 30

Project Engineer: Dr. Michael P. Nemeth
Mail Stop 190
NASA Langley Research Center
Hampton, VA 23665-5225
(804) 864-3184

Objective: To develop analytical procedures for anisotropic structural components that accurately predict the response for tailored structures.

CRASH CHARACTERISTICS OF COMPOSITE FUSELAGE STRUCTURES

82 July 1 - 94 September 30

Project Engineer: Mr. Huey D. Carden
Mail Stop 495
NASA Langley Research Center
Hampton, VA 23665-5225
(804) 864-4151

Objective: To study the crash characteristics of composite transport fuselage structural components.

**EXPERIMENTAL AND ANALYTICAL CHARACTERIZATION OF THE MECHANICAL
BEHAVIOR OF METAL MATRIX COMPOSITES**

80 June 1 - 93 September 30

Project Engineer: Dr. W. Steven Johnson
Mail Stop 188E
NASA Langley Research Center
Hampton, VA 23665-5225
(804) 864-3463 FTS 928-3463

Objective: To experimentally investigate the fatigue, fracture, and thermomechanical behavior of MMC's to insure airframe structural integrity at elevated temperatures. Both continuously reinforced laminates and discontinuous particulate and whisker reinforced MMC's will be included in the study.

**DEVELOPMENT OF ANALYTICAL MODELS OF THE THERMOMECHANICAL
BEHAVIOR OF METAL MATRIX COMPOSITES**

87 June 1 - 93 September 30

Project Engineer: Dr. C. A. Bigelow
Mail Stop 188E
NASA Langley Research Center
Hampton, VA 23665-5225
(804) 864-3462 FTS 928-3462

Objective: To develop finite-element codes, laminate-analysis codes, and micromechanics models necessary to analytically investigate mechanics issues related to the fatigue, fracture, and thermomechanical behavior of MMC's.

ANALYSIS OF PLY CRACKING INITIATION

91 October 1 - 94 September 30

Project Engineer: Dr. John H. Crews, Jr.
Mail Stop 188E
NASA Langley Research Center
Hampton, VA 23665-5225
(804) 864-3457 FTS 928-3457

Objective: To develop tests and micromechanics stress analyses for microcracking and ply cracking in laminated composites.

MECHANICS MODELS OF ADVANCED TEXTILE COMPOSITES

88 June 1 - 94 September 30

Project Engineer: Mr. Clarence C. Poe, Jr.
Mail Stop 188E
NASA Langley Research Center
Hampton, VA 23665-5225
(804) 864-3449 FTS 928-3449

Objective: To develop finite-element models of the deformation and local stress states that reflect the local fiber curvature of advanced textile composites. Mathematical descriptions of the unit cell architecture will be the basis for the models. Failure criteria will be developed to optimize these materials with regard to in-plane and out-of-plane strength. Experiments will be conducted to support model development and verify predictions.

INTERLAMINAR SHEAR FRACTURE TOUGHNESS

89 May 1 - 92 September 30

Project Engineer: Ms. Gretchen B. Murri
Mail Stop 188E
Aerostructures Directorate, USAARTA (AVSCOM)
NASA Langley Research Center
Hampton, VA 23665-5225
(804) 864-3466 FTS 928-3466

Objective: Cyclic end-notched flexure tests will be used to measure the mode II strain energy release rate of two materials in fatigue. Results will be used to develop ASTM test standards for strain energy release rate under fatigue loading.

DELAMINATIONS IN TAPERED COMPOSITE LAMINATES WITH INTERNAL PLY DROPS

88 October 1 - 92 September 30

Project Engineer: Ms. Gretchen B. Murri
Mail Stop 188E
Aerostructures Directorate, USAARTA (AVSCOM)
NASA Langley Research Center
Hampton, VA 23665-5225
(804) 864-3466 FTS 928-3466

Objective: To characterize delamination failures in tapered composites containing internal ply-drops. Experimental results from a variety of materials and lay-ups will be compared with finite element and closed-form solutions.

**IMPACT RESPONSE AND DAMAGE IN STITCHED, WOVEN, AND BRAIDED
GRAPHITE FIBER COMPOSITES**

87 October 1 - 94 October 31

Project Engineer: Mr. C. C. Poe, Jr.
Mail Stop 188E
NASA Langley Research Center
Hampton, VA 23665-5225
(804) 864-3467 FTS 928-3467

Objective: To characterize damage in three-dimensional braided composites subjected to hard object impact at low energy levels.

MIXED-MODE DELAMINATION TESTING

87 September 1 - 92 September 30

Project Engineer: Mr. James R. Reeder
Mail Stop 188E
NASA Langley Research Center
Hampton, VA 23665-5225
(804) 864-3456 FTS 928-3456

Objective: To measure the delamination fracture toughness of laminated composites material subjected to combined mode I and mode II loadings and thereby develop a mixed mode delamination failure criterion. The new mixed-mode-bending specimen will be used for testing.

HIGH TEMPERATURE LONG-TERM APPLICATIONS OF POLYMERIC COMPOSITES

90 January 1 - 98 September 30

Project Engineer: Dr. W. S. Johnson
Mail Stop 188E
NASA Langley Research Center
Hampton, VA 23665-5225
(804) 864-3463

Objective: To assess the influence of thermal-mechanical fatigue and long term durability on the mechanical properties of polymeric matrix composites for use on advanced supersonic commercial transports. Temperatures will approach 450°F for 60,000 flight hours.

TIME DEPENDENT COMPOSITE CHARACTERIZATION FOR POLYMER COMPOSITES

90 January 1 - 95 September 30

Project Engineer: Dr. Thomas S. Gates
Mail Stop 188E
NASA Langley Research Center
Hampton, VA 23665-5225
(804) 864-3400 FTS 928-3400

Objective: To develop constitutive models for nonlinear, rate dependent behavior. The analysis will be supported by experimental data to account for creep, relaxation, and physical aging.

EXPERIMENTAL EVALUATION OF ADVANCED COMPOSITE MATERIAL FORMS

84 June 1 - 93 June 1

Project Engineer: Mr. H. Benson Dexter
Mail Stop 188B
NASA Langley Research Center
Hampton, VA 23665-5225
(804) 864-3094 FTS 928-3094

Objective: To determine mechanical properties and establish damage tolerance of 2-D and 3-D woven, stitched, knitted, and braided composite materials. Data base mostly completed on woven stitched knitted and braided materials. Additional testing in new interlock braids and knits will be completed in FY 93.

MICROMECHANICS MODELING OF COMPOSITE THERMOELASTIC BEHAVIOR

86 October - 93 September 30

Project Engineer: Dr. David E. Bowles
Mail Stop 191
NASA Langley Research Center
Hampton, VA 23665-5225
(804) 864-3095 FTS 928-3095

Objective: Develop analytical methods to investigate thermally induced deformations and stresses in continuous fiber-reinforced composites at the micro-mechanics level, and predict how these deformations and stresses affect the dimensional stability of the composite.

DESIGN, ANALYSIS, AND FABRICATION OF PRECISION OPTICAL BENCHES
89 June 1 - 93 September 30

Project Engineer: Dr. David E. Bowles
Mail Stop 191
NASA Langley Research Center
Hampton, VA 23665-5225
(804) 864-3095 FTS 928-3095

Objective: Analytically and experimentally investigate the effects of constituent properties (fiber, matrix, core, adhesive) and bench design on thermally induced deformations and stresses in composite optical bench structures. Develop fabrication techniques for producing lightweight ultra-stable composite optical benches.

ADVANCED COMPOSITE MATERIALS FOR ULTRA-HIGH PRECISION REFLECTOR
HONEYCOMB PANELS
88 October 1 - 95 September 30

Project Engineer: Dr. Stephen S. Tompkins
Mail Stop 188B
NASA Langley Research Center
Hampton, VA 23665-5225
(804) 864-3096 FTS 928-3096

Objective: Develop advanced structural graphite reinforced composite material systems that are dimensionally stable and durable in the LEO and GEO space environments. Using these material systems, fabricate ultra high precision, light weight, core reinforced panels for reflectors and optical benches. Critical requirements for the panels are: a) high inplane and flexural stiffness, b) low moisture distortion, c) near zero thermal expansion, and, d) panel face-sheet material replicate high accurate mold surface (surface accuracy less than 1 micron RMS).

THERMAL AND MECHANICAL STABILITY OF COMPOSITE MATERIALS
83 October 1 - 93 September 30

Project Engineer: Dr. Stephen S. Tompkins
Mail Stop 188B
NASA Langley Research Center
Hampton, VA 23665-5225
(804) 864-3096 FTS 928-3096

Objective: Develop and evaluate structural composite materials (resin-, metal-, and ceramic-matrix) that are dimensionally stable and/or have stable thermal and mechanical properties when subjected to simulated long-term LEO and GEO space service environments.

ULTRASONIC NDE OF CARBON-CARBON MATERIALS FOR NASP

Project Engineer: Dr. Eric I. Madaras
Mail Stop 231
NASA Langley Research Center
Hampton, VA 23665
(804) 864-4993 FTS 928-4993

Objective: To develop ultrasonic measurement techniques for characterizing the integrity of carbon-carbon composite materials under consideration for use in the NASP project.

EFFECTS OF THROUGH-THE-THICKNESS REINFORCEMENT ON ULTRASONIC INSPECTION OF COMPOSITE LAMINATES

Project Engineer: Dr. Patrick H. Johnston
Mail Stop 231
NASA Langley Research Center
Hampton, VA 23665
(804) 864-4966 FTS 928-4966

Objective: To measure the spatial variations of sound velocity in stitched and other three-dimensional fiber architecture composites and to relate these to measurement artifacts in ultrasonic measurements of these composites resulting from them, with a focus toward developing detection methods which are insensitive to these phase-distortions.

CHARACTERIZATION OF COMPOSITES BASED ON ANALYSIS OF THE FREQUENCY DEPENDENCE OF ULTRASONIC ATTENUATION

Project Engineer: Dr. Patrick H. Johnston
Mail Stop 231
NASA Langley Research Center
Hampton, VA 23665
(804) 864-4966 FTS 928-4966

Objective: To measure the ultrasonic attenuation coefficient of composites as a function of frequency and to relate these results to models of the flaw types present, such as porosity or delaminations due to impact damage.

NONDESTRUCTIVE EVALUATION OF PULTRUSION PROCESSING

Project Engineer: Mr. F. Raymond Parker
Mail Stop 231
NASA Langley Research Center
Hampton, VA 23665
(804) 864-4965 FTS 928-4965

Objective: To instrument a pultrusion die with ultrasonic sensors to enable one to monitor the cure properties of the composite in the die by measuring the change in ultrasonic velocity in the composite and to detect the presence of porosity in the composite by measuring the attenuation of the ultrasonic signal in the composite.

PROPAGATION OF PLATE MODES IN ACOUSTIC EMISSION SIGNALS IN COMPOSITE PLATES

Project Engineer: Mr. William Prosser
Mail Stop 231
NASA Langley Research Center
Hampton, VA 23665-5225
(804)864-4960 FTS 928-4960

Objective: To characterize the propagation of plate mode acoustic waves in thin composite plates by measuring the velocity of the extensional mode and the dispersion of the flexural mode as well as the effect of source orientation on the amplitude of the two modes, allowing a better understanding of the propagation of acoustic emission (AE) signals in composite structures.

EFFECT OF STRESS ON THE ENERGY FLUX DEVIATION OF ULTRASONIC WAVES IN GRAPHITE-EPOXY COMPOSITES

Project Engineer: Mr. William Prosser
Mail Stop 231
NASA Langley Research Center
Hampton, VA 23665-5225
(804)864-4960 FTS 928-4960

Objective: To model the shift in the energy flow of ultrasonic waves due to the application of stress and nonlinear elastic effects in composite materials to serve as the basis of a new NDE technique to characterize stress in a composite.

THERMAL NDE OF COMPOSITE ROTORCRAFT STRUCTURES

Project Engineer: Mr. Joe Zalameda
Mail Stop 231
NASA Langley Research Center
Hampton, VA 23665
(804) 864-4793 FTS 928-4793

Objective: To develop NDE systems for rapid, inexpensive, and efficient inspection of composite rotorcraft structures in both industrial and field environments, including investigations toward combining thermal and ultrasonic NDE techniques for the inspection of composite impact damage.

THERMOGRAPHIC NDE OF COMPOSITES

Project Engineer: Dr. William P. Winfree
Mail Stop 231
NASA Langley Research Center
Hampton, VA 23665-5225
(804)864-4963 FTS 928-4963

Objective: To develop thermographic techniques for characterization of defects in composite materials and structures with particular emphasis on impact damage and porosity detection.

THERMOGRAPHIC CHARACTERIZATION OF STRESS INDUCED DAMAGE IN COMPOSITES

Project Engineer: Ms. D. Michele Heath
Mail Stop 231
NASA Langley Research Center
Hampton, VA 23665
(804) 864-4964 FTS 928-4964

Objective: To develop a remote thermographic technique for monitoring stress induced damage in composite materials during cyclic fatigue testing and during static loading.

SMART MATERIALS AND STRUCTURES

Project Engineer: Dr. Robert Rogoswki
Mail Stop 231
NASA Langley Research Center
Hampton, VA 23665-5225
(804)864-4990 FTS 928-4990

Objective: Investigate methods for embedding and interrogating optical fiber sensors for health monitoring of composite materials and structures.

HIGH STRENGTH, DELAMINATION RESISTANT CARBON-CARBON COMPOSITES
FOR HYPERSONIC VEHICLE AIRFRAME APPLICATIONS

Project Engineer: Mr. Philip O. Ransone
Mail Stop 191
NASA Langley Research Center
Hampton, VA 23665-5225
(804) 864-3503

Objective: To develop thin, high strength, oxidation-resistant carbon-carbon composite materials with good interlaminar strengths. Approaches include woven and stitched through-the-thickness reinforcements, alternate fiber sizings, and composite processing variations.

CONTRACTS

COLLAPSE AND FAILURE MODES IN ADVANCED COMPOSITE STRUCTURES NSG-1483

78 January 15 - 93 January 14

Project Engineer: Dr. James H. Starnes, Jr.
Mail Stop 190
NASA Langley Research Center
Hampton, VA 23665-5225
(804) 864-3168

Principal Investigator: Dr. Wolfgang G. Knauss
California Institute of Technology
Pasadena, CA 91125
(213) 356-4524/4528

Objective: To experimentally and analytically study time-dependent effects on buckling and failure of composite structures with discontinuities.

STRUCTURES AND MATERIALS TECHNOLOGIES FOR AIRCRAFT COMPOSITE PRIMARY STRUCTURES

NAS1-19347

91 September 1 - 98 August 31

Project Engineer: Mr. Marshall Rouse
Mail Stop 190
NASA Langley Research Center
Hampton, VA 23665-5225
(804) 864-3182

Principal Investigator: Dr. Ravi Deo
M.S. 3853/MF
Northrop Corporation
1 Northrop Ave
Hawthorne, CA. 90250-3277
(213) 332-2134

Objective: To develop and validate structures and materials technologies for wing and fuselage structures that would be applicable to subsonic and/or supersonic commercial transport aircraft.

ADVANCED COMPOSITE STRUCTURAL DESIGN TECHNOLOGY FOR
COMMERCIAL TRANSPORT AIRCRAFT

NAS1-19348

91 September 1 - 98 August 31

Project Engineer: Dr. James H. Starnes, Jr.
Mail Stop 190
NASA Langley Research Center
Hampton, VA 23665-5225
(804) 864-3168

Principal Investigator: Mr. R. E. Barrie
Lockheed Aeronautical Systems Co.
D/73-C1 Zone 0150
86 S. Cobb Drive
Marietta, GA 30063
(404) 494-8161

Objective: To design, analyze, fabricate, and test generic advanced-composite structural components for subsonic and supersonic transport aircraft applications in order to develop verified design technology.

STRUCTURES AND MATERIALS TECHNOLOGY FOR AIRCRAFT COMPOSITE
PRIMARY STRUCTURES

NAS1-19349

Project Engineer: Dr. Mark J. Stuart
Mail Stop 190
NASA Langley Research Center
Hampton, VA 23665-5225
(804) 864-3170

Principal Investigator: Mr. R. E. Horton
Boeing Commercial Airplanes
Mail Stop 6H-CF
P.O. Box 3707
Seattle, WA 98124-2207
(201) 234-0118

Objective: To design, analyze, fabricate, and test generic advanced-composite structural components for subsonic and supersonic transport aircraft applications in order to develop verified design technology.

STRUCTURAL OPTIMIZATION FOR IMPROVED DAMAGE TOLERANCE

NAG-1-168

81 September 1 - 92 October 15

Project Engineer: Dr. James H. Starnes, Jr.
Mail Stop 190
NASA Langley Research Center
Hampton, VA 23665-5225
(804) 864-3168 FTS 928-3168

Principal Investigator: Dr. Raphael T. Haftka
Virginia Polytechnic Institute and State University
Blacksburg, VA 24061
(703) 231-4860

Objective: To develop a structural optimization procedure for composite wing boxes that includes the influence of damage-tolerance considerations in the design process.

FAILURE ANALYSIS AND DAMAGE TOLERANCE OF COMPOSITE AIRCRAFT STRUCTURES

NAS1-17925

85 February 23 - 92 December 30

Project Engineer: Dr. Damodar R. Ambur
Mail Stop 190
NASA Langley Research Center
Hampton, VA 23665-5225
(804) 864-3174

Principal Investigator: Mr. R. E. Barrie
Lockheed Aeronautical Systems Co.
D/73-C1 Zone 0150
86 South Cobb Drive
Marietta, GA 30063
(404) 494-8161

Objective: To develop advanced structural concepts and to advance the analytical capability to predict composite structural failure.

ANISOTROPIC SHELL ANALYSIS

NAG-1-901

88 October 1 - 93 September 30

Project Engineer: Dr. Michael P. Nemeth
Mail Stop 190
NASA Langley Research Center
Hampton, VA 23665-5225
(804) 864-3184

Principal Investigator: Dr. Michael W. Hyer
Virginia Polytechnic Institute and State University
Blacksburg, VA 24061
(703) 231-5372

Objective: To develop accurate analyses for the response of anisotropic composite shell structures.

THICKNESS DISCONTINUITY EFFECTS

NAG-1-537

85 October 1 - 93 September 30

Project Engineer: Dr. James H. Starnes, Jr.
Mail Stop 190
NASA Langley Research Center
Hampton, VA 23665-5225
(804) 864-3168

Principal Investigator: Dr. Eric R. Johnson
Virginia Polytechnic Institute and State University
Blacksburg, VA 24061
(703) 231-6126

Objective: To develop verified analytical models of compression loaded laminates with thickness discontinuities and dropped plies.

COMPOSITE FUSELAGE TECHNOLOGY

NAG-1-982

89 April 7 - 93 April 7

Project Engineer: Dr. James H. Starnes, Jr.
Mail Stop 190
NASA Langley Research Center
Hampton, VA 23665-5225
(804) 864-3168

Principal Investigator: Dr. P. A. Lagace
Massachusetts Institute of Technology
Cambridge, MA 02139
(617) 253-3628

Objective: To conduct experimental and analytical studies of pressurized composite fuselage shells subjected to damage.

STIFFNESS TAILORING OF COMPOSITE PLATES FOR IMPROVED STABILITY AND STRENGTH UNDER COMBINED LOADING

NAG-1-1141

90 June 1 - 92 November 1

Project Engineer: Dr. Mark J. Stuart
Mail Stop 190
NASA Langley Research Center
Hampton, VA 23665-5225
(804) 864-3170

Principal Investigator: Dr. S. B. Biggers
Clemson University
Clemson, SC 29634
(803) 656-0139

Objective: Conduct experimental and analytical studies to tailor membrane and bending stiffnesses for a composite plate that will result in improved buckling resistance and/or postbuckling strength.

MECHANICAL PROPERTIES OF 3-D WOVEN FABRIC

NCC-1-130

88 August 1 - 93 May 1

Project Engineer: Dr. Gary L. Farley
Mail Stop 190
Aerostructures Directorate, USAARTA (AVSCOM)
NASA Langley Research Center
Hampton, VA 23665-5225
(804) 864-3091

Principal Investigator: Dr. John M. Kennedy
Department of Mechanical Engineering
Clemson University
Clemson, SC
(803) 656-5632

Objective: Establish the mechanical response and damage tolerance characteristics of 3-D woven fabrics.

PROGRESSIVE FAILURE MODEL FOR LAMINATED COMPOSITES

NAG-1-979

89 March 1 - 92 February 28

Project Engineer: Dr. Charles E. Harris
Mail Stop 188E
NASA Langley Research Center
Hampton, VA 23665-5225
(804) 864-3449 FTS 928-3449

Principal Investigator: Dr. David H. Allen
Aerospace Engineering Department
Texas A&M University
College Station, TX 77843

Objective: To develop a damage-dependent constitutive model as the mechanics foundation for a progressive failure methodology to predict the residual strength and life of laminates.

THERMAL VISCOPLASTICITY IN METAL MATRIX COMPOSITES

L-24457C

87 July 1 - 92 January 31

Project Engineer: Dr. W. S. Johnson
Mail Stop 188E
NASA Langley Research Center
Hampton, VA 23665-5225
(804) 864-3463 FTS 928-3463

Principal Investigator: Dr. Yehia A. Bahei-El-Din
Department of Civil Engineering
Rensselaer Polytechnic Institute
Troy, NY 12180-3590
(518) 276-8043

Objective: This contract is to develop an analytical method for estimating thermal viscoplasticity stresses and strains in continuous fiber-reinforced metal matrix composites due to fabrication and/or subsequent thermal cycling and mechanical loadings.

DEVELOPMENT OF ADVANCED WOVEN COMPOSITE MATERIALS AND STRUCTURAL FORMS

NAS1-18358

86 August 29 - 92 August 31

Project Engineer: Mr. H. Benson Dexter
Mail Stop 188B
NASA Langley Research Center
Hampton, VA 23665-5225
(804) 864-3094 FTS 928-3094

Principal Investigator: Ms. Janice Maiden
Textile Technologies, Inc.
2800 Turnpike Drive
Hatboro, PA 19040
(215) 443-5325

Objective: To develop textile technology to produce 2-D and 3-D woven preforms and structural elements with integral stiffening, multilayers, and multidirectional reinforcement. Last task for hot-stiffened panel expected to be completed by August '92. This contract will expire at completion of that task.

VISCOELASTIC RESPONSE OF COMPOSITE/HONEYCOMB PANELS FOR
PRECISION REFLECTORS

NAG-1-343

88 August 16 - 93 December 31

Project Engineer: Dr. D. E. Bowles
Mail Stop 191
NASA Langley Research Center
Hampton, VA 23665-5225
(804) 864-3095 FTS 928-3095

Principal Investigator: Dr. M. W. Hyer
Virginia Polytechnic Institute and State University
Blacksburg, VA 24061
(703) 231-5372

Objective: Analytically and experimentally investigate the visco-elastic response of sandwich panels fabricated from composite face sheets and honeycomb cores.

ADVANCED COMPOSITE FABRICATION AND TESTING

NAS1-18954

89 August - 94 August

Project Engineer: Mr. Marvin B. Dow
Mail Stop 188B
NASA Langley Research Center
Hampton, VA 23665-5225
(804) 864-3090 FTS 928-3090

Principal Investigator: Mr. Anthony Falcone
Boeing Aerospace
Seattle, WA 98124
(206) 234-2678

Objective: To process and test experimental composite materials and state-of-the-art systems including woven, braided, knitted, and stitched fiber forms. Processing shall include resin transfer molding, pultrusion, and thermoforming.

MICROMECHANICAL MODELING OF FIBER-MATRIX INTERACTIONS IN CARBON-CARBON COMPOSITES

NAG1-343

91 January - 92 August

Project Engineer: Dr. Howard G. Maahs
Mail Stop 188B
NASA Langley Research Center
Hampton, VA 23665-5225
(804) 864-3498

Principal Investigator: Dr. M W. Hyer
Virginia Polytechnic Institute and State University
Blacksburg, VA 24061
(703) 231-5372

Objective: To analytically investigate the potential for crenelated fibers to provide increased mechanical fiber-matrix interaction in carbon-carbon composites, thus increasing the interlaminar strength of these materials.

SURFACE TREATMENT, SIZING, AND INTERFACE STUDIES OF CARBON FIBERS IN COMPOSITES

NCC1-161

92 February - 95 February

Project Engineer: Dr. Howard G. Maahs
Mail Stop 188B
NASA Langley Research Center
Hampton, VA 23665-5225
(804) 864-3498

Principal Investigator: Dr. Peter M. A. Sherwood
Kansas State University
Manhattan, KS 66506-3701
(913) 532-6689

Objective: To characterize the active chemical species on carbon fiber surfaces and correlate the nature and distribution of these species with the mechanical properties of carbon-carbon and polymeric matrix composites employing these fibers as the reinforcement. To systematically produce fiber variants with different surface treatments and with sizings of different chemistry, with the goal of optimizing key composite properties of interest.

ADVANCED COMPOSITE STRUCTURAL CONCEPTS AND MATERIAL
TECHNOLOGIES FOR PRIMARY AIRCRAFT STRUCTURES

NAS1-18888

1989 April - 1995 May

Project Engineer: Dr. Randall C. Davis
Mail Stop 241
NASA Langley Research Center
Hampton, VA 23665-5225
(804) 864-5435 FTS 928-4535

Principal Investigator: Mr. A. Jackson
Lockheed Aeronautical Systems Company
D/73-C1 Zone 0150
86 South Cobb Drive
Marietta, GA 30063
(404) 494-8164

Objective: To develop and verify innovative textile preform concepts and fabrication processes that exploit the full potential of integrated design/manufacturing procedures to achieve light-weight and cost-effective primary structures; and to develop a strong structural mechanics technology base to predict the performance of advanced concepts.

NOVEL MATRIX RESINS WITH IMPROVED PROCESSABILITY AND PROPERTIES
FOR PRIMARY AIRCRAFT STRUCTURES

NAS1-18841

1989 April - 1992 April

Project Engineer: Dr. P. Hergenrother
Mail Stop 226
NASA Langley Research Center
Hampton, VA 23665-5225
(804) 864-4270 FTS 928-4270

Principal Investigator: Dr. E. P. Woo
Dow Chemical Company
1712 Building
Midland, MI 48674
(517)-636-1072

Objective: Develop new high performance resins with improved durability, toughness and processability. The resins will be targeted for aircraft structural applications with maximum use temperatures ranging from 180°F to 450°F. New resins such as toughened cyanates, modified epoxies, acetylene chromenes, bisbenzocyclobutenes and cyclic oligomers will be synthesized. Composites of the new resins will be fabricated via resin transfer molding or conventional prepreg and evaluated.

ADVANCED MATERIALS AND PRODUCT FORMS

NAS1-18834

1989 April - 1995 May

Project Engineer: Dr. N. Johnston
Mail Stop 188M
NASA Langley Research Center
Hampton, VA 23665-5225
(804) 864-3493 FTS 928-3493

Principal Investigator: Mr. J. T. Hartness
BASF
13504-A South Point Blvd.
Charlotte, NC 28217
(704)-588-7976

Objective: Develop improved matrix resins and unique material forms that offer increased performance and improved processability over state-of-the-art structural composite materials. Two prepreg concepts will be developed and evaluated. The first will use either thermoplastic or thermoset polymer powders to impregnate fiber tows or woven preforms. The second will employ thermoplastics spun into fibers and intimately blended with the reinforcing fibers.

THE MICROMECHANICS OF FATIGUE FAILURE IN WOVEN AND STITCHED COMPOSITES

NAS1-18840

1989 April - 1995 May

Project Engineer: Mr. C. C. Poe
Mail Stop 188E
NASA Langley Research Center
Hampton, VA 23665-5225
(804) 864-3467 FTS 928-3467

Principal Investigator: Dr. Brian Cox
P.O. Box 1085
Rockwell International
1049 Camino Dos Rios
Thousand Oaks, CA 91360
(805)-373-4128

Objective: Develop experimental techniques to characterize the initiation and growth of fatigue damage. Determine the effect of damage on the internal stresses and the global composite stiffness. Based on damage characterization, develop micromechanical model for predicting fatigue behavior of new material architectures.

DAMAGE TOLERANCE OF COMPOSITE PLATES

NAS1-18778

1989 April - 1995 May

Project Engineer: Mr. W. C. Jackson
Mail Stop 188E
NASA Langley Research Center
Hampton, VA 23665-5225
(804) 864-3468 FTS 928-3468

Principal Investigator: Dr. G. S. Springer
Department of Aeronautics and Astronautics
Stanford University
Stanford, CA 94305
(415)-723-4135

Objective: Develop an analysis to predict the complete damage state during and after low-velocity impact and to predict the residual properties. The analysis will be sufficiently general to account for the unique properties of thermoplastic matrix materials while applying to other matrices as well. A three-dimensional finite element model will be developed to calculate stresses, strains, and displacements in a composite during impact based on Hertzian contact forces. The model will define impactor position, velocity, and force as a function of time and will be general regarding material properties and composite layup. The model will predict fiber and matrix damage and trace delamination growth. The analysis will be verified through impact tests wherein the impact force and the extent of damage will be measured. Both destructive and nondestructive techniques will be used to determine the extent of damage.

ADVANCED FIBER PLACEMENT FUSELAGE TECHNOLOGY PROGRAM

NAS1-18887

1989 April - 1995 May

Project Engineer: Mr. W. T. Freeman
Mail Stop 241
NASA Langley Research Center
Hampton, VA 23665-5225
(804) 864-2945 FTS 928-2945

Principal Investigator: R. L. Anderson
M.S. X11K4
Hercules Incorporated
P.O. 98
Magna, Utah 84044
(801)-251-2077

Objective: To develop breakthrough technology for cost effective fabrication of damage tolerant composite fuselage structures. A seven-axis tow placement technique will be used to achieve low cost manufacturing of highly efficient complex structural forms. Major emphasis shall be on innovative manufacturing methods that may offer options for highly efficient primary aircraft structures. A variety of crown, window belt, and keel panels will be manufactured at Hercules and delivered to the Boeing Commercial Airplane Group for evaluation.

INNOVATIVE COMPOSITE AIRCRAFT PRIMARY STRUCTURES (ICAPS)

NAS1-18862

89 March 31 - 94 September 30

Project Engineer: Mr. Marvin B. Dow
Mail Stop 188B
NASA Langley Research Center
Hampton, VA 23665-5225
(804) 864-3090 FTS 928-3090

Principal Investigator: Mr. Alan Markus
McDonnell Douglas Corporation
Douglas Aircraft Company
3855 Lakewood Blvd.
Long Beach, CA 90846
(213) 593-4880

Objective: Develop and demonstrate innovative woven/stitched fiber preforms and resin matrix impregnation concepts for transport wing and fuselage structures. Demonstrate tow placement processes for transport fuselage structures. Conduct a study of materials and structures for high speed transport aircraft. For such future aircraft, perform long-term, elevated temperature evaluations of polymeric matrix composite materials, investigate accelerated testing methodology, and develop structural panel concepts.

ADVANCED TECHNOLOGY COMPOSITE AIRCRAFT STRUCTURES

NAS1-18889

1989 April - 1995 May

Project Engineer: Mr. W. T. Freeman
Mail Stop 241
NASA Langley Research Center
Hampton, VA 23665-5225
(804) 864-2945 FTS 928-2945

Principal Investigator: Dr. Larry Ilcewicz
Boeing Commercial Airplanes
M.S. 31C-65
P.O. Box 3707
Seattle, WA 98124
(206) 393-9630

Objective: To support NASA's goal to revitalize the nation's capacity for aeronautical innovation over the next decade by developing technology needed to apply composites to primary structures on commercial transport aircraft by the late 1990's. The technology shall provide a high level of technical confidence and demonstrate acceptable cost effectiveness for these specific objectives: (1) Develop basic technologies required to support cost effective damage tolerant pressurized fuselage structural designs and verify breakthrough technology results with mechanical tests. (2) Demonstrate advanced material placement processes and flexible automation for low cost assembly of pressurized transport fuselage structures. (3) Demonstrate the use of thermoplastic materials with advanced manufacturing techniques for fuselage clips, fittings, frames, and window belt reinforcements. (4) Develop the associated design, analysis and process technologies so that commercial application readiness and cost effectiveness can be realistically assessed. (5) Since the fuselage has the highest percentage of corrosion and fatigue problems on transport aircraft, composites will be evaluated for their potential to reduce repair and maintenance costs associated with airline life-cycle supportability. (6) Composite center fuselage elements will be developed because weight reductions at the airplane center line are more effective in increasing payload, due to the offsetting dead-weight relief effects. The contract was modified in 1991 to include development of a Designer's Cost Model.

NOVEL COMPOSITES FOR WING AND FUSELAGE APPLICATIONS

NAS1-18784

89 April 28 - 93 July 31

Project Engineer: Mr. H. Benson Dexter
Mail Stop 188B
NASA Langley Research Center
Hampton, VA 23665-5225
(804) 864-3094 FTS 928-3094

Principal Investigator: Mr. James Suarez
Grumman Aerospace Corporation
Aircraft Systems Division
South Oyster Bay Road
Bethpage, NY 11714-3582
(516) 575-6552

Objective: Integrate innovative design concepts with cost-effective fabrication processes to achieve damage tolerant structures that can perform at a design ultimate strain level of at least 6000 micro in./in. Integral structures will be fabricated using weaving and knitting/stitching concepts. Resin transfer molding will be used for low cost resin application and consolidation. Contract has been redirected to focus on cross-stiffened window belt elements that are integrally woven/stiffened and lower side quadrant fuselage panel.

SCIENCE-BASED APPROACH TO RESIN TRANSFER MOLDING OF AIRCRAFT STRUCTURES

NAS1-19347 TASK NO. 2

1991 November 18 - 1994 November 30

Project Engineer: Mr. Jerry W. Deaton
Mail Stop 188B
NASA Langley Research Center
Hampton, VA 23665-5225
(804) 864-3087 FTS 928-3087

Principal Investigator: Dr. R. L. Ramkumar
Aircraft Division
Northrop Corporation
One Northrop Avenue
Hawthorne, CA 90250-3277
(310) 331-7102

Objective: To develop analytical models of RTM processes in carbon fiber preforms compacted by stitching, braiding, or weaving. The model will account for CAD interfaces, multiple inlets, ports, and inserts. Models will be validated by fabricating representative structural elements and stiffened panels. An RTM guideline for composite materials selection and tooling design will be generated.

INNOVATIVE COMPOSITE FUSELAGE STRUCTURES

NAS1-18842

1989 April - 1995 May

Project Engineer: Mr. M. Rouse
Mail Stop 190
NASA Langley Research Center
Hampton, VA 23665-5225
(804) 864-3182

Principal Investigator: Dr. R. B. Deo
M.S. 3853/MF
Northrop Corporation
1 Northrop Ave
Hawthorne, CA. 90250-3277
(213) 332-2134

Objective: Develop innovative concepts for fighter aircraft fuselage structures that will improve structural efficiency while reducing manufacturing costs. Analysis methods and structural mechanics methodologies appropriate for the new structural concepts will also be developed and validated through tests of elements and components. Analysis techniques will be developed in three major areas: (1) structural details, (2) structural stability, and (3) scaling laws. This contract was redirected in 1991 to develop structural concepts and materials technology of future supersonic commercial transports.

FIBER WAVEGUIDE SENSORS FOR INTELLIGENT MATERIALS

NAG -1-895

1988 SEPTEMBER - 1991 OCTOBER

Project Engineer: Dr. Robert Rogoswki
IRD, Nondestructive Evaluation Science Branch
Mail Stop 231
NASA Langley Research Center
Hampton, VA 23665-5225
(804)864-4990 FTS 928-4990

Principal Investigator: Dr. Richard O. Claus
Department of Electrical Engineering
Virginia Polytechnic Institute and State University
Blacksburg, VA 24061

Objective: Development of fiber-optic based opto-electronic sensing instrumentation for the characterization of materials and structures.

ULTRASONIC NONDESTRUCTIVE CHARACTERIZATION OF COMPOSITES WITH 3-DIMENSIONAL ARCHITECTURES

NSG-1-601

1981 September – 1992 March

Project Engineer: Dr. Patrick H. Johnston
IRD, Nondestructive Evaluation Science Branch
Mail Stop 231
NASA Langley Research Center
Hampton, VA 23665
(804) 864-4966 FTS 928-4966

Principal Investigator: Dr. James G. Miller
Department of Physics
Washington University
St. Louis, MO 33130

Objective: The overall goal of our research program is the development and application of quantitative ultrasonic techniques to problems of nondestructive evaluation of composite materials. We specifically are focused on applications of frequency analysis of ultrasonic propagation to determine material properties in composite laminates and more complex fiber geometries.

INVESTIGATION OF ACOUSTIC PROPERTIES OF COMPOSITE MATERIALS

NAG -1-1063

1983 September – 1991 October

Project Engineer: Dr. Patrick H. Johnston
IRD, Nondestructive Evaluation Science Branch
Mail Stop 231
NASA Langley Research Center
Hampton, VA 23665
(804) 864-4966 FTS 928-4966

Principal Investigator: Dr. Barry T. Smith
Department of Physics
College of William and Mary
Williamsburg, VA 23185

Objective: The research involves an investigation of the ultrasonic properties of composite materials in order to characterize and assess damage. Current focus lies upon impact damage in carbon-carbon and stitched and woven laminates.

NONDESTRUCTIVE EVALUATION OF CARBON-CARBON COMPOSITES
1989 September – 1995 September

Project Engineer: Dr. Eric I. Madaras
IRD, Nondestructive Evaluation Science Branch
Mail Stop 231
NASA Langley Research Center
Hampton, VA 23665
(804) 864-4993 FTS 928-4993

Principal Investigator: Dr. Ron Kline
Department of Aerospace and Mechanical Engineering
University of Oklahoma
Norman, OK 73019

Objective: The research involves methods of measuring the elastic moduli of carbon-carbon materials and integrating the results with FEM codes to predict the behavior of components. Also, research related to nondestructive evaluation of carbon-carbon coatings is being conducted.